Petroleum geology of North Greenland

edited by
Flemming G. Christiansen

GRØNLANDS GEOLOGISKE UNDERSØGELSE

GGU

Bulletin 158

1989

GRØNLANDS GEOLOGISKE UNDERSØGELSE
Bulletin 158

Petroleum geology of North Greenland

edited by
Flemming G. Christiansen

1989

Dansk sammendrag

Oliepotentialet af det Nedre Palæozoiske sedimentbassin i Nordgrønland – et landområde som er flere gange større end Danmark – er blevet vurderet ved at undersøge udbredelsen af mulige moderbjergarter for olie og disses senere thermale historie. Et stort prøvemateriale blev indsamlet i felten og ved korte boringer til max. 40 m dybde i somrene 1984 og 1985 og er senere analyseret ved en lang række kemiske og fysiske metoder. To enheder rige på organisk materiale, den Kambriske Henson Gletscher Formation og de nederste dele af de Silure skifre, er mulige moderbjergarter for olie. Begge enheder er vidt udbredte i Nordgrønland og kan kortlægges i overfladen, ligesom deres mulige udbredelse i undergrunden kan vurderes ud fra tolkning af aflejringsmiljøer og den regionale struktur. Begge de mulige moderbjergarter har et moderat til højt indhold af organisk materiale, som ved passende opvarmning kan være blevet omdannet til olie.

Ved hjælp af en række forskellige analyseparametre er det påvist, at en sådan opvarmning fandt sted i det meste af Nordgrønland for ca. 350 millioner år siden. I den nordlige del af området var varmepåvirkningen imidlertid så kraftig, at den dannede olie er blevet nedbrudt til grafit samt gas, som er sivet ud ved overfladen. I den sydlige del af regionen har påvirkningen været mindre kraftig, og her findes i dag mange eksempler på olierester ved overfladen, f.eks. sorte olie-plettede sandsten, beg-fyldte koraller og udsivende asfalt langs sprækker. Dette antyder muligheden for egentlige olieforekomster i undergrunden.

Beregningerne viser, at der ialt er blevet dannet mellem 25 og 100 milliarder m^3 olie, hvoraf dog kun en yderst ringe del kan forventes at være bevaret som olie-felter. De mest lovende områder er i de sydlige dele af Wulff Land og Warming Land, måske også i Washington Land.

Fig. 1. Shallow core drilling at 81°16′N, 42°23′W, the hitherto northernmost borehole completed by GGU.

Fig. 1. Kort boring ved 81° 16′ nordlig bredde, 42° 23′ vestlig længde – GGU's hidtil nordligste borehul.

Preface

Estimating the distribution and extent of fuel resources of Greenland is one of the major objectives of the Geological Survey of Greenland (GGU).

This work is the first comprehensive assessment of the hydrocarbon potential of the Lower Palaeozoic Franklinian basin in North Greenland, which is one of the few remaining unexplored frontier basins in the world.

The project forming the backbone of this report was a logical outgrowth of a systematic geological study of the whole basin initiated by GGU in 1978. At the same time it represents the continuation of a tradition started in central East Greenland where systematic geological mapping was followed by a comprehensive evaluation of the hydrocarbon potential. In recent years this tradition has been continued in the Mesozoic basin of northern East Greenland and in due course is expected to continue in the Late Palaeozoic – Mesozoic Wandel Sea basin in the north-eastern corner of Greenland and in the onshore Mesozoic basin of West Greenland.

The Franklinian basin is one of the northernmost basins in the world, and systematic investigations are challenging from a logistical and planning point of view.

Sampling in 1980 of all potential source rocks in the basin formed the basis for the first reconnaissance level evaluation. Screening of this material allowed subsequent focusing on the most promising sequences during the 1984–85 field seasons. A specially constructed helicopter-portable shallow core drill was applied in the subsequent stage. The retrieved cores were subjected to a comprehensive analytical programme including study of LECO and Rock Eval pyrolysis, thermal maturity, palynology, palynofacies, thermal alteration index (TAI), 'vitrinite' and graptolite reflectance, fluorescence, gas chromatography/mass spectrometry, carbon isotopes, X-ray diffraction of kerogen, fission track, fluid inclusions, porosity and permeability, coupled with detailed field work around the drilling sites.

This multidisciplinary approach is rarely seen and reflects not only the excellent three dimensional exposures but also the skilful planning, project management and scientific insight by the project leader.

It is a great pleasure to see the completion of a project which I have followed from its initiation with reconnaissance type work to the present synthesis of a broad-spectred data set reflecting an impressive list of analytical procedures.

Structural style, facies evolution, character and maturation of organic matter have been successfully integrated into a sophisticated multi-facetted synthesis.

Finn Surlyk,
Professor, dr. scient.,
Geologisk Centralinstitut,
University of Copenhagen,
Øster Voldgade 10,
DK-1350 Copenhagen K,
Denmark.

Abstract

Lower Palaeozoic sediments of the Franklinian basin are well exposed in a broad zone across North Greenland. The region was characterized by major generally east–west trending facies belts throughout the depositional period. In the southern shelf areas predominantly carbonate sedimentation took place, bordered to the north by outer shelf and slope mudstones. In the north mainly siliciclastic deep-water sedimentation prevailed in the trough.

All shale and dark carbonate units were studied and extensively sampled, followed by shallow core drilling of the most interesting intervals. The analytical programme included LECO/Rock Eval, palynological, petrographic, reflectance and fluorescence, gas chromatography, mass spectrometry, carbon isotope and X-ray diffraction studies of source rocks and migrated bitumens, porosity and permeability measurements of potential reservoir rocks, and fluid inclusion and fission track studies to reveal the thermal history.

Two major organic-rich units of potential source quality occur in the region: the Lower to Middle Cambrian Henson Gletscher Formation and lateral equivalents, and the Lower Silurian shales, of which especially the interval of late Llandovery age seems promising. Both units have moderate to high contents of organic carbon, typically between 3 and 6%, and a good to excellent generative potential of immature samples. The organic matter in the Henson Gletscher Formation is dominated by amorphous kerogen, whereas the Silurian shales also contain minor contents of graptolites, chitinozoans and scolecodonts.

Geochemically, the kerogen in both source rocks is of Type II. The extractable organic matter is rather similar in gross composition. The Cambrian extracts have lighter carbon isotope composition and lower pristane/phytane ratios when compared to those of the Silurian, and a different distribution of hopane and sterane biomarkers.

The thermal maturity of the source rocks ranges from immature or early mature in the southernmost areas to postmature or low metamorphic in the northernmost areas, with only a narrow mature transition zone. This simple and consistent maturity pattern, with the exception of a few anomalies caused by intrusions or tectonism, has been mapped across most of North Greenland.

Evidence of hydrocarbon generation and migration is widespread in the region, observed as oil-stained carbonates or sandstones, as solid bitumen or as seeping asphalt. Most of the examples are closely associated with nearby source rocks, but numerous bitumens in the southernmost areas without any known source rock point towards important long-distance migration of oil. The chemical composition of these bitumens is in accordance with a Cambrian source rock.

The similarity between the thermal maturity pattern and the tectono-metamorphic zones, fission track data, and abrupt changes in thermal maturity between Lower Palaeozoic and Upper Palaeozoic or Mesozoic sediments all suggest that the maturation and most of the petroleum generation took place before or during the Ellesmerian orogeny in Late Devonian or Early Carboniferous time.

Large amounts of hydrocarbons were generated; estimates of the total generative potential based on most likely values of depositional areas, thickness of source rocks and geochemical data suggest values in the range of 25–100 × 10^9 m^3 of petroleum. More than 90% of this amount was probably generated and even prospects with low migration efficiencies could contain significant accumulations. The two most obvious play types, the Silurian carbonate reef and the sandstones in the Henson Gletscher Formation, seem disappointing due to high thermal maturity and deep erosional level. The best prospectable play type is accumulations in the southern part of the region as a result of long distance migration.

List of contributors

John Boserup, Flemming G. Christiansen, Hans F. Jepsen, Niels Henry Larsen, Grete Søgaard Nielsen & Henrik Nøhr-Hansen
Grønlands Geologiske Undersøgelse, Øster Voldgade 10, DK-1350 Copenhagen K, Denmark.

Carsten Guvad, Christian J. W. Koch, Svend Stouge, Erik Thomsen & Preben Østfeldt
Danmarks Geologiske Undersøgelse, Thoravej 31, DK-2400 Copenhagen NV, Denmark.

Bjørn Buchardt
Institut for Historisk Geologi og Palæontologi, Øster Voldgade 10, DK-1350 Copenhagen K, Denmark.

Kirsten Hansen & Jørgen Jensenius
Institut for Petrologi, Øster Voldgade 10, DK-1350 Copenhagen K, Denmark.

CONTENTS

Chapter 1

Background

F. G. Christiansen

The present work is mainly based on the results of the 'Nordolie' project (1984–1987) that was undertaken to study the distribution and thermal maturity of potential hydrocarbon source rocks in central and western North Greenland (Christiansen & Rolle, 1985). The project was carried out concurrently with a geological mapping programme by the Geological Survey of Greenland (GGU) that also encompassed important petroleum-related disciplines such as stratigraphy, sedimentology and structural geology. This provided the first systematic survey of the possibilities of exploring hydrocarbons in the region.

Field work was carried out in 1984–1985 and a comprehensive report of the findings, which includes data published earlier, was prepared (Christiansen, 1988). The present publication is a condensed version of that report.

Physiography

The study area of more than 40 000 km^2 is situated between 80° and 83°N. It encompasses a number of major land areas (Washington Land, Hall Land, Nyeboe Land, Warming Land, Wulff Land, Nares Land and Freuchen Land), separated by permanently ice-covered fjords, glaciers and the Inland Ice (figs 2 and 3). A number of smaller islands and nunataks provide good exposures. Approximately half of the study area is ice-free land.

The physiography is quite variable and controlled to a large extent by bedrock lithology and structure with the geomorphic regions corresponding to the main stratigraphic–structural provinces (Davies, 1972; Dawes & Christie, in press). Hence the southern part of the region, characterized by flat-lying or gently northerly dipping carbonate strata, is dominated by plateaus with elevations up to about 1000 m. The plateaus are dissected by steep-sided, flat-floored valleys, lakes and glaciers into mesa-like blocks. The central and northern areas form lowland with an undulating surface dominated by gently dipping to slightly folded sandstones and shales. To the north, in the mainly clastic strata of the folded region along the northern coast, higher and rougher terrain with peaks over 1200 m is widespread.

Many of the north–south trending fjords and valleys provide well-exposed and often picturesque sections through the succession.

Preliminary studies of the physiographic and biological environment in relation to petroleum exploration were carried out in 1984–1985 by the Greenland Fisheries and Environmental Research Institute (GFM) and the Greenland Technical Organization (GTO). The biological part of the study (Grønlands Fiskeri- og Miljøundersøgelser, 1986) confirmed the barren nature of the region with few areas of continuous vegetation (*c.* 1%).

The coasts of the study area are ice-locked all year. GGU's field work was launched by C-130 Hercules aircraft operating through Thule Air Base (U.S. Air Force), the Canadian Forces Station at Alert, or Station Nord (Royal Danish Air Force) (fig. 2). Natural landing strips were established for local transport with Twin Otter. Most of the field work was supported by Bell 206 Jet Ranger helicopter.

North Greenland is characterized by a high-Arctic climate with long cold winters and short cool summers. Only June, July and August display average temperatures above freezing point. However, towards the Inland Ice the valleys have pleasant conditions for field work during the summer. During most of the winter period temperatures are from −25°C to −30°C. Precipitation is low (less than 200 mm per year), predominantly as snow. In the summer logistics in the coastal areas can be hampered for days by dense fog owing to local open water.

Early expeditions to North Greenland

The first geological knowledge of the region between Washington Land and Peary Land dates back to the end

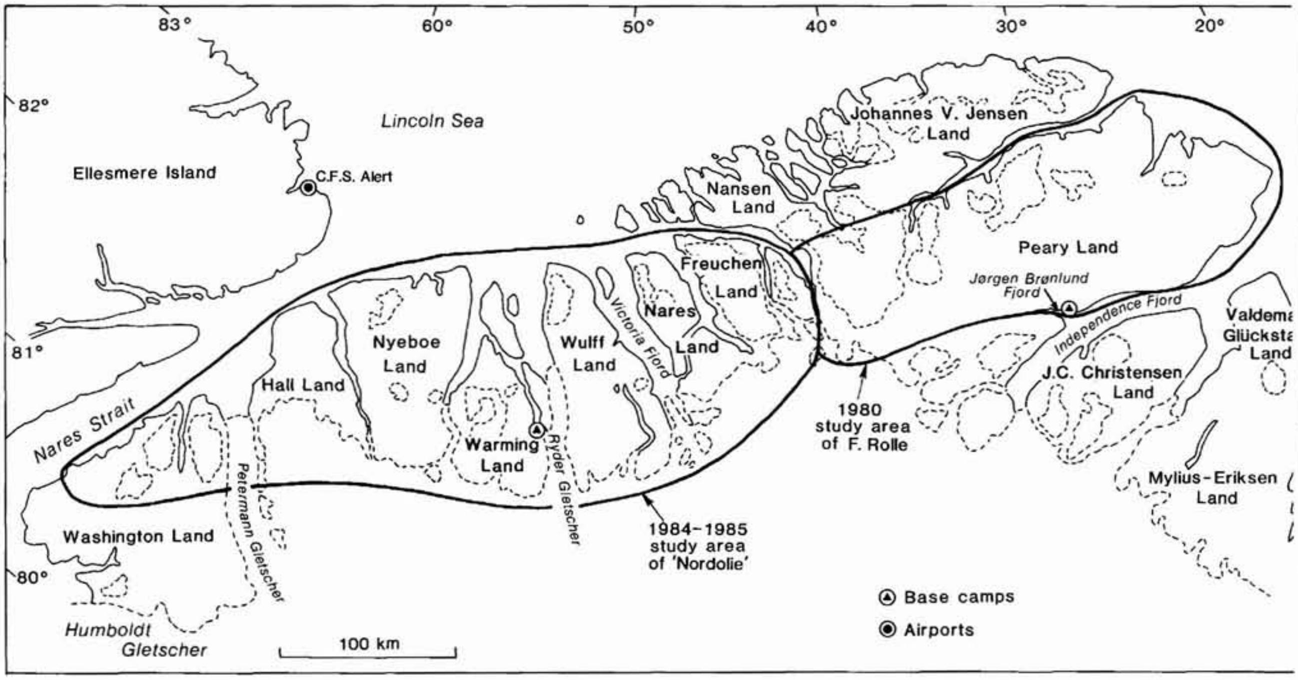

of the last century – approximately to the beginning of the modern oil history. The first discovery of oil in a well by J. A. Drake, Titusville, Pennsylvania was in 1859, 12 years before Charles Francis Hall in the ship USS *Polaris* landed on the west coast of Hall Land. The main goals of Hall's North Polar Expedition, 1871–1873, and the following Royal Navy Arctic Expedition, 1875–1876 (under G. S. Nares), the U.S. Lady Franklin Bay Expedition, 1881–1884 (led by A. W. Greely), and the expeditions of R. E. Peary 1898–1902, 1905–1906, 1908–1909 were geographic exploration and 'flag waving'.

Scattered but important geological results were obtained. The most interesting details are summarized by Peter R. Dawes and co-workers (Dawes, 1971, 1976, 1984a; Dawes & Haller, 1979; Dawes & Christie, 1982).

The first systematic geological survey of North Greenland, including cartographic work of this 'terra incognita', was carried out by Lauge Koch on the 2nd Thule Expedition, 1916–1918 (led by Knud Rasmussen) and as leader of the Bicentenary Jubilee Expedition, 1920–1923. The results include important topographic and geological maps and stratigraphic–structural studies of the Lower Palaeozoic succession (e.g. Koch, 1925, 1929; Dawes & Haller, 1979). The regional geological elements of Koch's work, obtained under extremely severe conditions, remain essentially unaltered today.

The succeeding significant geological studies in northern Greenland were mainly made outside the present study area but were important in a regional assessment. J. C. Troelsen participated in the Danish Thule and Ellesmere Land Expedition 1939–1941 and revised Proterozoic and Lower Palaeozoic stratigraphy on both sides of Nares Strait (Troelsen, 1950). Additional stratigraphic and structural results were obtained during the Danish Northeast Greenland Expedition 1938–1939 and the Danish Peary Land Expedition 1947–1950 led by Eigil Knuth (e.g. Nielsen, 1941; Troelsen, 1949; Ellitsgaard-Rasmussen, 1955).

Modern expeditions

Aircraft have played an increasingly important role in the modern expeditions in North Greenland and geological knowledge has multiplied, especially in the last decade. Of importance to the present study are the results obtained during Operation Grant Land – a joint venture of the Geological Surveys of Canada and Greenland – in 1965–1966 (Allaart, 1965; Norford, 1972; Dawes, 1984a), the Peary Land Expeditions 1966–1970 (Jepsen, 1971), the Joint Services Expedition 1969 (Dawes & Soper, 1970, 1979), and GGU field work in southern Peary Land in 1974 (Christie & Peel, 1977) and Washington Land 1975–1977 (e.g. Henriksen & Peel, 1976; Hurst, 1980a,b).

More recently GGU has carried out systematic geological mapping and regional studies throughout North Greenland from Nares Strait to the Wandel Sea. These

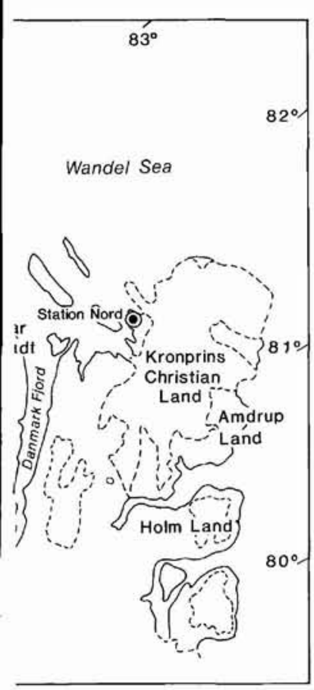

Fig. 2. Map of northern Greenland showing the location of the 'Nordolie' study area, the previous study area in the east, and the geographic names used in the text.

expeditions, led by Niels Henriksen, worked in 1978–1980 in central and eastern North Greenland from a base camp in southern Peary Land, while in 1984–1985 the region to the west was studied from a base camp in southern Warming Land (fig. 2; Dawes, 1984b; Henriksen, 1985a,b, 1986, 1987). Many papers have appeared as a result of these five field seasons; details of structure and stratigraphy have been worked out and a flood of new stratigraphic names have appeared on maps and in new systematic descriptions.

Commercial activities

Commercial petroleum activities have only taken place in North Greenland in a single period from 1968 to 1973 by a group of companies under Greenarctic Consortium. The consortium was founded in February 1969, with the aim of exploring minerals and hydrocarbons in northern Greenland. Ponderay Exploration Company, an Edmonton-based independent oil company, headed the consortium which included a number of Canadian shareholders as well as two small Danish companies, Internationalt Mineselskab A/S and Nordkalotten Mineselskab A/S. The Danish subsidiary company Ponderay Polar A/S (wholly owned by Greenarctic Consortium) held a non-exclusive five-year concession to explore for minerals and oil north of latitude 74° 30′.

Field work was carried out in the summers of 1969, 1971 and 1972 by geologists mainly from J. C. Sproule and Associates Ltd., a consulting company well known for pioneering work on the economic potential of the Arctic. Also in 1971 an aeromagnetic study was flown by Grumman Ecosystem Corporation, a subsidiary of Grumman Aircraft with major interests in Greenarctic Consortium. Results from this commercial activity were not published, apart from an abstract (Stuart-Smith, 1970) and a short paper on Silurian reefs in Peary Land (Mayr, 1976). However, permission was granted for GGU to include data in review papers on North Greenland (e.g. Dawes, 1976), and on petroleum geology of Greenland (Henderson, 1976). Other information is contained in a review of hydrocarbons in the Canadian Arctic (Stuart-Smith & Wennekers, 1977). A number of confidential reports prepared for Greenarctic Consortium consider hydrocarbon prospects in both the Lower Palaeozoic strata and the Wandel Sea Basin. Upper Ordovician and Silurian reefs or basal Cambrian sandstones were proposed as the main targets for future exploration. Neither oil seepage nor bitumen impregnation were reported, but carbonates with a petroliferous odour were noted in the Cambrian Brønlund Fjord Formation and the Ordovician Wandel Valley Formation. The lack of interest in and knowledge of source rocks, which is typical for all hydrocarbon exploration prior to the seventies, is also apparent in the Greenarctic study: "The Paleozoic section within this area is comprised almost entirely of carbonates and shales of marine origin, and can therefore be considered as potential source rocks".

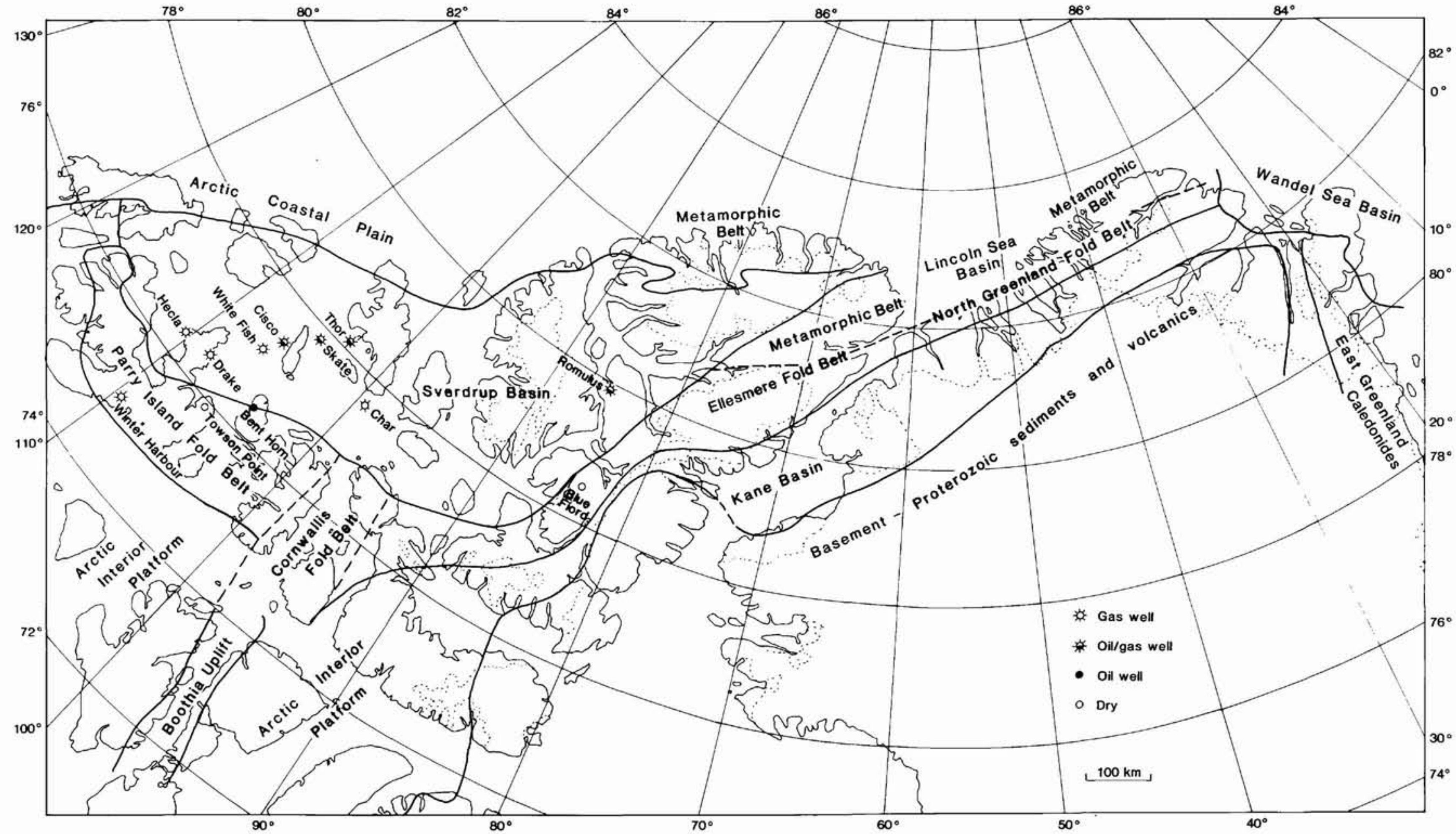

Fig. 3. Geological provinces in Arctic Canada and northern Greenland. Compiled after numerous sources. The locations of some of the mentioned wells in the Sverdrup and Franklinian basins are indicated.

Influence from Canadian activities

The obvious geological connection and the similarity of climatic conditions between North Greenland and the Canadian Arctic Islands makes a comparison of the hydrocarbon activities, and the implications of the results obtained so far very relevant.

Compared to North Greenland, activities in Canada started much earlier and have now reached an early-mature stage with more than 180 completed wells (see reviews by Stuart-Smith & Wennekers (1977), Rayer (1981), Nassichuk (1983), and Embry *et al.* (in press)). The highlights of the exploration history in the Canadian Arctic Islands include (see localities in fig. 3):

1960: first exploration permits.
1962: first well completed (Winter Harbour, some gas in Devonian sandstone).
1967: Panarctic Oils Ltd formed.
1969: first major gas discovery (Drake Point, 5.3 TCF in Jurassic sandstone).
1972: first oil discoveries (Thor, Triassic sandstone; Romelus, Triassic sandstone).
1974: first off-shore well (Hecla N-52, ice-strengthened platform, 128 m water depth).
1974: oil discovery at Bent Horn, Cameron Island (in Devonian carbonates).
1980: discovery of major gas fields through thick layer of ice (White Fish, Cretaceous sandstone; Char, Jurassic sandstone).
1981: first major Mesozoic oil discoveries (Skate, Jurassic sandstone; Cisco, Jurassic sandstone).
1985: first production (Bent Horn A-02 drilled in 1976, Middle Devonian Blue Fiord reefal limestone; 100 000 barrels of crude shipped to refinery in Montreal).

The drilling activities culminated in the early seventies (23 wells completed within 1973). In the eighties, a constant level of 4 to 5 wells per year has been maintained, by far the most active operator being Panarctic Oils Ltd. Exploration since the mid-seventies has concentrated in the Mesozoic succession in the Sverdrup Basin where a number of major gas fields have been discovered; less effort was devoted to the Lower Palaeozoic Franklinian Basin (neither the folded deep-water siliciclastics of the 'Franklinian Geosyncline' nor the stable shallow-water carbonates of the 'Arctic Interior Platform'; fig. 3).

Nassichuk (1983) estimated the mean oil and gas potential as follows (discovered and undiscovered recoverable resources):

Arctic Interior Platform: 1.1×10^9 barrels of oil, 8.5 TCF gas (no discoveries as yet).

Franklinian Geosyncline: 0.5×10^9 barrels of oil, 7.8 TCF gas (only minor discoveries).

Sverdrup Basin: 2.9×10^9 barrels of oil, 69.9 TCF gas (minor oil discoveries, more than 15 gas discoveries with recoverable reserves of approximately 15 TCF). Estimates by Procter *et al.* (1984) show almost the same range of values.

The major discoveries of gas have been made in clastic reservoirs of Triassic and Jurassic age in the Sverdrup Basin and are of particular relevance to future studies in the Wandel Sea Basin in eastern North Greenland.

In Canada, Early Palaeozoic basin development simulates that of North Greenland. To the south there is a stable platform dominated by shallow-water carbonates; to the north deep-water siliciclastics occur with a complex border zone of carbonate reefs and debris which roughly corresponds to the southern limit of Ellesmerian (Late Palaeozoic) folding.

A detailed source rock study comprising material from 21 wells penetrating the Lower Palaeozoic succession suggested several potential source rock units in the deep-water sequence (Powell, 1978). Intervals in the Upper Ordovician to Silurian Cape Phillips Formation (comparable to the Silurian shales in North Greenland) and in the Devonian Bathurst Island, Eids, Weatherall and Bird Fiord Formations contain rich oil-prone organic matter. The main problem with the source rocks in the Lower Palaeozoic in Canada seems to be the high thermal maturity. Many of the intervals penetrated by drilling are thermally postmature and the generation probably took place already in Middle to Late Devonian time (Powell, 1978).

Hydrocarbon staining and bitumen occurrences at the surface have been reported from many locations, especially in Ordovician to Devonian carbonates (e.g. Sproule, 1966; Rayer, 1981, figs 12, 13, 43). Oil shows in wells are restricted to three structures: Blue Fiord, Towson Point, Bent Horn. In the latter case several wells have been tested with a production of up to 5000 barrels/day from Middle Devonian carbonates (Rayer, 1981). In September 1985 crude from this field was shipped to Montreal and this continued in the summers of 1986, 1987 and 1988.

The main oil prospects in Canada include only one type that is relevant to North Greenland, namely reservoirs in Ordovician to Devonian reefs along the shelf margin or in isolated reefs encased in shale. Other play types are related to folding and diapirism of Ordovician evaporites (not recognized in North Greenland) and to Upper Devonian sandstones (not present in North Greenland due to deep erosional level or non-deposition).

The accumulative knowledge from the Canadian Arctic has had important geological implications for North Greenland. It is notable that the Greenarctic operations overlapped with one of the most active and optimistic periods in the Canadian Arctic Islands. The withdrawal roughly took place at a time when activities were redirected and concentrated on Mesozoic prospects in the Sverdrup Basin. The low activities in the Franklinian basin at present must be taken as evidence of very little interest in Palaeozoic prospects in this setting and in this part of the world.

Initiation of 'Nordolie'

The Greenarctic enterprise in northern Greenland was influenced by commercial activities in the Canadian Arctic and was also inspired by findings, especially of reef complexes, in Greenland during Operation Grant Land in 1965 and 1966. Kerr (1967) used Greenland data in his regional appraisal and showed that the Silurian reef complex of the Arctic Islands continues into the Hall Land – Washington Land area, while Dawes (1971) indicated its regional extent across North Greenland. Subsequent to Greenarctic's withdrawal, development of ideas of the petroleum geology, both in form of analytical work, reports and papers, was sporadic in North Greenland due to concentration of resources in the major exploration programme off-shore West Greenland in the mid-seventies.

Norford (1972) mentioned residual bitumen at Kap Tyson in western Hall Land and provided a few TOC analyses of nearby shales. Henderson (1976) quoted several unpublished OLEXCON reports with analytical data of organic-rich shales in Washington Land, Hall Land and Nyeboe Land. Perregaard (1979) reported promising analytical results of two organic-rich lime mudstones (and one organic-lean limestone) of Silurian age from Washington Land. Possible source rocks for petroleum in the Brønlund Fjord Group and potential traps associated with the unconformity at the base of the Wandel Valley Formation and east–west trending faults in Peary Land were mentioned for the first time by Peel (1979). Many of the geologists participating in GGU's Peary Land activities in 1978 and 1979 collected random samples of dark, often stinking, limestone, dolomite and shale. Subsequent analytical work on 64 samples (later included in Rolle & Wrang, 1981) gave promising results.

Consequently, hydrocarbon studies were included in GGU's Peary Land programme in 1980 (Rolle, 1981). This work aimed at systematic source rock sampling with preliminary examination of most of the Lower Palaeozoic succession and more detailed investigations of the Brønlund Fjord Group. Analytical work of the sampled material suggested the presence of potential source rocks in Peary Land (Rolle & Wrang, 1981), and hence formed the background for new and more detailed studies. These, carried out in 1984 and 1985, aimed at a combined geological–geochemical study of potential source and reservoir rocks, and a source rock programme was integrated in GGU's regional studies of central and western North Greenland.

Chapter 2

Review of the Lower Palaeozoic basin in North Greenland with special emphasis on petroleum geology

F. G. Christiansen

The Lower Palaeozoic sediments of North Greenland were deposited in the eastward extension of the Franklinian basin of Ellesmere Island, and are exposed today in a broad E–W trending zone across North Greenland about 800 km long and up to 200 km wide (figs 4 and 5).

Numerous accounts on the geology of this region have appeared, particularly over the last decade following field work by GGU in 1978–1980 and 1984–1985 (*Rapp. Grønlands geol. Unders.* **88, 99, 106, 126, 133**). A number of reviews with quite different approaches summarize the geology with respect to the history of exploration (Dawes & Christie, 1982, Christie & Dawes, in press), general geology (Dawes, 1971, 1976; Dawes & Peel, 1981; Higgins, 1986), stratigraphy (Peel, 1982, 1985), deformation (Higgins *et al.,* 1985) and basin development (Surlyk & Hurst, 1984; Higgins *et al.,* in press). Reviews concerning the geological implications for future petroleum activities have, however,

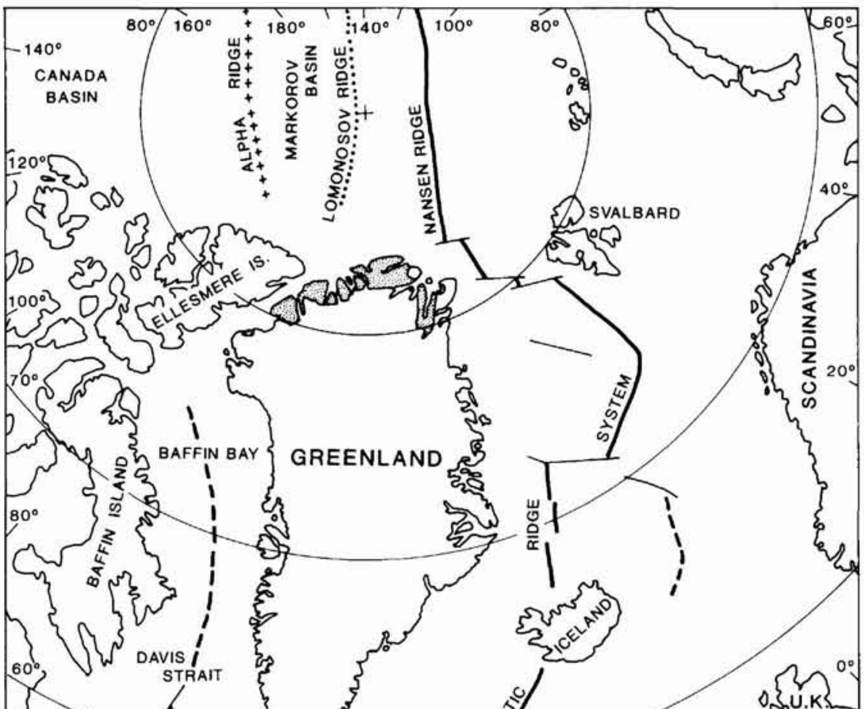

Fig. 4. Map showing the tectonic position of the Lower Palaeozoic sediments in North Greenland. Dark tone: exposures of the Lower Palaeozoic Franklinian basin in North Greenland, full lines: active spreading zones, thin lines: fracture zones, dash lines: extinct spreading zones (?), lines of crosses: ridge of uncertain origin, line of dots: ridge of continental origin.

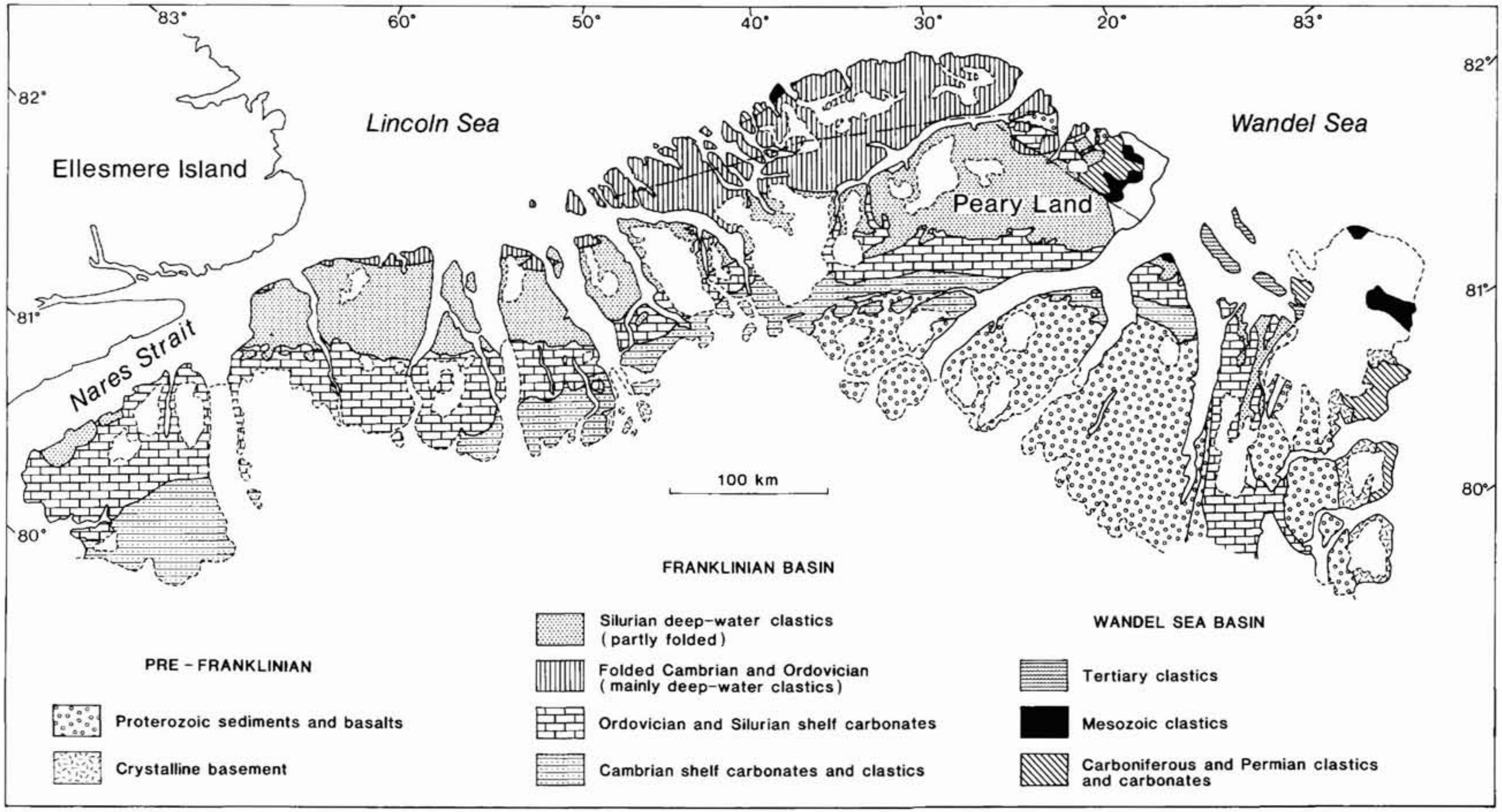

Fig. 5. Geological map of North Greenland. Simplified and modified after Dawes (1976), Higgins *et al.* (in press), and Christiansen *et al.* (in press).

been very limited (Henderson, 1976; Christiansen *et al.*, in press).

Tectonic setting

The segment of the Franklinian basin represented in North Greenland developed in Early Palaeozoic time and is now exposed along the northern margin of the Greenlandic Precambrian shield. Cratonic rocks (Archaean–Proterozoic crystalline basement and Middle to Late Proterozoic volcanics and sediments) underlie at least the southern part of the basin in North Greenland.

During the time of basin development, from latest Proterozoic or earliest Cambrian to Devonian time, the Greenland craton formed part of the Laurentia continent with a palaeogeographic position of the study area between latitudes 5°S and 15°N (Scotese *et al.*, 1979). On the basis of the east–west sediment transport direction, parallel to the continental margin, Surlyk & Hurst (1983) proposed that the basin took the form of a relatively narrow trough with a northern barrier. Two main hypotheses were proposed: the presence of a narrow ocean with the spreading axis ridge forming the barrier or an aulacogen model with rifting from the Iapetus Ocean extending deeply into the continent. Earlier, a back-arc model had been proposed with the Pearya Geanticline in northern Ellesmere Island and its intrusions and volcanic rocks forming in this setting (Frisch, 1974; Christie, 1979; Trettin & Balkwill, 1979; Trettin, 1987). However, there is no evidence in the Greenland part of the basin in support of this model.

The final closure of the Iapetus Ocean in the Late Silurian and the subsequent continental collision formed the East Greenland Caledonian fold belt. This episode also strongly affected the Greenland part of the Franklinian basin; most of the Silurian turbidites were derived from the rising Caledonide mountains (Surlyk, 1982; Hurst *et al.*, 1983), and the subsidence history was affected by loading and local uplift (causing for instance the unconformity below the Wandel Valley Formation) (Surlyk & Hurst, 1984).

The Ellesmerian orogeny brought deposition in the Franklinian basin to a close in Late Devonian to Early Carboniferous time (fig. 6) and gave rise to the North Greenland fold belt. The fold belt trends approximately east–west, as do the metamorphic zones, roughly parallel to the margin of the deep-water trough (Dawes & Soper, 1973; Dawes, 1976; Higgins *et al.*, 1985); this implies collision with a northern continental mass of either cratonic or arc affinity, probably the Siberian block.

Plate tectonic reconstructions are important in petroleum exploration because by extrapolation they shed light on the development of the least known parts of the tectonic and sedimentary history. Often this approach is applied to predict potential source and reservoir facies and prospect types. Various basin classifications have been proposed over the past 20 years (e.g. Klemme, 1971; Bally & Snelson, 1980; Stoneley, 1981; Bois *et al.*, 1982; St. John *et al.*, 1984; Kingston *et al.*, 1985). These

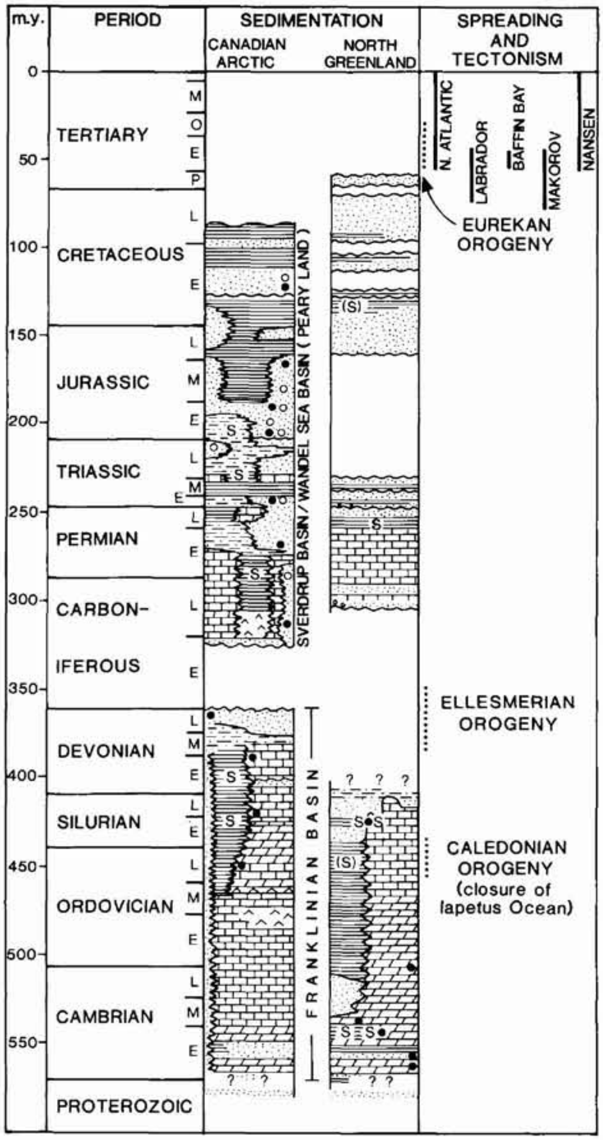

Fig. 6. Simplified diagram showing the relations between stratigraphy, sedimentation, source rock deposition(s), hydrocarbon occurrences (filled circles: oil and bitumen, open circles: gas), ocean spreading and tectonism in North Greenland and Canadian Arctic. Based on numerous sources mentioned in text, in particular Dawes & Kerr (1982 and papers herein), Kerr (1980), Rayer (1981).

classification systems are generally difficult to apply to North Greenland, particularly due to lack of data in respect to the northern border of the basin and the limited knowledge of the Late Palaeozoic and Mesozoic histories. It should, however, be noted that the Franklinian basin differs from many oil-producing Lower Palaeozoic basins; the latter are mainly of an intra-cratonic type with very long and slow subsidence histories (e.g. the Michigan basin and several basins in Australia, South America and northern Africa). An oil-producing basin with a strong resemblance to North Greenland in age and tectonic setting occurs in Alberta, Canada. Many other Lower Palaeozoic basins with similarities to North Greenland only have a very low petroleum potential, mainly because of very deep subsidence and later orogenesis caused by continental collision (e.g. the Lower Palaeozoic successions in the Caledonides in Europe and North America).

Basin evolution and source rock deposition

The tectonic/sedimentological evolution of the Lower Palaeozoic deep-water basin in North Greenland was described in terms of 9 development stages by Surlyk & Hurst (1983, 1984), an approach recently expanded to incorporate the shelf areas by Higgins *et al.* (in press).

Throughout the depositional period, the region was characterized by major generally east–west trending facies belts (fig. 5). In the southern shelf areas mainly carbonate shallow-water deposition took place, bordered to the north by outer shelf and slope mudstones (fig. 6). In the north mainly siliciclastic deep-water sedimentation prevailed in the trough. With time, the facies boundaries moved southwards during a stepwise basin expansion. The major facies boundaries were probably controlled by deep crustal faults, some of which have no surface expressions today, while others were reactivated during Ellesmerian deformation (see e.g. Soper & Higgins, 1987). Of particular importance to the present study is the Navarana Fjord escarpment (Hurst & Surlyk, 1983; Surlyk & Hurst, 1984; Escher & Larsen, 1987; Surlyk & Ineson, 1987a,b) which separated carbonate and turbidite deposition in Late Ordovician to Early Silurian time. The Permin Land flexure (Surlyk & Hurst, 1983, 1984), largely corresponding to the Early Silurian hinge line of Sønderholm *et al.* (1987), also has important implications for the petroleum geology. This lineament or flexure seems to have developed as a response to loading from the thick and rapidly deposited Lower Silurian turbidites. It is considered as a flexure line with increasing subsidence to the north and is not necessarily controlled in position by deeper crustal structures. The flexure controls the position of the Early to Late Silurian reef-belt, which developed as a series of large slope mounds along the northern margin of the platform (Sønderholm & Harland, 1989a).

Towards the south, shelf sedimentation was dominated by carbonates, with the exception of a single period of siliciclastic sedimentation in earliest Cambrian time. In the Early Cambrian, carbonate deposition extended to a position just north of the present northern coast of Nyeboe Land; in Late Ordovician to Early Silurian, the Navarana Fjord escarpment defined the boundary between the carbonate platform and the deep-water trough. Later during the Early Silurian (late Llandovery) the platform margin moved to a more southerly position controlled by the Permin Land flexure. The southern limit of carbonate deposition is not known due to cover by the Inland Ice but the platform was probably at least 200 km wide and may have been considerably wider as in the Canadian Arctic Interior Platform (fig. 3). The thickness of the shelf deposits suggests a slightly decreasing subsidence rate from the Early Cambrian to the earliest Silurian with a relatively uniform history along depositional strike and a much higher subsidence rate in the Early to Late Silurian (M. Sønderholm, personal communication, 1988). However, the eastern part of the shelf sequence in Peary Land was uplifted and partially eroded in the earliest Ordovician, corresponding to the strata underlying the unconformity at the base of the Wandel Valley Formation, probably in response to Caledonian tectonism to the east (Hurst & Surlyk, 1983; Surlyk & Hurst, 1984).

Trough sedimentation was dominated by turbiditic sandstones with minor siltstones and conglomerates. The Ordovician succession is relatively thin compared to the Cambrian and Silurian part reflecting considerable variation in subsidence rate. The trough may be traced for more than 800 km along strike in North Greenland and continues into Ellesmere Island. The width is not known but was probably between 100 and 200 km throughout much of the depositional period with the exception of the Early Silurian to Late Silurian (earliest Devonian?) when the deep-water basin expanded strongly towards the south.

The outer shelf and slope deposits, which are particularly interesting in the present study due to their source potential, comprise a mixture of mainly black shales, lime mudstones and conglomerates. The configuration of the outer shelf and slope varied considerably with time and therefore has strong implications for the source potential. In earliest Cambrian time this zone was very wide but apparently without source rock deposition due to well oxygenated conditions. In the Early to Middle Cambrian, outer shelf deposition took place in a wide belt under mainly anoxic conditions, and good source rocks formed. This pattern changed from the Middle Cambrian throughout most of the Ordovician when outer shelf-slope sedimentation occurred in a narrower zone. During Late Ordovician to Early Silurian time the Navarana Fjord escarpment defined a narrow by-pass margin between shallow-water carbonate deposition and deep-water siliciclastic sedimentation, and the formation of organic-rich units was very restricted. A wide outer shelf prevailed in mid-Silurian time when black shales overlapped the shallow-water carbonates. This was a period of major source rock deposition.

Stratigraphy, reservoir and source rock studies

The lithostratigraphic nomenclature applied in the present study to the Lower Palaeozoic shelf sequence and slope and trough sequence is shown in figs 7 and 8. Information on the different units is summarized below, either at formation or group level and includes data on: main lithology, distribution and thickness, reference to general descriptions and to information of reservoir and source rock quality.

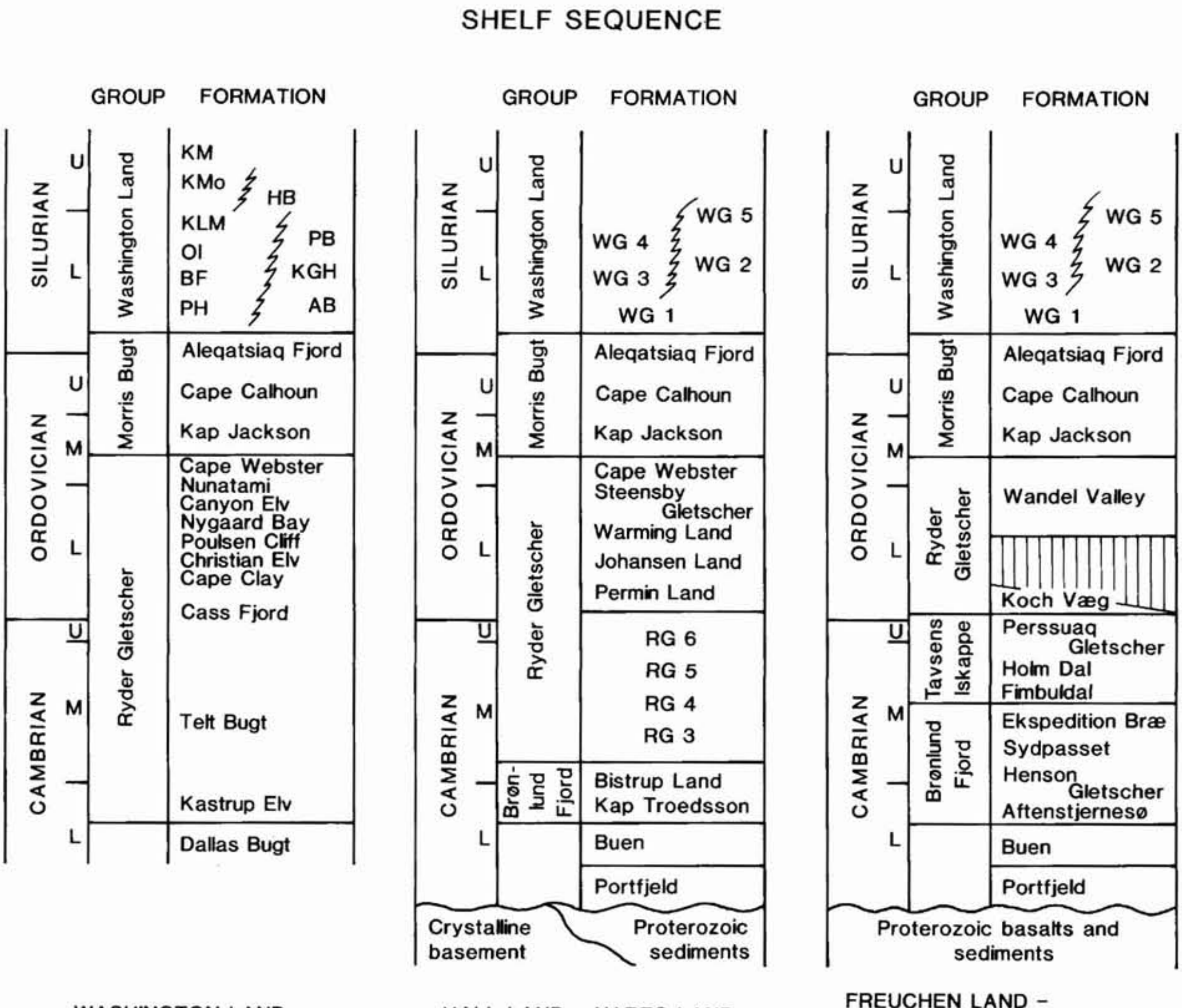

Fig. 7. Stratigraphic nomenclature of the shelf sequence in central and western North Greenland. Modified after Henriksen (1987) and Higgins *et al.* (in press). AB: Adams Bjerg, BF; Bessels Fjord, HB: Hauge Bjerg, KGH: Kap Godfred Hansen, KLM: Kap Lucie Marie, KM: Kap Maynard, KMo: Kap Morton, OI: Offley Island, PB: Pentamerus Bjerge, PH: Petermann Halvø, RG: Ryder Gletscher Group; WG: Washington Land Group.

Crystalline basement

Lithology: gneisses with minor amphibolite and supracrustals.
Distribution: only exposed at the head of Victoria Fjord and in Inglefield Land.
References: Henriksen & Jepsen (1985), Hansen *et al.* (1987).
Reservoir rocks: not likely.

Proterozoic sediments

Lithology: sandstones and volcanics.
Distribution: Inglefield Land and Peary Land, probably thin in central North Greenland.
Thickness: 25 m in Wulff Land to more than 2 km in Peary Land.
References: Jepsen (1971), Christie & Ineson (1979), Clemmensen (1979), Collinson (1979, 1980), Dawes *et al.* (1982), Peel *et al.* (1982).
Reservoir rocks: possible?, most sandstones are altered by dykes and volcanics.
Source rocks: not likely.

Lower Palaeozoic shelf sequence

Lower Cambrian shelf siliciclastics and carbonates

Lithostratigraphy: Skagen Group.
Lithology: siltstones and sandstones in lower part, dolomites in upper part.
Distribution: known in northern Wulff Land and easternmost Peary Land.
Thickness: 500–600 m in northern Wulff Land.
References: Christie & Ineson (1979), Friderichsen *et al.* (1982), Higgins & Soper (1985), Surlyk & Ineson (1987a).
Reservoir rocks: oolitic and pisolitic grainstones possible.
Source rocks: none, shales contain less than 1% TOC (Christiansen *et al.*, 1985).

Lower Cambrian shelf carbonates

Lithostratigraphy: Portfjeld Formation.
Lithology: dolomites.
Distribution: throughout North Greenland.
Thickness: 200–800 m, generally increasing northwards towards the shelf edge.
References: Jepsen (1971), Christie & Ineson (1979), O'Connor (1979), Surlyk & Ineson (1987a), Higgins *et al.* (in press).
Reservoir rocks: ?, asphalt seepage in Wulff Land, bitumen in upper part of the formation in Freuchen Land and Peary Land.
Source rocks: none, very low TOC contents with the exception of a 10–15 m thick interval of dark cherty dolomite near the base of the formation in Peary Land (O'Connor, 1979; Rolle & Wrang, 1981).

Lower Cambrian shelf siliciclastics

Lithostratigraphy: Buen and Dallas Bugt Formations.
Lithology: mainly sandstones in the lower part, mainly shales in the upper part.
Distribution: throughout North Greenland.
Thickness: 250–500 m, generally decreasing towards the north.
References: Jepsen (1971), Christie & Ineson (1979), Hurst & Peel (1979), Peel & Christie (1982), Davis & Higgins (1987), Higgins *et al.* (in press).
Reservoir rocks: poor to good, porosities in strongly cemented sandstones are up to 10% (see Chapter 7), hydrocarbon staining common in the southern part of Wulff Land.
Source rocks: none, very low content of TOC in shales, all 21 recorded values are below 0.2% (Rolle & Wrang, 1981; Christiansen *et al.*, 1985).

Lower Cambrian – Middle Ordovician shelf carbonates

Lithostratigraphy: Brønlund Fjord, Tavsens Iskappe and Ryder Gletscher Groups.
Lithology: dolomites, limestones with some shales and sandstones (Brønlund Fjord and Tavsens Iskappe Groups), dolomites with minor sandstones (Ryder Gletscher Group).
Distribution: throughout North Greenland.
Thickness: 900–1500 m, decreasing towards the north and east.
References: Henriksen & Peel (1976), Christie & Peel (1977), Ineson & Peel (1980, 1987, in press), Ineson (1985), Peel & Wright (1985), Sønderholm & Due (1985), Christiansen *et al.* (1987), Higgins *et al.* (in press).
Reservoir rocks: several possibilities, sandstones in Henson Gletscher and Sæterdal Formations of the Brønlund Fjord Group, vuggy carbonates in the Aftenstjernesø and Henson Gletscher Formations of the Brønlund Fjord Group. Macroscopic bitumen and hydrocarbon staining are common in these units (see Chapter 7).

Source rocks: The Henson Gletscher Formation contains good to excellent source rocks and has consequently been one of the main targets of the present study (Christiansen & Rolle, 1985; Christiansen *et al.*, 1985, 1986, 1987; see further details in later chapters).

Middle Ordovician to Lower Silurian shelf carbonates

Lithostratigraphy: Morris Bugt Group.
Lithology: limestones.
Distribution: throughout North Greenland.
Thickness: 620–760 m.

SLOPE AND TROUGH SEQUENCE

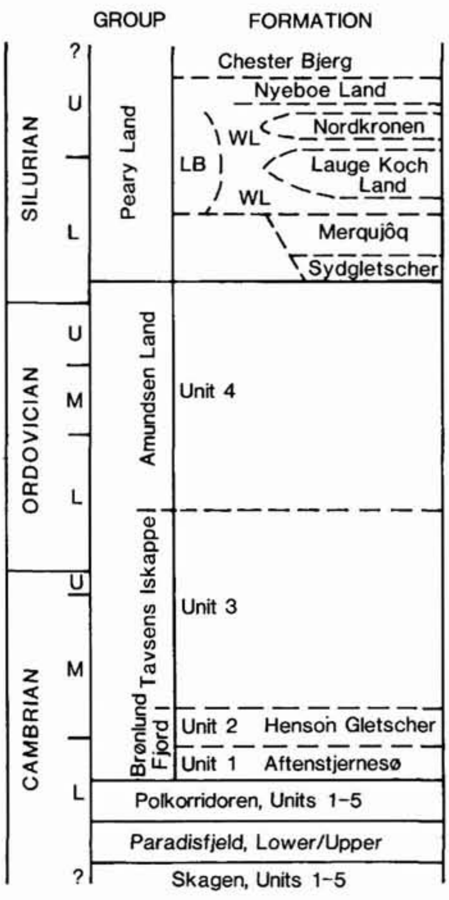

Fig. 8. Stratigraphic nomenclature of the slope and trough sequence in central and western North Greenland. Modified after Henriksen (1987) and Higgins *et al.* (in press). LB: Lafayette Bugt, WL: Wulff Land.

References: Peel & Hurst (1980), Sønderholm *et al.* (1987), Higgins *et al.* (in press), Smith *et al.* (1989), Sønderholm & Harland (1989a,b).
Reservoir rocks: ?, some bitumen in Aleqatsiaq Fjord Formation.
Source rocks: none, a few intervals in Aleqatsiaq Fjord Formation contain more than 1% TOC (Christiansen *et al.*, 1985).

Silurian shelf carbonates

Lithostratigraphy: Washington Land Group.
Lithology: limestones and dolomites, both as platform and reef facies.
Distribution: throughout North Greenland.
Thickness: 200–1500 m.
References: Hurst (1980a,b, 1981, 1984), Sønderholm *et al.* (1987), Sønderholm & Harland (1989a,b).
Reservoir rocks: likely, especially some of the reef complexes which are juxtaposed with shales of source rock and seal quality. Bitumen is common in debris from the reefs.
Source rocks: none, some of the back and inter-reef lime mudstones contain 1–2% TOC but display a poor hydrocarbon potential (Christiansen & Nøhr-Hansen, 1989).

Lower Palaeozoic slope and trough sequence

Lower Cambrian deep-water carbonates

Lithostratigraphy: Paradisfjeld Group.
Lithology: carbonate mudstones and conglomerates.
Distribution: widely exposed in north Peary Land and Nansen Land.
Thickness: at least 1 km.
References: Dawes & Soper (1973), Friderichsen *et al.* (1982), Friderichsen & Bengaard (1985).
Reservoir rocks: none, possible reservoirs only occur in postmature areas.
Source rocks: not likely.

Lower Cambrian deep-water siliciclastics

Lithostratigraphy: Polkorridoren Group.
Lithology: sandstones and shales.
Distribution: widely exposed in north Peary Land and Nansen Land.
Thickness: at least 2 km.
References: Dawes & Soper (1973), Friderichsen *et al.* (1982), Higgins *et al.* (1985).

Reservoir rocks: none, possible reservoirs only occur in postmature areas.

Source rocks: not likely.

Middle Cambrian to Lower Silurian slope and trough sediments

Lithostratigraphy: Vølvedal and Amundsen Land Groups (Brønlund Fjord and Tavsens Iskappe Groups).

Lithology: sandstones, shales, chert, carbonate mudstones and conglomerates.

Distribution: throughout North Greenland from Nyeboe Land to Amundsen Land.

Thickness: 60–450 m in the area studied (mainly slope facies), about 1 km in Amundsen Land (trough facies).

References: Friderichsen *et al.* (1982), Surlyk & Hurst (1984), Higgins & Soper (1985), Davis & Higgins (1987), Ineson & Peel (in press), Higgins *et al.* (in press).

Source rocks: The recognition of the correlation between the Henson Gletscher Formation and unit 2 of Higgins & Soper (1985) considerably increases the known source potential of the Cambrian succession. In addition the black shales of unit 4 of Soper & Higgins (Amundsen Land Group) are organic-rich. Analyses from Nyeboe Land and Freuchen Land show several TOC values in excess of 5%, despite the high thermal maturity (Christiansen *et al.*, 1985; U. H. Jacobsen, personal communication 1988).

Silurian sandstone turbidites and shales

Lithostratigraphy: Peary Land Group.

Lithology: sandstones, shales and conglomerates.

Distribution: throughout North Greenland.

Thickness: from less than 1 km in the southernmost exposures to more than 5 km in the northernmost areas.

References: Hurst (1980a), Hurst & Surlyk (1982), Surlyk & Hurst (1984), Larsen & Escher (1985, 1987), Surlyk & Ineson (1987a,b).

Reservoir rocks: ?, the sandstone turbidites of the Merqujôq, Lauge Koch Land and Nyeboe Land Formations are fine-grained and the porosity/permeability values are low.

Source rocks: The Silurian shales contain good to excellent source rocks and have been considered in detail in the present study (Christiansen *et al.*, 1985, 1986; Christiansen & Nøhr-Hansen, 1989; see further details in later chapters). The lower part of the Lafayette Bugt and Wulff Land Formations (Thors Fjord Member) are particularly rich in organic matter.

Chapter 3

Analytical programme and applied methods

F. G. Christiansen, J. Boserup, B. Buchardt, C. Guvad, K. Hansen, C. J. W. Koch, J. Jensenius, G. S. Nielsen, H. Nøhr-Hansen, S. Stouge, E. Thomsen and P. Østfeldt

The laboratory phase of the 'Nordolie' project included geochemical, microscopical and petrophysical methods (fig. 9). These methods vary considerably in approach and degree of sophistication. Laboratory work has been carried out in Copenhagen at the laboratories of the Geological Survey of Greenland (GGU), the Geological Survey of Denmark (DGU), and the Geological Institute, University of Copenhagen.

Sampling

Considerable time was devoted to stratigraphic, sedimentological and structural studies of potential reservoir and source rock sequences with the highest priority during field work given to sampling of fine-grained units for analytical work. During the summers of 1984 and 1985 two teams carried out field work and sampling from 33 camp sites in central and western North Green-

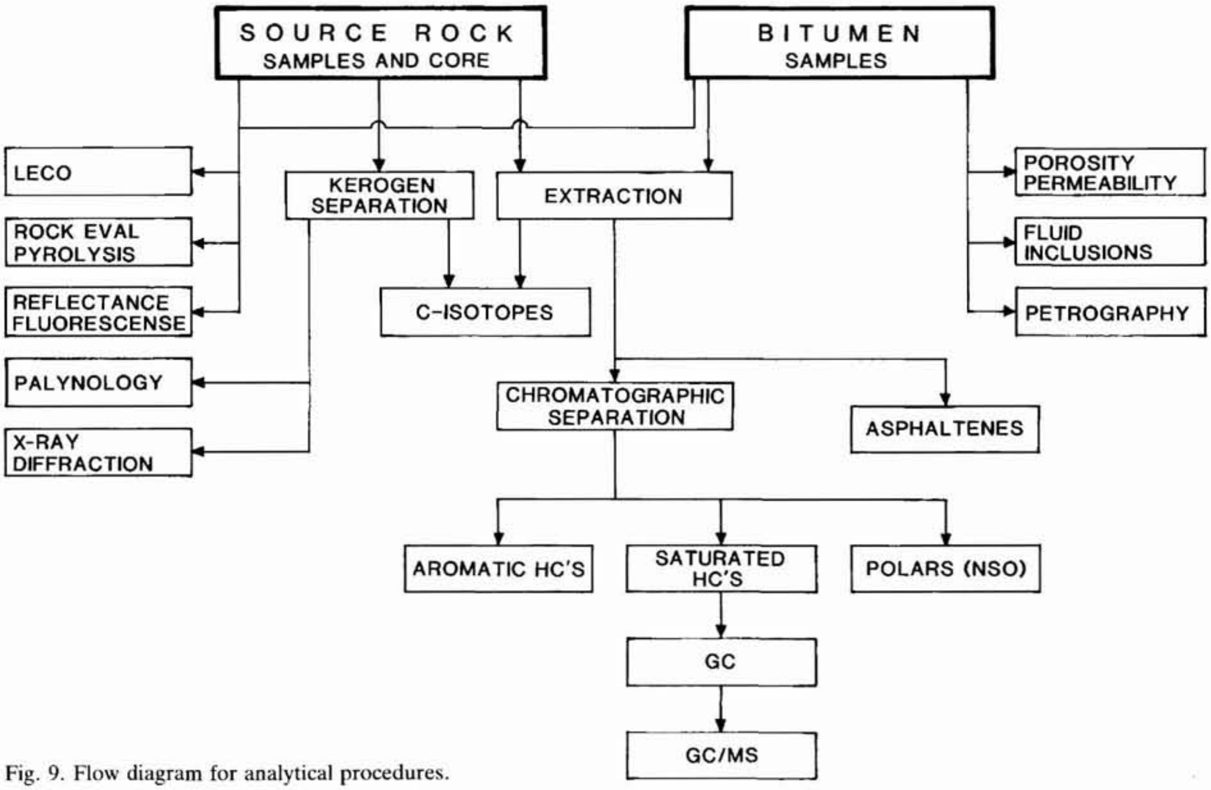

Fig. 9. Flow diagram for analytical procedures.

land (Christiansen & Rolle, 1985; Christiansen *et al.*, 1986); approximately 70 localities were visited by helicopter. In addition to the 989 samples collected by geologists directly involved in the source rock study, a limited number of samples (approximately 75) collected by other geologists were also studied. The study of the Peary Land region, which is only briefly treated in the present work, is mainly based on 275 samples collected by Flemming Rolle in 1980 (Rolle, 1981) plus approximately 50 samples collected by a number of other geologists in 1978 to 1980.

The samples collected were selected to be representative of the studied interval. Whenever possible, samples were collected from unweathered intervals below the surface, as weathering is known to influence the organic geochemistry of surface samples (Leythaeuser, 1973; Clayton & Swetland, 1978; Forsberg & Bjorøy, 1983). All samples were wrapped in aluminium foil to avoid contamination during transport and storage. So far no contaminants have been detected in any of the analysed surface samples.

Drilling programme

A drilling programme was carried out in order to obtain unweathered and statistically representative samples of the most interesting source rock units (see Christiansen *et al.*, 1986 for details). The drilling unit, which was constructed and later modified a number of times by J. Boserup and A. Clausen at GGU, has been successfully employed in Jameson Land, East Greenland (Surlyk, 1983; Surlyk *et al.*, 1984), in North Greenland (Christiansen *et al.*, 1986), and on Traill Ø, East Greenland (Marcussen *et al.*, 1987).

Thirteen holes were drilled to a maximum depth of 40 m. Approximately 345 cumulative metres were drilled and except for the uppermost metres at each site the recovery was close to 100%. All cores were described at the drill site using a scale of 1:50 or 1:100 and most holes were logged by gamma ray measurements (logs of the Silurian cores are shown by Christiansen & Nøhr-Hansen, 1989).

After logging, the core pieces were wrapped in aluminium foil and packed in standard core boxes made of hard plastic. Unfortunately, the plastic seems to have caused minor contamination with C_{12}, C_{14}, C_{16}, C_{18}, C_{20} *n*-alkanes in some of the analysed core samples (see fig. 11).

Handling and storage

All samples and core boxes were transported to Copenhagen by air during or shortly after the two field seasons. The sampled material is stored at GGU, mostly in closed standard sample cases. During preparation (e.g. cutting, crushing) contact with equipment or containers made of organic compounds (e.g. rubber, plastic) was avoided.

LECO and Rock Eval pyrolysis

The LECO and Rock Eval analyses were carried out at the source rock laboratories at DGU and GGU. More than 600 samples were analysed, mainly during the months immediately following the two field seasons with later supplementary analyses of a smaller number of specific samples. Both types of analyses are based on crushed whole rock material using 200 mg and 100 mg of sample, respectively.

The total carbon content (TC), the total organic carbon content (TOC), and hence the total inorganic carbon content (TIC = TC − TOC) were determined by combustion in a LECO IR 212 furnace before and after treatment with hot concentrated HCl, respectively.

The Rock Eval pyrolysis method (Espitalié *et al.*, 1977) is universally applied by oil and service companies in the characterization of source rock potential, types of organic matter, and thermal maturity (Horsfield *et al.*, 1983; Horsfield, 1984; Tissot & Welte, 1984). However, the method should be used with caution because of variation due to differences in material type and mineral matrix (Espitalié *et al.*, 1980, 1984; Evans & Felbeck, 1983; Katz, 1983) and presence of migrated bitumen (Clementz, 1979). In order to reduce errors and misinterpretations the material from North Greenland was analysed employing the same laboratory procedure and the same instrumentation throughout.

During the Rock Eval pyrolysis the powdered samples are heated at steadily increasing temperatures from 300°C to 550°C. The release curve of the pyrolysate typically shows two peaks (fig. 10). The low temperature peak, S1 (mg HC/g rock) at 300°C is due to hydrocarbons already present in the sample. The second, S2 (mg HC/g rock) between 410°C and 520°C, correlates with hydrocarbons generated by thermal alteration of the kerogen. The CO_2 generated during pyrolysis in the temperature interval 300°C to 390°C is trapped and analysed by thermal conductivity detection as a third peak S3 (mg CO_2/g rock). With increasing thermal maturity the area of the S2 peak decreases and the peak is displaced towards higher temperatures. The temperature of maximum generation (T_{max}) during pyrolysis is used as a maturity parameter (fig. 10).

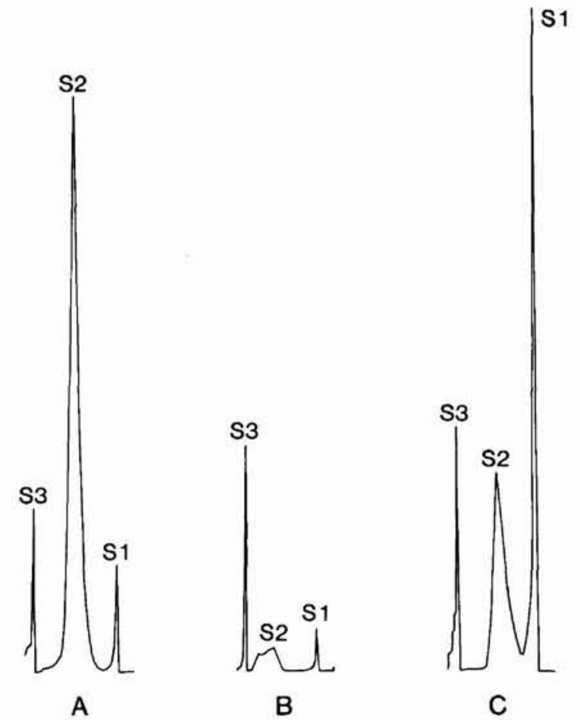

TOC: 2.82%	TOC: 2.26%	TOC: 0.97%
S1: 0.64	S1: 0.16	S1: 3.09
S2: 14.20	S2: 0.81	S2: 4.43
S3: 0.62	S3: 0.30	S3: 0.33
Tmax: 432° C	Tmax: 465° C	Tmax: 423° C

Fig. 10. Selected pyrogrammes showing typical relations of S1, S2, S3, T_{max} and TOC for (A) immature to mature source rock (sample 316775, Lafayette Bugt Formation, Washington Land), (B) mature to postmature source rock (sample 324490, Thors Fjord Member, Warming Land), (C) bitumen-impregnated sandstone (sample 322205, Buen Formation, Wulff Land).

Palynological studies

Palynological preparation and studies were carried out at GGU. Kerogen from more than 455 samples was examined optically in order to obtain information on the Thermal Alteration Index (TAI), kerogen composition, relative kerogen content and content of palynomorphs.

The kerogen was separated from 20 g of each sample by standard palynological preparation, in which minerals are dissolved by HCl and HF. The first slide was made after this acid treatment. The second slide was made of organic residue which had been sieved on a 10 micron nylon mesh. Occasionally a third slide was made after brief oxidation (3 to 5 minutes) with fuming HNO_3 followed by washing with a weak KOH solution.

The organic residue was mounted in a permanent medium Eukitt® (produced by O. Kindler, West Germany). The first and second slides were used in the evaluation of maturity and kerogen content, the third for biostratigraphic purposes. The slides were studied with translucent microscopy applying an Olympus BH-2 microscope. The S.E.M. observations were carried out on Au-coated sieved and oxidized kerogen using a Cambridge or a Phillips Scanning Electron Microscope at the Geological Institute, University of Copenhagen.

Gas chromatography and gas chromatography/mass spectrometry

Gas chromatography (GC) and gas chromatography/mass spectrometry (GC/MS) analyses were carried out at the source rock laboratories at DGU and GGU. Following preliminary interpretation based on screening methods (LECO/Rock Eval and palynological studies), 54 samples of source rocks and bitumen were selected for GC analysis. Sixteen of these samples were analysed using the GC/MS technique after evaluation of the gas chromatograms (checking for 'biomarkers' in the C_{27} to C_{32} range) (Østfeldt, 1987b). About 115 samples from Peary Land had been analysed prior to the initiation of the Nordolie project (Rolle & Wrang, 1981). Many of these samples are, however, postmature and lean in organic material and provide only little information on the petroleum geology of the region.

Crushed samples (50–100 g except for the pure bitumens) were extracted with methylene chloride for 24 h in a Soxhlett extraction apparatus. The extract was filtered, the solvent removed by evaporation, and the amount of extract determined.

The extract (50–100 mg) was separated on an open silica column by stepwise elution with *n*-hexane, methylene chloride and methanol, yielding saturated, aromatic and polar (= hetero compounds) fractions, respectively. Asphaltenes are retained on the column. After evaporation of the solvent, the weight of the individual fractions was determined, and the relative distribution of saturate (sa), aromatic (ar) and polar (po) compounds was calculated.

GC analyses of the total saturate fraction were carried out on a Hewlett Packard 5840 gas chromatograph, fitted with a 25 m × 0.3 mm (int. diam.) fused silica capillary column coated with a cross-linked methyl silicone stationary phase. The column was operated from 80° to 300°C at 6°C/min. and the effluent detected with a FID detector. From the gas chromatogram, the pristane to phytane (Pr/Ph) and pristane to C_{17} *n*-alkane (Pr/nC_{17}) ratios were calculated (see fig. 11).

GC/MS analyses were carried out using a Finngan 1020 GC/MS system connected with an on-column injector onto a 25 m × 0.22 mm (int. diam.) fused silica capillary column coated with cross-linked methyl silicone phase. The column was operated from 70° to 310°C at 5°C/min. The column led directly into the ion source of the mass spectrometer operating at an ionizing voltage of 70 eV.

The mass spectrometer was operated in the Multiple Ion Detection (MID) mode, scanning 10 ions (m/e 82, 123, 177, 183, 191, 205, 217, 218, 231, and 259) every second. From the integrated ion-chromatograms of m/e 191 (triterpanes), 217 and 218 (steranes and diasteranes), several source, lithology and maturity-dependent parameters were calculated (see Østfeldt, 1987a,b for details). The other seven ion-chromatograms (not integrated) were used to support the tentative peak assignment.

Reflectance and fluorescence studies

Reflectance and fluorescence measurements of graptolites, kerogen and bitumen were carried out at the source rock laboratories of DGU and GGU. The graptolite-rich samples were collected for initiation of a research programme on graptolite reflectance (Stouge *et al.*, 1988) and about 45 samples were prepared shortly after the two field seasons. About 75 samples were selected for reflectance and fluorescence measurements of kerogen and bitumen after initial evaluation of screening data (Thomsen & Guvad, 1987). Only samples with relatively high TOC values or visible fluorescence in the palynological slides were considered further.

The investigations were carried out on whole rock samples, either crushed to a grain size of 2 to 3 mm or prepared as rock fragments orientated perpendicular to the lamination. The samples were embedded in a cold setting epoxy resin and then ground and polished using

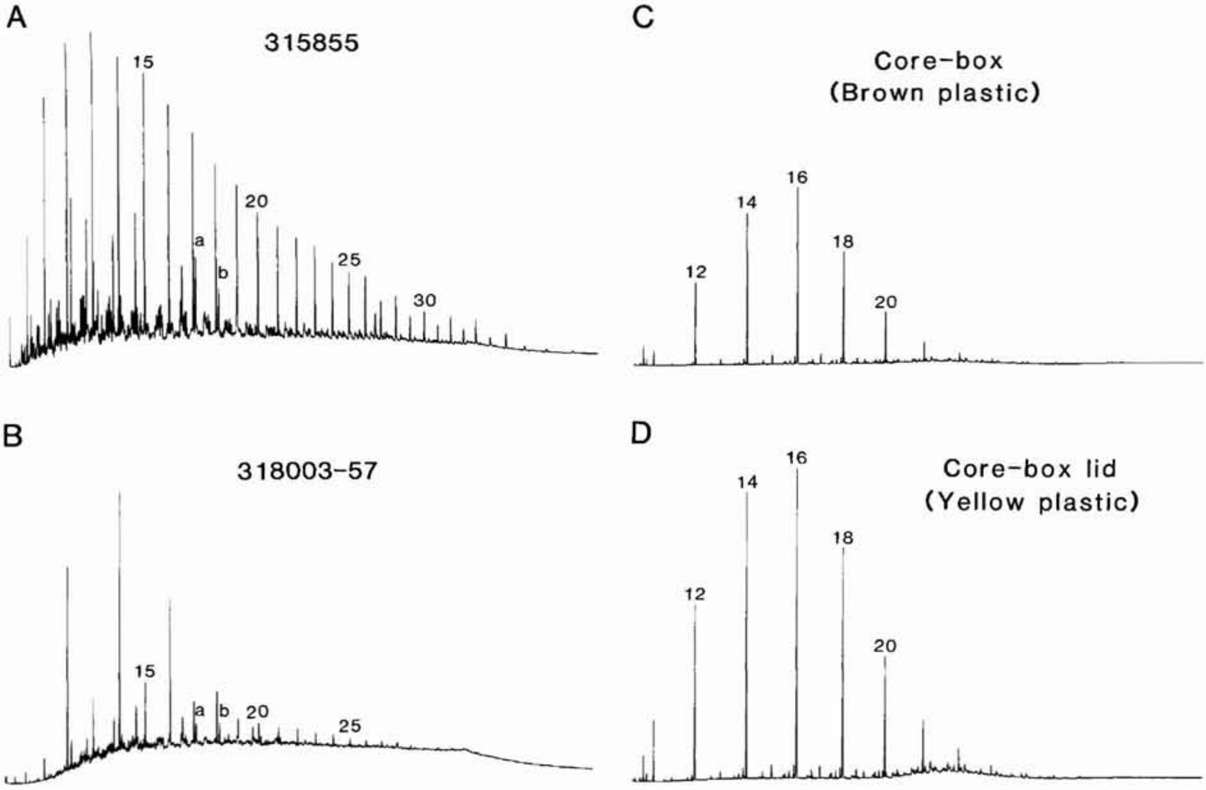

Fig. 11. Selected gas chromatograms of the saturated fraction. a: pristane, b: phytane, numbers are *n*-alkane carbon numbers. (A) Mature source rock. Sample 315855, Henson Gletscher Formation, Freuchen Land. (B) Polluted bitumen rock, note anomalously high values of C_{12}, C_{14} and C_{16} *n*-alkanes. Sample 318003–57, Henson Gletscher Formation, Freuchen Land. (C) Extract of core-box (brown plastic). Note the high contents of C_{12}, C_{14}, C_{16}, C_{18} and C_{20} *n*-alkanes. (D) Extract of core-box lid (yellow plastic). Note the composition similar to the core-box.

1/4 micron diamond powder for the final polish. Two microscope systems have been employed for measurement, in both cases using oil immersion: A reflected-light Zeiss photomicroscope equipped with an MP03 photometer and digital readout, using a 40× Epi-pol oil immersion objective, working with a plane glass reflector. Data are collected and processed by an MPS 3000 microcomputer. A Leitz MPV-SP reflected-light microscope equipped with a pol-opak illuminator, plane glass reflector and a 32× oil immersion objective. Data are collected and processed by an MPS 3000 microcomputer.

Illumination for both systems was through a green filter with peak transmission at 546 nm. The photomultipliers were calibrated against standards with reflectance values of 0.516 and 1.26% R_o^v. Quantitative measurements of fluorescence were carried out using the Zeiss microscope system, fitted with a continuous filter monochromator and a 100W high-pressure mercury lamp connected to a stabilized power supply. For UV excitation the Zeiss F1 fluorescence reflected-light illuminator is used with a 25× neofluar objective.

Carbon isotope studies

Carbon isotope measurements of kerogen, bitumen and source rock extracts were carried out at the Stable Isotope Laboratory at the Geological Institute, University of Copenhagen. This method was brought into use in the later part of the project, mainly in order to correlate observed migrated bitumens with the two main source rock units but also to provide additional information on the depositional environment.

Measurements were carried out on both kerogen and extracts of the source rock (n = 16) and extracts of the migrated bitumen (n = 25). The total extract (see previous section on GC) was employed, typically from the same samples as used in the GC, GC/MS programme. Kerogen was separated from rock samples by decalcification with HCl followed by methylene chloride extraction to remove bitumen and dried at 90°C.

Combustion to CO_2 (of both carbon in kerogen and in extracts) was carried out in an oxygen–helium atmosphere at 900°C with copper oxide as catalyst. The evolved gas was purified over copper and silver at 600°C and transferred to a Finngan MAT 250 triple collector mass spectrometer. The ratio between ^{13}C and ^{12}C is reported as per mille deviations from the PDB-standard using the δ-function (Epstein *et al.*, 1951). Reproducibility is better than 0.05‰ on the δ-scale.

X-ray diffraction of kerogen

X-ray diffraction of kerogen concentrates was carried out at the Laboratory of Clay Mineralogy, DGU (Koch, 1987). This method, rarely applied in source rock studies, was introduced in the final stage of the working programme with the special aim of characterizing and ranking thermally postmature samples.

Fifteen organic-rich samples were prepared, eight of these represent a profile through the Cambrian–Ordovician outer shelf and slope sequence with a known systematic increase in thermal maturity. The remaining Silurian samples have a known, but highly scattered, thermal maturity.

Depending on the content of organic carbon 10–25 g of powdered sample was treated with 15% HCl at a temperature of 80°C (see details in Koch, 1987). Following centrifugation, washing with destilled water and drying, the solid material was treated with concentrated HF at 80°C for two days and finally dried.

The kerogen concentrate was investigated by X-ray diffractometry using a Phillips 1050 vertical goniometer equipped with a graphite monochromator in the diffracted beam and using CoKα as radiation. In addition to the kerogen study a semiquantitative evaluation of the mineral content of the samples was made. The X-ray diffractogram in fig. 12 illustrates the procedure for determination of the two parameters d_{002} and WHH_{002} (position and width at half height of the 002 'graphite peak'). A number of other peaks show the presence of mineral phases (either relicts or minerals formed during preparation).

Fission track studies

Fission track studies of apatite and zircon from sandstones were carried out at the Geological Institute, University of Copenhagen. This method was included in the later part of the 'Nordolie' project in order to obtain chronological information on thermal episodes and history of uplift.

Fifteen samples representing two cross sections, one in the area where the Henson Gletscher Formation outcrops and one in the Silurian shales in Nyeboe Land, were prepared. Sample material of 0.5 to 1.5 kg was crushed and separated by magnetic and heavy liquid methods (see details in Hansen, 1988). The separates were mounted in epoxy or teflon, polished, and etched to reveal spontaneous tracks.

Age determinations were carried out using the external detector method (Gleadow & Lowering, 1978) with the Fish Canyon and Mt. Dromedary apatites and zircons as age standards following the zeta calibration

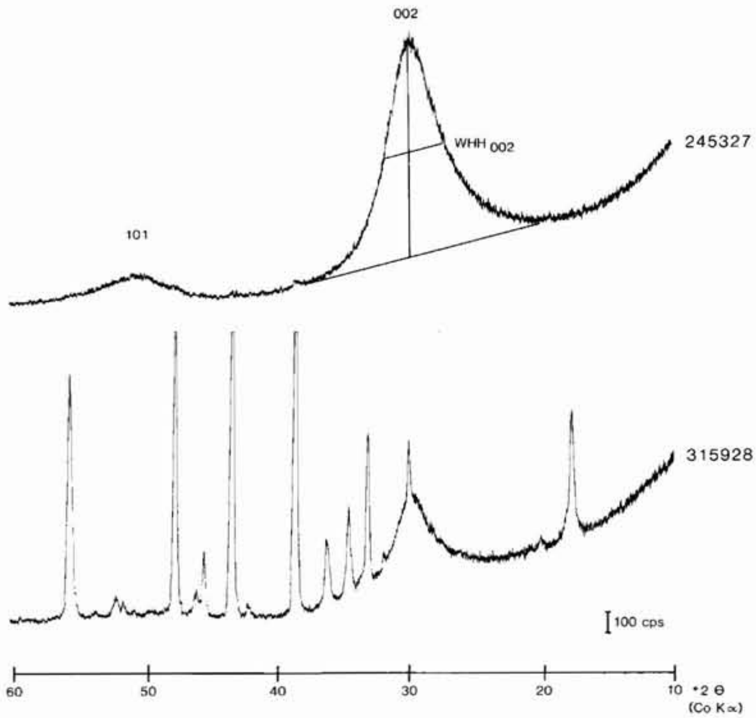

Fig. 12. X-ray diffractograms of samples 245327 and 315928 showing the procedure for determination of d_{002} and WHH_{002}. The sharp peaks indicate the presence of pyrite and fluorides formed during preparation.

procedure described by Hurford & Green (1983). NBS SRM 612 and Corning CN1 and CN2 glasses were employed for monitoring the neutron fluence. The polished and etched apatites and zircons were irradiated together with high quality low-uranium mica detectors at the J1 facility of the HERALD reactor in Aldermaston, U.K., or at the Risø National Laboratory, Denmark.

All measurements for calculating the fission track length distribution in apatite were carried out on horizontal, confined tracks as suggested by Gleadow *et al.* (1986).

Fluid inclusion studies

Studies of fluid inclusions and stable isotopes of diagenetic calcite and dolomite associated with bitumen were carried out at the Geological Institute, Copenhagen University. These methods were employed in the later part of the project in order to obtain information on the temperature and chemistry of pore waters at the time of diagenetic growth and migration of hydrocarbons (Jensenius, 1987).

Only samples from four localities, all with macroscopically identified bitumen, were investigated.

Fluid inclusion microthermometry was performed with the aid of a Chaimeca heating and freezing stage (Poty *et al.*, 1976) calibrated from 96°C to 400°C. The stable isotopes were analysed by the following procedure at the Stable Isotope Laboratory, Geological Institute, University of Copenhagen. Approximately 30 mg of carbonate were crushed to a grain size between 64 and 150 μm, treated with sodium hypochlorite to remove migrated hydrocarbons and kerogen, followed by reaction in vacuum with concentrated H_3PO_4. The evolved CO_2 was cleaned over dry ice isoproponal mixture and subsequently admitted to the Finngan Mat-250 isotope mass spectrometer.

Porosity/permeability

Measurements of the petrophysical parameters (porosity, permeability and grain density) were carried out commercially by the Core Analysis Laboratory of DGU. Approximately 60 orientated plugs (25 mm × 25 mm), mostly from Cambrian sandstones, were analysed. Following drying, the specific permeability is measured by flowing nitrogen through the plug. The porosity and grain density is determined applying a double chambered helium porosimeter and a picometer with calibrated mercury pump (Springer, 1987).

Thin sections of all analysed samples from the plugs or nearby slabs have been stained for carbonate identification by Dickson's method (Allman & Lawrence, 1972) and studied in detail.

Chapter 4

Palynological studies of the organic matter

H. Nøhr-Hansen

Palynological studies of the kerogen in potential source rocks and other sediments in petroliferous basins provide important data on quality, quantity and type of the organic matter. In addition the palynomorphs are useful for biostratigraphic correlation. The colour and preservation of palynomorphs and other kerogen particles are of value in thermal maturity evaluation (Staplin, 1969; Burgess, 1974; Dow, 1977). The kerogen composition, described as organic facies (Jones, 1987) or palynofacies (Combaz, 1964; Batten, 1981; Tyson, 1987), is yet another powerful tool in source rock characterization and evaluation.

Although palynological kerogen analysis is frequently used on Mesozoic and Cenozoic organic material and many of the resulting data are published, this is not the case in studies of Lower Palaeozoic sequences where palynomorphs are used mainly for biostratigraphic purposes and only rarely in organic facies and environmental studies (Aldridge *et al.*, 1979; Dorning, 1987) or in source rock studies (Legall *et al.*, 1981). The amorphous kerogen in Palaeozoic sediments has only been sporadically described from a palynological point of view (Venkatachala, 1981; Batten, 1984).

The present chapter concentrates on providing a systematic presentation of the results of palynological studies of the organic matter from selected intervals of the Lower Palaeozoic sequence in North Greenland. In addition to the organic-rich potential source rock units, most other lithological units from the Lower Palaeozoic sequence in North Greenland have been investigated.

The organic content of 455 samples was isolated by standard palynological preparation (Chapter 3). These samples had previously formed the basis for preliminary thermal maturity studies (Christiansen *et al.*, 1985, 1987), and were employed in a combined kerogen classification and thermal maturity study of the Silurian material (Christiansen & Nøhr-Hansen, 1989). The MGUH numbers used in the figure captions indicate that specimens are stored in the Geological Museum of the University of Copenhagen.

Classification of organic matter

The organic matter of the samples studied is dominated by amorphous kerogen without any structures reminiscent of its precursor. The very sparse information obtained from the amorphous kerogen, combined with a low palynomorph content and the absence of terrestrial material, makes it impossible to carry out a traditional kerogen facies analysis. Instead a tentative classification based on content and relative composition of the total kerogen was introduced (Christiansen & Nøhr-Hansen, 1989). Three types of kerogen are discerned: (1) large coherent particles of amorphous kerogen, (2) finely disseminated amorphous kerogen, and (3) palynomorphs. The total content of kerogen was evaluated, employing for each sample both the slide of unsieved organic material and the slide of sieved organic material (Chapter 3), and classified as poor, moderate or rich.

Samples dominated by finely disseminated amorphous kerogen are generally those poor in kerogen (Plate 1 A and B) and they display low TOC values ($<$ 1%). The kerogen from these samples often occurs in a silica gel in the unsieved organic material (Plate 1 A). Samples with a moderate kerogen content contain small to moderate amounts of large kerogen particles (Plate 1 C and D) and display TOC values in the range 1 to 3%. Samples rich in kerogen are generally dominated by large particles of amorphous kerogen (Plate 1 E and F) and display high TOC values ($>$ 3%).

Palynomorphs constitute only a minor amount of the total organic material from North Greenland (commonly 1–2% and never more than 20%). Chitinozoans, graptolite fragments, scolecodonts, acritarchs and spores were observed.

Solid bitumen is widespread in a number of samples. This may present some problems in the TAI (Thermal Alteration Index) evaluation since the migrated bitumen has often been through a different thermal history than the autochthonous kerogen. Another problem

Unit	Thickness	Lithology	n	Acritarchs	Chitinozoans	Scolecodonts	Trilete spores	Graptolite fragments	Kerogen
Ryder Gletscher Fm 3–6	< 650		7						P–M
Buen Fm & Polkorridoren Gp	250–500		3						P–M,B
Portfjeld Fm	150–300								
Pre-Portfjeld	< 30		3						P–M

Unit	Thickness	Lithology	n	Acritarchs	Chitinozoans	Scolecodonts	Trilete spores	Graptolite fragments	Kerogen
Tavsens Iskappe Gp	400–700		4			2			P B
Ekspedition Bræ Fm	30–80		3	(2)					P B
Sydpasset Fm	10–70		2	(1)					M
Henson Gletscher Fm	40–130		57						M–R,B
Aftenstjernesø Fm	50–70		5						P–M
Buen Fm & Polkorridoren Gp	250–500		1						P B
Portfjeld Fm	250–300								
Pre-Portfjeld	< 30		1						P

Fig. 13. Stratigraphic distribution based on 86 analysed Cambrian samples in the western (above) and eastern (below) part of North Greenland, thickness (m), lithology, number of analysed samples, number of samples with recorded palynomorphs (acritarchs, chitinozoans, scolecodonts, trilete spores, graptolite fragments), relative kerogen composition (finely disseminated amorphous kerogen: dotted, large amorphous particles of kerogen: black, palynomorphs: blank), relative kerogen content: empty (E), poor (P), moderate (M), and rich (R), and bitumen content (B).

with solid bitumen is the resemblance of palynomorph membranes to bitumen flakes which have been squeezed between minerals. Examples of bitumen in palynologically prepared samples are illustrated in Plate 10.

Cambrian shelf sequence

Organic matter from 86 Cambrian samples was analysed (fig. 13), the majority collected from the Henson Gletscher Formation (Ineson & Peel, in press; Christiansen *et al.*, 1987).

The organic matter from lime mudstones and interbedded shales is dominated by large particles of granular to spongy amorphous kerogen, whereas finely disseminated amorphous kerogen only occurs in moderate amounts. The relative kerogen content is moderate to high. Palynomorphs were not recorded from the Henson Gletscher Formation. Most of the other Cambrian units are dominated by finely disseminated amorphous kerogen and have a poor to moderate kerogen content.

Most of the Cambrian succession is barren of palynomorphs (fig. 13). It is remarkable that algae (Plate 2 A-F), which resemble the acritarch genus *Leiosphaeridia*, are only recorded from dolomite of the Sydpasset Formation and from lime mudstone of the Ekspedition

Unit	Thickness	Lithology	n	Acritarchs	Chitinozoans	Scolecodonts	Trilete spores	Graptolite fragments	Kerogen
Washington Land Gp	> 800		14		1	2			E–P,B
Aleqatsiaq Fjord Fm	250–340		28	17	13	14	(6)	3	P–M
Cape Calhoun Fm	30–60		4	3	3	3		3	P
Troedsson Cliff Mb	170–230		14	12	11	11	5	7	P
Gonioceras Bay Mb			10	7	5	9		2	P B
Cape Webster Fm	175–200		6						E–P,B
Stensby Gletscher Fm, Canyon Elv Fm, Nunatami Fm	90–125		15	4	1	4	(1)		E–P,B
Warming Land Fm	50–150		1						

Unit	Thickness	Lithology	n	Acritarchs	Chitinozoans	Scolecodonts	Trilete spores	Graptolite fragments	Kerogen
Børglum River Fm	430		4			4			P,B
Wandel Valley Fm	~ 360		3						P

Fig. 14. Stratigraphic distribution of 92 analysed Ordovician samples from the western (above) and eastern (below) part of the region, thickness (m), lithology, number of analysed samples, number of samples with recorded palynomorphs (acritarchs, chitinozoans, scolecodonts, trilete spores, graptolite fragments), relative kerogen composition (finely disseminated amorphous kerogen: dotted, large amorphous particles of kerogen: black, palynomorphs: blank), relative kerogen content: empty (E), poor (P), moderate (M), and rich (R), and bitumen content (B).

Bræ Formation; the latter also contains lumps of algae or spore-like palynomorphs (Plate 2 G-I). Both formations have a poor to moderate kerogen content. A few scolecodonts were recorded from the Tavsens Iskappe Group, which spans the Cambrian–Ordovician boundary.

Ordovician shelf and trough sequence

Organic matter from 92 samples of Ordovician shelf and trough deposits was analysed (fig. 14).

The organic-rich northern trough facies are postmature with regard to oil generation, whereas the shelf carbonates have a low organic content dominated by early mature finely disseminated amorphous kerogen.

Acritarchs (Plate 3 A and B) were recorded in 43 samples from the Ordovician succession and although the flora is of low diversity, the acritarchs seem to be biostratigraphically useful (K. J. Dorning, personal communication, 1986). Chitinozoans occur in 34 samples with a generally low diversity, but a number of biostratigraphically significant species have been recorded (Grahn & Nøhr-Hansen, 1989). Graptolite fragments (Plate 3 C) occur in 15 samples, and scolecodonts (Plate 3 D) occur in 47 samples.

The Troedsson Cliff Member and Aleqatsiaq Fjord Formation yielded the largest numbers of palynomorphs. The Troedsson Cliff Member is particularly interesting due to its content of presumed trilete spores (Plate 3 G-L) described in detail by Nøhr-Hansen & Koppelhus (1988). Two samples from the Aleqatsiaq Fjord Formation contain algal structures (Plate 3 E and F).

Silurian outer shelf and trough sequence

The organic matter of 277 Silurian samples from outcrops and shallow cores was systematically analysed (fig. 15; Christiansen & Nøhr-Hansen, 1989). The majority of the samples (259) are black shales from the Thors Fjord Member (lower part of the Wulff Land Formation), the Wulff Land Formation and the age-equivalent Lafayette Bugt Formation. Locally these shales reach more than 400 m in thickness.

The Thors Fjord Member is dominated by large amorphous kerogen particles and is tentatively characterized as rich in kerogen. The Lafayette Bugt Formation has a moderate kerogen content with a weak dominance of large amorphous kerogen particles. In contrast, the upper part of the Wulff Land Formation is dominated by finely disseminated amorphous kerogen and has a relatively poor kerogen content.

The Silurian shales in general have a low content of palynomorphs compared to the Ordovician carbonates. Chitinozoans (Plate 4 A and B) and graptolite fragments (Plate 4 C and D) are common. Scolecodonts are less abundant and trilete spores occur in only a few samples. Acritarchs have only been reported from one Upper Silurian sample in western Hall Land (Armstrong & Dorning, 1984). Chitinozoans were recorded in 120 samples. The diversity is low, but the species are stratigraphically distinct (Grahn & Nøhr-Hansen, 1989). A chitinozoan biostratigraphy combined with biostratigraphic schemes on graptolites (Bjerreskov, 1986) and conodonts (Armstrong & Aldridge, 1982) are useful for correlation of the source rock intervals.

The graptolite fragments recorded have no biostra-

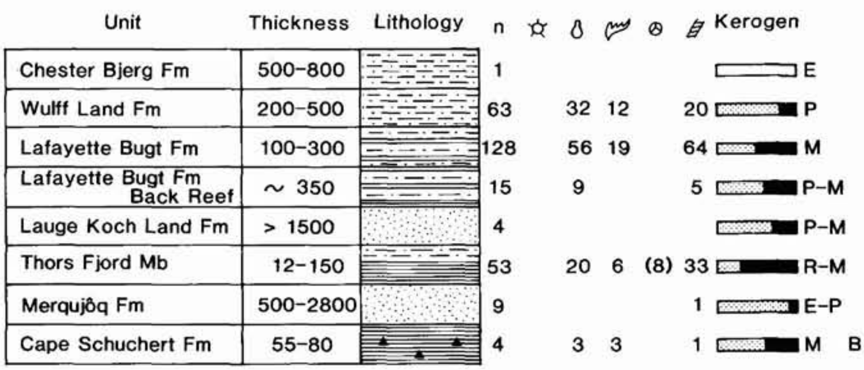

Fig. 15. Stratigraphic distribution of 277 analysed Silurian samples, thickness (m), lithology, number of analysed samples, number of samples with recorded palynomorphs (acritarchs, chitinozoans, scolecodonts, trilete spores, graptolite fragments), relative kerogen composition (finely disseminated amorphous kerogen: dotted, large amorphous particles of kerogen: black, palynomorphs: blank), relative kerogen content: empty (E), poor (P), moderate (M), and rich (R), and bitumen content (B).

tigraphic value, but measurements of graptolite reflectance contribute to the evaluation of the thermal maturity (Stouge *et al.*, 1988; Chapter 6).

The scolecodonts, which were observed in 40 samples, have so far not proved useful in either biostratigraphic or maturity studies.

Degraded and disintegrated palynomorphs, probably trilete spores having the appearance of degraded bitumen, were recorded from a few samples from the Lafayette Bugt, Wulff Land and Nyeboe Land Formations (Plate 4 E-H). The Lafayette Bugt Formation also contains spherical folded bodies (Plate 4 I) resembling the acritarch-like algae from the Cambrian Ekspedition Bræ Formation and rounded to drop-shaped palynomorphs (Plate 4 L).

Plant megafossils were reported from the Nyeboe Land Formation of Ludlow age (Larsen *et al.*, 1987). The same samples contain, in addition to the above mentioned degraded spore-like bodies (Plate 4 G and H), tubular structures (Plate 4 J and K) comparable to the material illustrated from Ordovician (Vavrdová, 1984), Llandovery (Duffield, 1985) and Wenlock (Strother & Traverse, 1979) successions elsewhere.

Amorphous kerogen

The state of preservation of the kerogen and the dominance of large amorphous kerogen particles indicate that the shale-dominated units with a moderate to rich kerogen content (figs 13 and 15) were deposited in oxygen-poor environments. In contrast, the carbonate-dominated units with a relatively poor to moderate kerogen content (fig. 14) represent more oxygenated depositional environments.

The differentiation, classification, and origin of amorphous kerogen are poorly known. Since most hydrocarbon targets are within Mesozoic deposits, very few palynological publications present descriptions of Lower Palaeozoic amorphous kerogen. Among the few Lower Palaeozoic examples are Venkatachala's (1981) illustrations of Precambrian to Ordovician filamentous algae. Venkatachala interpreted these algae as remains of blue-green algae (or cyanobacteria) which formed algal mats. Biodegradation of these filamentous algae leads to the formation of flaky or granular organic matter (Venkatachala, 1981, p. 184).

Batten (1984) illustrated Lower Palaeozoic lumps of amorphous kerogen with shapes interpreted as inherited from faecal pellets. He also mentioned that apparently amorphous masses occasionally prove to be composed largely of acritarchs.

Remains of blue-green algae were rarely identified in the palynological slides although commonly observed in thin-sections (Larsen, 1989). However, probably filamentous algae very similar to those reported by Venkatachala (1981) were recorded from a single Upper Ordovician – Lower Silurian sample (Plate 3 F).

Neither faecal pellets nor amorphous masses composed of acritarchs were recorded in the present organic material. Biodegradation and thermal alteration have destroyed any direct sign of the precursors of the amorphous kerogen from North Greenland.

Palynomorph distribution – depositional or preservational control

Palynomorphs were recorded in 76% of the analysed samples of Ordovician limestone, all of which were deposited in relatively shallow water, and in 67% of the Silurian shales which represent deeper water deposition. Thus the Ordovician versus Silurian palynomorph distribution illustrates a shallow to deep-water trend which, despite the age difference, clearly indicates the preferred habitat of the organisms.

Acritarchs, chitinozoans and scolecodonts were recorded from 38 to 54% of the analysed Ordovician samples, whereas graptolite fragments occur in only 17% of the samples (Table 1).

Table 1. The distribution of palynomorphs in the Ordovician limestone samples

	Number of analysed samples	Ac	Ch	Sc	Gr	Number of barren samples
Washington Land Gp	14	0	1	2	0	12
Aleqatsiaq Fjord Fm	28	17	13	14	3	3
Cape Calhoun Fm	4	3	3	3	3	0
Troedsson Cliff Mb	14	12	11	11	7	1
Gonioceras Bay Mb	10	7	5	9	2	0
Børglum River Fm	4	0	0	4	0	0
Steensby Glet. Fm	15	4	1	5	0	5
	89	43	34	48	15	21
% of analysed samples	100	48	38	54	17	24

Chitinozoans and graptolite fragments are represented in 43% and 44% of the Silurian samples, respectively. Scolecodonts occur in only 14%, and acritarch-like palynomorphs in less than 1% of the Silurian samples (Table 2).

The presumed benthic scolecodonts seem to prefer a shallow-water and/or limestone environment in contrast to the planktonic graptolites. The frequency of scoleco-

Table 2. The distribution of palynomorphs in the Silurian shale samples

	Number of analysed samples	Ac	Ch	Sc	Gr	Number of barren samples
Chester Bjerg Fm	1	0	0	0	0	1
Wulff Land Fm	63	0	32	12	20	26
Lafayette Bugt Fm	128	0	56	19	64	37
Lafayette Bugt Fm back reef	15	0	9	0	5	3
Thors Fjord Mb	53	0	20	6	33	11
Cape Schuchert Fm	4	0	3	3	1	1
Amundsen Land Gp	13	0	0	0	0	13
	277	0	120	40	123	92
% of analysed samples	100	0	43	14	44	33

dont and graptolite fragments in the Silurian deep-water deposited shales is the opposite of that in the shallow-water facies. The distribution of the supposedly planktonic chitinozoans indicates that this group tolerated shallow as well as deep-water conditions.

It is remarkable that acritarchs were not recorded from the Silurian shales in North Greenland, since acritarchs have been reported in moderate to large numbers in all marine lithologies except reef limestone, sandstone and conglomerate, in the Silurian of Britain and Ireland (Aldridge *et al.*, 1979). In North Greenland acritarchs are common in the Ordovician limestones, whereas only one Silurian sample, also a limestone, has revealed acritarchs (Armstrong & Dorning, 1984). Likewise, the very few Cambrian acritarch-like palynomorphs recorded from North Greenland were recovered from carbonates. The present distribution pattern is in accordance with the observations of both Aldridge *et al.* (1979) and Dorning (1987) who suggest that microfossils are more diverse, abundant and well-preserved in Palaeozoic platform carbonates than in graptolitic shale and sandstone turbidite sequences.

The analyses of the Ordovician and Silurian samples revealed 24 and 33% of the samples, respectively, to be barren of palynomorphs. The deviation is small and probably not significant. The Ordovician organic matter is generally less mature than the Silurian.

Although the data have not been strictly treated statistically, the palynomorph distribution clearly illustrates environmentally controlled trends.

Chapter 5

Composition of organic matter in source rocks

B. Buchardt, F. G. Christiansen, H. Nøhr-Hansen, N. H. Larsen and P. Østfeldt

Oil-production from Lower Palaeozoic sediments is relatively limited compared to that from sediments of Late Palaeozoic, Mesozoic and Tertiary age (Bois *et al.*, 1982). This raises a simple question: is the low potential of Lower Palaeozoic basins due to limited abundance and poor quality of source rocks, or is it the long, deep and often more complex subsidence and thermal history combined with possible later deformation which has reduced the potential compared to younger basins?

Knowledge of the composition of the organic matter in the source rocks is very important in this context. Previous studies of oils from producing basins and organic matter from organic-rich units of Early Palaeozoic age are still limited in number and in choice and combination of analytical methods. The few detailed examples include the Michigan basin (e.g. Powell *et al.*, 1984; Rullkötter *et al.*, 1986), the Baltic Alum shales (Buchardt *et al.*, 1986), various Australian basins (e.g. McKirdy *et al.*, 1983, 1984; Glickson *et al.*, 1985), and comparison of Ordovician oils and source rocks from several basins (e.g. Reed *et al.*, 1986; Hatch *et al.*, 1987). Little information is available from the largest producing Lower Palaeozoic basins in the world in Algeria and Sibiria.

In the following, systematically recorded information from microscope studies, either of palynological specimens or of algae observed in thin section, is combined with a number of organic geochemical parameters obtained by pyrolysis, gas chromatography (GC), gas chromatography/mass spectrometry (GS/MS), and carbon isotope studies. The presentation concentrates on the two major organic-rich units in North Greenland: the Lower to Middle Cambrian Henson Gletscher Formation and the Lower Silurian shales. The hydrocarbon potential, thermal maturity and geological relations of these two potential source rocks have previously been described on the basis of field and screening data (Christiansen *et al.*, 1987; Christiansen & Nøhr-Hansen, 1989). The organic matter in the two source rock units is here characterized geochemically. This is followed by a discussion of the possible control of source rock formation with emphasis on depositional environment, palaeogeography and climate, possible upwelling, regional sea level variation, and basin development.

Microscope studies

The results of studies under the microscope are presented in detail in the preceding chapter and by Larsen (1989). Palynologically, the source rocks are dominated by aggregated and finely disseminated amorphous kerogen with only minor amounts of palynomorphs and rare remains of filamenteous algae. Shelf carbonates with a considerably lower content of organic matter than the source rocks have a relatively higher abundance of palynomorphs.

Systematic studies of more than 400 thin sections provided an overview of a large number of algal groups in the Lower Palaeozoic sediments in North Greenland (Larsen, 1989). However, this study only recorded algae in shallow-water carbonate facies without any source rock potential. Visually well defined algal remains have not been reported from the source rocks, probably because of the small size or lack of resistant cell-walls of algae in this depositional setting. Furthermore, degradation and compaction are often intense in the shales compared to the carbonates, so that the original structure is unlikely to be preserved.

Pyrolysis

More than 600 samples were studied by Rock Eval pyrolysis (Christiansen *et al.*, 1985, 1987; Christiansen & Nøhr-Hansen, 1989; Chapters 3 and 6). In particular the Hydrogen Index (HI) and the Oxygen Index (OI), plotted in a modified van Krevelen diagram, provide information on the composition of the organic matter and its hydrocarbon potential. However, the majority of the analysed source rocks are postmature and display low HI values which makes it impossible to discern the

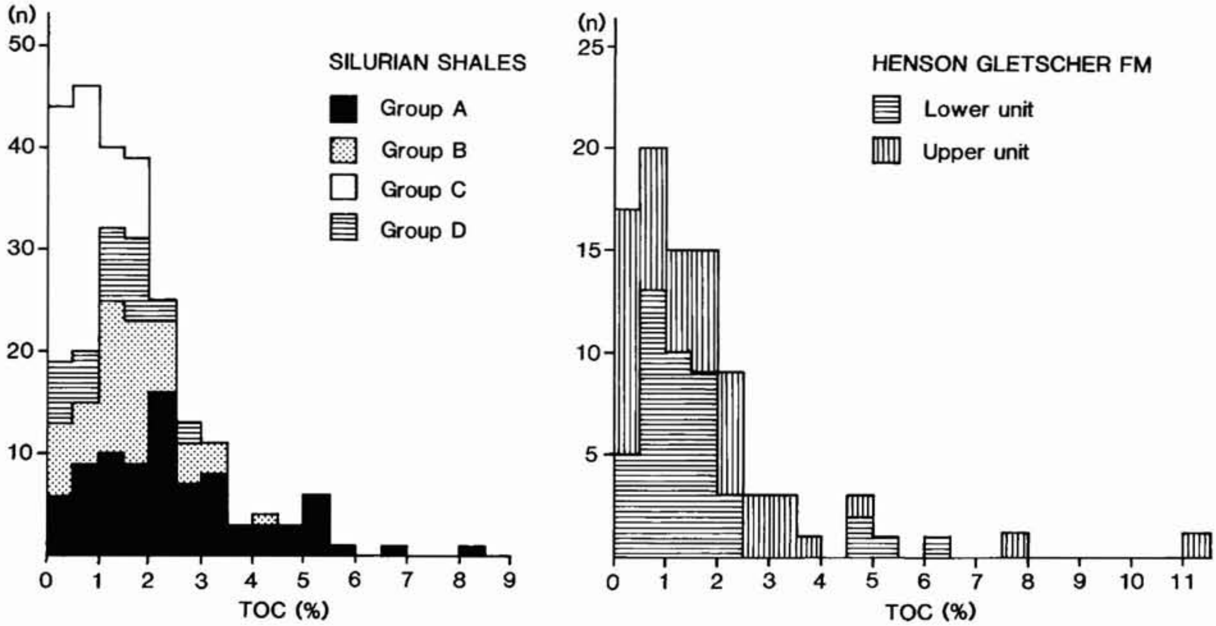

Fig. 16. Histograms showing the total organic carbon (TOC) distribution in the Cambrian Henson Gletscher Formation and in the Silurian shales. See details and subdivision in Christiansen *et al.* (1987) and Christiansen & Nøhr-Hansen (1989).

kerogen type. The kerogen from a minor number of early mature samples, mainly from Silurian shales in Washington Land and Nares Land, has been classified as typical Type II kerogen (Christiansen & Nøhr-Hansen, 1989, fig. 16), which is generally considered as derived from marine organisms, probably algae and bacteria.

The TOC distribution in the Silurian shales and the Henson Gletscher Formation is shown in fig. 16. Despite the high thermal maturity most of the shales and lime mudstones have relatively high TOC contents. In the Silurian shales, particularly group A (lower part of Thors Fjord Member and Lafayette Bugt Fm) which overlaps platform carbonates, is rich in organic carbon whereas the uppermost shales (group C) (upper part of Wulff Land and Lafayette Bugt Formations) and the back-reef shales display lower TOC contents (see details in Christiansen & Nøhr-Hansen, 1989). The Henson Gletscher Formation has a more uniform distribution with only a minor difference between the upper and lower part (fig. 16).

Gas chromatography and gas chromatography/mass spectrometry

A total of 31 potential source rock samples, 12 Cambrian and 19 Silurian, were analysed by gas chromatography (GC). In addition six of these samples, two Cambrian and four Silurian, were analysed by gas chromatography/mass spectrometry (GC/MS) (see analytical details in Chapter 3 and Østfeldt, 1987b). Additional geochemical data were obtained from the associated bitumen occurrences (see Chapter 7).

The extracts of the Cambrian and Silurian source rocks closely resemble each other in organic geochemical composition. They are dominated by saturated hydrocarbons which are strongly paraffinic with a smooth distribution without any odd to even predominance (figs 17 and 18). Most samples have a pronounced light-end bias in the paraffin distribution due to the high thermal maturity. The strong thermal alteration is also the reason for the limited preservation of cyclic biomarkers in the C_{27} to C_{33} range (see details in Chapter 6). The pristane to phytane ratios of the studied Cambrian samples display lower values (range: 1.0–1.5, average: 1.32, SD: 0.17) than the Silurian (range: 0.9–2.0, average: 1.62, SD: 0.33) (fig. 19).

The interpretation of source parameters from cyclic biomarkers is hampered by the small number of immature to early mature samples. Four of the Silurian source rocks and two associated bitumen samples display homogeneous biomarker distributions and are hence considered as representative of this succession. The Cambrian material is more complicated since only two source rock samples, and none of the associated bitumens, have preserved measurable biomarkers.

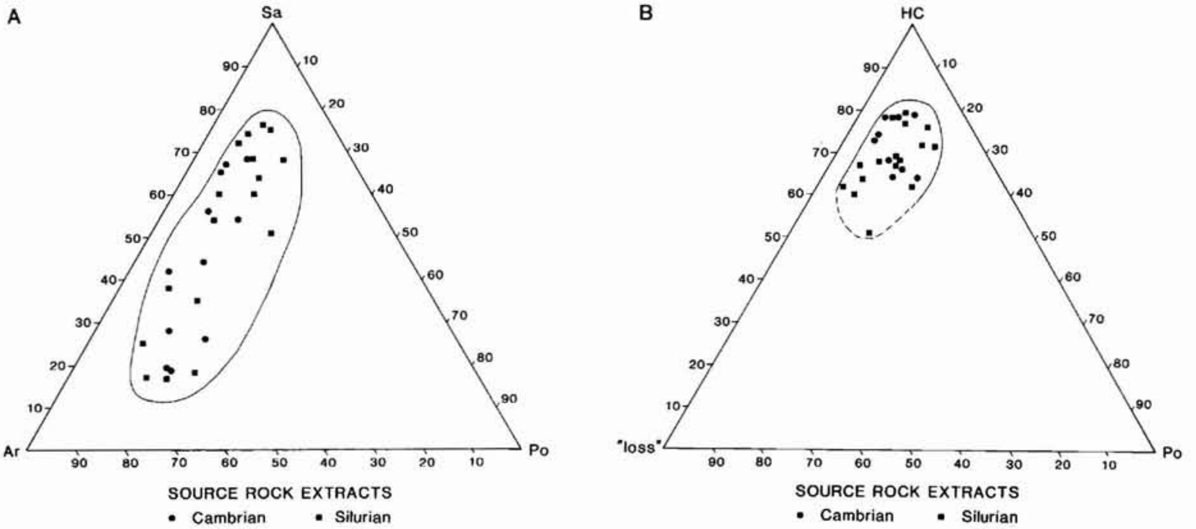

Fig. 17. Triangular diagrams showing the relative proportions in source rock extracts of (A) saturated, aromatic, and polar compounds and (B) hydrocarbons (saturates plus aromatics), polar compounds, and 'loss'. The 'loss' during column chromatography corresponds mostly to the asphaltene content.

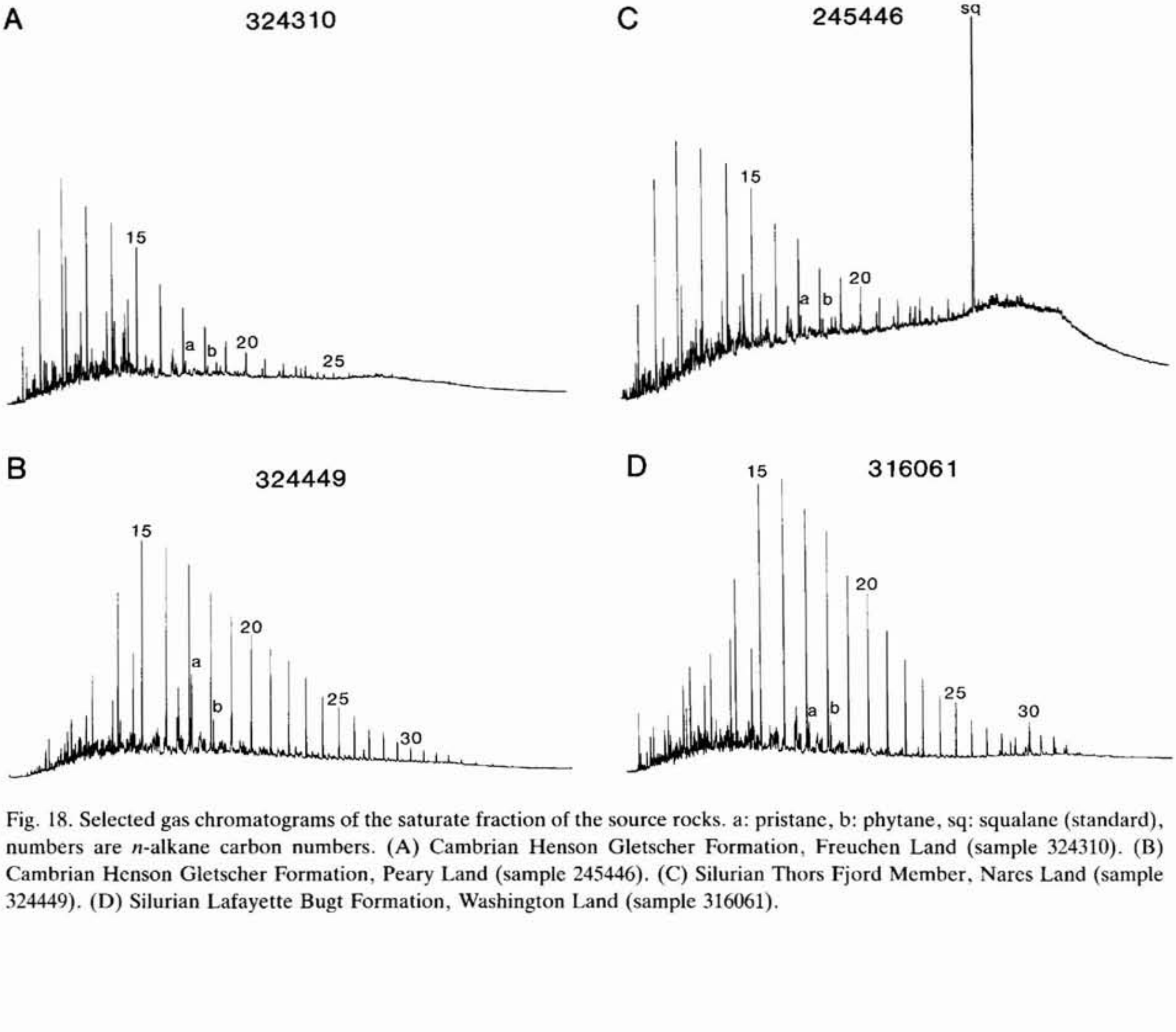

Fig. 18. Selected gas chromatograms of the saturate fraction of the source rocks. a: pristane, b: phytane, sq: squalane (standard), numbers are *n*-alkane carbon numbers. (A) Cambrian Henson Gletscher Formation, Freuchen Land (sample 324310). (B) Cambrian Henson Gletscher Formation, Peary Land (sample 245446). (C) Silurian Thors Fjord Member, Nares Land (sample 324449). (D) Silurian Lafayette Bugt Formation, Washington Land (sample 316061).

Many of the possible long distance migrated bitumens in the southern part of the region (see Chapter 7) have also preserved biomarkers.

The two Cambrian source rocks display a rather unusual, but uniform, biomarker distribution with relatively large amounts of tricyclic deterpenoid compounds, minor amounts of steroid biomarkers (mainly C_{29} steranes, fig. 21), and lack of cyclic triterpenoids (fig. 20 A). The Silurian source rocks (and bitumen samples) contain both steroid and treterpenoid biomarkers including hopanes (fig. 20 B). The sterane distribution is completely dominated by C_{29} steranes (figs 20 B and 21).

The long distance migrated bitumens (group C in Chapter 7) are moderately to severely biodegraded but contain detectable cyclic biomarkers such as steroids, triterpenoids and hopanes (fig. 20 C). It is remarkable that all eight analysed bitumen samples contain the triterpenoid biomarker gammacerane in relatively high amounts, since this compound has not been recorded from any of the two known source rock units.

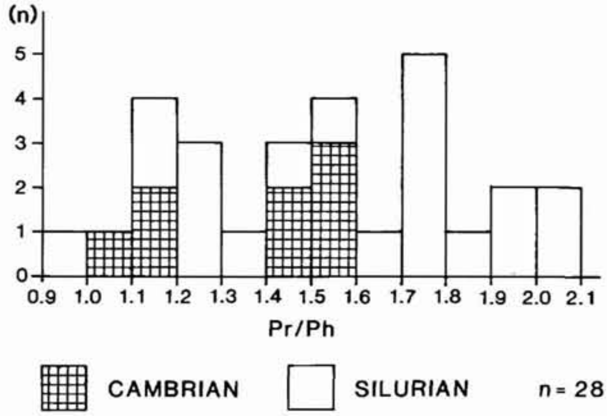

Fig. 19. Histogram showing the variation in pristane (Pr) to phytane (Ph) ratio in extracts of Cambrian and Silurian rocks.

Carbon isotopes

Carbon isotopic compositions were determined for 16 samples of Cambrian and Silurian organic-rich rocks. The data include both kerogen and soluble organic matter (extracts). $\delta^{13}C$-values for both extracts and kerogens fall within a range from −26.5 to −32.0‰ (figs 22 and 23). Cambrian kerogens and extracts are depleted in the heavy carbon isotope compared to the Silurian samples (−29.7 to −31.2‰ for Cambrian, −26.9 to −30.5‰ for Silurian samples). The only exception is the Silurian sample 324446, which has a $\delta^{13}C$-value comparable to that of the Cambrian material.

Extracts from Cambrian samples are slightly enriched in ^{13}C in relation to corresponding kerogens. Silurian extracts, on the other hand, are indistinguishable from the corresponding kerogens.

The carbon isotopic composition of kerogen of Early Palaeozoic age has been reported by Welte *et al.* (1975), Galimov (1980), Glickson *et al.* (1985), Lewan (1986), Buchardt *et al.* (1986), and Hatch *et al.* (1987). The values vary from −26 to −32‰ with a dominance in the range below −28‰. The North Greenland samples fall within this range.

Soluble organic matter is generally believed to be depleted in ^{13}C as compared to corresponding kerogen (Galimov, 1980; Schoell, 1984). In kerogen of predominantly amorphous composition, however, the difference seems to be insignificant (Buchardt & Cederberg, 1987; Buchardt & Lewan, unpublished data). The minor differences observed in the present material is therefore in accordance with other data.

Control of chemical composition

The variation in chemical composition of kerogen and soluble organic matter in source rocks is related to type of primary organic matter, the depositional environment and thermal maturation. The carbon isotopic composition is mainly dependent on the type of organic matter, environment and early diagenesis (Deines, 1980; Lewan, 1986) whereas thermal maturation has only minor influence on the composition (Lewan, 1983; Buchardt *et al.*, 1986). The pristane to phytane ratio also seems to be related to depositional conditions and it is generally accepted that high ratios reflect predominantly oxidizing environments whereas low ratios are found in organic matter deposited under reducing conditions (Tissot & Welte, 1984). The distribution of cyclic biomarkers has strong implications for the interpretation of the type of organic matter and the environment, especially from Mesozoic to Recent sediments, but most parameters are overprinted by maturity effects in thermally mature to postmature sediments.

In Mesozoic to Cenozoic deposits differences in composition are most commonly related to either a marine or a terrestrial origin of the kerogen. In North Greenland, however, few terrestrial palynomorphs and plant remains are reported (Larsen *et al.*, 1987; Nøhr-Hansen & Koppelhus, 1988), and the kerogen is presumed to be mainly of marine origin. This is in contrast to the Lower Palaeozoic source rocks formed in a fresh or brackish water environment in the Michigan, Chinese and Australian intracratonic basins. It should be noted that well-

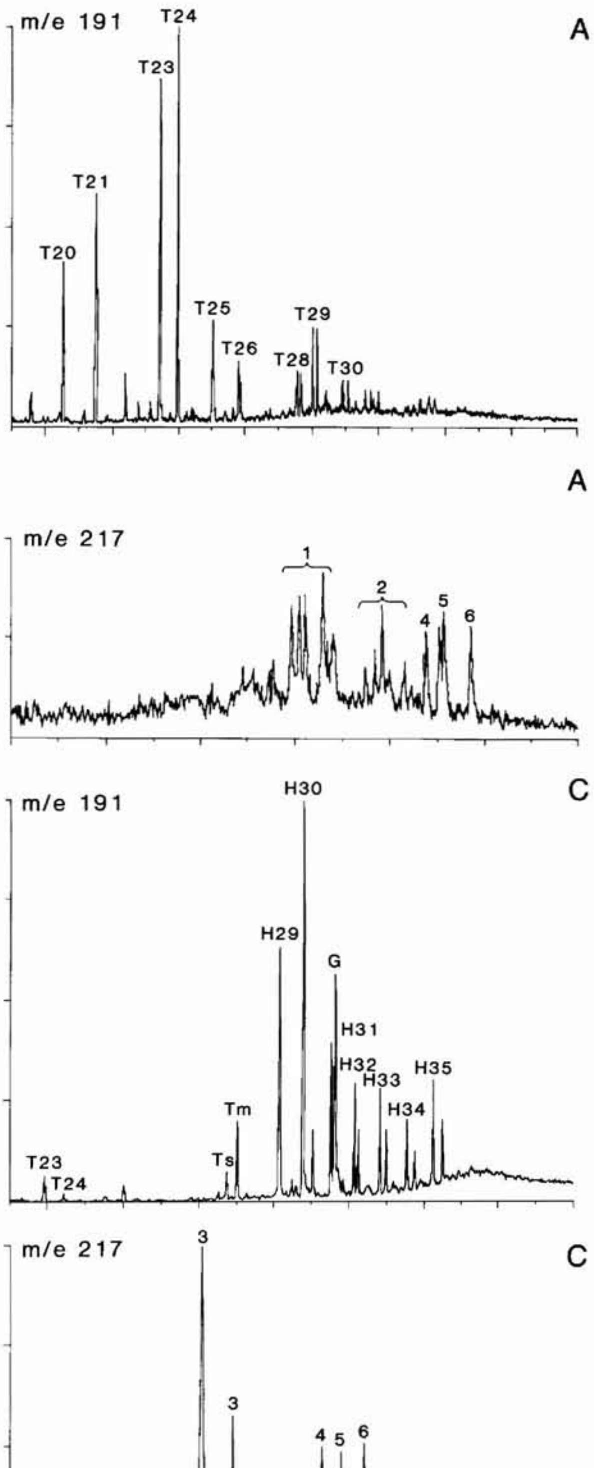

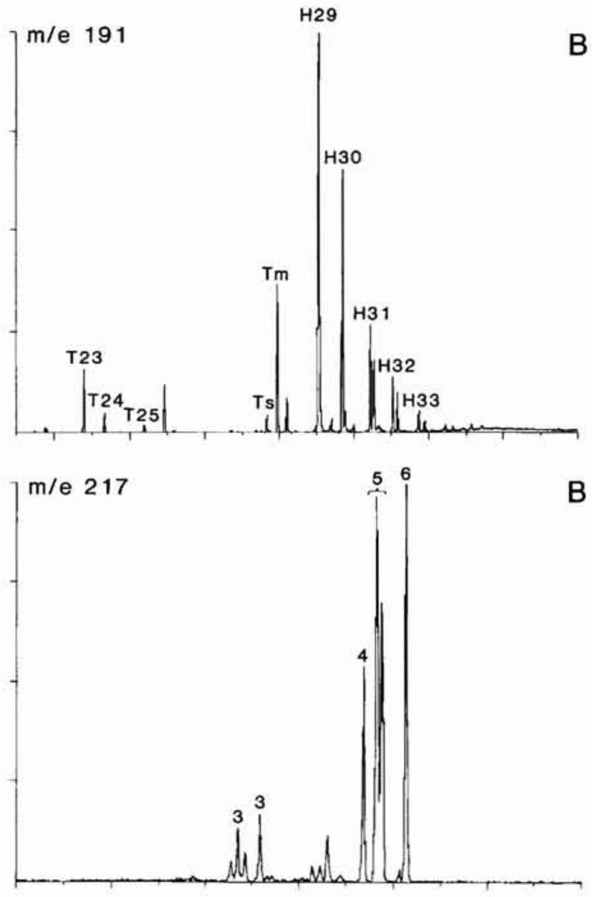

Fig. 20. Selected ion chromatograms (m/e 191 and m/e 217) of the saturate fraction of: (A) source rock in Cambrian Henson Gletscher Formation, Freuchen Land (sample 324310). (B) source rock in Silurian Lafayette Bugt Formation, Washington Land (sample 316061). (C) Long-distance-migrated bitumen in Portfjeld Formation, southern Wulff Land (sample 324200E).

Code to peak identification:

(m/e 191): T20–T30: tricyclic diterpenoids with carbon numbers indicated, H29–H35: 17α, 21β hopanes with carbon number indicated (from H31 both 22S and 22R configuration), Ts: 18α-trisnorhopane II, Tm: 17α-trisnorhopane, G: gammacerane (m/e 217): 1: 27 carbon steranes $\alpha\alpha$ and $\beta\beta$, 2: 28 carbon steranes $\alpha\alpha$ and $\beta\beta$, 3: 29 diasteranes (20R and 20S), 4: 29 carbon steranes ($\alpha\alpha$-20S), 5: 29 carbon steranes ($\beta\beta$, 20R and 20S), 6: 29 carbon steranes ($\alpha\alpha$ -20R).

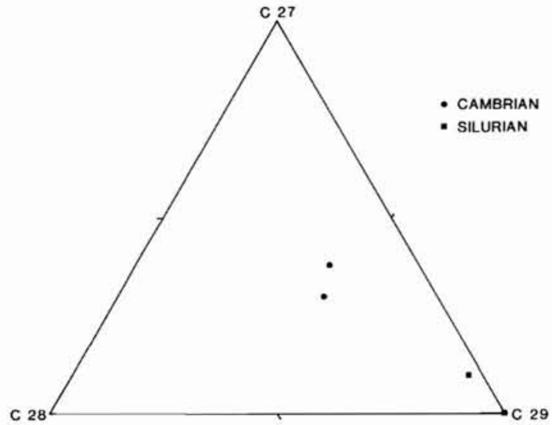

Fig. 21. Triangular diagram showing the relative proportion of the C_{27}, C_{28} and C_{29} steranes in Cambrian and Silurian source rocks.

defined remains of higher terrestrial plants are unknown from deposits older than Early Devonian (Glensel & Andrews, 1987).

Visually, only minor differences have been recorded between the organic matter in the Cambrian and Silurian source rocks (Chapter 4). It is completely dominated by apparently identical amorphous kerogen with only a minor content of palynomorphs. The amorphous kerogen probably derived from marine planktonic organisms. The observed differences in geochemical composition of Cambrian and Silurian kerogen are hence mainly ascribed to deviating environments or variation in early diagenetic modifications.

The higher pristane to phytane ratios in the Silurian rocks, as compared to the Cambrian, point to a more oxidizing environment at the time of deposition of Silurian source rocks. The ^{13}C-depleted kerogens are characterized by pristane/phytane ratios below 1.5 whereas ^{13}C-enriched samples have ratios between 1.5 and 2.1 (fig. 24). Similar relationships have been observed for Mesozoic deposits (Buchardt & Cederberg, 1987). The isotopic difference may be explained by preferential preservation of ^{13}C-depleted lipid-derivates in more reducing environments (Galimov, 1980).

Pristane and phytane are considered the primary derivates of the phytyl side-chain of the chlorophyll molecule (e.g. Illich, 1983). The presence in relatively high amounts in both the Cambrian and Silurian source rocks is taken as evidence of active photosynthesis in the precursors to the major part of the organic matter. In contrast, several world-wide distributed Ordovician source rocks have very low pristane and phytane contents and a kerogen composition dominated by *Gloeocapsamorpha prisca* Zalessky 1916 (Reed *et al.*, 1986). Geochemical evidence of this 'primitive' prokaryotic organism has not been recorded in the present study.

Selected biomarkers such as the steranes, hopanes and gammacerane may provide information on the possible precursors of the organic matter. Ourisson *et al.* (1979) claimed that prokaryotic organisms are the major source of hopanes in hydrocarbons whereas eukaryotic organisms and other higher organisms are the main sources of steranes. It is only the Silurian source rocks and the associated bitumens which contain hopanes. Since no major evolutionary steps in algae and bacteria are known to have taken place from Cambrian to Silurian times it would be expected that the Silurian source rocks were dominated by similar or less primitive organisms compared to the Cambrian, and hence have a lower hopane content. The hopane content is, however, easily changed during thermal maturation. Both the Cambrian and Silurian source rocks contain steranes. The C_{29} steranes, which in Mesozoic rocks are consid-

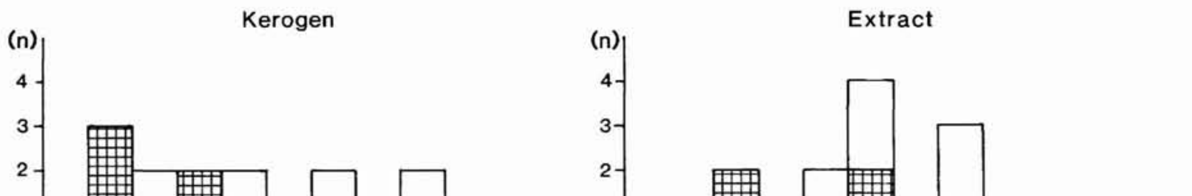

Fig. 22. Histogram showing the variation in $\delta^{13}C$ composition of kerogen and extracts in Cambrian and Silurian source rocks.

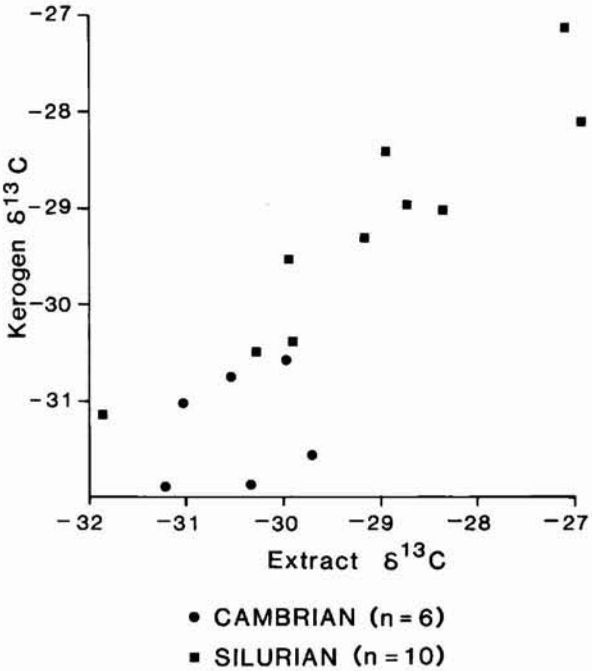

Fig. 23. Cross plot of isotopic composition in extracts versus kerogens.

ered to be terrestrial in origin (Huang & Meinschein, 1976), are dominant in the Silurian shales and occur in moderate amounts in the Cambrian source rocks (fig. 21). This dominance of C_{29} steranes is commonly observed in Lower Palaeozoic rocks (Waples, 1985 p. 162; Moldowan *et al.*, 1985; Grantham, 1986). The triterpenoid biomarker gammacerane, which has only been recorded from the long distance migrated bitumens, was also originally proposed as a component of non-marine origin (Hills *et al.*, 1966). This interpretation has since been questioned and although the origin is still unclear it should be noted that the compound is most abundant in Mesozoic sediments from hypersaline environments, especially lacustrine (e.g. Moldowan *et al.*, 1985; Philp & Lewis, 1987).

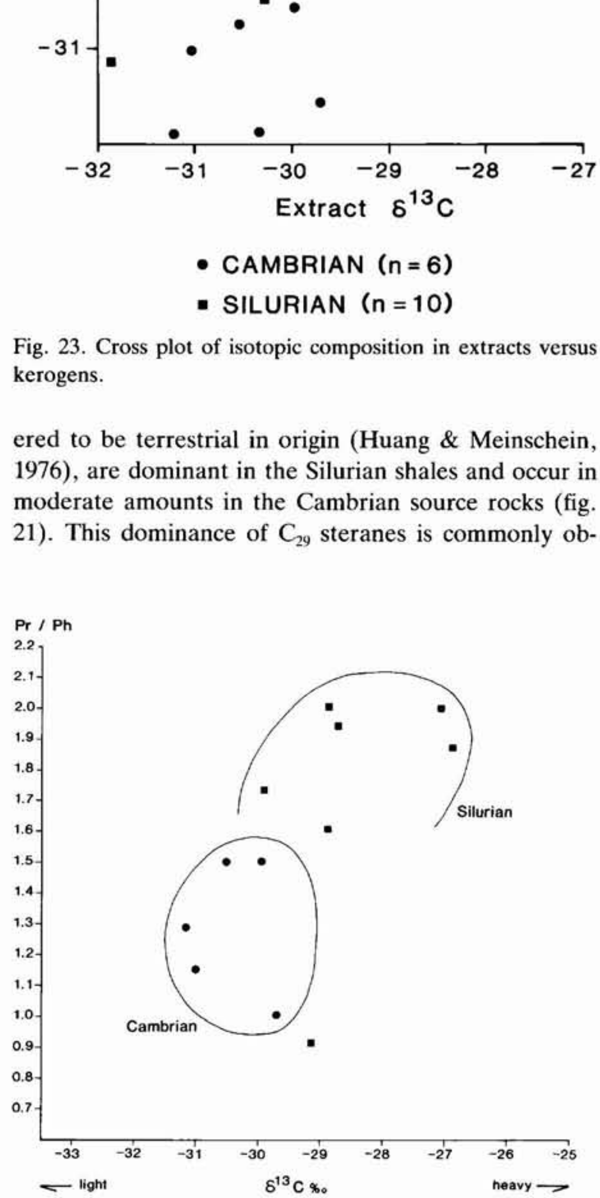

Fig. 24. Cross plot of isotopic composition versus pristane to phytane ratio of Cambrian and Silurian source rock extracts (only organic-rich units included).

The recorded combined parameters from GC, GC/MS and C-isotope analyses make it possible to distinguish geochemically between the Cambrian and Silurian source rocks. The difference in composition seems to be mainly controlled by variation in depositional environment rather than variation in precursors of the organic matter. It is suggested that the Cambrian source rocks formed under more reducing conditions than the Silurian.

Control of source rock deposition

Deposition of source rocks in the Early Palaeozoic, and black shales in general, was controlled in time and space by a large number of more or less interdependent factors (see e.g. Thickpenny & Leggett, 1987): organic production versus biochemical degradation, climate, sea level stand, palaeogeography, upwelling zones, sedimentation rate, water depth, etc.

Compared to younger sediments exact knowledge of some of these fundamental factors is often limited. In North Greenland the spatial and chronological relations of source rock deposition are controlled by a combination of local factors controlling basin development, and the global configuration (palaeogeography, climatic belts, global sea-level, evolution of organisms) at the time of deposition.

In Late Cambrian times North Greenland was situated approximately 10° south of the equator and the basin margin had an east–west orientation (Scotese *et al.*, 1979 fig. 9). During the Early Ordovician it drifted northwards to a position 15° north of the equator. The position of Laurentia (North America and Greenland) did not change much in the following period and in mid-Silurian time North Greenland was still at a position of 15° north with a northwest to southeast trend of the basin margin (Scotese *et al.*, 1979 fig. 18). The equatorial position of the Franklinian basin throughout most of its depositional history points towards a stable tropical climate with a possible variation caused by the crossing of the equator and the counterclockwise rotation. This climatic interpretation is further supported by the algae study which indicates a tropical or subtropical climate at the time of deposition (Larsen, 1989).

The palaeogeographic position with an east–west trend of the basin margin is not in accordance with a control of source rock deposition by 'classical coastal upwelling', a model which has been suggested for many basins (e.g. Parrish, 1982, 1987; Schopf, 1983). Berry & Wilde (1978) proposed a general model of black shale deposition controlled by progressively ventilated oceans; during glacial times with low sea levels, well-oxygenated conditions prevailed whereas extensive shelf areas were covered with anoxic water in the interglacial periods of high stands of sea level. This model implies generally anoxic waters, and very long periods of anoxic conditions, in Early Palaeozoic time. Black shale deposition in Europe was particularly concentrated in three intervals: Middle to Late Cambrian, Caradoc (in Late Ordovician), and Llandovery (Silurian), all characterized by periods of rising sea levels (McKerrow, 1979; Leggett *et al.*, 1981; Thickpenny & Leggett, 1987). Compared to this temporal pattern the situation in North Greenland seems different. The Early to Middle Cambrian Henson Gletscher Formation was deposited in a period of inferred falling global sea level whereas the most organic-rich parts of the Silurian shales formed during a major sea-level rise in the Llandovery (see Leggett *et al.*, 1981). Considered in detail it should be noted that the organic-rich Silurian shales in North Greenland are slightly younger than the maximum deposition of black shales in Europe. Furthermore, the onset of source rock deposition was diachronic; it started earlier towards the west (Washington Land) than in the central part of North Greenland (Christiansen & Nøhr-Hansen, 1989).

The Silurian source rock deposition was related to the foundering of the carbonate platform. This is a combined effect of sea-level rise due to the Gondwana deglaciation and possible downflexuring caused by loading of the thick turbidite sequence deposited to the north (Higgins *et al.*, in press; see also Chapter 2). The foundering platform was covered by up to 100 m of black shales deposited in an anoxic environment (the Thors Fjord Member). During continued high-rate subsidence this pattern changed to more oxygenated deposits of deep-water grey shales and sandstone turbidites.

In the Cambrian case, source rock deposition took place in a period with a wide outer shelf. The onset of the anoxic conditions followed a change from siliciclastic to dominating carbonate deposition and ended when platform carbonates prograded northwards over the muddy/siliciclastic outer shelf.

It is concluded that deposition of organic-rich sediments with a good primary hydrocarbon potential was widespread in Early Palaeozoic times in North Greenland. Two major organic-rich units were deposited, one in Early to Middle Cambrian time and one in Early Silurian time. The organic matter in both units seems to have been derived from the same types of precursors as those to the amorphous kerogen. Geochemically, the two units are discerned employing several, mainly environmentally controlled, parameters.

Chapter 6

Thermal maturity

F. G. Christiansen, C. J. W. Koch, H. Nøhr-Hansen, S. Stouge, E. Thomsen and P. Østfeldt

Two of the aims of the 'Nordolie' project were to investigate the thermal maturity pattern of potential source rocks in North Greenland and to provide information on the thermal history of the basin.

Organic diagenesis of source rocks is a function of the burial and thermal history of a basin with the two most important factors being temperature and time. In the present study a multidisciplinary approach has been applied to the maturity concept and a large number of different maturity parameters with varying sensitivities have been combined. Each sedimentary basin in the world has its own unique thermal history which is expressed by the maturity parameters. Consequently it is important to establish the local empirical relations between the various parameters and especially in oil-related studies to deduce parameters corresponding to the possible onset of both oil generation and oil cracking, in other words to define 'the oil window'.

In Lower Palaeozoic basins a number of particular problems arise due to their age. The history of such old basins is often complicated to unravel. This is also true in central North Greenland where no post-Silurian deposits have been preserved (see Chapter 2). The lack of plant material in the early stages of evolution inhibits the use of the universal maturity parameters such as vitrinite reflectance (e.g. Tissot & Welte, 1984) and spore coloration (Staplin, 1969) and instead less reliable reflectance measurements are carried out on amorphous kerogen and bitumen; the Thermal Alteration Index (TAI) is determined from the colour of amorphous kerogen. On the other hand the limited variation in composition of the organic matter (dominance of Type II kerogen) is an advantage in the interpretation of geochemical maturity parameters, especially the T_{max} of the Rock Eval pyrolysis and the parameters derived from high molecular weight cyclic biomarkers.

Thermal maturity mapping of most sedimentary basins, especially petroliferous, starts as a one-dimensional study (single well data) and expands to two-dimensional (few wells projected onto cross-sections) or even three-dimensional studies (control from numerous wells). In all cases an expected down-hole increase in maturity facilitates interpretation; the main problem is the variation in type of organic matter with depth, i. e. comparison of parameters measured on different materials. In North Greenland the basin is deeply eroded and well exposed but there are no wells. No details were known on maturity gradients prior to sampling although an increase towards the north was expected due to the position of the metamorphic belt.

The maturity study presented below is essentially two-dimensional, the present-day surface being projected into a horizontal plane. This broad simplification seems valid although the terrain is rough; only minor variations of maturity with altitude have been observed (see a following section).

The maturity mapping concerns the outcropping organic-rich units. An attempt to predict the maturity spatially for any given unit has been made. In this context the thick organic-lean sequences are problematic, especially the shallow-water carbonates towards the south and the turbidite sandstones towards the north. The only applicable maturity parameters in such sediments are the Conodont Alteration Index (Epstein *et al.*, 1977) and X-ray diffraction data on clay minerals (e.g. Foscolos *et al.*, 1976). Both parameters provide little specific data on petroleum generation and destruction and provide no reliable input data for thermal modelling, although various authors have tried to correlate them to other, better established indicators (Heroux *et al.*, 1979; Bustin *et al.*, 1985a).

Measured maturity parameters

The analytical programme including details on sample preparation and laboratory techniques is described in Chapter 3. Most of the measured parameters are based on physical and chemical properties of the residual kerogen or its generation products, hydrocarbons (bitumen).

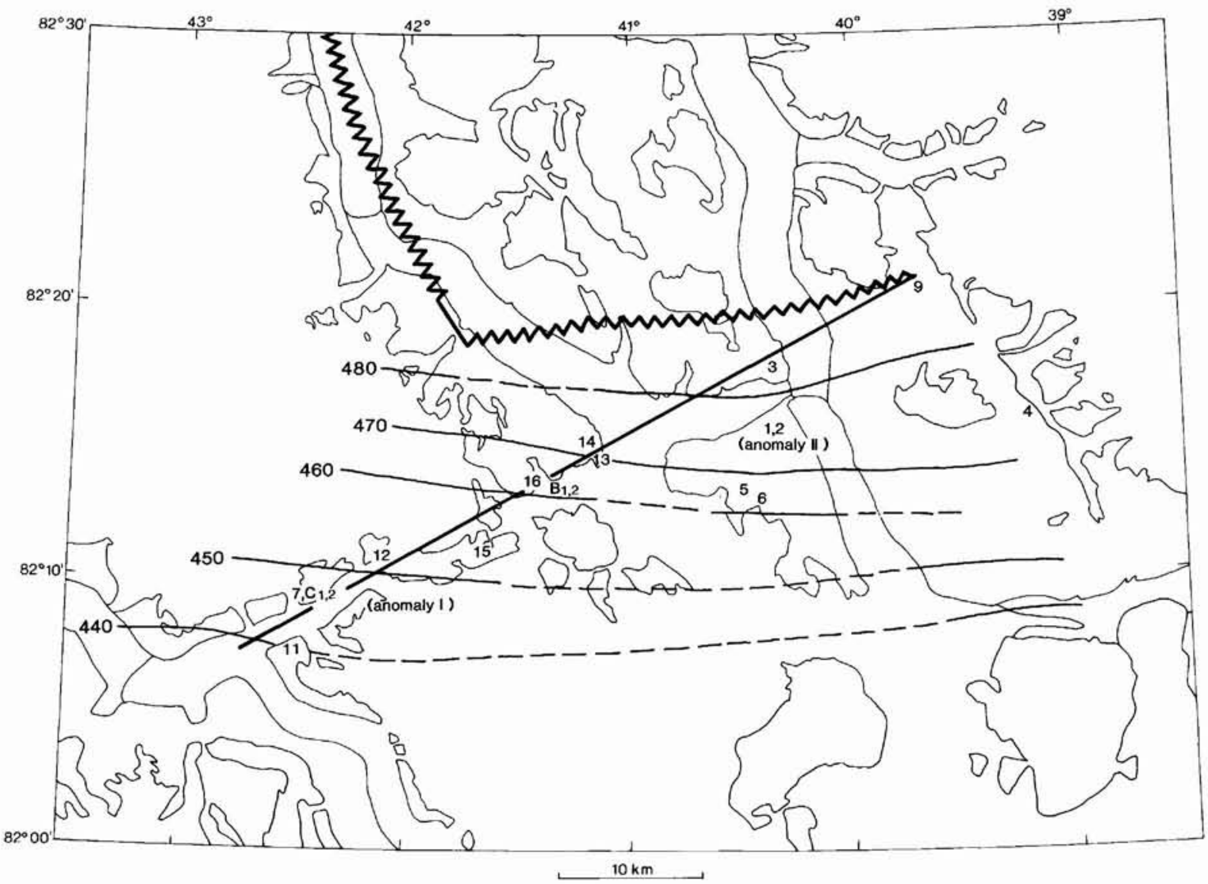

Fig. 25. Maturity map of the area where the Henson Gletscher Formation is exposed. The iso-T_{max} lines are taken from Christiansen *et al.* (1987), the line corresponds to the maturity profile shown in fig. 36.

For screening purposes a combination of Rock Eval pyrolysis (T_{max}) and palynological studies (TAI) has been applied. Preliminary results covering most of the region were published by Christiansen *et al.* (1985) and these were followed by more detailed studies on the Cambrian and Silurian source rocks (Christiansen *et al.*, 1987; Christiansen & Nøhr-Hansen, 1989).

A number of other maturity parameters have subsequently been included in the study, generally determined on a much smaller number of samples, but employing more sophisticated techniques. Gas chromatography (GC) and gas chromatography/mass spectrometry (GC/MS) provide several maturity parameters both from extraction data and from specific molecular compounds. Coal petrographic methods on polished samples give reflectance and in rare cases fluorescence values for both kerogen and bitumen. In addition graptolite reflectance studies have been carried out. Finally a number of less commonly used methods such as X-ray diffraction of kerogen ('kerogen crystallinity') were applied at a later stage.

In the following the different parameters obtained are presented regionally method by method. This is followed by considerations of thermal maturity parameters and the boundaries of the oil window. The interdependence of the various parameters, both regionally (composite maps and profiles) and sample by sample (cross plots), is discussed in a succeeding section. Finally, the few local thermal anomalies are described and the limited data available from Peary Land are reviewed.

Rock Eval pyrolysis: T_{max}

Rock Eval pyrolysis is the most widely applied technique in this maturity study. More than 600 samples were analysed providing more than 260 reliable T_{max} values. All pyrogrammes were inspected visually, whereupon a number of T_{max} values were excluded from

Fig. 26. Maturity map of central and western North Greenland, based mainly on data for the Silurian from Christiansen & Nøhr-Hansen (1989). The line in Washington Land corresponds to the maturity profile shown in fig. 37, the numbers in brackets refer to the rank in maturity in the composite maturity profile in fig. 38.

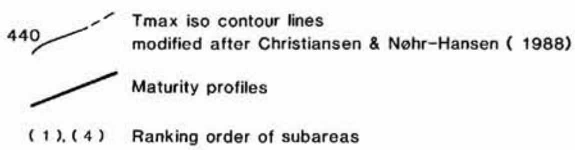

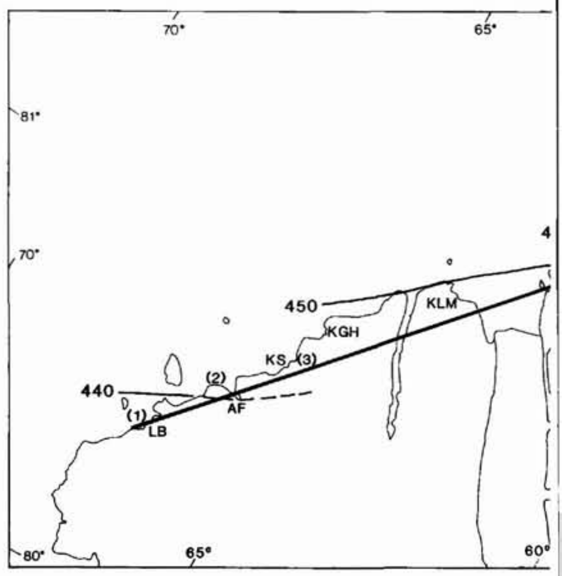

further consideration. Samples with small S2 values (< 0.2 mg HC/g rock) were omitted; only values from visually well defined S2 peaks were included (see fig. 10). Bitumen-stained samples were also excluded; these were typically recognized by high S1/TOC and S1/S2 ratios, skewness of S2 peaks towards the S1 peak and overlap between S1 and S2 peaks (see fig. 10). Generally these bitumen-stained samples exhibit anomalously low T_{max} values which are not representative of the thermal maturity.

Usually there is only minor variation of T_{max} values within individual cores, sections or smaller areas. For T_{max} values < 440°C a scatter of ± 5° is typical; for values ~ 450°C a variation of ± 10° is commonly observed, and the variation increases for poorly defined T_{max} values above 470°C (see e.g. figs 35–39). These variations are small compared to most Mesozoic basins, and would be much smaller if only the most organic-rich samples were considered (e.g. TOC > 2%). The constant Type II kerogen composition prior to subsidence and thermal alteration (see Chapter 5; Christiansen & Nøhr-Hansen, 1989) can be expected to reduce the variation compared to regions with lacustrine (mainly Type I kerogen) or terrestrially dominated (mainly Type III kerogen) deposits.

As a consequence it is possible to utilize T_{max} average values in the preparation of thermal maturity maps, typically calculated for single sections or smaller areas. Two examples are shown in figs 25 and 26, one including the area where the Henson Gletscher Formation is exposed, the other covering the whole region. The tentatively drawn iso-T_{max} lines clearly define a distinct thermal maturity trend with a strong gradient from south to north.

The maturity map for the Cambrian source rocks is relatively detailed and the calculated values are typically spaced at intervals of 5 to 10 km. Due to the systematic increase in maturity from south to north contouring the T_{max} values is easy. The iso-T_{max} lines are closely spaced; the distance from the 440° ('early mature') to the 460° ('end of generation') is only 8 to 12 km, and from 440° to 500° (no hydrocarbons preserved at all) about 25 km (fig. 25). The map of the whole region is based mainly on values from the Silurian shales (fig. 26). In this case the values are more scattered with typical distances between 10 and 30 km. Contouring the data is difficult, and the result is probably not as accurate as the Cambrian map, since the iso-lines have the same trend as the strike of the exposed Silurian shales. The distance between iso-lines increases towards the west and south, especially for the early mature to mature areas in Hall Land and Washington Land (fig. 26).

Thermal Alteration Index (TAI)

Measurements of the Thermal Alteration Index (TAI) were widely applied for screening purposes in combination with Rock Eval analyses (Christiansen *et al.*, 1985, 1987; Christiansen & Nøhr-Hansen, 1989). In order to obtain consistent results the samples were all examined by one person (HN-H) using constant microscope conditions. The TAI value was visually evaluated from the colour of the rim of the relatively large amorphous kerogen particles using a scale from 1 to 5 with a

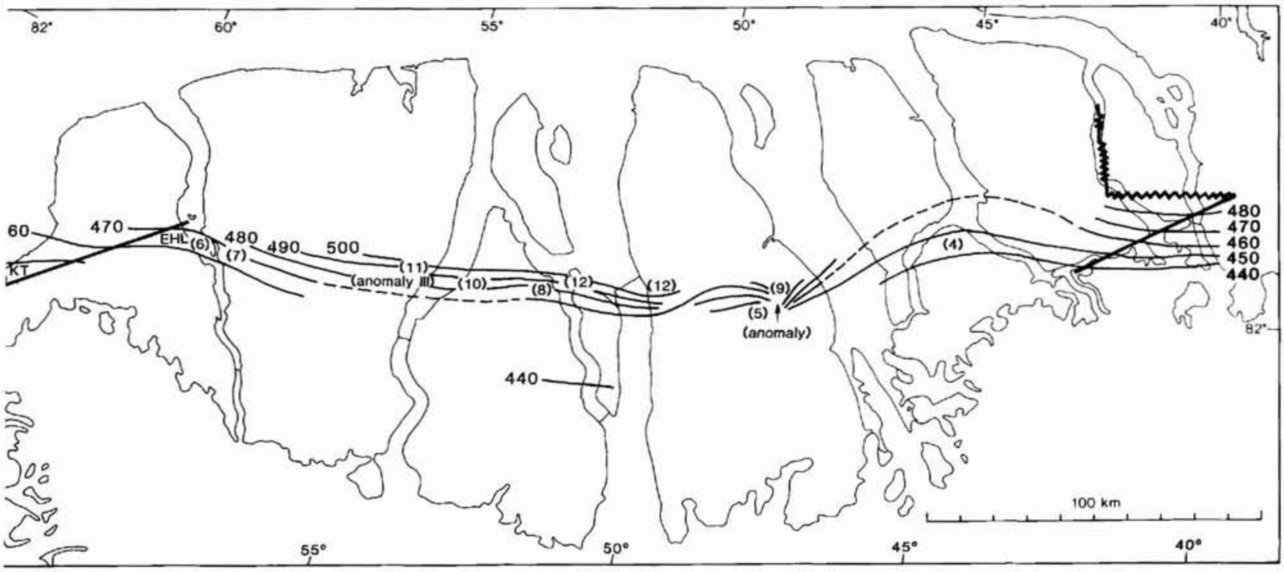

± subdivision (Staplin, 1969; Burgess 1974; Dow, 1977). Selected examples with a progressive coloration are shown in Plate 5. Increase in thermal alteration not only changes the colour of the kerogen but also the structure. Immature to early mature kerogen which has expelled only minor amounts of hydrocarbons has a fluffy structure (not illustrated), mature kerogen has a granular to flaky appearance (Plate 6 A) whereas post-mature amorphous kerogen has a more spongy character (Plate 6 B). Newly generated bitumen was also observed in the palynological slides. It occurs typically as angular particles reflecting the crystal faces of pores or as fine stringers (see Chapter 7 and Plate 10). The bitumen often has a paler colour than the associated kerogen and was therefore avoided in TAI determinations.

The TAI values are fairly constant within single cores or smaller areas, typically with one or two, occasionally three, dominating values (e.g. 2^+, 2^+ – (3^-) or (2^+) – (-3^-) -3) (figs 35–38; Christiansen *et al.*, 1985, fig. 5; Christiansen & Nøhr-Hansen, 1989, fig. 6). Hence it has been possible to prepare TAI maps with tentatively drawn iso-TAI lines for the Cambrian Henson Gletscher Formation (Christiansen *et al.*, 1987) and for the Silurian shales (Christiansen & Nøhr-Hansen, 1989). Both maps are in good agreement with maps of T_{max} confirming the distinct trend with rapidly increasing maturity from south to north (see also the profiles in figs 35 to 38).

Gas chromatography and gas chromatography/mass spectrometry

GC and GC/MS analyses provide a number of maturity parameters, both from extraction data and from specific molecular compounds. Furthermore evaluation of gas chromatograms may, at least qualitatively, support interpretation of the thermal maturity. The analytical programme included investigations of both extracts of shale and lime mudstones (source rocks) ($n > 25$) and of migrated bitumens ($n > 25$). The source rock data are easily applied in the thermal maturity study whereas the bitumen data should be treated with caution as they represent not only the thermal history of source rocks prior to expulsion but also the post-migrational history of the reservoir.

The analysed samples are divided into three main catagories according to maturity (fig. 27):

1) Samples with very low extractabilities; almost all of the original hydrocarbons are cracked to carbon and methane. These samples occur in the postmature zone where the T_{max} is higher than 480°C or not defined.

2) Samples with low to high extractability but without any preserved high molecular weight cyclic biomarkers such as steranes and hopanes. These samples are from the mature to postmature zone with corresponding T_{max} values between 440°C and 480°C.

3) Samples with high extractabilities and with cyclic biomarkers present. They only occur in early mature areas south of the 440°C iso-T_{max} line.

Fig. 27. Map of central and western North Greenland showing regional variation of maturity parameters derived from the GC and GC/MS methods.

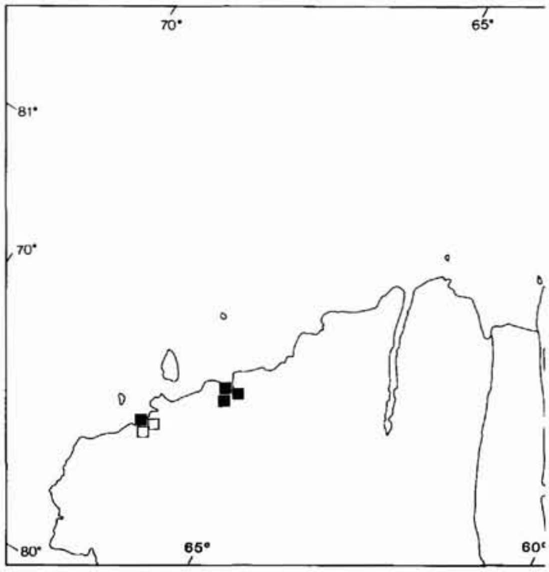

The first category is not considered further. The data from the second category are additionally supported by the gas chromatograms which show that the saturates are highly paraffinic with a pronounced light-end bias (Østfeldt, 1987b). This suggests a high maturity, probably ranging from peak generation to post generation. The samples cannot, however, be ranked in detail using this method only. The third group is also dominated by paraffins, extending up to C_{35}, and with some light-end bias towards light hydrocarbons. The presence of cyclic biomarkers allows the thermal maturity and history of these early mature samples to be determined in detail, employing isomerization ratios of steranes and hopanes.

Four ratios, all rising with increasing thermal maturity, were applied (fig. 28; see review by Mackenzie, 1984, and analytical details by Østfeldt, 1987a,b, and in Chapter 3).

C_{31} and C_{32} hopanes were measured for the 22R to 22R + 22S conversion both of which reach equilibrium values of 0.6 at pre- to early oil window maturity. Both Washington Land source rocks and bitumen and also the migrated bitumens from southern Warming Land and Wulff Land have reached these values (fig. 28). C_{29} steranes were measured for the 20R to 20R + 20S conversion. The equilibrium value of approximately 0.5 is reached just before peak generation. Such values were obtained in southern Warming Land and Wulff Land whereas the Washington Land samples display slightly lower values (fig. 28). The $\beta\beta/\alpha\alpha + \beta\beta$ ratio reaches equilibrium late in the oil window with a value of about 0.63 using the present technique. It is questionable whether any of the samples have reached equilibrium; especially the values for the samples from Warming Land and Wulff Land are rather scattered (fig. 28), probably due to biodegradational effects (see Chapter 7).

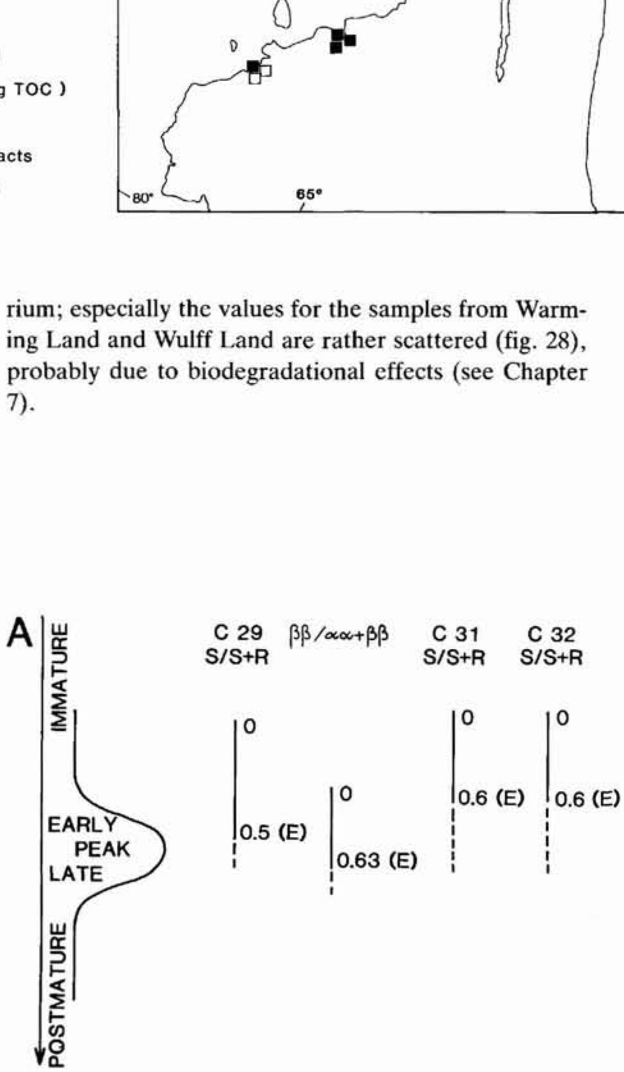

Fig. 28. Thermal maturity parameters based on isomerization of steranes and hopanes. (A) Empirical relations between measured values, equilibrium values and oil generation. Based on Mackenzie (1984) and Østfeldt (1987a). (B) Measured values from Washington Land (filled squares: source rock extracts; open squares: bitumen) and southern Warming Land and Wulff Land (open triangles: bitumen).

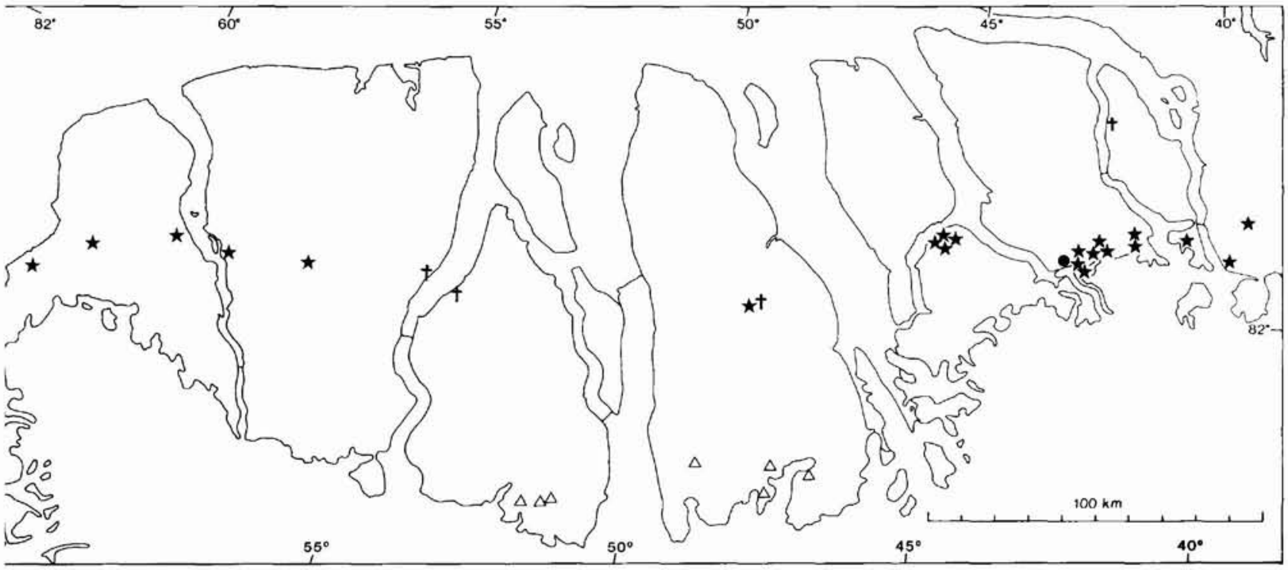

Organic petrological parameters

Organic petrological investigations of samples from North Greenland have been carried out in order to:

1) support the thermal maturity mapping based on screening methods (T_{max} and TAI) with reflectance measurements on kerogen and indigenous bitumen (R_o^k, R_o^{kb}, R_o^b), especially in the area where the Cambrian Henson Gletscher Formation is exposed;

2) study the migrated bitumens, both in order to use bitumen reflectance (R_o^B) in the maturity study (this chapter) and for a general discussion of the migration and diagenesis history (Chapter 7);

3) use fluorescence measurements as maturity indicators in these Early Palaeozoic sediments where most

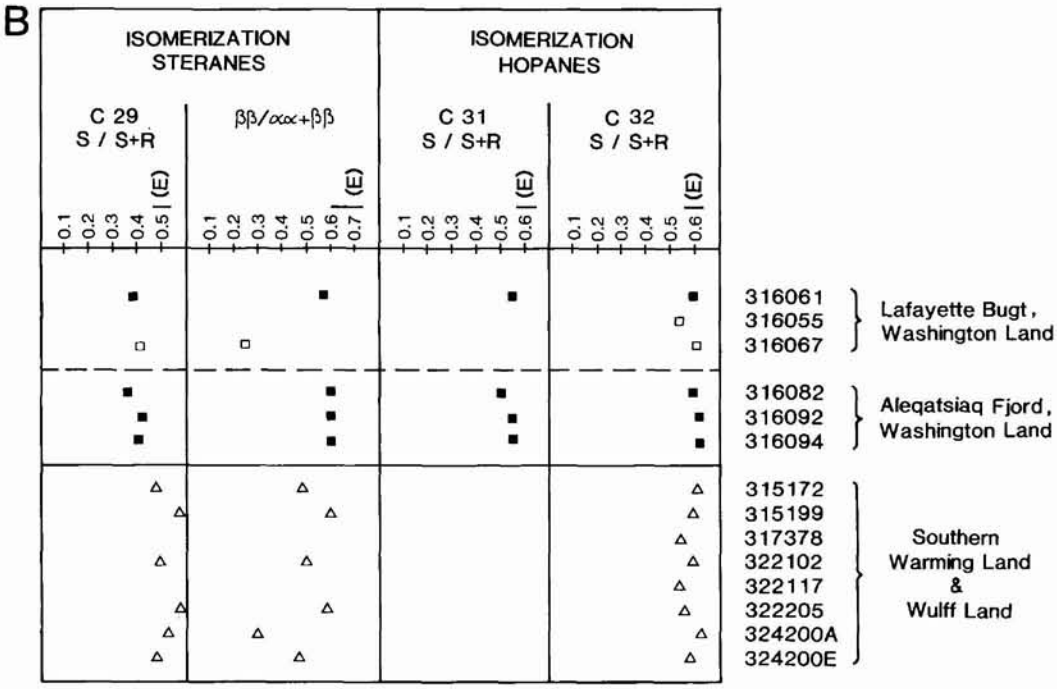

other organic petrological parameters are rather difficult to apply;

4) calibrate the until now little applied maturity parameter based on graptolite reflectance (R_{max}^G, or alternatively R_r^G or R_{min}^G) with other parameters.

Details are provided by Stouge *et al.* (1988) and Thomsen & Guvad (1987).

Due to lack of vitrinite *sensu stricto* in the Early Palaeozoic, the reflectance studies were restricted to kerogen and its maturation products, indigenous bitumen in the source rocks or migrated bitumen. Previous examples of reflectance measurements in Lower Palaeozoic sediments with relevance to the present work include studies of bitumen (Robert, 1974; Sikander & Pittion, 1978; Ogunyami *et al.*, 1980), graptolites and other zooclasts (e.g. Goodarzi *et al.*, 1985; Goodarzi & Norford, 1985; Bertrand & Heroux, 1987) and 'vitrinite-like compounds' in the kerogen (e.g. Kisch, 1980; Buchardt *et al.*, 1986).

The studied kerogen from North Greenland is amorphous (Type II) and derived from marine algae (Chapters 4 and 5). In terms of organic constituents it is dominated by the liptinite maceral group (Gutjahr, 1983). However, some stringers of vitrinitic type of organic matter are also observed. Measurements were carried out mainly on these stringers (R_o^k) and on the generated bitumen (R_o^b), in many cases, especially at higher maturities, with a common population (R_o^{kb}). Reflectance of migrated bitumen (R_o^B) may also be applied as a maturity parameter, and a linear relation between reflectance of true vitrinite and solid bitumen has been suggested (Jacob, 1985).

The reflectance values from the Cambrian sequence in Freuchen Land support the maturity trend outlined by screening methods (figs 29, 30 and 36). The values are, however, rather scattered making ranking based on single samples questionable. The reflectance of kerogen and migrated bitumen (R_o^k, (R_o^{kb}), R_o^B) seems to follow the same trend with a general increase from $R_o \sim 0.75\%$

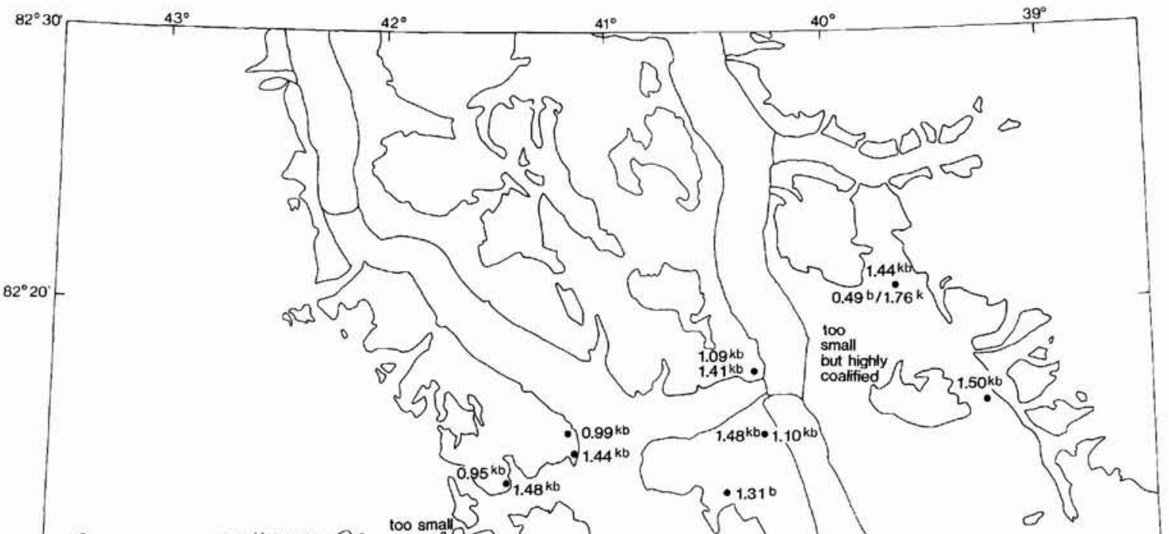

Fig. 29. Regional variation in reflectance values of shale and lime mudstone. R_o^k: reflectance of kerogen, R_o^b: reflectance of indigenous bitumen, R_o^{kb}: reflectance of kerogen and indigenous bitumen (one population in reflectogram); F: fluorescence of kerogen or indigenous bitumen.

(T_{max} < 440°C) in the southern part to $R_o \sim 1.75\%$ in the northern part of the area (T_{max} > 500°C) (figs 29 and 30). In contrast indigenous bitumen (R_o^b, (R_o^{kb})) often shows rather low values, even in highly mature areas, pointing towards a limited new generation of hydrocarbons late in the subsidence history.

In the remaining region a similar strong south to north gradient is supported by the reflectance values. All the samples from southern Warming Land and Wulff Land (T_{max} < 440°C) have R_o^B values in the range 0.1 to 0.5%. Also the Washington Land samples (T_{max} < 445°C) have low reflectance values with R_o^B from 0.15 to 0.6% and R_o^k, R_o^b and R_o^{kb} between 0.5 and 0.9% (figs 31, 32, 36, 37 and 38). In the mature to postmature areas in Nares Land, Wulff Land and Nyeboe Land significantly higher reflectance values have been recorded (figs 31 and 32).

Fluorescence of bitumen and liptinitic kerogen has only been reported from a limited number of samples, and systematic measurements of λ-max and Q values have only been carried out on bitumen samples from Washington Land, southern Freuchen Land and Nares Land (see details in Thomsen & Guvad, 1987).

Measurements of graptolite reflectance on a number of samples of Silurian shale with a regional distribution and a few Ordovician shales from the northern folded part of the region are included in the study.

Two of the measured parameters, R_{max}^G (maximum reflectance) and R_r^G (random reflectance), seem applicable in the regional maturity mapping and support the previously mentioned increase in maturity from south to north (fig. 33).

The lowest values are recorded from Washington Land (R_r^G < 0.77%, R_{max}^G < 0.87%), followed by southern Nares Land and southern Hall Land (fig. 33). The Silurian shales in the region between show higher, but relatively constant values. The few samples from the folded northern part of the region yield very high values of graptolite reflectance (R_r^G: 4.34–7.24%, R_{max}^G: 8.39–9.03%).

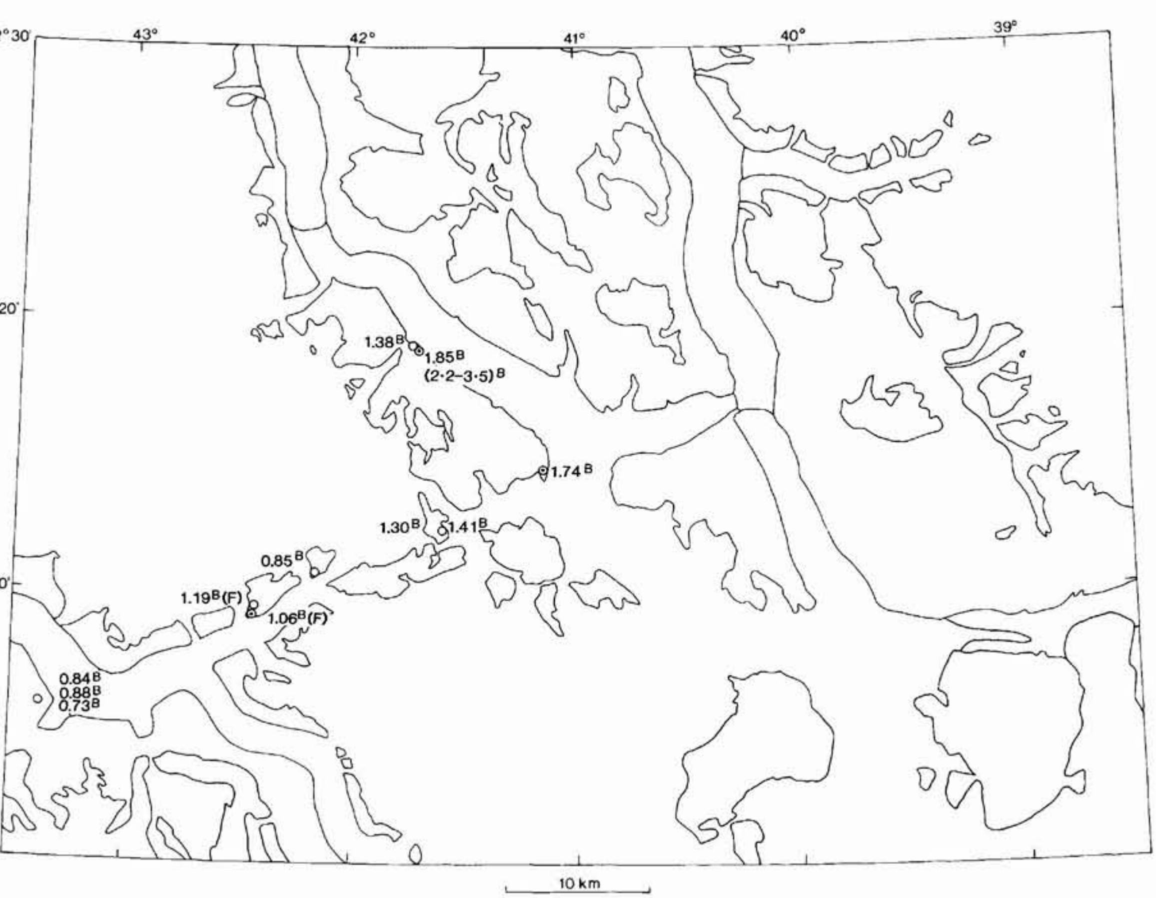

Fig. 30. Regional variation in reflectance values of migrated bitumen (circles with dots: macroscopic bitumen in vugs, veins; open circles: stained carbonates and sandstones). F: fluorescence of migrated bitumen.

Fig. 31. Regional variation in reflectance values of Silurian shales.

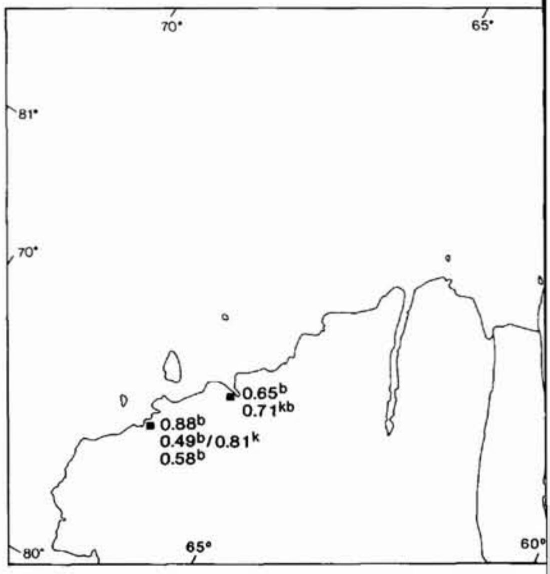

X-ray diffraction of kerogen

X-ray diffraction of kerogen provides a potential maturity indicator, although it has been little used in hydrocarbon studies (see Koch, 1987). The structural state of the kerogen, which changes with increasing thermal maturity, is described by employing two parameters d_{002} (d-spacing of 002 in 'graphite') and WHH_{002} (width at half height of the 002 peak in 'graphite') (see analytical details in Chapter 3; Wedeking & Hayes, 1981; Koch, 1987).

The material includes eight organic-rich Cambrian to Ordovician samples representing a profile with known increase in thermal maturity (figs 25 and 36) and seven organic-rich Silurian shales which are regionally scattered but easily ranked in order of increasing thermal maturity (figs 26 and 38; Koch, 1987).

The immature to early mature samples are characterized by very broad diffraction peaks, WHH values above 5, and an intense scattering in the angular range 10–30° 2θ (figs 34, 36 and 38). Samples with higher maturities (mature to postmature) show sharper diffrac-

Fig. 32. Regional variation in reflectance values of migrated bitumen (vugs, veins, stained carbonates and sandstones).

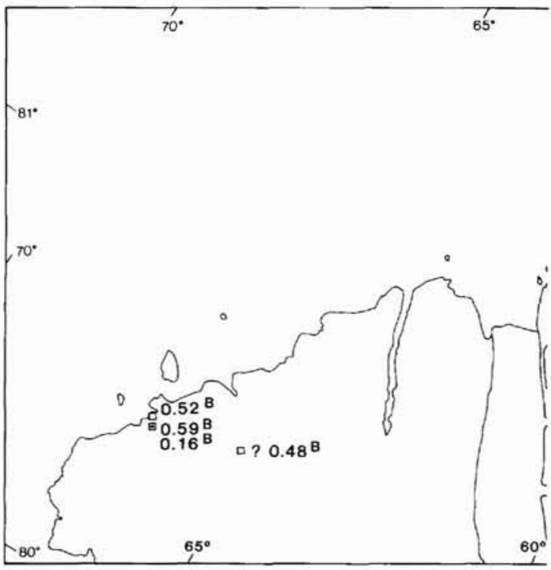

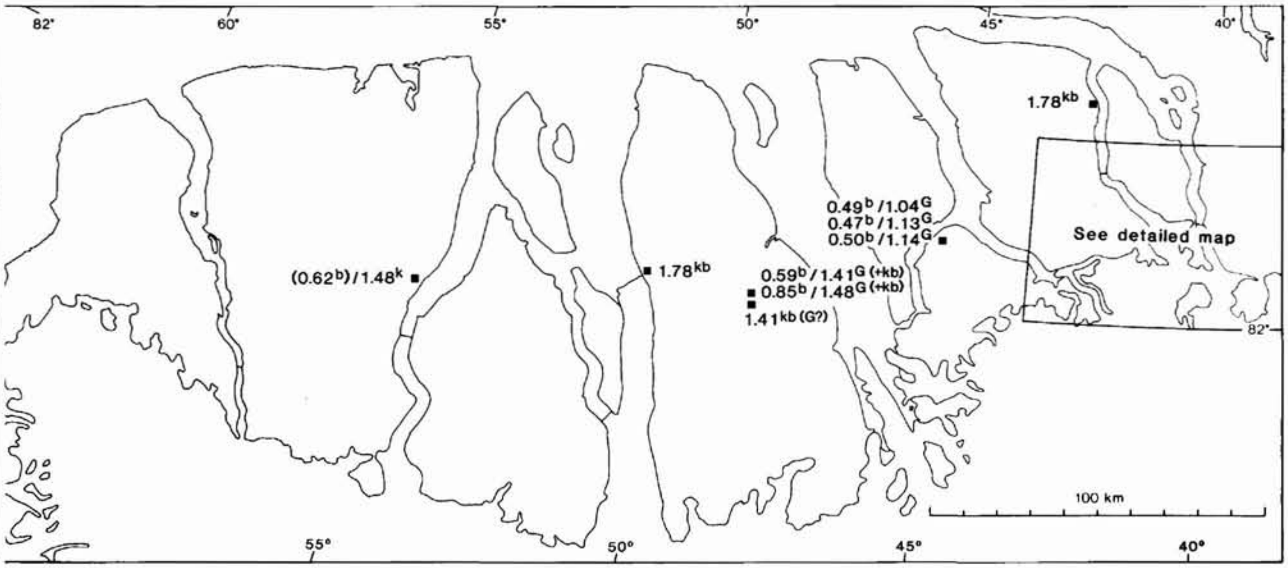

tion peaks, WHH values between 4 and 2.5, and a decrease in the scattering (figs 34 and 36). The two analysed postmature to low metamorphic samples have broad but well defined diffraction peaks, WHH between 4 and 5, and only little scattering (figs 34 and 36). The presence of 101 diffraction is noted in these samples.

Thermal maturity and the oil window

In the foregoing it has been demonstrated how each of the measured maturity parameters support the general mapped pattern of rapid increase in organic diagenesis from south to north. The parameters vary considerably in applicable range of maturity as well as in exactness. Only a few of the parameters provide specific information on the four most important thresholds in petroleum exploration: (1) onset of petroleum generation, (2) peak generation, (3) end of petroleum generation, (4) end of petroleum preservation.

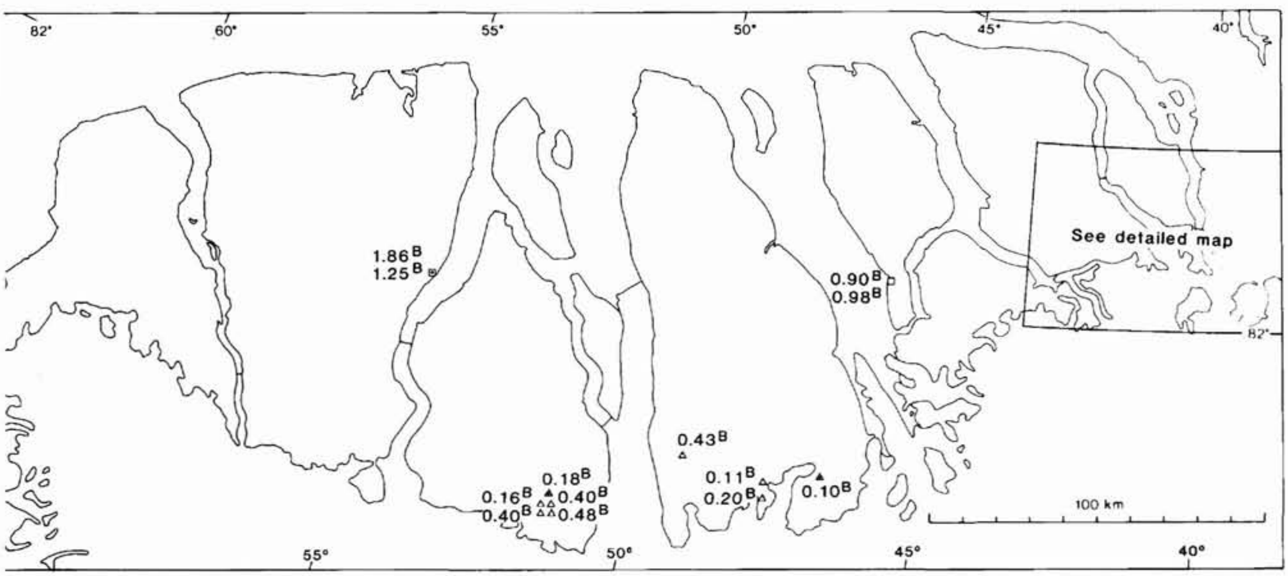

Fig. 33. Regional variation in reflectance values of graptolites.

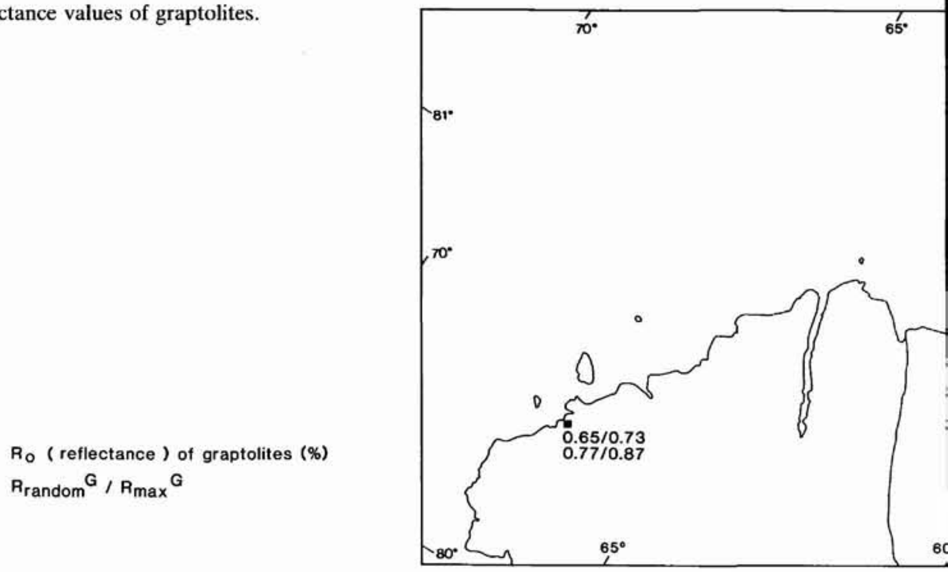

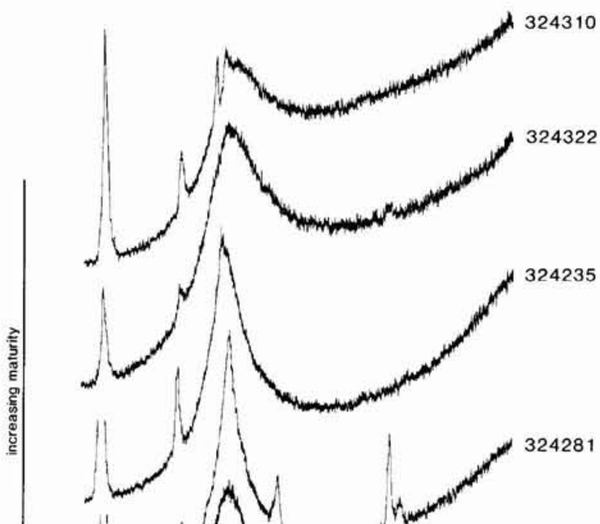

Fig. 34. X-ray diffractograms of Cambrian samples ranked in order of increasing thermal maturity (from south to north).

In North Greenland where the distribution and maturity gradient of source rocks are known in considerable detail, the generation of petroleum is systematically registered as a decrease in residual potential of the kerogen and as an increase in hydrocarbon content of the source rocks.

The variation of these factors with increasing thermal maturity, in this case expressed as T_{max} values, is shown as circumscribed curves of the Hydrogen Index, S1/TOC, and SOM/TOC (fig. 35). The Hydrogen Index curve, which reflects the residual generation potential of the organic matter, decreases drastically between T_{max} values of 438°C and 445°C ('peak generation'). The onset value is not known exactly but probably corresponds to a T_{max} value of ~ 435°C. No significant potential is present at maturities higher than a T_{max} of 460°C to 470°C ('end of generation'). The other two curves reflect the presence of generated hydrocarbons in the source rocks, either as the bitumen transformation ratio (mg SOM/g TOC) or as the Rock Eval parameter S1/TOC. Despite differences in number of analysed samples and in the techniques themselves, the two curves are similar (fig. 35). Maximum values are obtained at conditions corresponding to 'peak generation' and 'just after peak generation' (T_{max}: 440°C to 455°C). The petroleum content is drastically reduced at maturities between T_{max} of 470°C and 475°C ('bottom of preservation') and virtually no petroleum is preserved at T_{max} values higher than 485°C (fig. 35).

Although the two generation curves follow the classical 'Phillippi-trend' it must be noted that one quantitative difference from other petroleum provinces is that

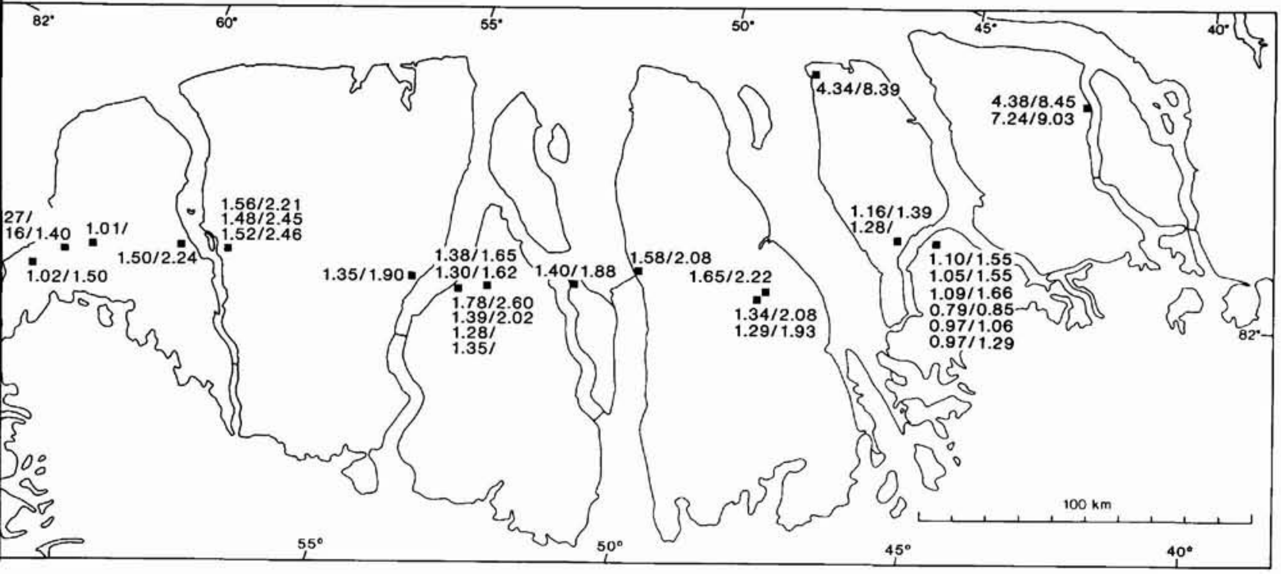

the highest bitumen ratios observed in North Greenland are only about 60 mg SOM/g TOC compared to maximum values between 150 and 200 in many other basins (Tissot & Welte, 1984). These high values are often from actively generating and expelling source rocks, conditions which the North Greenland source rocks reached during the Devonian (?) (see Chapter 8 for further discussion). Since that time significant amounts of hydrocarbons have been lost by further migration and degradation, by surface alteration and evaporation.

The interpretation of generation/degradation with increasing thermal maturity is further supported qualitatively by direct observation of petroleum or its altered relicts in the field, in palynological preparations and in polished samples. The decrease in generation potential of the kerogen is also observed as increasing coloration, degradation and reflectance. However, threshold values for onset, peak and end of generation can only be determinated empirically by comparison with the above-mentioned parameters.

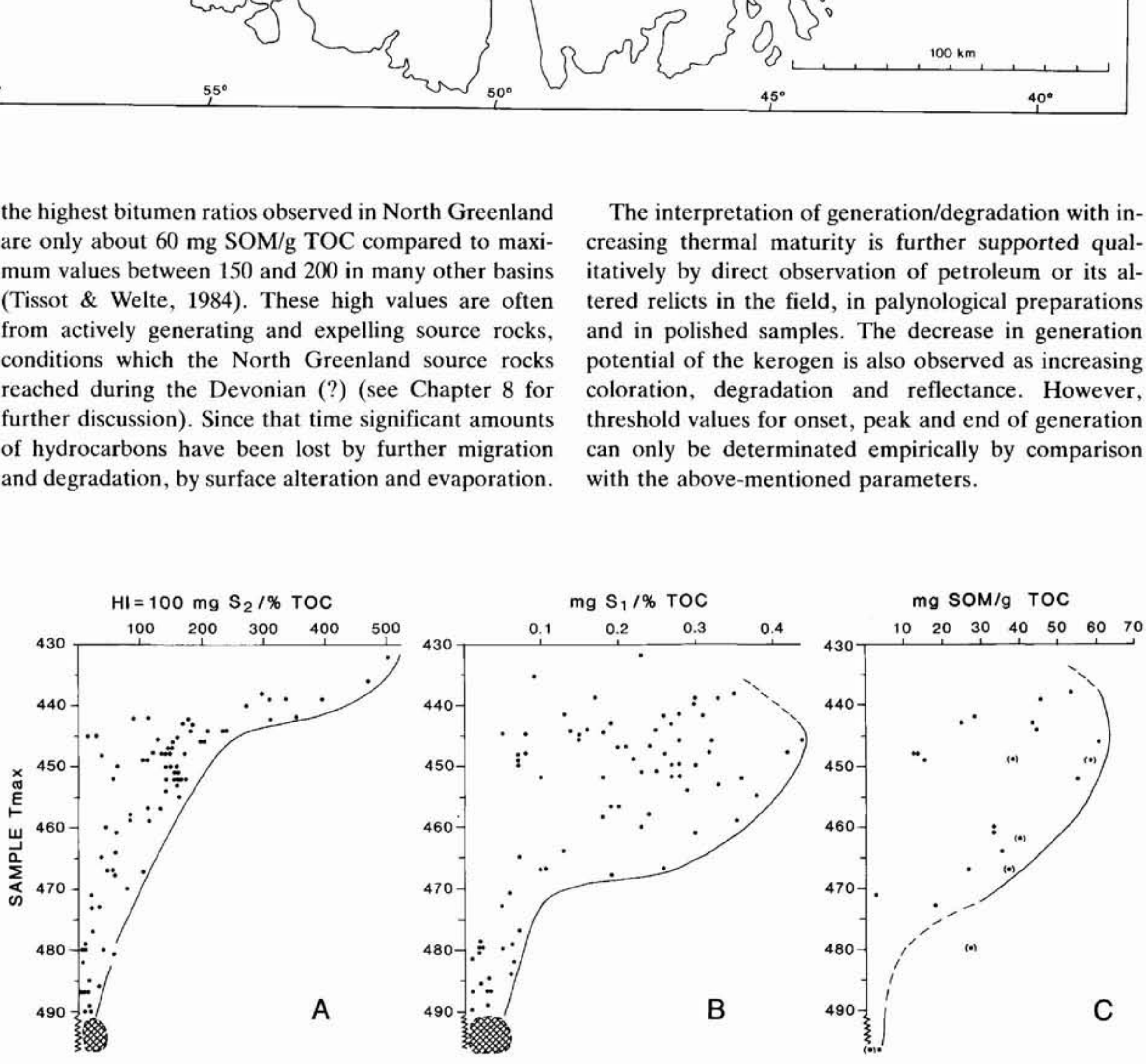

Fig. 35. Plots of hydrocarbon generation parameters versus thermal maturity (sample T_{max}) for Cambrian and Silurian source rocks. (A) Hydrogen Index (100 × mg S_2/% TOC), only samples with TOC > 2.0% are included. (B) (mg S_1/% TOC), only samples with TOC > 2.0% are included. (C) Extractability (mg SOM/g TOC), samples with TOC < 2.0% are in parenthesis.

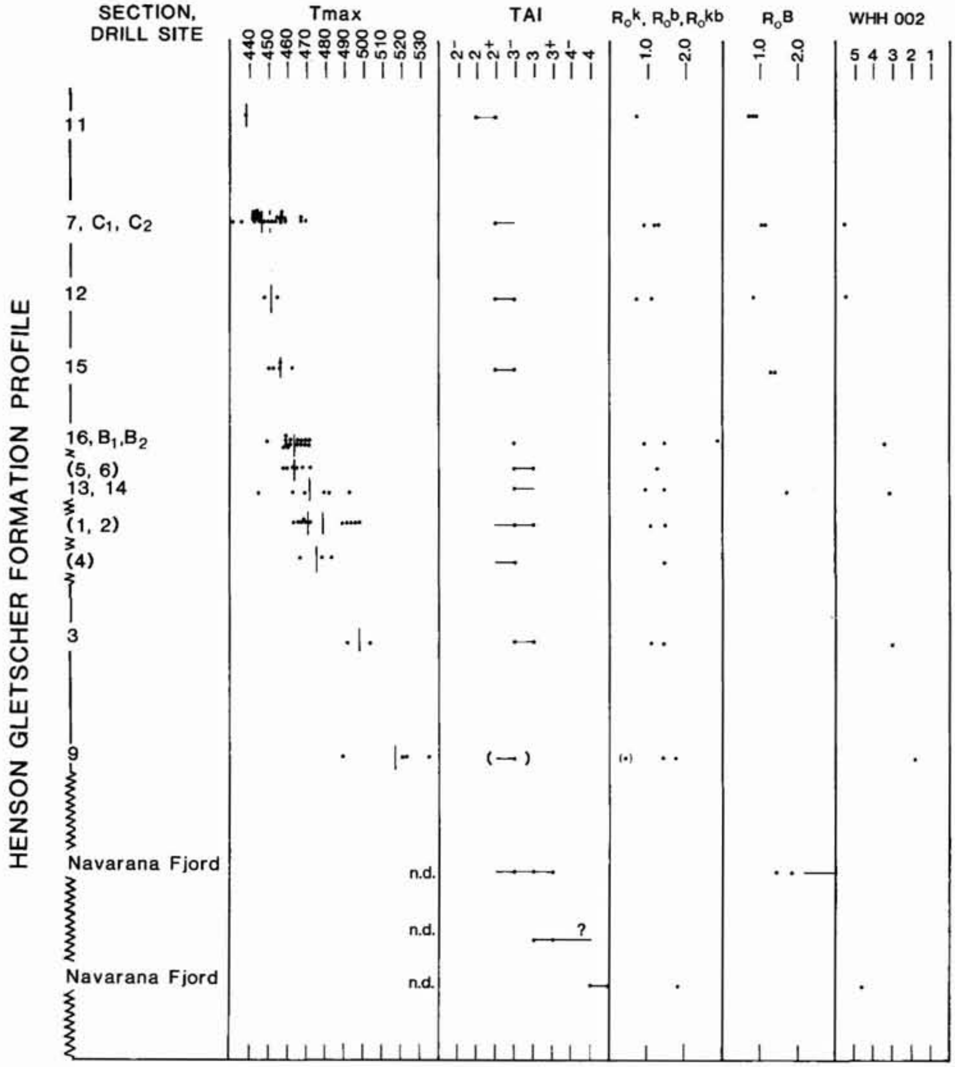

Fig. 36. Maturity profile through the area where the Henson Gletscher Formation is exposed showing the relations between most of the measured maturity parameters. See fig. 25 for location.

Empirical correlation of maturity parameters

The empirical relations between the maturity parameters employed are illustrated in various ways as profiles, composite profiles, cross plots and finally as a synoptic figure.

Two profiles at an oblique angle to the maturity trend illustrate the scatter and the sensitivity of the measured values. One of them is from the area where the Henson Gletscher Formation is exposed (fig. 36), the other is from the Silurian shales outcrop area in Washington Land and Hall Land (fig. 37). Similar information is shown in the composite profile (fig. 38) where subareas with outcropping Silurian shales are ranked in order of increasing maturity (based on T_{max} average values). All three profiles illustrate that a large number of analyses are necessary, and that none of the methods are fully adequate by itself.

A number of cross plots are included to show the direct relations between measured maturity indicators, especially of T_{max} versus other parameters. Fig. 39 shows the relation between calculated T_{max} average values (Reg. T_{max}) and T_{max} values for individual samples. In many subareas, especially with T_{max} below 460°C, only minor variation is observed. A number of observed anomalies (I, II and III) will be discussed in the following section.

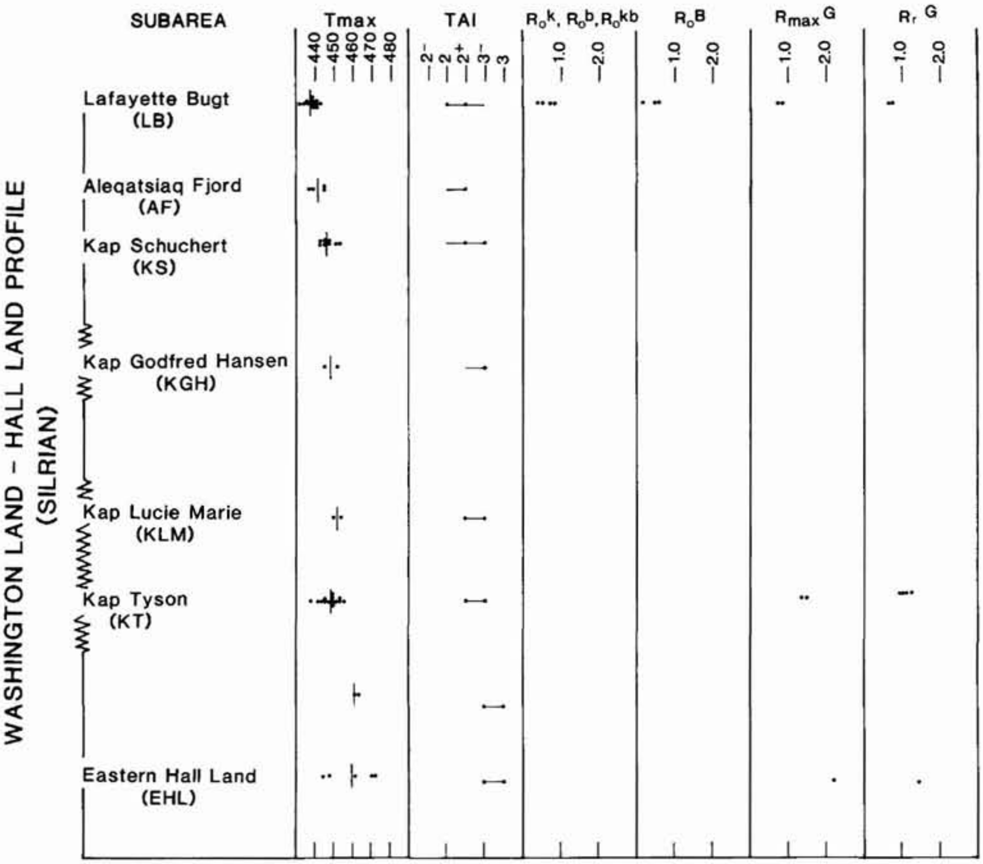

Fig. 37. Maturity profile through western Washington Land and Hall Land showing the relations between most of the obtained maturity parameters. See fig. 26 for location.

A consistent relation between Reg. TAI values and Reg. T_{max} is observed (fig. 40). The TAI values are most sensitive at early to peak generation (below T_{max} of 450°C) and at the beginning of metamorphism with only little distinction between.

The relation between reflectance of kerogen (R_o^k and R_o^{kb}) and Reg. T_{max} or sample T_{max} is not sufficiently clear to be easily applicable. A considerable scattering around a roughly linear (?) correlation may be suggested (fig. 41).

Reflectance of migrated bitumen (R_o^B) is much more sensitive to increasing thermal maturity and displays a well defined correlation with the Reg. T_{max} (fig. 42). The reflectance of graptolites, whether expressed as R_r^G or as R_{max}^G, shows a distinct correlation with measured T_{max} values (fig. 43). Both graptolite parameters are very sensitive in the T_{max} range from 435°C to 460°C and show a dramatic increase in postmature to low metamorphic rocks.

There is also a consistent relation between the regional T_{max} values and WHH_{002} with a roughly linear trend in the T_{max} range from 450°C to 520°C and the high, but scattered, WHH values at $T_{max} < 450$°C (fig. 44). The pattern of high WHH values in the postmature samples from the northern part of the region is not fully outlined but appears comparable to the results by Wedeking & Hayes (1983).

All measured parameters with increasing maturity showing onset, peak, end of oil generation, end of oil preservation and beginning of metamorphism are compiled in fig. 45. Note the following empirically determined threshold values which seem to be valid for both the Cambrian and the Silurian source rocks in North Greenland:

Onset of petroleum generation: Reg. T_{max}: 435–437°C, TAI: 2^-–2, R_o^k: 0.5–0.8, R_o^B: 0.1–0.5, R_{max}^G: 0.5–0.9, R_r^G: 0.5–0.7, WHH: > 6.

Peak generation: Reg. T_{max}: 440–445°C, TAI: 2–2^+, R_o^k: 0.7–1.0, R_o^B: 0.5–1.0, R_{max}^G: 0.7–1.2, R_r^G: 0.6–1.1, WHH: 4.5–6.

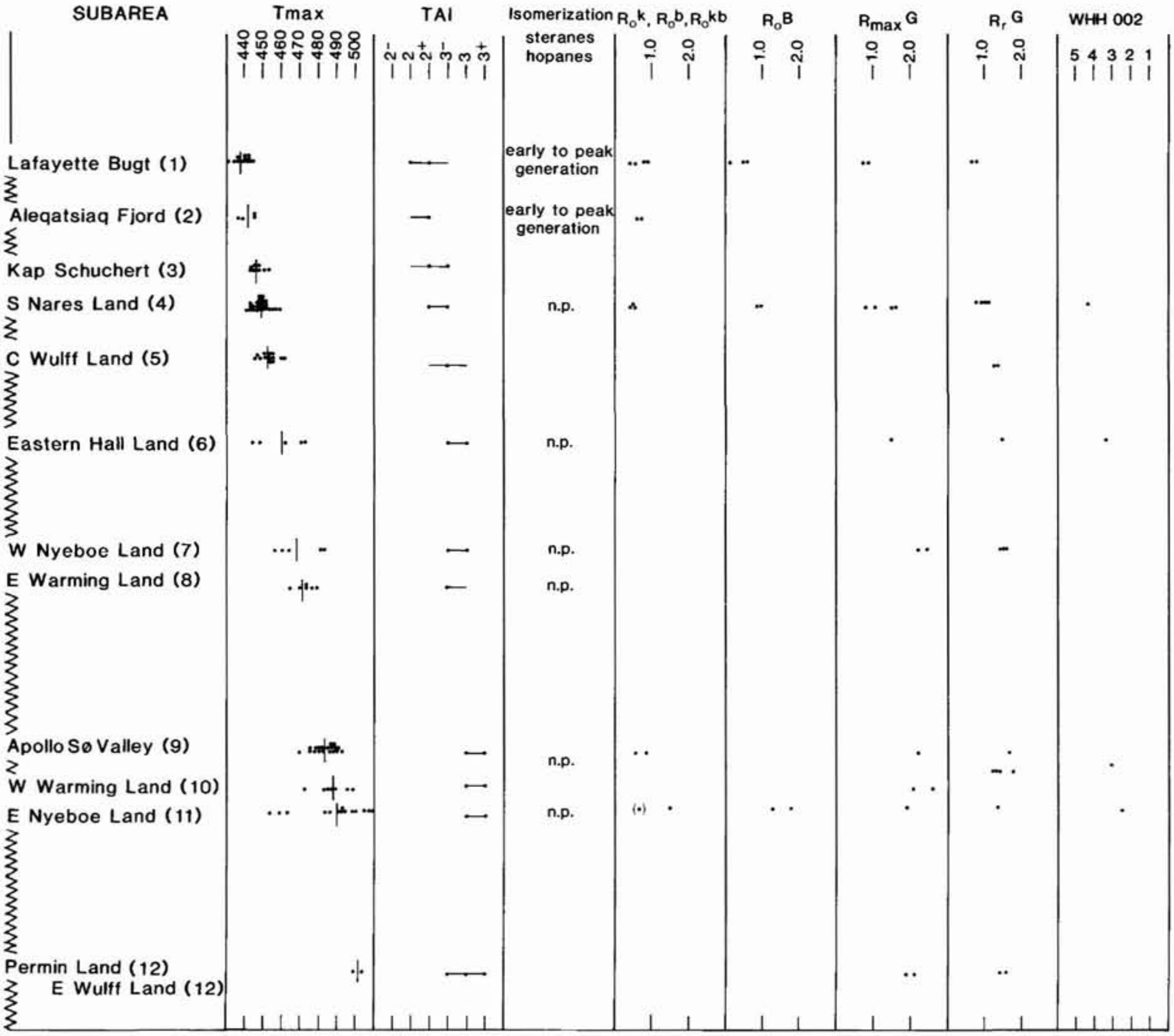

Fig. 38. Composite maturity profile of the Silurian shales showing the relations between most of the measured maturity parameters. The ranking of the different subareas is based on T_{max} data. The location of the areas is shown (with number) in fig. 26.

End of generation: Reg. T_{max}: 465°C, TAI: 3^-–3, $R_o{}^k$: 1.0–1.5, $R_o{}^B$: 1.0–1.5, $R_{max}{}^G$: 1.4–2.4, $R_r{}^G$: 1.1–1.6, WHH: 4–3.5.

End of preservation: Reg. T_{max}: 475°C, TAI: 3^-–3, $R_o{}^k$: 1.1–1.6, $R_o{}^B$: 1.2–1.8, $R_{max}{}^G$: 1.5–2.5, $R_r{}^G$: 1.2–1.7, WHH: 3.5–3.

These threshold values and the empirical relations between the measured maturity indicators in general are comparable with many previously proposed maturation schemes (e.g. Dow, 1977; Heroux *et al.*, 1979; Tissot & Welte, 1984; Bustin *et al.*, 1985a,b; Macauley *et al.*, 1985). However, a number of minor differences should be noted:

1) Large variation in reflectance values of kerogen in North Greenland and relatively low values of the preservation limit.

2) A surprisingly good correlation of $R_o{}^B$ (reflectance of migrated bitumen) with other parameters.

3) Lack of fluorescence in many early mature to mature source rocks.

4) A systematic and good correlation between WHH_{002} and other indices throughout the maturity scale.

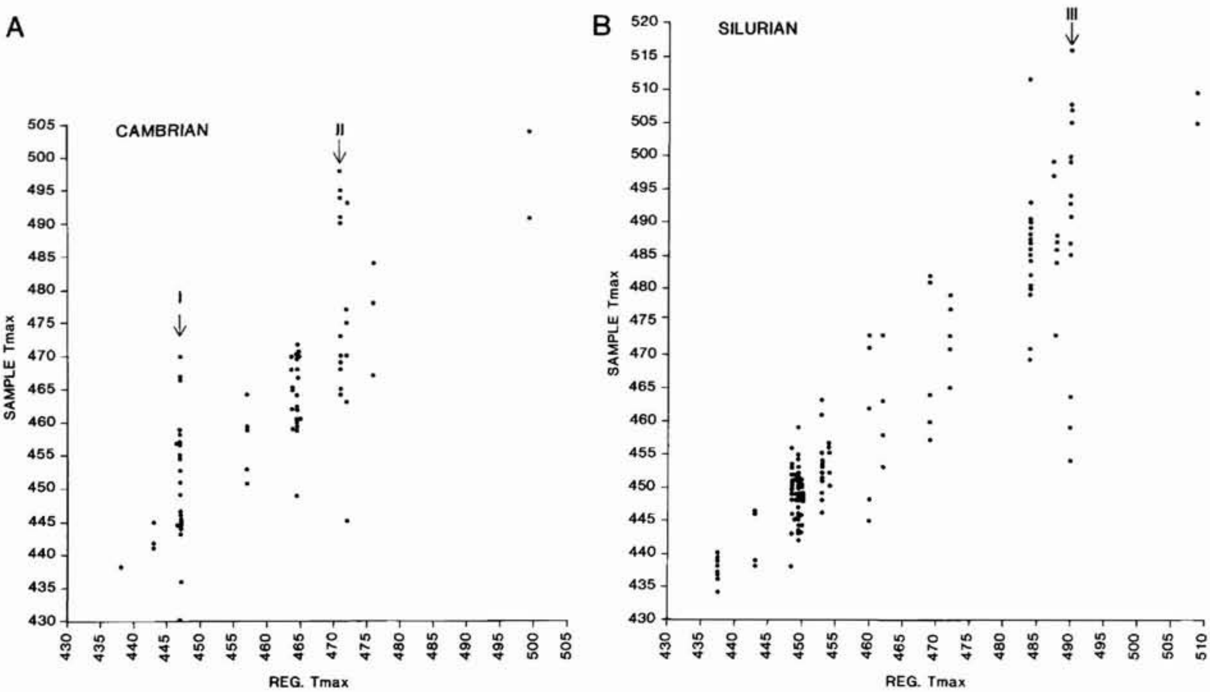

Fig. 39. Relation between calculated T_{max} average for subareas (Reg. T_{max}) and T_{max} of individual samples. A: Cambrian source rocks; B: Silurian source rocks. The Roman numbers refer to areas with thermal maturity anomalies (see figs 25, 26 and 46).

The above compilation illustrates that the various parameters applied vary considerably in exactness, sensitivity and range of application. All the recorded parameters are very sensitive and applicable in the range from early mature to peak generation conditions. In the range from peak to late or end of generation only a few of the data available provide a significant distinction (mainly T_{max} and WHH, to a lesser degree R_o^B). In the

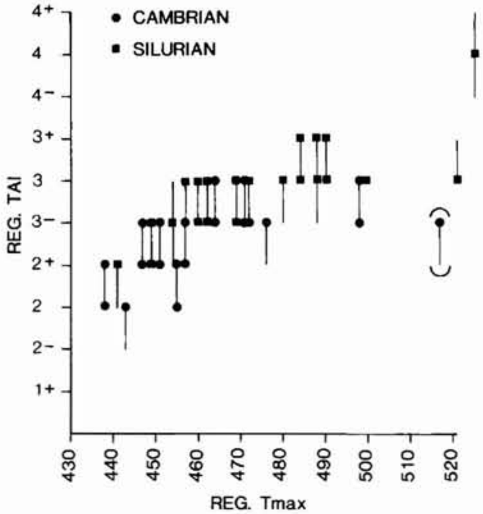

Fig. 40. Relation between Reg. T_{max} and Reg. TAI.

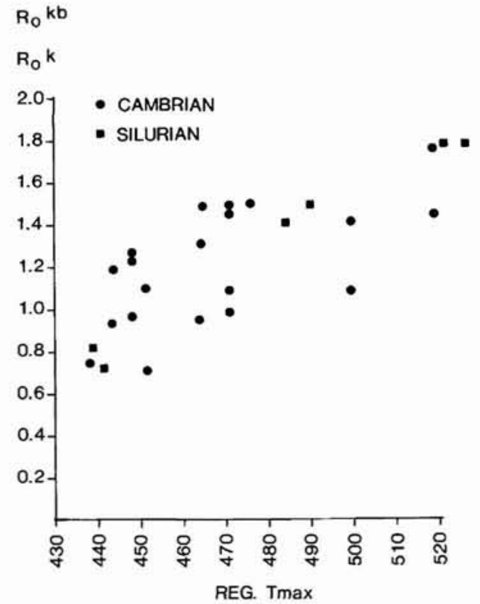

Fig. 41. Relation between Reg. T_{max} and reflectance of kerogen and indigenous bitumen (R_o^k and R_o^{kb}).

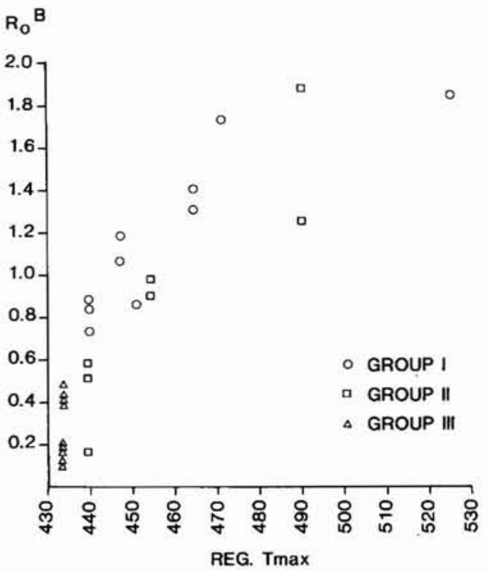

Fig. 42. Relation between Reg. T_{max} and reflectance of migrated bitumen (R_o^b).

postmature to low metamorphic range detailed mapping seems difficult due to the loss of hydrocarbons (no T_{max}). Some of the reflectance values (R_{max}^G, R_o^G, R_o^B, (R_o^{kb})) and WHH are the most sensitive parameters in this range.

Local maturity anomalies

Although most of the data presented support a very distinct maturity pattern, a number of anomalies have been recorded in the form of either single sections, localities, or smaller areas. The anomalies were detected by variation in T_{max} or occasionally in TAI, and later supported by reflectance and GC analyses.

Two obvious examples occur in the Cambrian sequence, and two more in the Silurian. In the area around the type section of the Henson Gletscher Formation (fig. 25) the T_{max} values are very scattered. Samples with well defined S2 peaks have T_{max} close to 470°C whereas other samples have considerably higher values in the range 480°C to 490°C (figs 36 and 39). These local high maturation values are probably associated with the

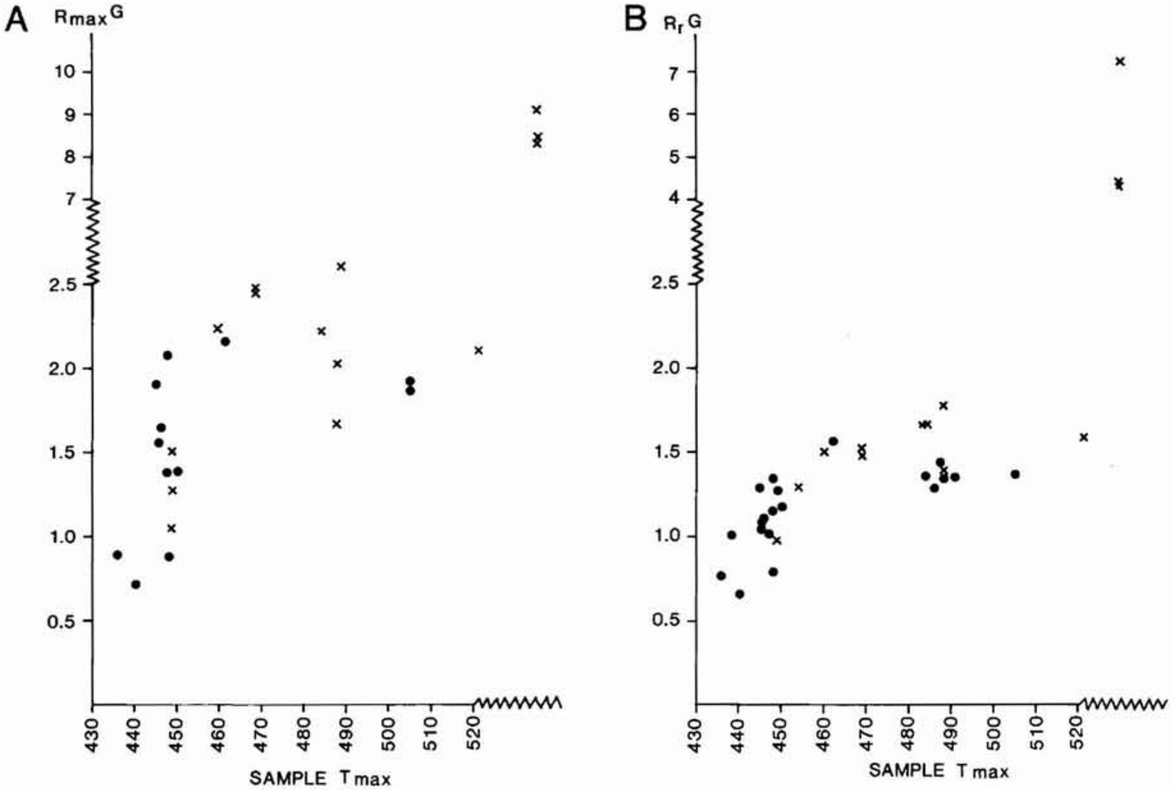

Fig. 43. Relation between T_{max} and reflectance of graptolites. (A) Sample T_{max} (dots; crosses are regional values from samples without any measured or defined T_{max} value) versus R_{max}^G. (B) Sample T_{max} (dots; crosses are regional values from samples without any measured or defined T_{max} value) versus R_r^G.

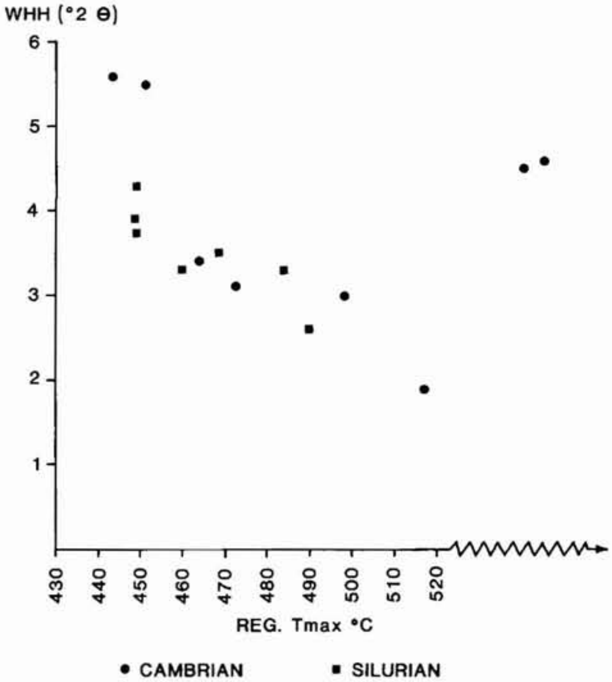

Fig. 44. Relation between Reg. T_{max} and X-ray diffraction of kerogen (WHH_{002} = width at half height).

fault zones or basic dykes present in the area. Also the area around the C1 and C2 drill sites (fig. 25) displays scattered T_{max} values. In this case the well defined T_{max} values close to 445°C are from the uppermost shales of the Henson Gletscher Formation, whereas the lower shales have higher and poorly defined values in the range 455°C to 470°C.

Both Silurian anomalies show a striking variation in maturity depending on stratigraphic and topographic height (fig. 46). At two locations, around the N1 and N2 drill sites in eastern Nyeboe Land and in central Wulff Land (the valley compared to neighbouring hills), the shales overlying the carbonate shelf sequence have a very high maturity (T_{max} 480°C) and those a few hundred metres higher a considerably lower maturity (fig. 46). These systematic differences are comparable to those at the C1–C2 locality and are too large to be caused by differences in subsidence depth and too well documented to be caused by analytical errors.

The local high maturity of the lowermost shales is more likely to be the result of major shearing/thrusting along the contact zone between carbonates and shales which may represent a major décollement surface (Larsen & Escher, 1985), or as interaction of hot basinal fluids penetrating through the same zone. In the case of

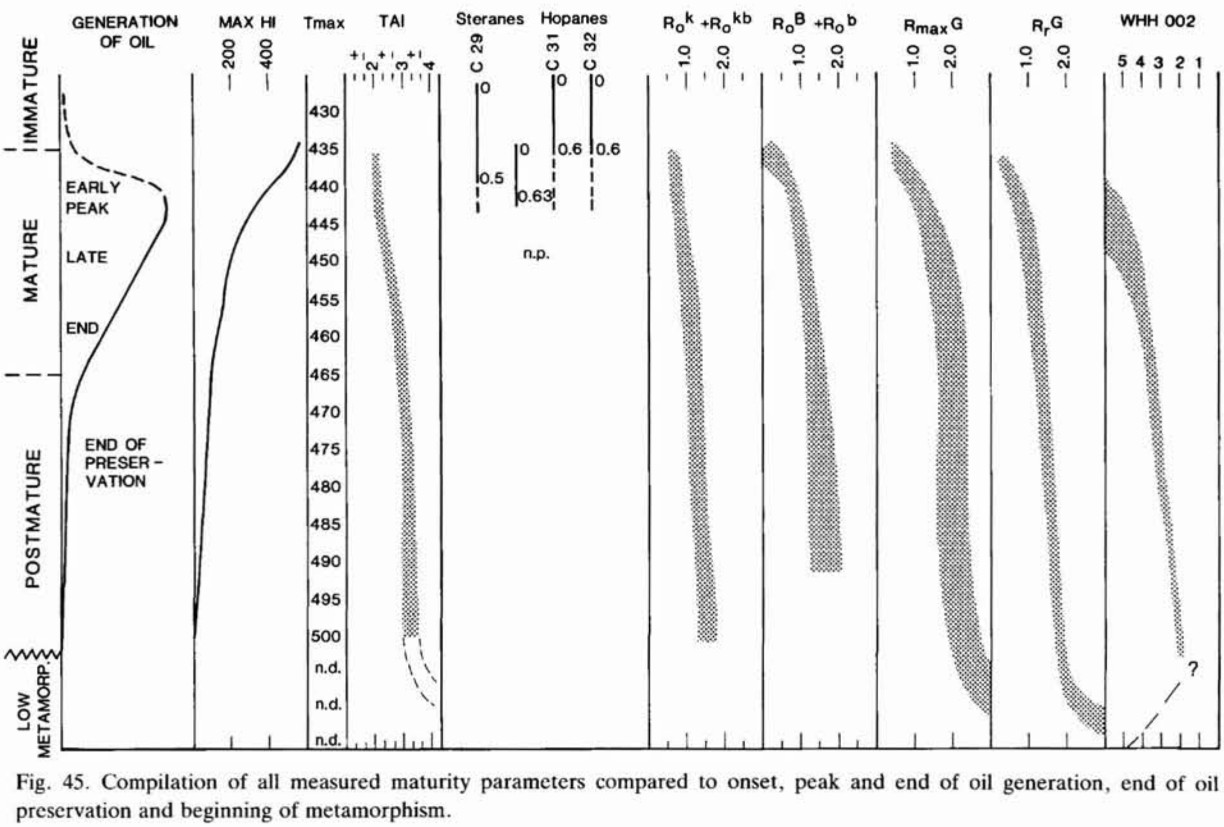

Fig. 45. Compilation of all measured maturity parameters compared to onset, peak and end of oil generation, end of oil preservation and beginning of metamorphism.

the valley in central Wulff Land an additional factor may have been a fault/joint zone striking parallel to the lake, which could also have permitted migration of hot fluids.

Thermal maturity of the Peary Land region

In the Peary Land region the available data are less systematic as regards both regional distribution and measured parameters. However, knowledge of the distribution of potential source rocks and their thermal maturity pattern west of this region allows a re-evaluation of analytical work carried out previously by Rolle (1981) and Rolle & Wrang (1981).

The Silurian deep-water sequence including organic-rich shales can be traced for at least 250 km east of Freuchen Land before it is overlain/truncated by thermally immature to mature Upper Palaeozoic and Mesozoic sediments (fig. 47; Christiansen *et al.*, in press). The Henson Gletscher Formation can only be traced for about 80 km in the western part of Peary Land and the lack of organic-rich units in the Cambrian shelf sequence further east makes detailed maturity mapping difficult.

More than 120 samples of Lower Palaeozoic sediments from the Peary Land region were analysed with GC (Rolle & Wrang, 1981) and the same samples have since been complemented by Rock Eval analyses. A small number of additional samples have been analysed recently by various other methods.

All of the studied Silurian shales have, despite reasonably high TOC contents (1–3%), virtually no generation potential (S2 < 0.1 mg HC/g sample), very low extractabilities (< 10 mg SOM/g TOC), no defined T_{max} values, and are consequently considered as postmature or even low metamorphic (fig. 47).

Most other samples with TOC > 1% are from the Brønlund Fjord Group, especially from the Henson Gletscher Formation, and are, with the exception of one locality, included in the 'Nordolie' study area (see figs 15, 19 and 30). In the Løndal area, just south of Hans Tavsen Iskappe (fig. 47), the Henson Gletscher Formation seems early mature with a T_{max} average of 441°C, high extractability, preserved cyclic biomarkers, and a high generative potential (S2 up to 25 mg HC/g sample, HI up to 300).

Organic-rich shales (1–10% TOC) from the Ordovician Vølvedal and Amundsen Land Groups occurring in Johannes V. Jensen Land are postmature to low metamorphic with no defined T_{max} values and very low extractabilities (fig. 47). One sample containing highly coalified impsonite has a R_o^b of 4.70 (Thomsen & Guvad, 1987) corresponding to a vitrinite reflectance of approximately 3.3 using the equation of Jacob (1985).

Most of the remaining samples provide very little information on the thermal maturity due to their low organic carbon and hydrocarbon content. The presence of minor amounts of migrated bitumen cannot be excluded, the gas chromatograms of these samples all have a strong light-end bias suggesting a high maturity.

Despite the limited data base, it is concluded that the

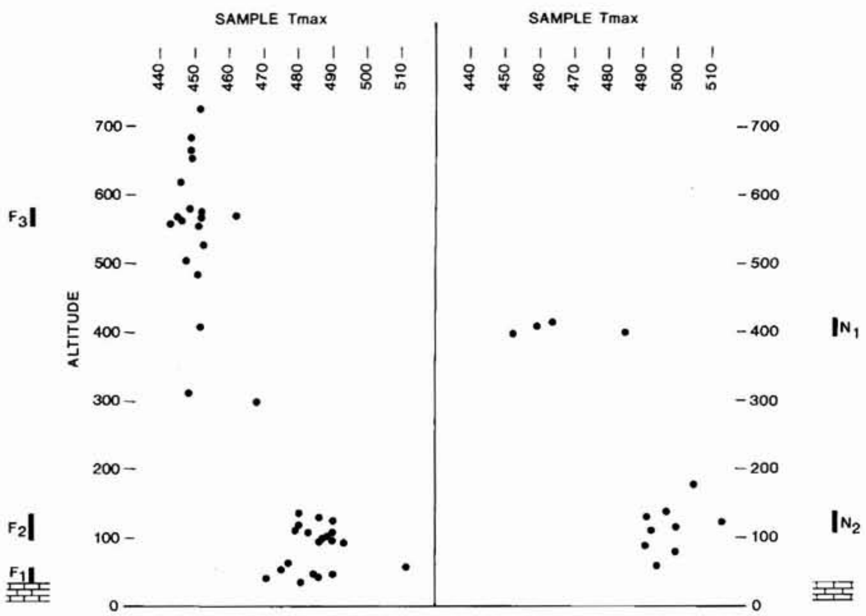

Fig. 46. Variation in maturity (T_{max}) with increasing vertical distance from the shale-carbonate contact in central Wulff Land and eastern Nyeboe Land. F_1, F_2, F_3, N_1 and N_2 indicate cores.

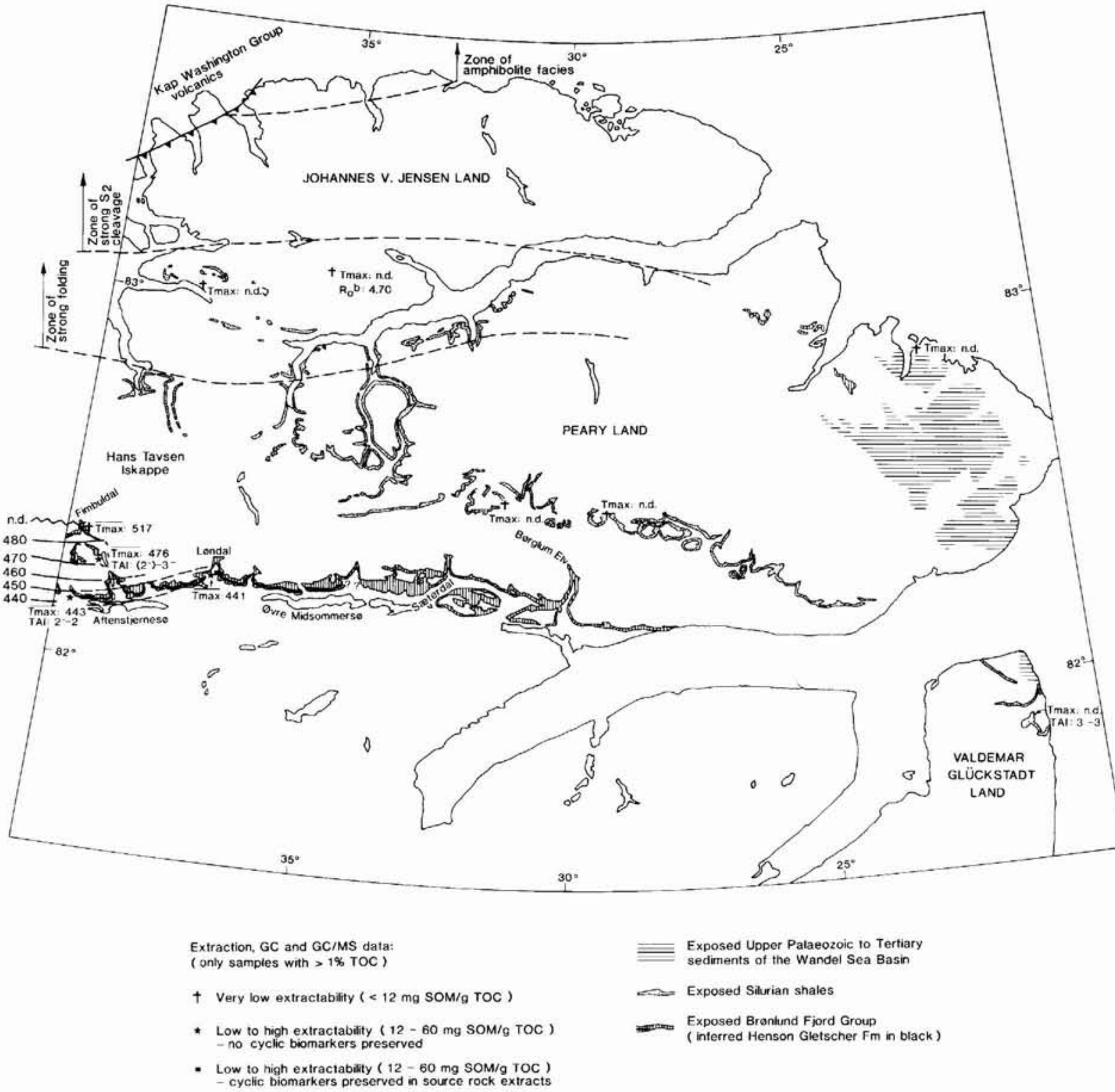

Fig. 47. Simplified map of the Peary Land region based on Geological Map of Greenland 1:500 000 sheet 8, Peary Land. The distribution of Silurian shales (stippled), the Cambrian Brønlund Fjord Group with the Henson Gletscher Formation (vertically hatched/black) and Upper Palaeozoic, Mesozoic and Cenozoic Wandel Sea Basin sediments (horizontally hatched) is indicated. Furthermore the following maturity values are shown: T_{max} (e.g. 441 or n.d.), TAI, reflectance of bitumen/kerogen, extractability (very low: cross, low to high: star; only shown for samples with more than 2% TOC). The tectono-metamorphic zones are taken from Higgins *et al.* (1985).

northern postmature (to low metamorphic) zone of central and western North Greenland continues eastwards where it covers all of Johannes V. Jensen Land and most, if not all, of the southern part of Peary Land. The expected transition to mature or immature areas towards south cannot be mapped with the data available.

Summary

The thermal maturity pattern of the organic-rich units in North Greenland has been mapped by screening methods and later by a number of other, more sophisticated, methods. All measured maturity indicators have been empirically correlated with special emphasis on

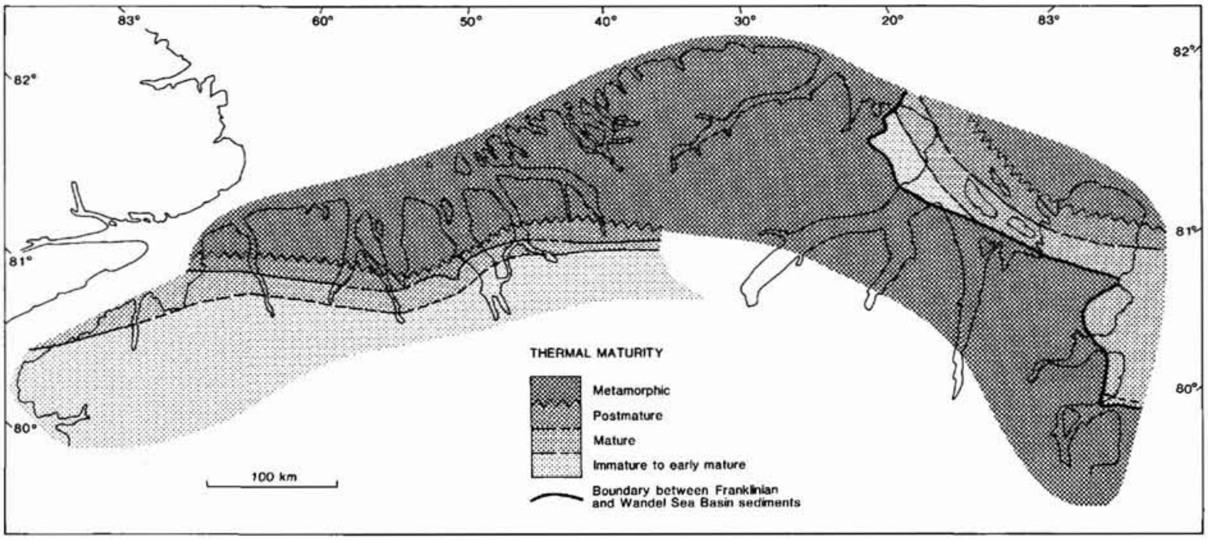

Fig. 48. Simplified thermal maturity map of North Greenland based on all available data. The Lower Palaeozoic pattern is based on data from the present chapter, Upper Palaeozoic and Mesozoic values are from Christiansen *et al.* (in press).

threshold values for (1) onset of petroleum generation, (2) peak generation, (3) end of generation and (4) end of petroleum preservation.

Generally a consistent and simple maturity pattern is observed, with the exception of a few maturity anomalies probably caused by intrusions or tectonism. The regional pattern is simplified in fig. 48 which shows a very large northern area, which is considered as low metamorphic in terms of organic diagenesis. South of this zone, two relatively narrow east–west trending zones with thermally postmature and mature surface rocks are defined. The southern part of the region includes thermally immature to early mature surface rocks.

Chapter 7

Bitumen occurrences

F. G. Christiansen, B. Buchardt, J. Jensenius, H. F. Jepsen, H. Nøhr-Hansen, E. Thomsen and P. Østfeldt

The previous chapters have demonstrated the existence of two potential source rock units in North Greenland and a thermal history which suggests that significant amounts of hydrocarbons were once generated.

For any future exploration in the region the direct evidence of generation and migration, namely bitumen occurrences, provides important additional information for the source rock study. Although highly sophisticated geophysical methods dominate petroleum exploration today, the importance of oil seeps and visual bitumen must not be underrated. Many of the important oil-producing regions of the world were first discovered through surface seeps, and in an undrilled sedimentary basin the existence of seeps is the first and only indication that petroleum is present. In the late 1800s and early 1900s seeps were the main factor in localizing drill sites (Moore, 1984). Since that time structural analyses, firstly on the basis of surface and well data and secondly from geophysical data, have played an ever increasing role. Surface indications are, however, particularly common in folded, faulted and deeply eroded sediments and consequently still important in areas with these characteristics (Link, 1952; Hunt, 1979) like most onshore basins in Greenland.

Terminology

The terminology of solid bitumen and similar substances is complicated, confusing and dependent on the mode of information. The traditional classification scheme is based on solubility, fusibility and H/C ratio (see Rogers *et al.*, 1974; Hunt, 1979). More recent classifications are based on either detailed geochemistry (Curiale, 1986) or fluorescence/reflectance values (Jacob, 1983, 1985).

In the present study the term bitumen is used for products of once-liquid oil (more or less thermally altered and/or biodegraded) which was generated and migrated from a source rock. Most bitumens are due to the generally high thermal maturity of the source rocks (see Chapter 6) considered as the 'allochthonous' post-oil type (Curiale, 1986).

In the field, a distinction was made between bitumen-stained samples (dark sandstones or carbonates, often with a petroliferous odour), macroscopic hard solid bitumen, and macroscopic soft to seeping asphalt. Geochemically, bitumen is considered as the soluble extractable organic matter from any of the three above distinct types and is described by conventional analytical parameters. Microscopically, bitumen is defined as the dark porous-filling organic matter of migrational origin. In polished sections the bitumen is classified using reflectance and fluorescence values (Jacob, 1985). With increasing thermal alteration (and biodegradation?) the reflectance increases and the fluorescence decreases giving the following rank in classification: asphalt, gilsonite, glance pitch, albertite, grahamite, epi-impsonite, cata-impsonite.

Stratigraphic and geographic distribution

Migrated hydrocarbons and their altered remains, observed as black asphalt and solid bitumen or as oil-stained limestone and sandstone, have been reported from numerous localities in central and western North Greenland. Stratigraphically and geographically three main relations of appearance are distinguished (fig. 49).

Group I: Migrated hydrocarbons associated with source rocks in the Cambrian Henson Gletscher Formation.

Group II: Migrated hydrocarbons associated with source rocks in the Silurian shales.

Group III: Migrated hydrocarbons which are not closely associated with any known source rocks. Restricted to Cambrian sediments in the southern part of the region.

The bitumens of *group I* are closely associated with the known source rocks in the Henson Gletscher Formation (Chapter 2; Christiansen *et al.*, 1987). Most

Fig. 49. Bitumen occurrences in North Greenland. Group I (circles), group II (squares), group III (triangles).

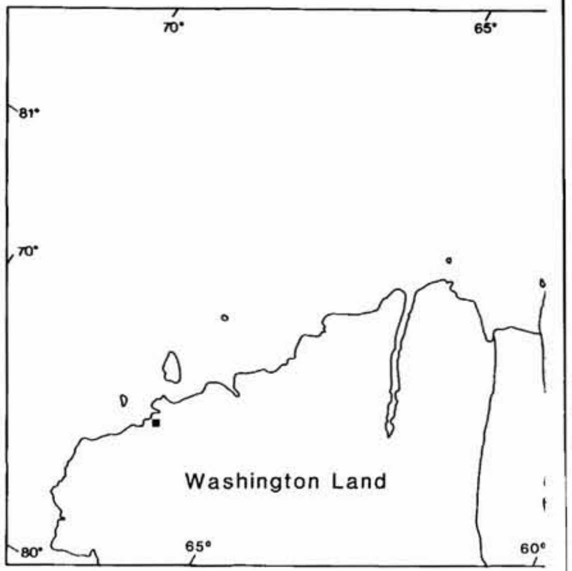

samples are situated within distances of less than 100 m vertically from the source rocks, in many places less than 10 m. The most commonly observed type is solid black bitumen occurring in vuggy and veined dolomite, either in the upper part of the Henson Gletscher Formation or in the enclosing Sydpasset and Aftenstjernesø Formations. Bitumen-stained sandstone is also common in the middle siliciclastic unit of the Henson Gletscher Formation (Christiansen *et al.,* 1987). A few examples have been recorded at a distance of several hundred metres from the source rocks, both stratigraphically above (Tavsens Iskappe Group) and below (Portfjeld Formation).

The bitumen of *group II* occurs within a few metres' or even centimetres' distance of Silurian shales, mainly in veins, vugs or corals in debris flow conglomerates of the Lafayette Bugt Formation. Relatively few occurrences are reported compared to group I, probably due to the high thermal maturity of most Silurian shales (Christiansen & Nøhr-Hansen, 1989; Chapter 6).

The bitumen samples of *group III* all come from the southern part of Warming Land and Wulff Land (fig. 49), an area without any known source rock. Asphalt seepage and asphalt filled vugs and veins occur in brecciated Portfjeld Formation less than 100 metres above the underlying Precambrian basement. The Buen Formation sandstones are dark and bitumen-stained at a number of localities. The upper part of the Ryder Gletscher Group contains both bitumen-stained sandstone and vuggy carbonates with black solid bitumen.

Composition and properties of bitumen

The bulk chemical composition and physical properties of the bitumen have been studied by GC (n = 26), GC/MS (n = 10), carbon isotope analyses of whole extracts (n = 25) and reflectance/fluorescence methods (n = 25) (see Chapter 3 for analytical details).

Most of the analytical results are consistent with the stratigraphic and geographic distribution of the bitumen and hence presented within this framework.

Group I (associated with Cambrian source rocks). The bitumens of group I are from a relatively mature area with few early mature and many mature and postmature samples. This high regional thermal maturity also affects the composition and properties of the bitumen. The reflectance of the bitumen is high (fig. 30); with the exception of few albertite/grahamite samples and some two-phased bitumens, most of the material is classified as epi-impsonite according to the terminology of Jacob (1985).

The extractability is low to moderate (30–200 mg SOM/g TOC) compared to other migrated hydrocarbons. This is probably due to the high maturity and is further supported by the lack of cyclic biomarkers and a strong light-end bias of the generally paraffinic saturates (fig. 52 A; Østfeldt, 1987). The effect of biodegradation ranges from low to moderate as expressed by the low to moderate content of polars (NSO-components) and asphaltenes (figs 50 and 51) and the Pr/nC_{17} relation (fig. 53).

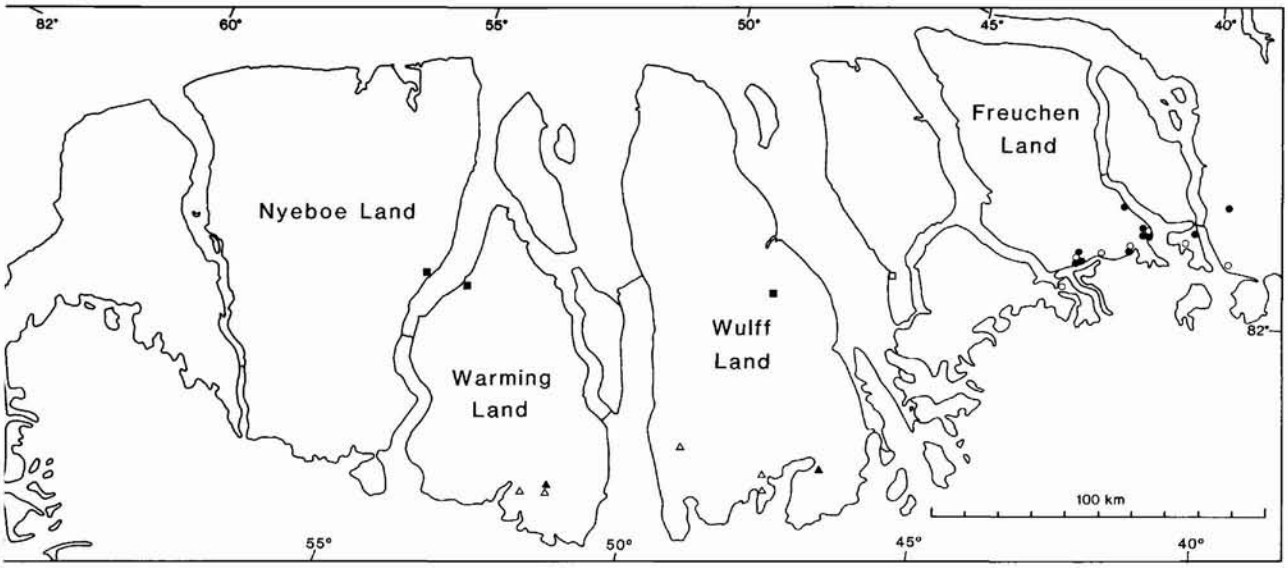

Pristane/phytane ratios are consistent and low (mean: 1.11 (SD: 0.35), range: 0.70 to 1.81). The carbon isotopic composition is also relatively constant and very depleted in ^{13}C (mean $\delta^{13}C$: −30.93‰ (SD: 0.80), range: −29.69‰ to −32.19‰) (fig. 54).

Group II (associated with Silurian source rocks). The small number of group II samples ranges considerably in regional thermal maturity with few early mature and a number of postmature samples. This variation in maturity of associated source rocks is also observed in the bitumen parameters. The bitumen reflectance varies in accordance with the regional maturity, the least mature samples contain glance pitch and albertite/grahamite, all the postmature samples epi-impsonite.

The two early mature samples have a high extractability (700–800 mg SOM/g TOC) and cyclic biomarkers are retained in the extracts. The biomarkers exhibit a ste-

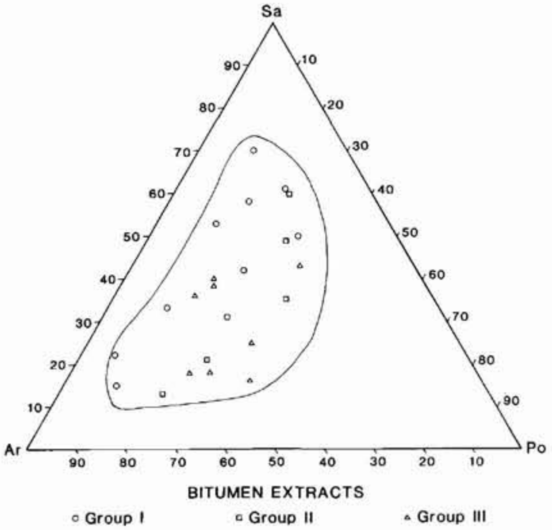

Fig. 50. Triangular diagram of the relative proportion of saturated, aromatic and polar compounds in extracts of bitumens.

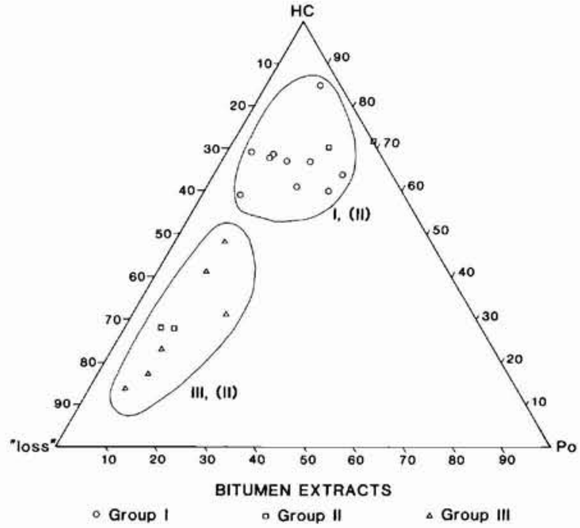

Fig. 51. Triangular diagram of the relative proportions of hydrocarbons (saturates + aromatics), polar compounds, and 'loss' in extracts of bitumens. The 'loss' during column chromatography corresponds mostly to the asphaltene content.

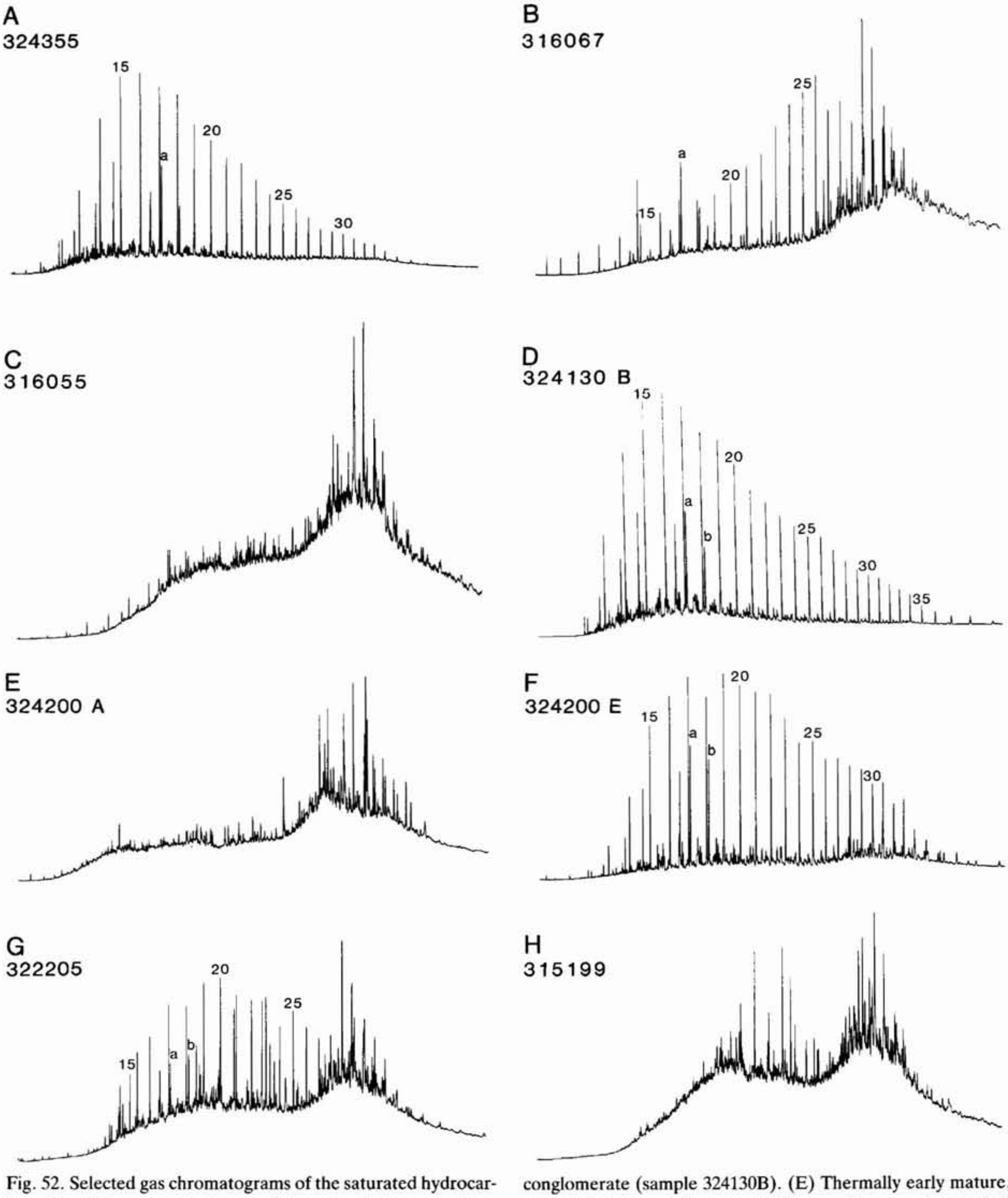

Fig. 52. Selected gas chromatograms of the saturated hydrocarbons from bitumen extracts. a: pristane, b: phytane, numbers are *n*-alkane carbon numbers. (A) Thermally mature, little biodegraded group I bitumen from sandstone (sample 324355). (B) Thermally early mature, mildly biodegraded group II bitumen from coral in conglomerate (sample 316067). (C) Thermally early mature, strongly biodegraded group II bitumen from coral in conglomerate (sample 316055). (D) Thermally postmature, little biodegraded group II bitumen from coral in conglomerate (sample 324130B). (E) Thermally early mature, strongly biodegraded group III bitumen from seeping asphalt (sample 324200A). (F) Thermally early mature, little biodegraded group III bitumen from asphalt filled vug (sample 324200E). (G) Thermally early mature, little biodegraded group III bitumen from sandstone (sample 322205). (H) Thermally early mature, strongly biodegraded group III bitumen from limestone (sample 315199).

rane distribution completely dominated by C_{29} steranes, relatively high Ts/Tm ratios and lack of gammacerane, all consistent with the interbedded source rocks (Østfeldt, 1987b; see also Chapter 5). The biodegradation of these two samples is moderate to high, evaluated from the relatively high content of polars and asphaltenes (figs 50 and 51), gas chromatograms (figs 52 B and C) and Pr/nC_{17} ratio (fig. 53).

The bitumen from the postmature areas has a very low extractability (5–30 mg SOM/g TOC) and the saturates are paraffinic with a strong light-end bias. This material seems only slightly biodegraded (figs 50, 51, 52 D, 53).

The pristane/phytane ratios of group II are considerably higher than those of group I (mean: 1.83 (SD: 0.27), range: 1.61 to 2.22). Also the carbon isotope composition is different from group I and considerably ^{13}C-enriched (mean $\delta^{13}C$: −26.50‰ (SD: 0.80), range: −25.16‰ to −27.12‰).

Group III (not closely associated with any source rock). All the samples from group III are from a thermally immature to early mature area and the bitumens do not show evidence of thermal alteration. The reflectance values are low with the material classified as gilsonite, glance pitch and albertite/grahamite.

The extractability is high to very high (most values ≥ 1000 mg SOM/g TOC). The extracts have a dominance of asphaltenes over hydrocarbons (fig. 51). Cyclic biomarkers are preserved in all samples with a sterane distribution entirely dominated by C_{29} steranes. The triterpenoid biomarker gammacerane is systematically detected in all samples, both in the slightly and the severely degraded (Østfeldt, 1987b).

The degree of biodegradation ranges from moderate to severe, evaluated from Pr/nC_{17} and relatively high contents of polars and asphaltenes (figs 50, 51 and 53). Many samples have no preserved normal alkanes, in some cases no isoprenoids either (figs 52 E and H). This biodegradation seems to be related to surface processes, since a clear difference is observed between seeping asphalt and asphalt from nearby closed spaces (figs 52 E and F).

The few samples with well defined pristane/phytane ratios show constant and low values similar to group I (mean: 1.03 (SD: 0.20), range 0.76 to 1.2) (fig. 54). The carbon isotopic composition is also comparable to group I, although slightly ^{13}C-enriched. If sample 324200A (strongly biodegraded and altered by surface evaporation) is omitted, the mean $\delta^{13}C$ is −29.48‰ (SD: 0.69) with a range between −28.59‰ and −30.82‰.

Correlation to source rocks

The composition and properties of the studied bitumen samples generally support a thermal history which is in accordance with the regional thermal maturity pattern. The group III samples reflect immature to early mature regional conditions, group I and II show a range

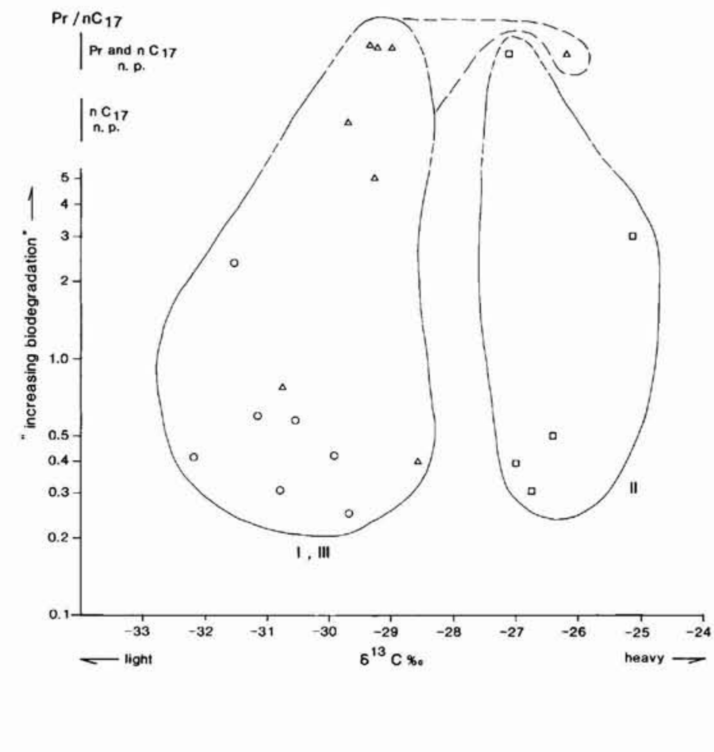

Fig. 53. Relation between carbon isotopic composition of total extracts and $Pristane/nC_{17}$ alkane ratio of the three bitumen groups (I: open circles, II: open squares, III: open triangles). The Pr/nC_{17} value is, under the assumption of a common source, mainly dependent of the degree of biodegradation. The uppermost part of the figure show samples where nC_{17} and both pristane and nC_{17}, respectively, have been completely lost during degradation.

from early mature to postmature. Biodegradation seems to be most severe in the richest extracts from early mature areas; this is particularly so in the group III samples.

Two of the parameters, the pristane/phytane ratio and the carbonate isotope composition (Lewan, 1983), are only little affected by thermal alteration and biodegradation and are hence applicable for correlation purposes. Furthermore, these data are recorded from most bitumen samples and from a number of samples of two of the possible sources of the bitumen (see also Chapter 5), the Cambrian Henson Gletscher Formation and the Silurian shales.

The bitumens associated with Cambrian (group I) and Silurian (group II) source rocks are easily discerned in cross plots of Pr/Ph versus $\delta^{13}C$ (fig. 54) with only little variation within the groups. The associated source rock groups show a similar pattern but with more scattered values with some overlap inhibiting a clear distinction (fig. 24).

The extracts of the Silurian shales and the associated bitumens reveal a similar range in Pr/Ph values whereas the extracts are depleted in ^{13}C compared to the bitumen. In the Cambrian samples the bitumen and source rocks have a similar range in isotopic composition whereas the Pr/Ph values are slightly higher in the source rock extracts. The similar biomarker distribution of the Silurian shales and the Silurian bitumen should be

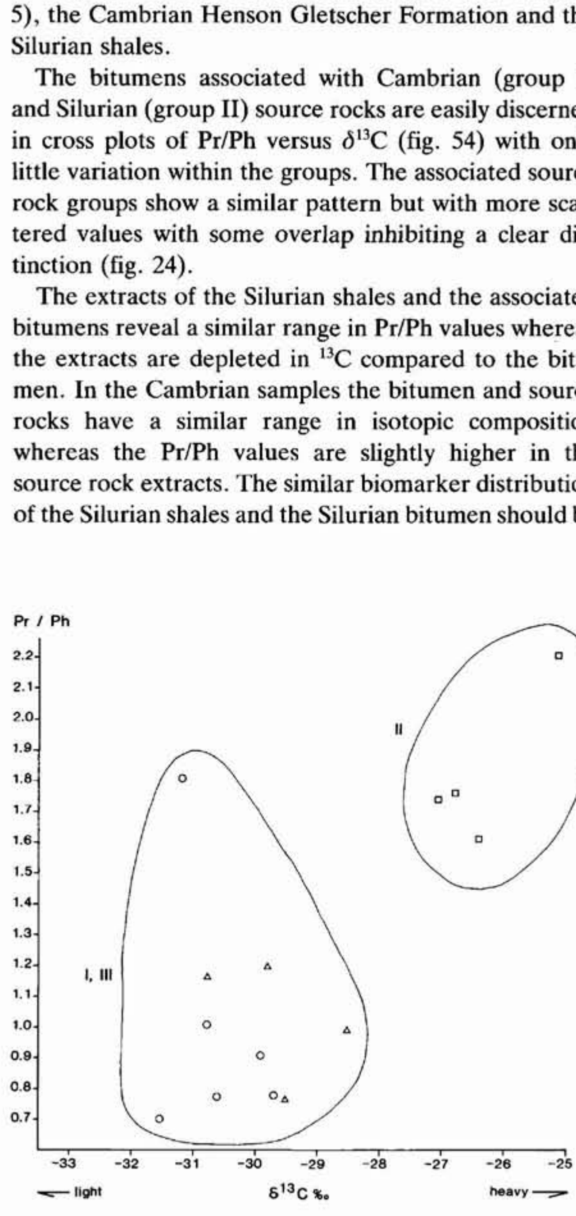

Fig. 54. Relation between carbon isotopic composition of total extracts and the pristane/phytane ratio of the three bitumen groups.

noted (Østfeldt, 1987b; see also Chapter 5). Unfortunately these compounds are not preserved in the Cambrian group I bitumen due to the high thermal maturity. Only two Cambrian source rocks contain cyclic biomarkers (see Chapter 5).

The group III samples have Pr/Ph ratios in the same range as the group I bitumen and the isotopic composition is slightly different (enriched in ^{13}C) compared to group I (fig. 54). This suggests that the source rocks of the two bitumen groups are geochemically similar. Assuming a common source, the difference in isotopic composition can be explained from the fact that only total extracts have been analysed. In normal oils saturated and aromatic hydrocarbons (which dominate in group I) are depleted in ^{13}C when compared to asphaltenes (which dominate in group III) (e.g. Schoell, 1984).

The hypothesis of a common source of the group I and III bitumens is, however, questionable when the few available cyclic biomarker distributions are considered. None of the group I bitumens, eight of the group III bitumens and two Cambrian source rocks contain preserved and detectable cyclic biomarkers. The group III bitumen and the Cambrian source rocks display distinct, but different distributions indicating a non-source relation. Particularly the ever present component gammacerane in the group III bitumens restricts the possible models since it points towards a source, or mixing with bitumen from a source, which was deposited in a hypersaline environment (see details in Chapter 5). In North Greenland such possibilities include unrecognized source rock within the Cambrian to Ordovician shallow-water carbonates or, more likely, a possible local variation in depositional environment of the Henson Gletscher Formation or its lateral equivalents (see fig. 66). Especially the transition from outer shelf Henson Gletscher Formation to contemporaneously deposited inner shelf or embayment carbonates is interesting in this context.

Host rocks

The observed migrated bitumens are hosted by a number of different rock types (Plates 7 to 9). Some of these are considered potential reservoir rocks (e.g. the Cambrian sandstones) whereas others, such as the vuggy and veined dolomites, probably do not qualify as potential reservoirs since the bitumen filled spaces are disconnected.

A detailed analysis of the diagenetic history of the potential reservoirs in North Greenland is beyond the scope of the present study. A general microscope investigation of bitumen-bearing samples, compared to reference samples without bitumen, provides some evidence of the conditions before, during and after hydrocarbon migration.

Sandstones. Bitumen-stained sandstones are restricted to the Cambrian (Lower Ordovician?) sequence with the most common examples in the Buen Formation, the Henson Gletscher Formation and Formation RG6. Other possibilities of the same type include the Morænesø, Sæterdal and Permin Land Formations (see Chapter 2).

The reservoir properties of the three most important sandstone units are summarized in fig. 55 and Table 3. The recorded values of porosity and permeability are not promising for any of the three reservoir targets. The relatively low values are due to intense quartz overgrowth leaving only minor inter-particle porosity. In some cases evidence of pressure solution or early signs of grain boundary migration are found, especially in samples from Peary Land. Early carbonate cement, predating hydrocarbon migration, is observed in several samples.

The hydrocarbon saturation in the pores has been calculated in several samples from the Buen and Henson Gletscher Formations based on Rock Eval and/or extraction data (Table 4). The Henson Gletscher Formation displays consistent saturation values below 12%, the Buen Formation a range between 36 and 63%. Considering the loss of hydrocarbons during surface evaporation and biodegradation (and loss during handling and preparation), the latter values seem high and indicate that the Buen Formation might have been oil-saturated or near-saturated at depth. This bitumen and its dark relicts are observed along grain boundaries, often associated with opaque minerals.

Carbonates. Carbonate rocks with bitumen-staining or black macroscopic bitumen in either primary or secondary spaces are common in both the Cambrian shelf succession and in the Silurian shelf and slope units. Three main types of appearance are distinguished: (a) dispersed bitumen in limestone or dolomite, (b) macroscopic discrete bitumen in primary intra- or interparticle spaces, and (c) macroscopic discrete bitumen in secondary spaces such as fractures, veins and vugs.

The three types are often closely associated within the same host rock unit but in several cases are related to different episodes (see e.g. Plate 9 with at least three 'generations' of bitumen).

The *dispersed bitumen* mainly occurs in graded limestones or dolomite grainstones in the Henson Gletscher Formation. The bitumen is observed along grain boundaries. Some of the dark dolomites are clearly postdated and partly dissolved by veins filled with saddle dolomite which is associated with another generation of bitumen (Plates 8 and 9).

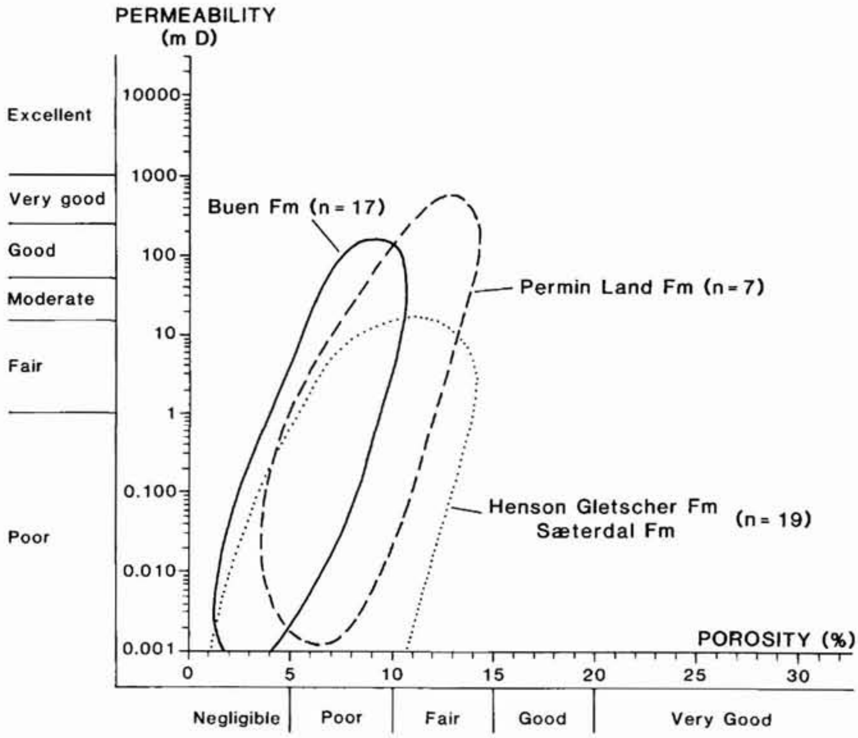

Fig. 55. Porosity/permeability variation of potential sandstone reservoirs.

Table 3. Summarized reservoir properties of

Lithostratigraphy	Outcrop pattern	Thickness	Composition[4]
Buen Fm[1]	Wulff Land– E. Peary Land	125–550 m	Quartz arenites (few subarkoses)
Henson Gl. Fm/ Sæterdal Fm[2]	Freuchen Land– C. Peary Land	<10–125 m	Subarkoses (with 15–30% dolomite)
Permin Land Fm[3]	Washington Land– Nares Land	12–53 m	Quartz arenites

1. *see* Jepsen (1971), Hurst & Peel (1979)

2. *see* Ineson (1985), Christiansen et al. (1987)

Macroscopic discrete bitumen in primary spaces is particularly common in Silurian limestones and conglomerates and especially the examples with intraparticle porosity (corals, crinoids) are impressive (Plate 9). The bitumen postdates growth of minerals with well defined crystal faces, mainly Fe-rich calcite, occasionally also Fe-rich dolomite, calcite or quartz (Plate 9). In contrast, reference samples without bitumen are dominated by calcite in similar, cemented primary pores.

Table 4. Oil saturation of Cambrian sandstones

Sample	$(S_1 + S_2)$ mg HC/g rock	SOM ppm	Porosity	Grain density	Saturation
Buen Formation					
322102	(2.72+6.09)		5.68	2.65	48%
		8560	5.68	2.65	47%
322205	(3.09+4.43)		5.46	2.62	42%
		11070	5.46	2.62	63%
324453	(3.40+4.72)		7.05	2.66	36%
Henson Gletscher Formation					
324256	(0.01+0.16)		2.95	2.69	2%
324269	(0.27+0.55)		6.30	2.69	4%
324309	(1.23+1.52)		7.51	2.67	12%
		1600	7.51	2.67	7%
324332	(0.05+0.22)		8.06	2.65	1%
324343	(0.08+0.26)		5.50	2.66	2%
324347	(1.31+1.41)		8.44	2.63	10%
324355	(0.40+0.80)		6.56	2.67	6%
		1710	6.56	2.67	8%

Density of HC ~ 0.85

Two Silurian samples, 316067 from the early mature areas in Washington Land and 324166 from the postmature areas in western Wulff Land were studied with fluid inclusion microthermometry (Jensenius, 1987). The calcite in 324166 contains abundant hydrocarbon inclusions and few one-phased aqueous inclusions. In sample 316067 the calcite inclusions are two-phased aqueous with homogenisation temperatures between 90°C and 150°C (fig. 56).

Macroscopic, discrete bitumen in secondary spaces is commonly reported in association with both source rocks and reservoir rocks of the previously mentioned types. Stylolites often contain organic-rich residues, and

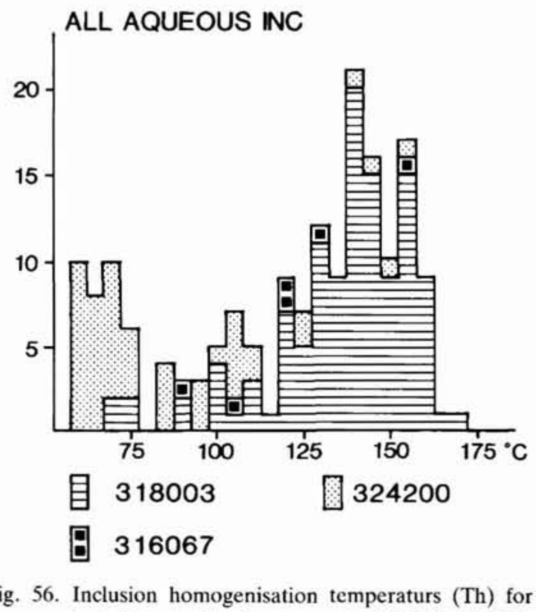

Fig. 56. Inclusion homogenisation temperaturs (Th) for all aqueous inclusions in the three samples 318003, 316067 and 324200. The low and high modes of 324200 correspond to calcite (C1) and dolomite (D2) hosted inclusions, respectively (see Jensenius, 1987, for details).

Typical grain size		Porosity	Diagenetic features
range:	0.1–1 mm	minor inter-particle	intense quartz overgrowth,
median:	0.2–0.4 mm	2–10%	occasionally early carbonate cement
range:	0.03–0.6 mm	minor inter-particle	intense quartz overgrowth
median:	0.05–0.1 mm	1.5–14%	
range:	0.05–0.4 mm	minor inter-particle	intense quartz overgrowth,
median:	0.1–0.15 mm	4–13%	occasionally early carbonate cement

3. *see* Peel (1980), Bryant & Smith (1985)

4. classification based on Folk (1968)

bitumen coating is commonly observed on fracture surfaces. The most common occurrence of secondary bitumen-filled spaces is in Cambrian dolomites, either in completely recrystallized sucrosic dolomites or in vugs and veins which are partly filled with crystalline material. Large saddle dolomite grains (Radke & Mathis, 1980) dominate, but examples of clear calcite, quartz, Fe-rich dolomite and calcite have also been reported (Plates 8 and 9).

Two examples were studied in detail combining petrographic, fluid inclusion and stable isotope techniques, namely the C1 core (samples 318003) from the mature to late mature part of Freuchen Land and the dolomite breccia which hosts an impressive asphalt seep in the thermally immature southern Wulff Land (sample 324200) (Plates 7 and 8).

The 318003 sections consist of dark grey, often bitumen-stained, dolomite grainstone, which are crosscut by numerous fracture zones. Most of these are subhorizontal, some are diagonal to the core and a few (especially the thinner ones) are vertical. Large saddle dolomite grains often replace the dolostone and are also present in the centre of partly open veins in association with bitumen (Plates 7, 8 and 9). Four main appearances are distinguished: (1) dispersed dark bitumen in the pores of the dolomite grainstone, (2) dark bitumen in stylolitic contacts between dolomite grainstone and saddle dolomite veins, (3) large black, often fractured, bitumen particles in the central part of the saddle dolomite veins, (4) yellow bitumen enclosing the large black bitumen particles (Plates 9 and 11). The two first types have similar reflectance values of about 0.9%, the third group somewhat higher (1.2%), whereas the yellow fluorescent bitumen has a very low reflectance (0.08%). The dolomite contains many green–yellow fluorescent hydrocarbon inclusions and some aqueous inclusions. The latter have homogenisation temperatures between 65°C and 170°C with a mode of 140°C (fig. 56), which after pressure corrections suggest a formation temperature of about 160–170°C (Jensenius, 1987). A minor variation in stable isotope composition between the dolomite grainstone (D0) and the saddle dolomite (D1) is shown (fig. 57).

Sample 324200 with the impressive asphalt-filled fractures exhibits a number of generations of carbonate minerals (Plate 8). The primary dolomite grainstone (D0), which typically contains stylolites, is postdated by replacive saddle dolomite (D1). A new generation of

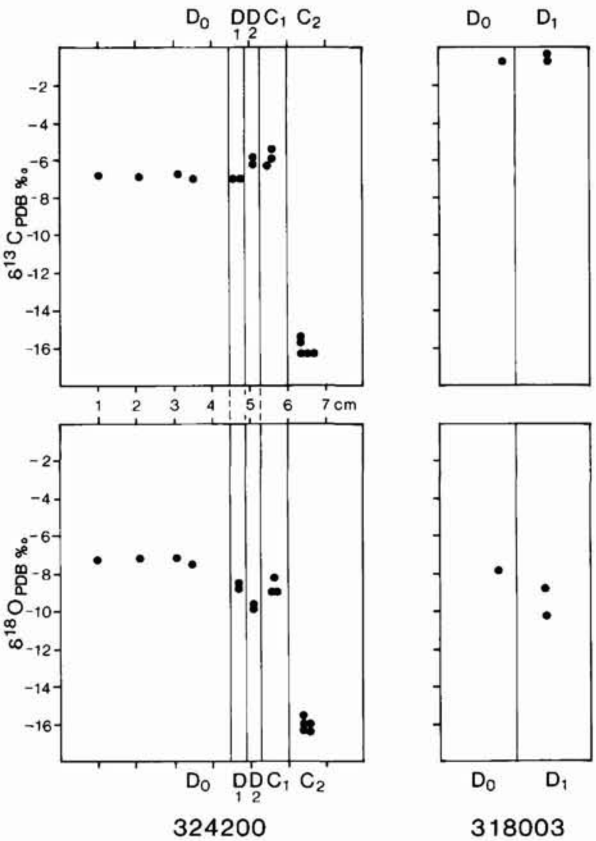

Fig. 57. Carbon and oxygen isotope values obtained in samples 318003 and 324200 showing the variations for the different generations of carbonate minerals (Plate 8).

fractures formed with subsequent precipitation of coarse-grained Fe-rich saddle dolomite (D2) and Fe-rich calcite (C1). The remaining voids are filled with asphalt, occasionally with a thin zone or crust of calcite (C2). Fluid inclusions (both hydrocarbon and aqueous types) were reported from the D2 and C1 zones. The homogenisation temperatures range between 34°C and 154°C with a mode around 60°C in the Fe-rich calcite and a considerably higher mode of about 100°C in the Fe-rich dolomite (fig. 56). These values correspond, after pressure correction, to precipitation temperatures of about 80–90°C and 115–125°C, respectively (Jensenius, 1987). The carbon and oxygen isotope values obtained display significant differences between the various generations of carbonate minerals (fig. 57).

Diagenetic history and hydrocarbon migration

The siliciclastic host rocks, which constitute several potential reservoirs, only express a limited part of the history. A general feature is the occurrence of early carbonate cement formed prior to hydrocarbon migration and an intense quartz overgrowth and pressure solution which is partly contemporaneous with the migration. Combining these features with the regionally maturity controlled variation of the physical and chemical parameters of the bitumen it seems that migration took place before and during the deepest subsidence.

The few examples of carbonate host rocks outline a complex diagenetic history but also provide specific data on the temperature and composition of the fluids associated with the mineral precipitation and hydrocarbon migration.

The dispersed bitumen and the bitumen in primary pores seem to reflect the regional maturity trend. The migration from source to host rock, often over very short distances, probably took place before and during the deepest subsidence. The bitumen-stained carbonates in the Henson Gletscher example are clearly post-dated by one or several episodes of dissolution and mineral precipitation associated with macroscopic solid bitumen. The fluid inclusion data (homogenisation temperature and freezing temperature) (fig. 56) and the stable isotope composition of the carbonate minerals (fig. 57) (see further details and discussion by Jensenius, 1987) suggest that the precipitation of the saddle dolomite took place from ^{18}O-shifted seawater with a $\delta^{18}O_{SMOW}$ composition around +6‰ at temperatures between 155°C and 165°C. These temperatures are too high to be caused by deep burial alone. The higher temperatures and the high reflectance of the macroscopic solid bitumen may be explained by the influence of hot solutions ascending from the deeper part of the basin, at feature which is commonly described from saddle dolomites associated with bitumen in Mississippi-valley type of mineralisation (e.g. Macqueen & Powell, 1983; Krebs & Macqueen, 1984).

In the asphalt seep from the thermally immature southern part of Wulff Land a completely different precipitation sequence is deduced (see details in Jensenius, 1987). The dolomite grainstone (D0) (no hydrocarbon

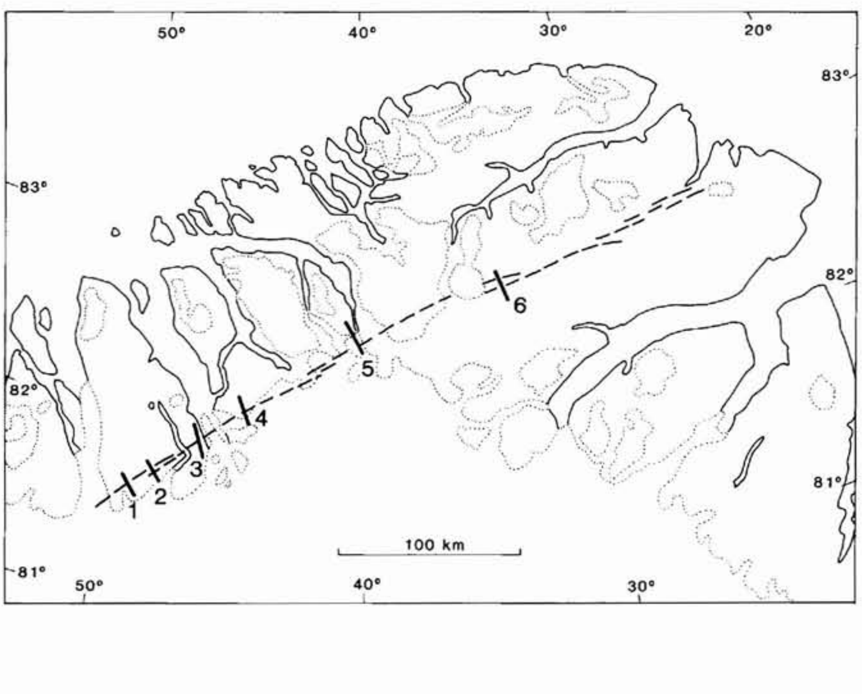

Fig. 58. Map showing the pattern of the major fault zone in the southern part of Wulff Land to Peary Land. Sections across the fault zone are shown in fig. 59.

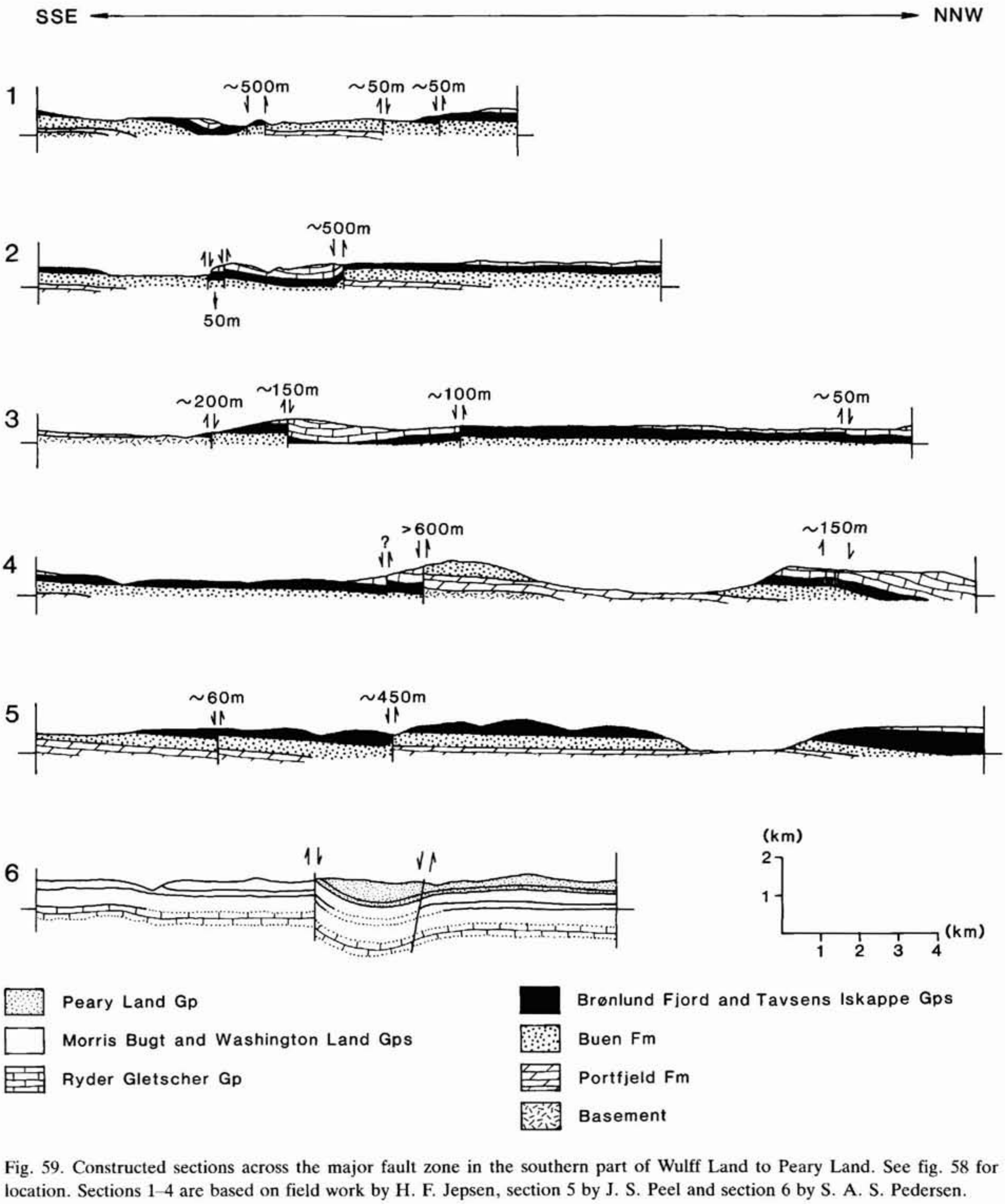

Fig. 59. Constructed sections across the major fault zone in the southern part of Wulff Land to Peary Land. See fig. 58 for location. Sections 1–4 are based on field work by H. F. Jepsen, section 5 by J. S. Peel and section 6 by S. A. S. Pedersen.

staining) recrystallized under the presence of slightly ^{18}O-shifted seawater ($\delta^{18}O_{SMOW}$: $+1 - -3\%$) at temperatures of 90°C to 100°C. The fracture-filling saddle dolomite (D1), and Fe-rich saddle dolomite (D2) precipitated at slightly higher temperatures between 105°C to 115°C and 115°C to 125°C, respectively. The Fe-rich calcite, related to the hydrocarbons, formed at temperatures between 80°C and 90°C, whereupon the remaining space in the fractures was filled with oil. Subsequent to degradation and shrinkage of the oil, highly ^{18}O-depleted modern Arctic meteoric water entered the rocks and precipitated thin crusts of calcite (C2). The proposed temperatures of precipitation are considerably lower than those of the saddle dolomites in the Henson Gletscher Formation, but also in this case somewhat higher than the expected temperature at the deepest subsidence. The lower temperatures of the Fe-rich calcite associated with the asphalt are in accordance with the geochemical results. The presence of cyclic biomarkers in the asphalt and the low reflectance clearly demonstrate that the hydrocarbons have not suffered any strong thermal alteration.

Structural setting and migration pathways

The structural setting of the three bitumen groups varies considerably from relatively simple to highly complex and therefore has strong implications on possible pathways and trapping of hydrocarbons.

The bitumens of group I (associated with the source rocks in the Cambrian Henson Gletscher Formation) occur in a simple structural setting characterized by shallow dips between 1.5° and 6° towards the north and northwest (Christiansen *et al.*, 1987). This pattern favours a simple up-dip migration towards the south through conduits closely associated with the source rocks (sandstones and coarse-grained carbonates). The few bitumens recorded at higher stratigraphic levels probably migrated along fractures and faults.

The bitumens of group II (associated with Silurian source rocks) also occur in a simple setting with shallow dips between 1° and 4° northwards (Christiansen & Nøhr-Hansen, 1989). The calcarenites and conglomerates, which host most of the recorded bitumen and therefore are considered the most likely migration conduits, occasionally display dips of more than 10° close to the reefs. The close association of source rocks and migration conduits favours an up-dip migration towards the south into platform carbonates or into Silurian reef complexes (see also fig. 69).

The bitumens of group III (in the southern part of the region without any known source rocks) occur in an area which generally is considered structurally simple with shallow northerly dips. The presumed long distance of migration and the variety of host rocks make detailed interpretation of possible pathways difficult.

A number of the reported bitumens are within or from the near vicinity of the major fault zone which has been traced from southern Wulff Land throughout the region to southern Peary Land (fig. 58). In the area north of the major fault zone, most of the Cambrian and Ordovician strata dip between 1.5° and 3° towards the north. A minor number of flexures and post-depositional faults have been observed. These faults only display minor vertical displacements, commonly with a northerly downfaulting between 30 and 75 m.

The configuration of the major fault zone is highly variable along strike (fig. 59). The zone is up to about 7 km wide and the individual faults display a variation in vertical displacement between 150 m of northerly downthrow to 600 m of southerly downthrow (fig. 59). The total vertical displacement is variable but in most cases with a southerly downthrow. Internally, the fault zone is dominated by synformal structures, occasionally with flank bed dips up to 30° (fig. 59). This structural style, especially the variation in thickness, number of individual faults and varying direction of vertical displacement, suggests a major strike-slip component of the fault zone. This deformation postdates any of the exposed sediments and it might have taken place before, after or contemporaneously with the expected main phase of hydrocarbon generation and migration during the Ellesmerian orogeny (see discussion in Chapter 8). Consequently, it is difficult with the present knowledge to deduce the migration history and implications of the observed type III bitumens. The most promising traps in terms of expected size seem to be situated immediately north of the major fault zone; this is also the area with the most simple (and probably most efficient) migration pathway.

Chapter 8

Timing of thermal episodes

F. G. Christiansen and K. Hansen

The two previous chapters have demonstrated a consistent pattern of thermal maturity and a distribution of bitumen occurrences suggesting that significant amounts of hydrocarbons were once generated and expelled with possible later migration. The timing of this migration has important economic aspects, especially in relation to the formation of traps and the degradation of accumulated hydrocarbons.

Precise dating of hydrocarbon generation, migration and accumulation is difficult unless these processes are clearly related to specific geological events such as: (1) formation of diagenetic minerals, which may be dated isotopically (e.g. smectite, illite, glauconite); or (2) magmatic events which may be dated isotopically (e.g. granite or dolerite intrusion). Indirect evidence, often producing relatively narrow time constraints, may be obtained from: (1) the subsidence history deduced from stratigraphic and sedimentological data; (2) drastic changes in thermal maturity or maturity patterns across unconformities; or (3) the thermal history (especially uplift) deduced from fission track age determinations and fission track length distributions.

Franklinian subsidence and Ellesmerian orogeny

Stratigraphic and sedimentological knowledge of the Franklinian basin in North Greenland, recently described in detail by Higgins *et al.* (in press), provides a good background for the consideration of the Early Palaeozoic subsidence history and its thermal maturity effect on the source rocks.

Shelf carbonates deposited along the southen margin of the Franklinian basin seem particularly suitable for calculation of the subsidence history. Preliminary determinations by M. Sønderholm (GGU, unpublished) suggest slow steady subsidence with a slightly decreasing rate of 15–20 mm/1000 y from Early Cambrian to Early Silurian time. Estimated rates for the Late Silurian indicate much higher values around 125–150 mm/1000 y. The sediments in the northern part of the region were laid down in a deep-water trough and indicate considerably higher subsidence rates throughout the Early Palaeozoic (especially in the Early Cambrian), apparently also with increasing values in the Silurian.

Little is known of possible continued subsidence as Devonian sediments are known only in the Canadian part of the Franklinian basin. However, it is clear that the Cambrian source rocks in the northernmost areas (north of the Navarana Fjord Escarpment), and probably also some of the Silurian shales, were already buried so deeply by Late Silurian or Early Devonian time that hydrocarbon generation took place. In the central and southern parts of the region it is not known whether the burial history can account for such an early generation of hydrocarbons.

The Late Palaeozoic Ellesmerian orogeny brought sedimentation in the Franklinian basin to a close (Trettin & Balkwill, 1979). In North Greenland it gave rise to the North Greenland fold belt, which has an E–W trend across most of the northern part of the region and roughly coincides with the trend of the deep-water trough. The rocks affected by deformation are mainly turbiditic sandstones and shales of Cambrian to Early Silurian age, and exhibit an increasing intensity of deformation and metamorphism towards the north (see fig. 60; Dawes, 1976; Higgins *et al.*, 1982, 1985; Soper & Higgins, 1987).

The youngest known sediments affected by the Ellesmerian orogeny in North Greenland are of latest Silurian, possibly earliest Devonian age (Peel, 1982; Higgins *et al.*, in press), whereas the oldest post-Ellesmerian sediments which unconformably overlie folded rocks are of Late Carboniferous age (Håkansson & Stemmerik, 1984; Stemmerik & Håkansson, in press). Rb-Sr isotopic dating of whole rocks and clay mineral fractions suggests a Late Devonian to Early Carboniferous age for the Ellesmerian metamorphism (Springer, 1981; N. Springer & J. D. Friderichsen, personal communication, 1988).

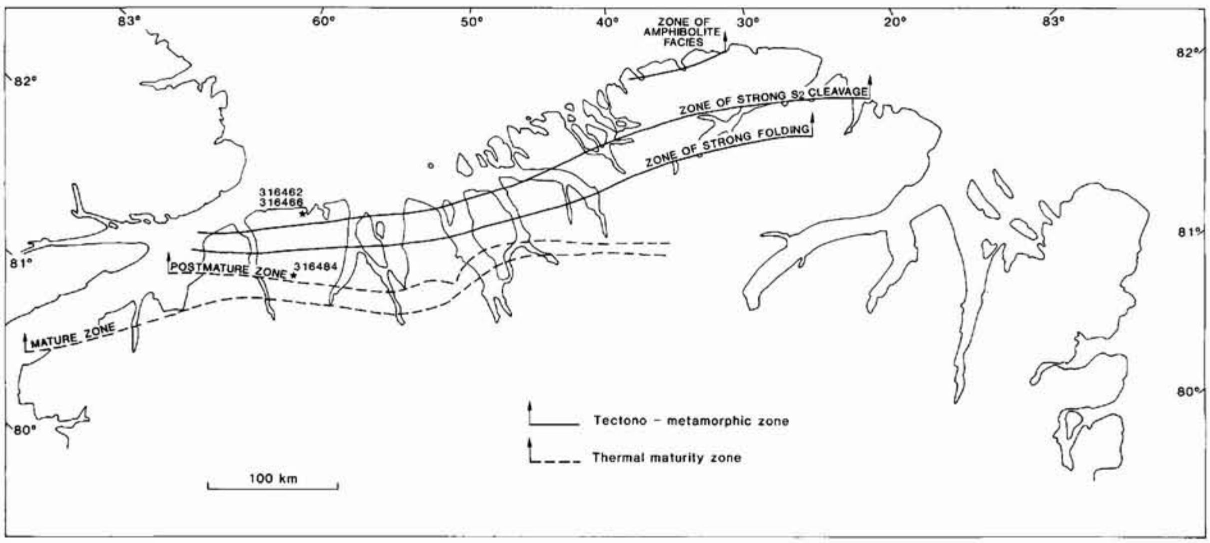

Fig. 60. Map of Ellesmerian tectono-metamorphic zones. Modified after Dawes (1976) and Higgins *et al.* (1982, 1985). The thermal maturity zonation is modified from Chapter 6. The locations of samples studied by the fission track method are indicated by stars.

The striking parallelism of the Ellesmerian tectono-metamorphic zones and the thermal maturity pattern (fig. 60) suggests that the strong thermal effect in the Early Palaeozoic source rocks is largely Ellesmerian. The thermal maturity increases markedly from thermally immature/early mature source rocks in the south to postmature source rocks over south–north distances of only 10–30 km as the fold belt is approached. A marked contrast in thermal maturity is observed in eastern Peary Land between thermally postmature or low metamorphic Silurian source rocks and overlying thermally immature or early mature Upper Palaeozoic and Mesozoic rocks (fig. 48; Christiansen *et al.*, in press). This implies at least two periods of burial or thermal events, one pre- or syn-Ellesmerian and one post-Ellesmerian, separated by a period of uplift.

Late Palaeozoic and Mesozoic sedimentation

Late Palaeozoic and Mesozoic sediments are restricted in North Greenland to relatively small areas in the northern and eastern parts of Peary Land (fig. 61; Dawes, 1976; Håkansson & Stemmerik, 1984). They rest unconformably on older rocks, or occur as fault-bounded inliers. In western North Greenland Late Palaeozoic and Mesozoic sediments have not been preserved, and it is not known where they were deposited. However, rocks of this age are widely preserved in northern Ellesmere Island (Trettin & Balkwill, 1979).

The absence of post-Ellesmerian sediments in western North Greenland may indicate that the area was subjected to uplift during Late Palaeozoic and Mesozoic time, while deposition in the Peary Land region may have been confined to fault-controlled basins.

Cretaceous–Tertiary magmatic and tectonic events

Cretaceous to Tertiary magmatic and tectonic activity is widespread in the eastern and northern part of North Greenland (fig. 61) (Soper *et al.*, 1982; Higgins *et al.*, 1985; Friderichsen & Bengaard, 1985). It is referred to the Eurekan orogeny, which affected the Canadian Arctic Islands as well as North Greenland (Trettin & Balkwill, 1972; Trettin *et al.*, 1979).

Dolerite dykes were intruded in dense N–S trending swarms along the north coast of Greenland, in north Peary Land and Nansen Land. Further south dykes are less frequent and have E–W to SE–NW trends (fig. 61). Geochemically the dykes are of alkaline type ('within-plate') (Soper *et al.*, 1982). The dykes cross-cut early Cretaceous sediments and are post-dated by the Kap Washington Group peralkaline volcanics and interbedded sediments which have a latest Cretaceous to earliest Tertiary age (Larsen *et al.*, 1978; Batten *et al.*, 1981; Batten, 1982; Larsen, 1982; Soper *et al.*, 1982). Friderichsen & Bengaard (1985) noted two dyke generations in Nansen Land, an early generation of densely distrib-

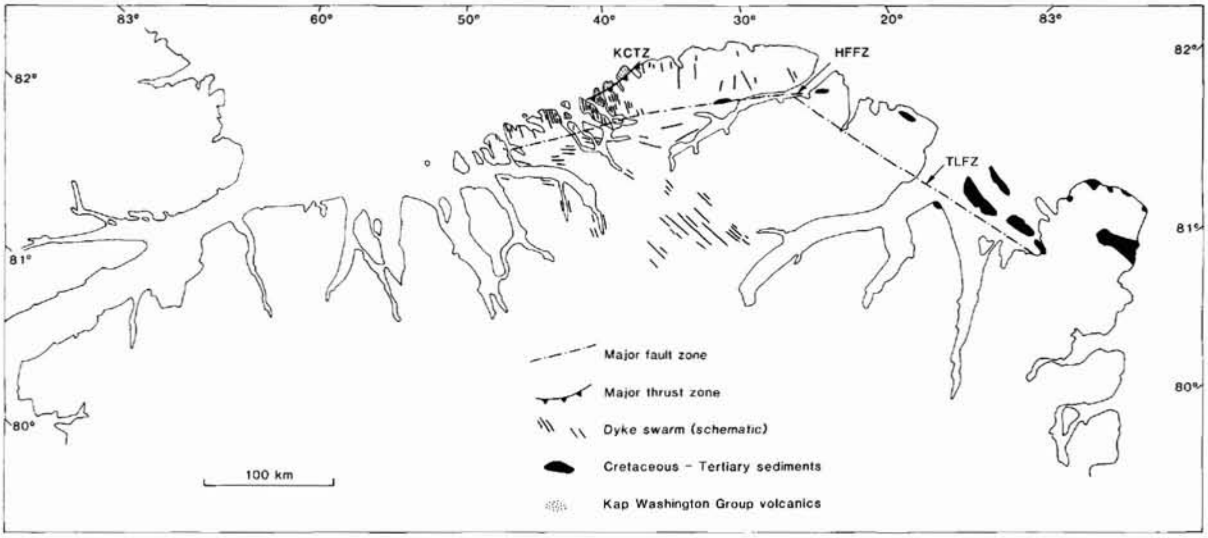

Fig. 61. Map of North Greenland showing Cretaceous–Tertiary magmatic and tectonic features. Modified after Soper *et al.* (1982). KCTZ: Kap Cannon thrust zone, HFFZ: Harder Fjord fault zone, TLFZ: Trolle Land fault zone.

uted N–S oriented dykes, and a later generation of scattered NW–SE to WNW–ESE oriented dykes.

Lower Palaeozoic metasediments of the North Greenland fold belt are thrust over the Kap Washington Group volcanics along the Kap Cannon thrust zone (fig. 61; Soper *et al.*, 1982). Isotopic ages suggest a Paleocene to Eocene age for the thrust event (Soper *et al.*, 1982).

Due to the limited occurrence of post-Ellesmerian sediments in North Greenland it is often difficult to distinguish Eurekan structures and events from those of Ellesmerian age. The most important Eurekan events are the northward thrusting on the Kap Cannon thrust zone and movements along the Harder Fjord and Trolle Land fault zones (fig. 61). In the Freuchen Land and inner J. P. Koch Fjord region, the scattered dolerite dykes are probably responsible for local anomalous thermal effect on the source rocks of the Henson Gletscher Formation (Chapter 6; Christiansen *et al.*, 1987).

Fission track analysis

A total of 15 samples from two profiles through thermally immature to postmature areas were prepared for fission track analyses, but only three of these yielded apatite grains of the appropriate size fraction (see details of preparation and analytical technique in Chapter 3).

All three samples are from Nyeboe Land (fig. 60); samples 316462 and 316466 are from turbiditic sandstones in the upper part of the Early Silurian Merqujôq Formation, whereas sample 316484 is from a sandstone in the Late Silurian Wulff Land Formation. The two first samples come from a thermally postmature to low metamorphic area in the steeply inclined Nyeboe Land linear belt (Dawes, 1982) where a cleavage is developed in the interlayered mudstone beds. The third sample is from a thermally postmature area, apparently undeformed, situated 50 km to the south (fig. 60).

The two northernmost samples, 316462 and 316466, show similar apatite fission track ages (Table 5). The

Table 5. Fission track ages of apatite and zircon

Sample	Ma ± 1 σ	No. grains	Ns	Ni	X^2(P%)
Apatite fission track ages					
316462	206.79±22.14	9	253	165	96.4
316466	207.18±21.53	9	275	179	89.2
316484	224.45±17.24	16	435	463	99.2
Zircon fission track ages					
316462*	457.73±45.40	8	552	125	4.9
	411.11±41.41	8	528	130	7.3
316484	347.74±34.30	9	482	141	88.8

*Two determinations; the very low probability of the chi-squared test (X^2(P%)), indicates that the interpretation of this age is difficult.

mean track lengths and track length distributions fall in the field of mixed and bimodal distributions of Gleadow *et al.* (1986) indicating a complex thermal history (Table 6; fig. 62). The bimodal character of 316462 and the broad based character of 316466 may be ascribed to a heating event in the 70–130°C range (Gleadow *et al.*, 1983) which only partly annealed earlier tracks. This event took place later than the age of 207 Ma. The southern sample, 316484, shows a slightly older age of 224 Ma and longer mean track length indicating a very limited late thermal overprint. This fission track age is expected to reflect the age of uplift through the 100°C isotherm.

Table 6. Confined track lengths of apatites

Sample	$t_{mean} \pm 1\ \sigma$ (μm)	No.	Type	Quality
316462	10.62±3.11	35	bimodal	?good
316466	9.01±3.19	15	mixed	poor
316484	10.99±2.53	130	mixed	good

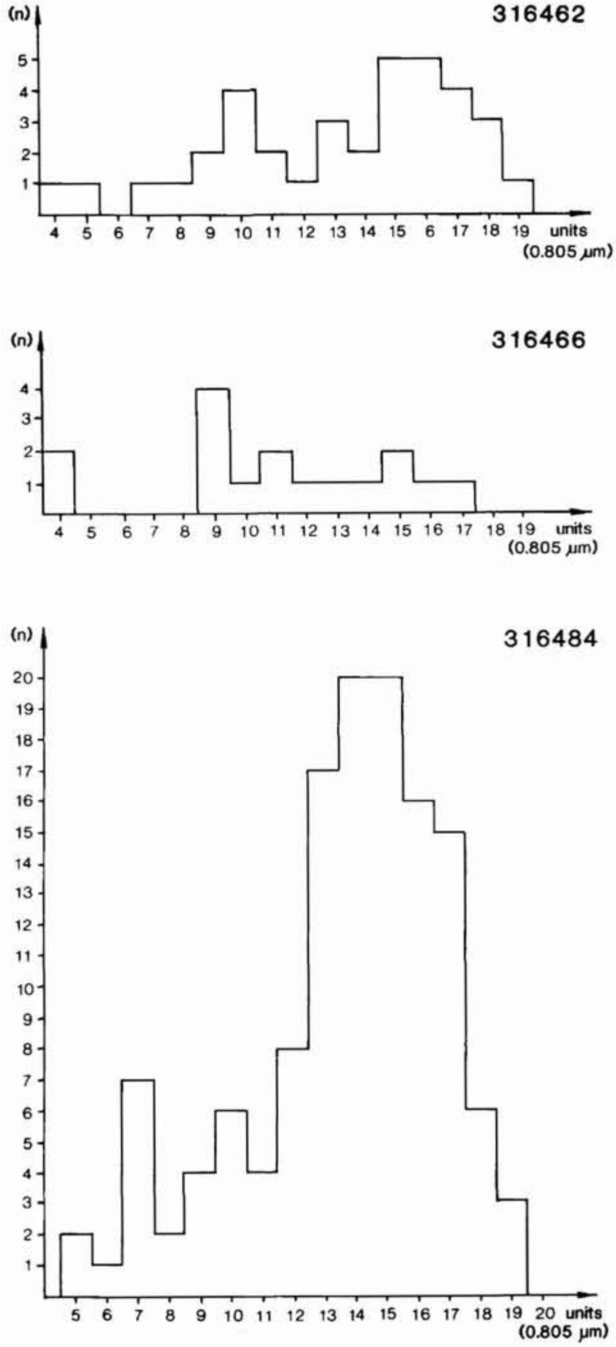

Fig. 62. Fission track length distributions. See details in Tables 5 and 6.

Fission track zircon age determinations were performed on two of the samples (Table 5). The obtained fission track ages are significantly different from each other. The northern sample, 316462, was reanalysed, but in both cases gave a low probability of the chi-squared test. The individual zircon grain ages of the sample are close to, or older than, the time of deposition (*c.* 280–700 Ma) and may imply that pre-sedimentary fission tracks were only partly annealed in the temperature interval around 240 ± 50°C (Hurford, 1986). The southern sample, 316484, is of much better analytical quality as expressed by the high probability of the chi-squared test, and the fission track age of 348 Ma obtained probably corresponds to the time of uplift through the 240°C isotherm.

A possible time-temperature history of the analysed samples is illustrated in fig. 63. All three sandstones were deposited in the Silurian and subjected to rapid subsidence shortly after deposition. During this subsidence and the following Ellesmerian orogeny the sandstones reached temperatures well above the apatite annealing range (100 ± 30°C) and possibly also close to the zircon annealing temperature (240 ± 50°C). Uplift through the 240°C isotherm took place shortly after the Ellesmerian orogeny, whereas uplift through the 100°C isotherm occurred in Late Triassic to Early Jurassic time. A possible late thermal overprint in the northern area was probably associated with Cretaceous to Tertiary magmatic activity.

Calculated cooling rates for sample 316484 give 8.9°C/Ma in the 240°C to 100°C interval and 4.5°C/Ma in the 100°C to 0°C interval. Using a geothermal gradient of 30°C/km, these values correspond to uplift rates of 36 m/Ma and 15 m/Ma, respectively. Such rates are comparable with post-Caledonian vertical movements in the

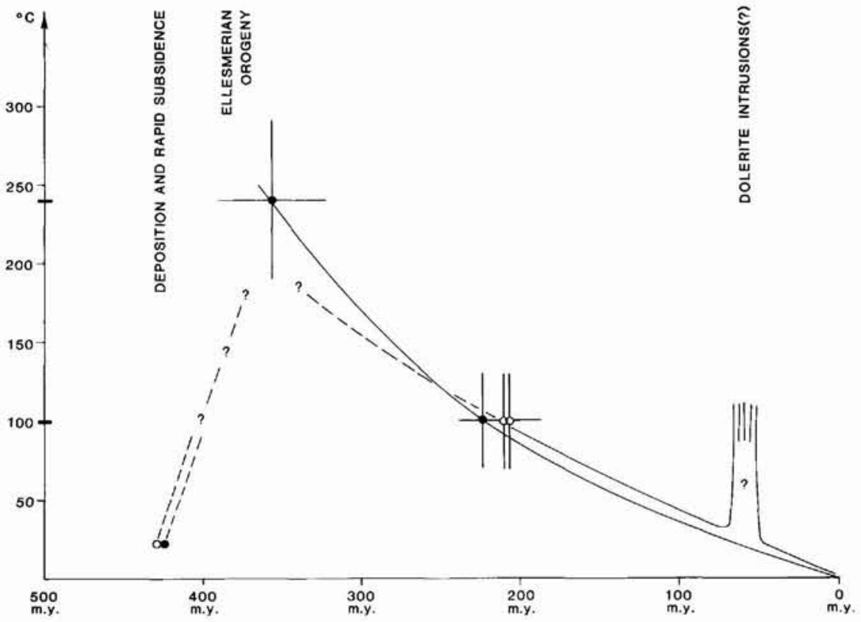

Fig. 63. Synoptic diagram showing the thermal tectonic history of the Silurian sediments in northern Nyeboe Land.

Scoresby Sund region of East Greenland (Hansen, 1985).

Implications

The thermal history as outlined by geological considerations, the thermal maturity pattern, and the age determinations of thermal episodes and uplift, is consistent with a simple model of hydrocarbon generation and possible accumulation. Both the Middle to Late Cambrian and the Early Silurian source rocks were subjected to rapid subsidence in the Late Silurian and suffered a strong thermal alteration during this subsidence and the subsequent Ellesmerian deformation. Most of the potential hydrocarbons were probably already generated at this time. After the Ellesmerian orogeny, uplift and cooling prevailed throughout most of the Mesozoic, possibly with local heating in the northernmost part of the region in the Cretaceous and Tertiary in association with the intense dyke intrusion.

Chapter 9

Quantitative aspects and economic implications

F. G. Christiansen

Many methods have been proposed for assessing the petroleum potential of a given region and each of these require different levels of information and knowledge (see numerous papers in Rice, 1986). Miller (1986) proposed a simplification into five basic categories of methodology:

1) Areal and volumetric yield, in combination with geological analogy.
2) Delphi or subjective consensus assessment.
3) Performance or behaviouristic extrapolation based on historical data.
4) Geochemical material balance.
5) Combinations of geological and statistical models.

These methods may be used during frontier to mature stages of exploration, either regionally, on single stratigraphic units or on specific plays or prospect types.

The present considerations of the hydrocarbon potential are based on the geochemical material balance approach. None of the other methods are adequate considering the stage of investigation and the available data.

The geochemical material balance approach is based on a stepwise evaluation of the hydrocarbon cycle (fig. 64):

1) Generative potential of source rocks.
2) Amount of hydrocarbons generated in source rocks.
3) Amount of hydrocarbons expelled from source rocks.
4) Loss during migration.
5) Amount of hydrocarbons trapped.
6) Loss during leakage, degradation.
7) Amounts of non-recoverable hydrocarbons in the reservoir.

This approach has been widely applied and is rapidly developing, thus increasing both the theoretical understanding and the sophistication of calculations (Welte & Yukler, 1981; Bishop *et al.*, 1983; Demaison, 1984; Kontorovich, 1984; Sluijk & Nederlof, 1984; Ungerer *et al.* , 1984).

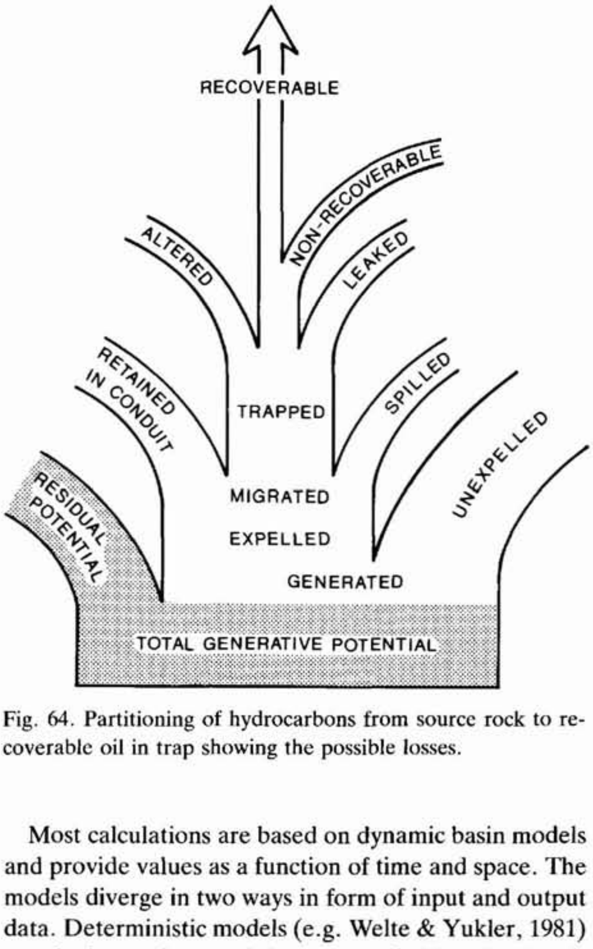

Fig. 64. Partitioning of hydrocarbons from source rock to recoverable oil in trap showing the possible losses.

Most calculations are based on dynamic basin models and provide values as a function of time and space. The models diverge in two ways in form of input and output data. Deterministic models (e.g. Welte & Yukler, 1981) use single numbers and the most probable value is calculated. Probablistic models (e.g. Bishop *et al.*, 1983; Sluijk & Nederlof, 1984) employ probability distributions for both input, calculation and output and are hence much more informative. However, very large databases and computer systems are necessary for utilizing this approach.

In the following preliminary appraisal of the hydrocarbon potential in North Greenland a simple deterministic non-dynamic calculation is used. Although the tectonic–sedimentological development of North Greenland is fundamentally well understood (Higgins *et al.*, in press), with a well established source rock distribution and thermal maturity pattern (Chapters 5 and 6), substantial data and work are still not available for detailed space-time-temperature modelling. Hence the main attempt in this chapter has been to estimate the order of magnitude by calculation of the ultimate potential of each source rock unit followed by discussion of generation and partitioning of hydrocarbons (see fig. 64).

Generative potential of source rocks

The hydrocarbon potential of source rocks is calculated using a simple material balance formula, either directly or summarized and integrated depending on the variation of input parameters:

Generated hydrocarbons =

drainage area × net thickness of source rock × density of source rock × yield × conversion constants.

The drainage area and net thickness are known from the preliminary studies of the two source rock units considered, the Henson Gletscher Formation (Christiansen *et al.*, 1987) and the Silurian shales (Christiansen & Nøhr-Hansen, 1988). The calculation only applies to the region between Hall Land and Freuchen Land (figs 65 and 66), where data control is good. Some of the source rocks are also distributed in Washington Land and Peary Land, but volumetric and geochemical values are not known in sufficient detail.

The yield of a given unit may be calculated as ultimate, residual or fractional (or by integration of subdivided units). The employed values are either recorded directly from the Rock Eval (S2 or S1 + S2) or from the TOC value (quantity) multiplied by either H/C (from elemental analysis) or Hydrogen Index (from Rock Eval) (quality). The conversion constant depends on the form of input data and the required output form (e.g. million barrels of hydrocarbon or million m^3 of hydrocarbon).

The calculations, as in other deterministic models, are based on a set of 'most likely' values. Calculations have also been performed on minimum and maximum values of area, thickness and yield in order to ascertain the sensitivity of the estimates.

In the Silurian succession the shales of Llandovery

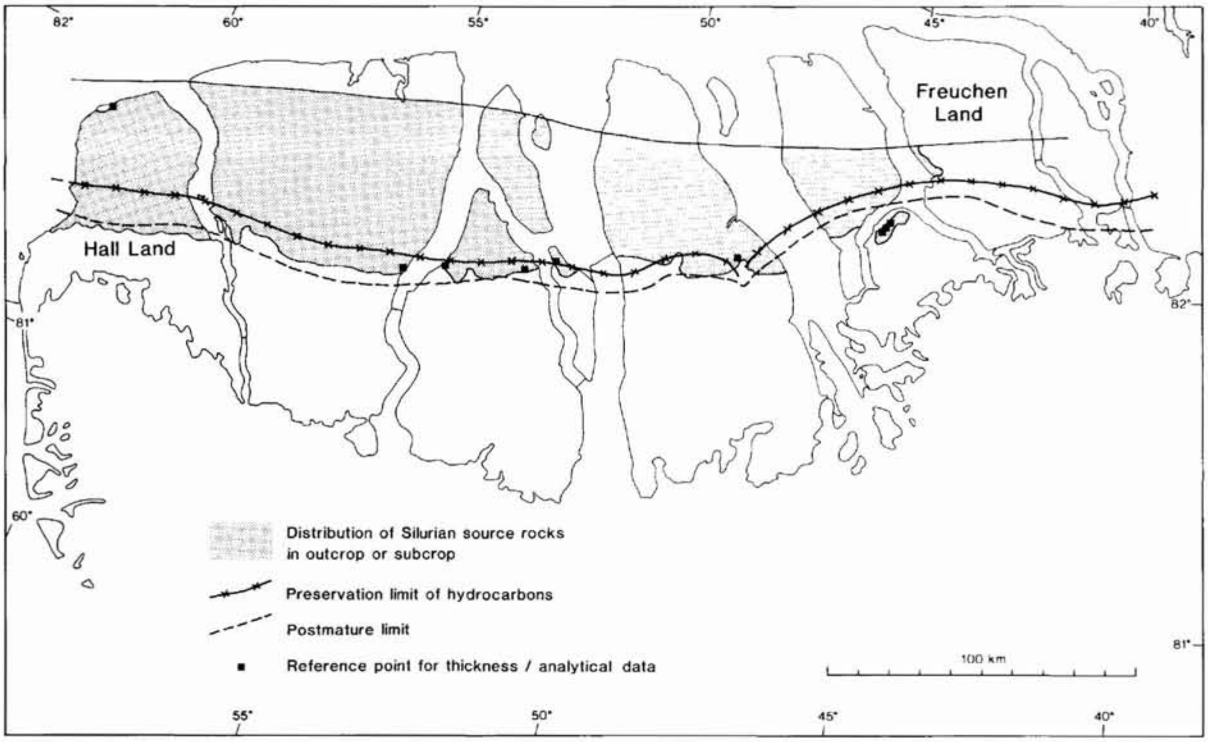

Fig. 65. Distribution of Silurian source rocks (shale groups A and B of Christiansen & Nøhr-Hansen, 1989) in outcrop and subsurface with reference points for measurements of thickness and analytical data. The preservation limit of hydrocarbons and the postmature limit of source rocks are indicated.

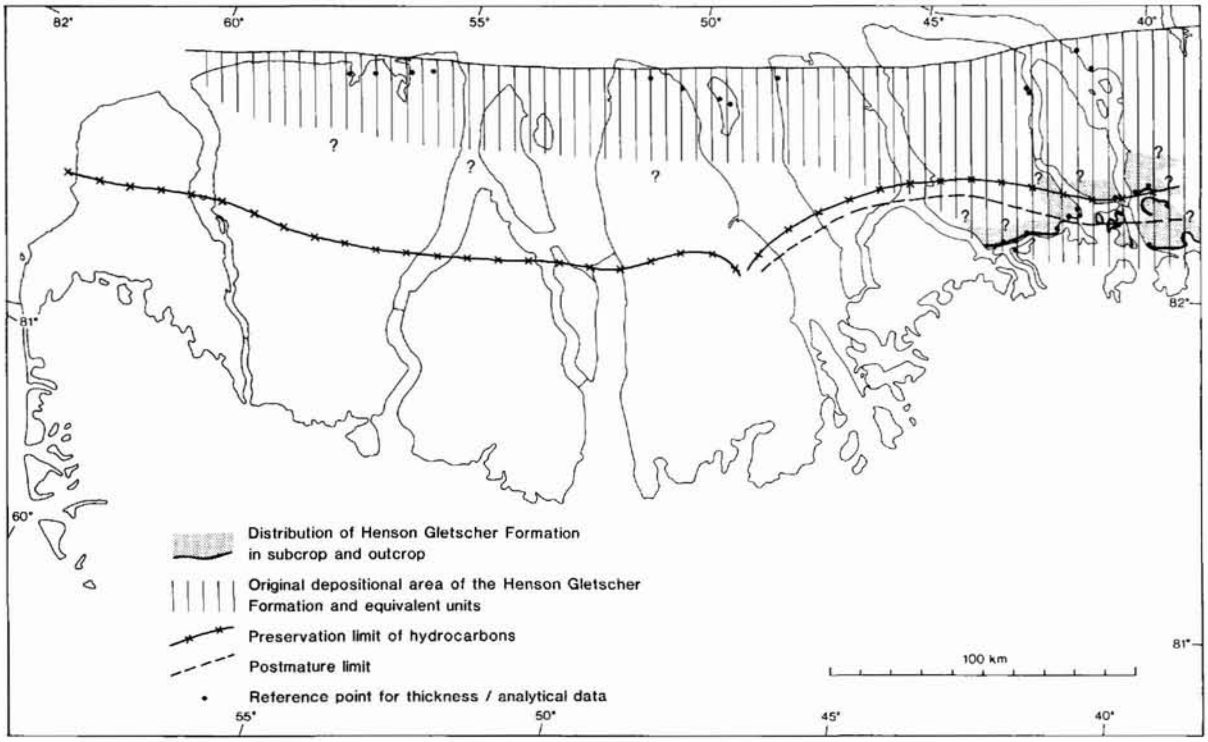

Fig. 66. Distribution of Cambrian source rocks with reference points for measurements of thickness and analytical data. The dark tone shows the outcrop and subcrop of the Henson Gletscher Formation (Christiansen *et al.*, 1987), and the vertical hatching indicates the total original depositional area of organic-rich rocks including unit 2 of the Cambrian – Lower Silurian starved basin sequence (Higgins & Soper, 1985; A. K. Higgins, personal communication 1987). The preservation limit of hydrocarbons and the postmature limit of source rocks are indicated.

age (group A and B of Christiansen & Nøhr-Hansen, 1989) have a significant potential. Organic-rich shales were apparently only deposited between the reef belt and the Navarana Fjord escarpment (fig. 65) covering an area of approximately 12 000 km^2 with tentatively estimated minimum and maximum values of 7500 km^2 and 17 500 km^2, respectively (Table 7).

In the Cambrian Henson Gletscher Formation estimates of the drainage area are more complex. The source rocks were traced in detail in a relatively small area until, due to the general shallow northerly dip, they disappear under younger strata (Christiansen *et al.*, 1987). The Henson Gletscher Formation outcrops over a distance of about 100 km (fig. 66) and an area of 3000 km^2 has been used in the calculation example (Table 7). However, the recent correlation between the Henson Gletscher Formation and unit 2 of the 'Cambrian – Lower Silurian starved basin sequence' (Higgins & Soper, 1985; Higgins *et al.*, in press) points towards a much wider distribution of organic-rich sediments, probably covering an area of approximately 15 000 km^2 (fig. 66, Table 7).

The applied net thickness values are also based on information from the two preliminary studies, in the Silurian case with a subdivision into a few intervals with certain average quantity and quality parameters of the organic matter.

The yield values are based on Rock Eval measurements. Due to the good correlation between percent TOC and generative potential (S1 + S2) for various ranks of maturity (figs 67 and 68) it has been possible to estimate the initial ultimate yield of the two units and to recalculate initial TOC values.

Typical immature Silurian shales with 2 and 4% TOC are expected to have generative potentials of 8 and 18 mg HC/g rock, respectively. At increasing maturity, e.g. at peak to late generation conditions of T_{max} between 445°C and 450°C, the generative potential is reduced to 3 and 7 mg HC/g rock, respectively (fig. 67). The Cambrian source rocks seem to have a slightly lower generative potential; the initial yield for shales and lime mudstones with 2 and 4% TOC is 7 and 16 mg HC/g rock, respectively.

Based on analyses of detailed measured sections and

Table 7. Calculation of generated hydrocarbons

	Drainage area km²	Thickness (m) with initial TOC%	Initial yield mg HC/g rock	Generated HC 10^3 mill. m^3 HC	'Palaeo-potential' with 1% efficiency mill. barrels HC
Silurian					
Most likely	12 000	5 (5% TOC)	26		
		20 (3% TOC)	14	32.25	2029
		75 (1.5% TOC)	6		
Maximum	17 500	10 (5% TOC)	26		
		25 (3% TOC)	14	77.11	4850
		100 (2% TOC)	8		
Minimum	7 500	20 (3% TOC)	14	9.60	604
		60 (1.5% TOC)	6		
Cambrian					
Maximum	15 000	30 (3.5% TOC)	14	19.69	1239
Minimum	3 000	30 (2.5% TOC)	9	2.53	159

drill cores (see results in Christiansen & Nøhr-Hansen, 1989) the TOC distribution of the Silurian shales has been simplified to a 'most likely' thickness of 5 m with 5% initial TOC, 20 m with 3% initial TOC and 75 m with 1.5% initial TOC.

In the Cambrian sequence an average total source

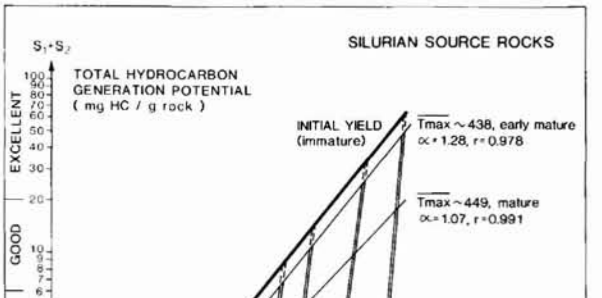

Fig. 67. Plot of %TOC versus generation potential (S1 + S2) for Silurian source rocks at various ranks of maturity. The linear relation is expressed as the slope (α) and the regression coefficient (r). The linear relation for an immature source rock is shown as a thick line, the maturation trend as double arrows.

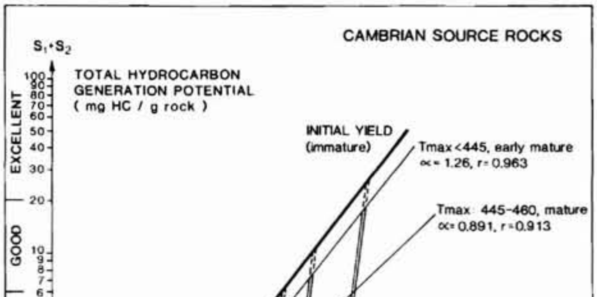

Fig. 68. Plot of %TOC versus generation potential (S1+S2) for Cambrian source rocks with various ranks of maturity. The linear relation is expressed as the slope (α) and the regression coefficient (r). The linear relation for an immature source rock is shown as a thick line, the maturation trend as double arrows.

rock thickness of 30 m has been applied in all calculations. Christiansen *et al.* (1987) mention a cumulative source thickness between 25 and 40 m (with an estimated average of 30 m) in the southern part of the region. Towards the north A. K. Higgins (personal communication, 1987) reports 10 measured sections with a formation thickness between 21 and 31 m (average 27 m); these values also include some sandstone intervals.

Only liquid hydrocarbons are considered in the calculations since any natural gas generated during the Ellesmerian orogeny will have leaked to the surface. The main potential of the source rocks is paraffinic crudes.

Amounts of hydrocarbons generated

Table 7 shows the amounts of hydrocarbons that would have been generated if all the studied source rocks had undergone a complete maturation history. Comparison of distribution and thermal maturity patterns (figs 65 and 66) not only suggests that most (> 90%) of the source rocks are completely mature but also that the major part have suffered such a strong thermal alteration that no hydrocarbons remain.

The calculated values are therefore considered as a reasonable estimate of the hydrocarbons generated during thermal maturation in Late Palaeozoic time. These estimates suggest that significant amounts of hydrocarbons were generated compared to many other petroliferous basins. This is further emphasized in the right column of Table 7, where the total 'palaeo-potential' is calculated assuming an efficiency of expulsion-migration-trapping-recovery of 1%. This 1% volume is close to the global percentage of generated hydrocarbons, which is considered economically recoverable (Durand, 1980). For comparison it should be noted that the production in Denmark and Norway in 1985 was 22 million barrels/year and 294 million barrels/year, respectively, and the reserves in the two countries 465 million barrels and 10 900 million barrels, respectively (Yarbrough, 1986). Nassichuk (1983) proposed reserves of approximately 500 million barrels in the Lower Palaeozoic basin of the Canadian Arctic based on volumetric yield considerations.

Conceptual plays

The present knowledge of basin evolution in North Greenland (e.g. Higgins *et al.*, in press) combined with the distribution and quality of source and reservoir rocks allow a tentative identification of a number of conceptual play models (fig. 69).

The most obvious Silurian play, also known from the Canadian Arctic (Rayer, 1981; Embry *et al.*, in press), is shelf margin limestones and reefs as reservoirs with juxtaposed shales acting as source and seal. The combination of source rocks with interbedded porous carrier beds (mainly carbonate conglomerates and calcarenites) favours a high migration efficiency. Table 8 illustrates some highly speculative calculations of the possible order of size of single fields. The available amounts of hydrocarbons are relatively easy to calculate; the efficiencies are not known but are suggested to be considerably higher for the organic-rich units than for the leaner parts. The maximum 'palaeo-potential' of the single reefs was probably in the range from a few tens to a few hundreds of million barrels, amounts which easily could have been trapped in the larger and probably also in the smaller reefs (Table 9).

Table 8. Calculation example, single field in Silurian reef

Drainage area km²	Thickness (m) initial TOC%	Initial yield mg HC/g rock	Efficiency %	'Palaeo-potential' mill. barrels HC
400	5 (5% TOC)	26	5	
	20 (3% TOC)	14	2	113
	75 (1.5% TOC)	6	0.5	

Table 9. Calculation example, reservoir capacity in single Silurian reef

	Reef volume km³	Porosity %	Capacity of reservoired HC mill. barrels
Maximum 10 km × 5 km × 0.5 km	25	20	31450
Minimum 1 km × 1 km × 0.3 km	0.3	10	190

The Silurian reef play is restricted by high thermal maturity and erosion level. Most of the reefs in the thermal mature zone are deeply eroded and are either exposed or shallowly buried down to only a few hundred metres of depth. The possible reefs further north, if present, occur down to 2 km below the surface, but are not likely to have any preserved hydrocarbons due to the high thermal maturity.

Two conceptual plays are suggested in the Cambrian sequence (fig. 69), both with their source in the Henson

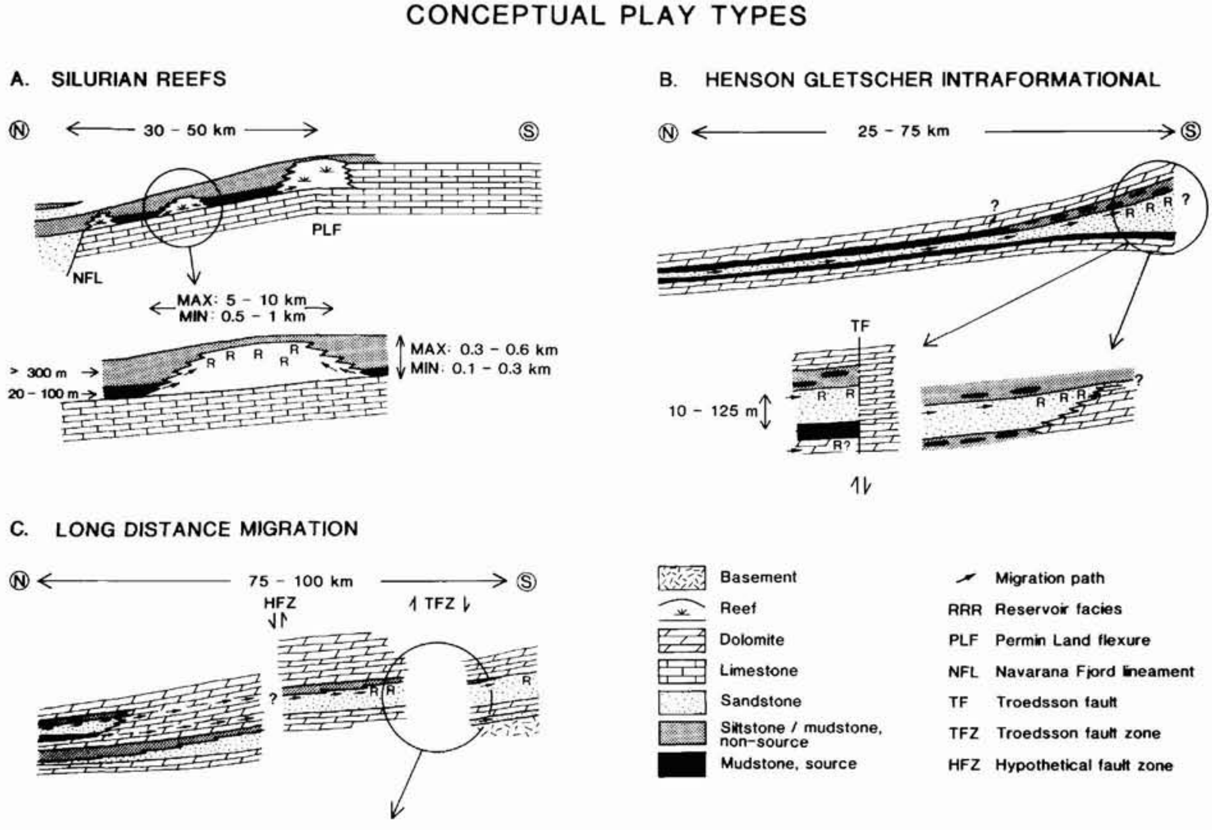

Fig. 69. Conceptual play types in central and western North Greenland. The schematic relations of potential source and reservoir rocks, migration pathways and seals are illustrated for three main prospect types, one Silurian and two Cambrian.

Gletscher Formation (or equivalent northern units). In both types the structural setting in the region with shallow northerly dip favours migration away from the most mature areas into thermally immature reservoirs towards the south.

The first play type includes intraformational reservoirs, especially sheet sandstones, but possibly also coarse-grained dolomites which are sealed by the enclosing source rocks. The nature of the middle siliciclastic unit is important for the migration history. Do the sheet sandstones form regionally continuous beds (blankets) which are highly efficient conduits, or do the sandstones laterally interdigitate with shale and lime mudstone? Trapping possibilities include both structural and stratigraphic types (fig. 69). Structural traps might have formed along major SW–NE trending faults or in nearby fault-induced anticlines. Stratigraphic traps might have formed where the reservoir sandstones of the Henson Gletscher Formation (or the Sæterdal Formation) interfinger with or laterally grade into impermeable intraformational bioturbated siltstones or into shallow-water dolomitized carbonates of the Ryder Gletscher Group. Due to the close association of source rocks with potential migration pathways, the efficiency of migration was probably high. This fact, combined with the large drainage areas, suggests that major accumulations could have formed at the time of maturation. However, the play is not prospective today. The areas where such stratigraphic traps were most likely to form are eroded and the areas with sufficiently buried potential traps are situated north of the inferred hydrocarbon preservation limit (fig. 66).

The second Cambrian play type includes reservoir rocks in strata older than the Henson Gletscher Formation, preferentially in the Lower Cambrian Buen Formation sandstones, but also Proterozoic sandstones or in possible but not yet recognized porous carbonates. This concept involves long distance migration, both laterally and along faults to older stratigraphic levels. Consequently the efficiency of migration is expected to be low (< 1%). The possibility of this play type, not only in Late Palaeozoic time but also today, is supported by the frequent staining of thermally unaltered bitumen in the potential reservoir rocks, the low thermal maturity of this part of the region, and the possible existence of subsurface structures. Both stratigraphic and structural traps are likely in this geological setting. The most simple prospective types would be that of fault-bounded reservoirs or large anticlines associated with major SW–NE faults (fig. 69).

Economic implications

The study of the hydrocarbon potential in central and western North Greenland has followed a stepwise evaluation of: (a) source rock deposition, (b) source rock quality and quantity, (c) thermal maturity history, and (d) generation products. Reservoir and trapping possibilities have not been considered in detail and only preliminary results are available. Several of these important factors provide positive indications of a petroleum potential. However, it is clear that the subsidence and thermal history of the source rocks are problematic. Most source rocks are thermally mature or postmature due to thermal alteration in Late Palaeozoic time. Hence the exploration prospectivity is considered limited, although clearly present.

Prospective plays involve generation of hydrocarbons more than 300 million years ago, long-distance migration and preservation in an uplifted and eroded basin. The expected limited cumulative efficiency of this playtype is partly compensated by the large amounts of generated hydrocarbons.

Among the most interesting results is the clear recognition of the regional thermal maturity pattern. Future petroleum geological activities can now be concentrated in relatively small areas outlined by the 'Nordolie' study. In addition examples of conceptual play types have been identified.

The present study also has implications for the petroleum assessment in the Canadian part of the Franklinian basin where the sedimentary succession is partly buried under Upper Palaeozoic and Mesozoic to Tertiary strata of the Sverdrup basin succession. The 'Nordolie' results may provide an important guideline for a re-evaluation of both source rocks (especially age, environment, quality and quantity, and thickness) and thermal history.

Acknowledgements

The 'Nordolie' project was supported economically by the Danish Ministry of Energy through project no. EFP–83–2251–305 and so was the contribution by J. Jensenius (EFP–84–2251–401). The studies by K. Hansen were supported by the Nordic Council of Ministers.

The authors are grateful to F. Rolle, O. Nykjær, J. Bojesen-Koefoed, O. Nygaard and K. Z. Jørgensen for their participation in the field work; to J. Boserup and G. S. Nielsen for handling, preparation and analytical work; and to M. Larsen and V. Hermansen for the endless job of typing. B. S. Hansen made the art-work with creative enthusiasm and J. Lautrup and assistants carried out the photographic work.

The following persons have kindly commented on various drafts of one or several chapters: P. R. Dawes, I. S. Eiríksdóttir, N. Henriksen, A. K. Higgins, F. Kalsbeek, H. C. Larsen, J. S. Peel, T. C. R. Pulvertaft and M. Sønderholm. Special thanks go to F. Surlyk and W. S. Watt for their time-consuming and effective comments and editing of the final report.

Finally, thanks to N. Henriksen for his enthusiastic and energetic leadership of the expeditions to North Greenland.

References

Aldridge, R. J., Dorning, K. J., Hill, P. J., Richardson, J. B. & Siveter, D. J. 1979: Microfossil distribution in the Silurian of Britain and Ireland. *In* Harris, A. L., Holland, C. H. & Leake, B. E. (edit.) The Caledonides of the British Isles – reviewed. *Spec. Publ. geol. Soc. Lond.* **8**, 433–438.

Allaart, J. H. 1965: The Lower Paleozoic sediments of Hall Land, North Greenland. Unpubl. intern. GGU rep., 11 pp.

Allman, M. & Lawrence, D. F. 1972: *Geological laboratory techniques*, 335 pp. London: Blandford Press.

Armstrong, H. A. & Dorning, K. J. 1984: Silurian palynomorphs from the Chester Bjerg Formation, Hall Land, western North Greenland. *Rapp. Grønlands geol. Unders.* **121**, 97–103.

Bally, A. W. & Snelson, S. 1980: Reals of subsidence. *Bull. Can. Petrol. Geol.* **28**, 9–75.

Batten, D. J. 1981: Palynofacies, organic maturation and source potential for petroleum. *In* Brooks, J. (edit.) *Organic maturation studies and fossil fuel exploration*, 201–223. London: Academic Press.

Batten, D. J. 1982: Palynology of shales associated with the Kap Washington Group volcanics, central North Greenland. *Rapp. Grønland geol. Unders.* **108**, 15–23.

Batten, D. J. 1984: Identification of amorphous sedimentary organic matter by transmitted light microscopy. *In* Brooks, J. (edit.) Petroleum geochemistry and exploration of Europe. *Spec. Publ. geol. Soc. Lond.* **12**, 275–287.

Batten, D. J., Brown, P. E., Dawes, P. R., Higgins, A. K., Koch, B. E., Parson, I. & Soper, N. J. 1981: Peralkaline volcanicity on the Eurasia basin margin. *Nature* **294**, 150–152.

Berry, W. B. N. & Wilde, P. 1978: Progressive ventilation of the oceans – an explanation for the distribution of the Lower Paleozoic black shales. *Am. J. Sci.* **278**, 257–275.

Bertrand, R. & Héroux, Y. 1987: Chitinozoan, graptolite, and scolecodont reflectance as an alternative to vitrinite and pyrobitumen reflectance in Ordovician and Silurian strata, Anticosti Island, Quebec, Canada. *Bull. Am. Ass. Petrol. Geol.* **71**, 951–957.

Bishop, R. S., Gehman, H. M. Jr., Young, A. 1983: Concepts for estimating hydrocarbon accumulation and dispersion. *Bull. Am. Ass. Petrol. Geol.* **67**, 337–348.

Bjerreskov, M. 1986: Silurian graptolites from N Greenland. *In* Hughes, C. P. & Rickards, R. B. (edit.) Palaeoecology and biostratigraphy of graptolites. *Spec. Publ. geol. Soc. Lond.* **20**, 181–189.

Bois, C., Bouche, P. & Pelet, R. 1982: Global geologic history and distribution of hydrocarbon reserves. *Bull. Am. Ass. Petrol.* **66**, 1248–1270.

Bryant, I. D. & Smith, M. P. 1985: Lowermost Ordovician sandstones in central North Greenland. *Rapp. Grønlands geol. Unders.* **126**, 25–30.

Buchardt, B. & Cederberg, T. 1987: EFP-83 projekt: Stabil isotop geokemi i moderbjergarter, olie og gas i Danmark, afsluttende rapport. Geologisk Centralinstitut, København, 33 pp.

Buchardt, B., Clausen, J. & Thomsen, E. 1986: Carbon isotope composition of Lower Palaeozoic kerogen: Effects of maturation. *In* Leythaeuser, D. & Rullkötter, J. (edit.) Advances in organic geochemistry 1985. *Org. Geochem.* **10**, 127–134.

Burgess, J. D. 1974: Microscopic examination of kerogen (dispersed organic matter) in petroleum exploration. *Spec. Pap. geol. Soc. Am.* **153**, 19–30.

Bustin, R. M., Barnes, M. A. & Barnes, W. C. 1985a: Diagenesis 10. Quantification and modelling of organic diagenesis. *Geoscience Canada* **12**, 4–21.

Bustin, R. M., Cameron, A. R., Grieve, D. A. & Kalkreuth, W. D. 1985b: Coal petrology, its principles, methods, and applications. *Geol. Ass. Can. Short Course Notes* **3**, 230 pp.

Christiansen, F. G. (edit.) 1988: Petroleum geology of North Greenland. Final report – 'Nordolie'. Unpubl. intern. GGU rep., Part I (text) 231 pp., part II (figures) 101 pp., Appendix I (previously completed papers 43 + 95 pp., Appendix II (key data) 87 pp.

Christiansen, F. G. & Nøhr-Hansen, H. 1989: The Silurian shales of central and western North Greenland: evaluation of hydrocarbon source rock potential. *Rapp. Grønlands geol. Unders.* **143.**

Christiansen, F. G. & Rolle, F. 1985: Project 'Nordolie': hydrocarbon source rock investigations in central North Greenland. *Rapp. Grønlands geol. Unders.* **125**, 17–21.

Christiansen, F. G., Nøhr-Hansen, H., Rolle, F. & Wrang, P. 1985: Preliminary analysis of the hydrocarbon source rock potential of central and western North Greenland. *Rapp. Grønlands geol. Unders.* **126**, 117–128.

Christiansen, F. G., Nykjær, O. & Nøhr-Hansen, H. 1986: Source rock investigations and shallow core drilling in central and western North Greenland – project 'Nordolie'. *Rapp. Grønlands geol. Unders.* **130**, 17–23.

Christiansen, F. G., Nøhr-Hansen, H. & Nykjær, O. 1987: The Cambrian Henson Gletscher Formation: a mature to postmature hydrocarbon source rock sequence from North Greenland. *Rapp. Grønlands geol. Unders.* **133**, 141–157.

Christiansen, F. G., Piasecki, S. & Stemmerik, L. in press: Petroleum, North Greenland. *In* Trettin, H. P. (edit.) *The Innuitian Orogen and Arctic platform: Canada and Greenland. The geology of North America* **E**. Ottawa: Geological Survey of Canada.

Christie, R. L. 1979: The Franklinian geosyncline in the Canadian Arctic and its relationship to Svalbard. *Norsk Polarinstitutt, Skrifter* **167**, 263–314.

Christie, R. L. & Dawes, P. R. in press: A history of exploration and geology in the Innuitian region. *In* Trettin, H. P. (edit.) *The Innuitian Orogen and Arctic platform: Canada and Greenland. The geology of North America* **E**. Ottawa: Geological Survey of Canada.

Christie, R. L. & Ineson, J. R. 1979: Precambrian–Silurian geology of the G. B. Schley Fjord region, eastern Peary Land, North Greenland. *Rapp. Grønlands geol. Unders.* **88**, 63–71.

Christie, R. L. & Peel, J. S. 1977: Cambrian–Silurian stratigraphy of Børglum Elv, Peary Land, eastern North Greenland. *Rapp. Grønlands geol. Unders.* **82**, 48 pp.

Clayton, J. L. & Swetland, P. J. 1978: Subaerial weathering of sedimentary organic matter. *Geochim. cosmochim. Acta* **42**, 305–312.

Clementz, D. M. 1979: Effect of oil and bitumen saturation on source rock pyrolysis. *Bull. Am. Ass. Petrol. Geol.* **63**, 2227–2232.

Clemmensen, L. B. 1979: Notes on the palaeogeographical setting of the Eocambrian tillite-bearing sequence of southern Peary Land, North Greenland. *Rapp. Grønlands geol. Unders.* **88**, 15–22.

Collinson, J. D. 1979: The Proterozoic sandstones between Heilprin Land and Mylius-Erichsen Land, eastern North Greenland. *Rapp. Grønlands geol. Unders.* **88**, 5–10.

Collinson, J. D. 1980: Stratigraphy of the Independence Fjord Group (Proterozoic) of eastern North Greenland. *Rapp. Grønlands geol. Unders.* **99**, 7–23.

Combaz, A. 1964: Les palynofacies. *Rev. Micropaleontol. Paris* **7**, 205–218.

Curiale, J. A. 1986: Origin of solid bitumens, with emphasis on biological marker results. *In* Leythaeuser, D. & Rullkötter, J. (edit.) Advances in organic geochemistry 1985. *Org. Geochem.* **10**, 559–580.

Davies, W. E. 1972: Landscape of northern Greenland. *Spec. Rep. Cold Reg. Res. Engng. Lab.* **164**, 67 pp.

Davis, N. C. & Higgins, A. K. 1987: Cambrian – Lower Silurian stratigraphy in the fold and thrust zone between northern Nyeboe Land and J. P. Koch Fjord, North Greenland. *Rapp. Grønlands geol. Unders.* **133**, 91–98.

Dawes, P. R. 1971: The North Greenland fold belt and environs. *Bull. geol. Soc. Denmark* **20**, 197–239.

Dawes, P. R. 1976: Precambrian to Tertiary of northern Greenland. *In* Escher, A. & Watt, W. S. (edit.) *Geology of Greenland,* 248–303. Copenhagen: Geol. Surv. Greenland.

Dawes, P. R. 1982: The Nyeboe Land fault zone: a major dislocation on the Greenland coast along northern Nares Strait. *In* Dawes, P. R. & Kerr, J. W. (edit.) Nares Strait and the drift of Greenland: a conflict in plate tectonics. *Meddr Grønland Geosci.* **8**, 177–192.

Dawes, P. R. 1984a: Operation Grant Land 1965–1966; a geological exploration programme in Ellesmere Island and North Greenland. *Rapp. Grønlands geol. Unders.* **121**, 5–17.

Dawes, P. R. 1984b: Programme NordGrøn (PNG) 1983–1985: regional mapping and geological studies in western and central North Greenland. *Rapp. Grønlands geol. Unders.* **120**, 18–24.

Dawes, P. R. & Christie, R. L. 1982: History of exploration and geology in the Nares Strait region. *In* Dawes, P. R. & Kerr, J. W. (edit.) Nares Strait and the drift of Greenland: a conflict in plate tectonics. *Meddr Grønland Geosci.* **8**, 19–36.

Dawes, P. R. & Christie, R. L. in press: Geomorphic regions of the Innuitian region. *In* Trettin, H. P. (edit.) *The Innuitian Orogen and Arctic platform: Canada and Greenland. The geology of North America* **E**. Ottawa: Geological Survey of Canada.

Dawes, P. R. & Haller, J. 1979: Historical aspects in the geological investigation of northern Greenland. Part 1: New maps and photographs from the 2nd Thule Expedition 1916–18 and the Bicentenary Jubilee Expedition 1920–1923. *Meddr Grønland* **200**(4), 38 pp.

Dawes, P. R. & Kerr, J. W. (edit.) 1982: Nares Strait and the drift of Greenland: a conflict in plate tectonics. *Meddr Grønland Geosci.* **8**, 392 pp.

Dawes, P. R. & Peel, J. S. 1981: The northern margin of Greenland from Baffin Bay to the Greenland Sea. *In* Nairn, A. E. M., Churkin, M. & Stehli, F. G. (edit.) *The ocean basins and margins* **5**, 201–264. New York: Plenum Publ. Corp.

Dawes, P. R. & Soper, N. J. 1970: Geological investigations in northern Peary Land. *Rapp. Grønlands geol. Unders.* **28**, 9–15.

Dawes, P. R. & Soper, N. J. 1973: Pre-Quaternary history of North Greenland. *In* Pitcher, M. G. (edit.) Arctic geology. *Mem. Am. Ass. Petrol. Geol.* **19**, 117–134.

Dawes, P. R. & Soper, N. J. 1979: Structural and stratigraphic framework of the North Greenland fold belt in Johannes V. Jensen Land, Peary Land. *Rapp. Grønlands geol. Unders.* **93**, 40 pp.

Dawes, P. R. & Soper, N. J. 1973: Pre-Quaternary history of North Greenland. *In* Pitcher, M. G. (edit.) Arctic geology. *Mem. Am. Ass. Petrol. Geol.* **19**, 117–134.

W. (edit.) Nares Strait and the drift of Greenland: a conflict in plate tectonics. *Meddr Grønland Geosci.* **8**, 89–104.

Deines, P. 1980: The isotopic composition of reduced organic matter. *In* Fritz, P. & Fontez, J. Ch. (edit.) *Handbook of environmental isotope geochemistry*. Vol. **1**, *The terrestrial environment,* 329–407. Amsterdam: Elsevier.

Demaison, G. 1984: The generative basin concept. *In* Demaison, G. & Murris, R. J. (edit.) Petroleum geochemistry and basin evaluation. *Mem. Am. Ass. Petrol. Geol.* **35**, 1–14.

Dorning, K. J. 1987: The organic palaeontology of Palaeozoic carbonate environments. *In* Hart, M. B. (edit.) *Micropalaeontology of carbonate environments*, 256–265. Chichester, England: Ellis Horwood Ltd.

Dow, W. G. 1977: Kerogen studies and geological interpretations. *J. geochem. Expl.* **7**, 79–99.

Duffield, S. L. 1985: Land-derived microfossils from the Jupiter Formation (Upper Llandoverian) Anticosta Island, Québec. *J. Paleont.* **59**, 1005–1010.

Durand, B. (edit.) 1980: *Kerogen. Insoluble organic matter from sedimentary rocks*, 519 pp. Paris: Editions Technip.

Ellitsgaard-Rasmussen, K. 1955: Features of the geology of the folding range of Peary Land, North Greenland. *Meddr Grønland* **127**(7), 56 pp.

Embry, A. F., Powell, T. C. & Mayr, U. in press: Petroleum resources, Arctic Islands. A. Petroleum. *In* Trettin, H. P. (edit.) *The Innuitian Orogen and Arctic platform: Canada and Greenland. The geology of North America* **E**. Ottawa: Geological Survey of Canada.

Epstein, A. G., Epstein, J. B. & Harris, L. D. 1977: Conodont color alteration – an index to metamorphism. *Prof. Pap. U.S. geol. Surv.* **995**, 27 pp.

Epstein, S., Buchsbaum, R., Lowenstam, H. A. & Urey, H. C. 1951: Carbonate-water isotopic temperature scale. *Bull. geol. Soc. Am.* **62**, 417–425.

Escher, J. C. & Larsen P.-H. 1987: The buried western extension of the Navarana Fjord escarpment in central and western North Greenland. *Rapp. Grønlands geol. Unders.* **133**, 81–89.

Espitalié, J., Laporte, J. L., Madec, M., Marquis, F., Leplat, P. 1977: Methode rapide de caracterisation des roches mères de leur potentiel pétrolier et de leur degré d'évolution. *Revue Inst. fr. Pétrole* **32**, 23–42.

Espitalié, J., Madec, M. & Tissot, B. 1980: Role of mineral matrix in kerogen pyrolysis: influence on petroleum generation and migration. *Bull. Am. Ass. Petrol. Geol.* **64**, 59–66.

Espatilié, J., Makadi, K. S. & Trichet, Y. 1984: Role of the mineral matrix during kerogen pyrolysis. *Org. Geochem.* **6**, 365–382.

Evans, R. J. & Felbeck, Jr. G. T. 1983: High temperature simulation of petroleum formation – II. Effects of inorganic sedimentary constituents on hydrocarbon formation. *Org. Geochem.* **4**, 145–152.

Folk, R. L. 1968: *Petrology of sedimentary rocks*, 170 pp. Austin, Texas: Hemphill's.

Forsberg, A. & Bjorøy, M. 1983: A sedimentological and organic geochemical study of the Botneheia Formation, Svalbard, with special emphasis on the effects of weathering on the organic matter in shales. *In* Bjorøy, M. *et al.* (edit.) *Advances in organic geochemistry 1981*, 60–68. London: Wiley & sons Ltd.

Foscolos, A. E., Powell, T. G. & Gunther, P. R. 1976: The use of clay minerals and inorganic and organic geochemical indicators for evaluating the degree of diagenesis and oil generating potential of shales. *Geochim. cosmochim. Acta* **40**, 953–966.

Friderichsen, J. D. & Bengaard, H.-J. 1985: The North Greenland fold belt in eastern Nansen Land. *Rapp. Grønlands geol. Unders.* **126**, 69–78.

Friderichsen, J. D., Higgins, A. K., Hurst, J. M., Pedersen, S. A. S., Soper, N. J. & Surlyk, F. 1982: Lithostratigraphic framework of the Upper Proterozoic and Lower Palaeozoic deep water clastic deposits of North Greenland. *Rapp. Grønlands geol. Unders.* **107**, 20 pp.

Frisch, T. 1974: Metamorphic and plutonic rocks of northernmost Ellesmere Island, Canadian Arctic Archipelago. *Bull. geol. Surv. Can.* **229**, 87 pp.

Galimov, E. M. 1980: $^{13}C/^{12}C$ in kerogen. *In* Durand, B. (edit.) *Kerogen*, 271–300. Paris: Editions Technip.

Gleadow, A. J. W. & Lovering, J. F. 1978: Thermal history of granitic rocks from western Victoria: a fission track dating study. *J. Geol. Soc. Aust.* **25**, 323–340.

Gleadow, A. J. W., Duddy, I. R. & Lovering, J. F. 1983: Fission track analysis: a new tool for the evaluation of thermal histories and hydrocarbon potential. *Austr. Petrol. Expl. Assoc. J.* **23**, 93–102.

Gleadow, A. J. W., Duddy, I. R., Green, P. F. & Lovering, J. F. 1986: Confined fission track lengths in apatite: a diagnostic tool for thermal history. *Contr. Mineral. Petrol.* **94**, 405–415.

Glensen, P. G. & Andrews, H. N. 1987: The evolution of early land plants. *American Scientist* **75**, 478–489.

Glickson, M., Gibson, D. L. & Philp, R. P. 1985: Organic matter in Australian Cambrian oil shales and Lower Palaeozoic shales. *Chem. Geol.* **51**, 175–191.

Goodarzi, F. & Norford, B. S. 1985: Graptolites as indicators of the temperature history of rocks. *J. geol. Soc. Lond.* **142**, 1089–1099.

Goodarzi, F., Snowdon, L. R., Gunther, P. R. & Jenkins, W. A. M. 1985: Preliminary organic petrography of Palaeozoic rocks from the Grand Banks, Newfoundland. *Marine Petrol. Geol.* **2**, 254–259.

Grahn, Y. & Nøhr-Hansen, H. 1989: Chitinozoans from Ordovician and Silurian shelf and slope sequences from North Greenland. *Rapp. Grønlands geol. Unders.* **144.**

Grantham, P. J. 1986: The occurrence of unusual C_{27} and C_{29} sterane predominance in two types of Oman crude oil. *Org. Geochem.* **9**, 1–10.

Grønlands Fiskeri- og Miljøundersøgelser 1986: Biologiske miljøundersøgelser i Nordgrønland 1984–85. Unpubl. rep., 113 pp.

Gutjahr, C. C. M. 1983: Introduction to incident-light microscopy of oil and gas source rocks. *Geol. Mijnbouw* **62**, 417–425.

Håkansson, E. & Stemmerik, L. 1984: Wandel Sea Basin – The North Greenland equivalent to Svalbard and the Barents Shelf. *In* Spencer, A. M. *et al.* (edit.) *Petroleum geology of North European margin*, 97–107. Norwegian Petroleum Society.

Hansen, B. T., Kalsbeek, F. & Holm, P. M. 1987: Archaean age and Proterozoic metamorphic overprinting of the crystalline basement at Victoria Fjord, North Greenland. *Rapp. Grønlands geol. Unders.* **133**, 159–168.

Hansen, K. 1985: Fission track age determinations of vertical movements in the crust caused by continental rifting: a fission track age study of the Scoresby Sund area; method and results. Unpublished lic.scient. thesis, Univ. Copenhagen, 119 pp.

Hatch, J. R., Jacobsen, S. R., Witzke, B. J., Risatti, J. B., Anders, D. E., Watney, W. L., Newell, K. D. & Vuletich, A. K. 1987: Possible late Middle Ordovician organic carbon isotope excursion: evidence from Ordovician oils and hydrocarbon source rocks, Mid-Continent and East-Central United States. *Bull. Am. Ass. Petrol. Geol.* **71**, 1342–1354.

Henderson, G. 1976: Petroleum geology. *In* Escher, A. & Watt, W. S. (edit.) *Geology of Greenland*, 489–505. Copenhagen: Geol. Surv. Greenland.

Henriksen, N. 1985a: Systematic 1:500 000 mapping and regional geological studies in central and western North Greenland. *Rapp. Grønlands geol. Unders.* **125**, 9–17.

Henriksen, N. 1985b: Systematic geological mapping in 1984 in central and western North Greenland. *Rapp. Grønlands geol. Unders.* **126**, 5–10.

Henriksen, N. 1986: Completion of field work for the 1:500 000 mapping and regional geological studies in central and western North Greenland. *Rapp. Grønlands geol. Unders.* **130**, 9–17.

Henriksen, N. 1987: Systematic geological mapping in 1985 in central and western North Greenland. *Rapp. Grønlands geol. Unders.* **133**, 5–12.

Henriksen, N. & Jepsen, H. F. 1985: Precambrian crystalline basement at the head of Victoria Fjord, North Greenland. *Rapp. Grønlands geol. Unders.* **126**, 11–16.

Henriksen, N. & Peel, J. S. 1976: Cambrian – Early Ordovician stratigraphy in southwestern Washington Land, western North Greenland. *Rapp. Grønlands geol. Unders.* **80**, 17–23.

Heroux, Y. Chagnon, A. & Bertrand, R. 1979: Compilation and correlation of major thermal maturation indicators. *Bull. Am. Ass. Petrol. Geol.* **63**, 2128–2144.

Higgins, A. K. 1986: Geology of central and eastern North Greenland. *Rapp. Grønlands geol. Unders.* **128**, 37–54.

Higgins, A. K. & Soper, D. J. 1985: Cambrian – Lower Silurian slope and basin stratigraphy between northern Nyeboe Land and western Amundsen Land, North Greenland. *Rapp. Grønlands geol. Unders.* **126**, 79–86.

Higgins, A. K., Mayr, U. & Soper, N. J. 1982: Fold belts and metamorphic zones of northern Ellesmere Island and North Greenland. *Rapp. Grønlands geol. Unders.* **130**, 9–17.

Higgins, A. K., Soper, N. J. & Friderichsen, J. D. 1985: North Greenland fold belt in eastern North Greenland. *In* Gee, D. G. & Sturt, B. A. (edit.) *The Caledonide Orogen – Scandinavia and related areas,* 1017–1029. London: John Wiley & Sons Ltd.

Higgins, A. K., Ineson, J. R., Peel, J. S., Surlyk, F. & Sønderholm, M. in press: The Franklinian basin in North Greenland. *In* Trettin, H. P. (edit.) *The Innuitian Orogen and Arctic platform: Canada and Greenland. The geology of North America* E. Ottawa: Geological Survey of Canada.

Hills, I. R., Whitehead, E. V., Anders, D. E., Cummins, J. J. & Robinson, W.E. 1966: An optically active triterpane, gammacerane in Green River, Colorado, oil shale bitumen. *Chem. Commun.* **20**, 752–754.

Horsfield, B. 1984: Pyrolysis studies and petroleum exploration. *In* Brooks, J. & Welte, D. (edit.) *Advances in petroleum geochemistry* **1**, 247–298. London: Academic Press.

Horsfield, B., Dembicki Jr, H. & Ho, T. T. Y. 1983: Some potential applications of pyrolysis to basin studies. *J. geol. Soc. Lond.* **140**, 431–443.

Huang, W.-Y. & Meinschein, W. G. 1976: Sterols as ecological indicators. *Geochim. cosmochim. Acta* **40**, 323–330.

Hunt, J. M. 1979: *Petroleum geochemistry and geology*, 615 pp. San Francisco: W. H. Freeman and Co.

Hurford, A. J. 1986: Cooling and uplift patterns in the Lepontine Alps, South Central Switzerland and an age of the vertical movement on the Insubric fault line. *Contrib. Miner. Petrol.* **92**, 413–427.

Hurford, A. J. & Green, P. F. 1983: The zeta age calibration of fission track dating. *Isotope Geosci.* **1**, 285–317.

Hurst, J. M. 1980a: Silurian stratigraphy and facies distribution in Washington Land and western Hall Land, North Greenland. *Bull. Grønlands geol. Unders.* **138**, 95 pp.

Hurst, J. M. 1980b: Paleogeographic and stratigraphic differentiation of Silurian buildups and biostromes of North Greenland. *Bull. Am. Ass. Petrol. Geol.* **64**, 527–548.

Hurst, J. M. 1981: Platform edge and slope relationships: Silurian of Washington Land, North Greenland and comparison to Arctic Canada. *Bull. Can. Petrol. Geol.* **29**, 408–419.

Hurst, J. M. 1984: Upper Ordovician and Silurian carbonate shelf stratigraphy, facies and evolution, eastern North Greenland. *Bull. Grønlands geol. Unders.* **148**, 73 pp.

Hurst, J. M. & Peel, J. S. 1979: Late Proterozoic (?) to Silurian stratigraphy of southern Wulff Land, North Greenland. *Rapp. Grønlands geol. Unders.* **91**, 37–56.

Hurst, J. M. & Surlyk, F. 1982: Stratigraphy of the Silurian turbidite sequence of North Greenland. *Bull. Grønlands geol. Unders.* **145**, 121 pp.

Hurst, J. M. & Surlyk, F. 1983: Initiation, evolution and destruction of an early Paleozoic carbonate shelf, eastern North Greenland. *J. Geol.* **91**, 671–691.

Hurst, J. M., McKerrow, W. S., Soper, N. J. & Surlyk, F. 1983: The relationship between Caledonian nappe tectonics and Silurian turbidite deposition in North Greenland. *J. geol. Soc. Lond.* **140**, 123–132.

Illich, H. A. 1983: Pristane, phytane, and lower molecular weight isoprenoid distributions in oils. *Bull. Am. Ass. Petrol. Geol.* **67**, 385–397.

Ineson, J. R. 1985: The stratigraphy and sedimentology of the Brønlund Fjord and Tavsen Iskappe Groups (Cambrian) of Peary Land, eastern North Greenland. Unpublished Ph.D. thesis, University of Keele, U.K., 310 pp.

Ineson, J. R. & Peel, J. S. 1980: Cambrian stratigraphy in Peary Land, eastern North Greenland. *Rapp. Grønlands geol. Unders.* **99**, 33–42.

Ineson, J. R. & Peel, J. S. 1987: Cambrian platform – outer shelf relationship in the Nordenskiöld Fjord region, central North Greenland. *Rapp. Grønlands geol. Unders.* **133**, 13–26.

Ineson, J. R. & Peel, J. S. in press: Cambrian shelf stratigraphy of the Peary Land region, central North Greenland. *Bull. Grønlands geol. Unders.*

Jacob, H. 1983: Recent studies on the genesis of natural solid oil bitumens. *Geol. Jahr. Reihe D* **59**, 61 pp.

Jacob, H. 1985: Disperse, feste Erdölbitumina als Migrations- und Maturitätsindikatoren im Rahmen der Erdöl-/Erdgas-Prospektion. Eine Modellstudie in NW-Deutschland. *Deutsche Gesellschaft Mineralölwissenschaft und Kohlechemie E.V., Forschungsbericht* **267**, 54 pp.

Jensenius, J. 1987: Fluid inclusion and stable isotope studies of diagenetic calcite and dolomite associated with seeping asphalt, North Greenland, 28 pp. *In* Jensenius, J. 1987: Fluid inclusion microthermometry and stable isotope studies applied to the diagenesis of sedimentary rocks. Unpublished lic. scient. thesis, University of Copenhagen.

Jepsen, H. F. 1971: The Precambrian, Eocambrian and early Palaezoic stratigraphy of the Jørgen Brønlund Fjord area, Peary Land, North Greenland. *Bull. Grønlands geol. Unders.* **96**, 42 pp.

Jones, R. W. 1987: Organic facies. *In* Brooks, J. (edit.) *Advances in petroleum geochemistry* **2**, 1–90. London: Academic Press.

Katz, B. J. 1983: Limitations of 'Rock-Eval' pyrolysis for typing organic matter. *Org. Geochem.* **4**, 195–199.

Kerr, J. W. 1967: Nares submarine rift valley and relative rotation of North Greenland. *Bull. Can. Petrol. Geol.* **15**, 483–520.

Kerr, J. W. 1980: A plate tectonic contest in Arctic Canada. *In* Strangway, D. W. (edit.) The continental crust and its mineral deposits. *Spec. Pap. geol. Ass. Can.* **20**, 457–486.

Kingston, D. R., Dishroon, C. P. & Williams, P. A. 1985: Global basin classification system. *Oil Gas J.* **83**(18), 238–262.

Kisch, H. J. 1980: Incipient metamorphism of Cambro-Silurian clastic rocks from the Jamtland Supergroup, central Scandinavian caledonides, western Sweden: illite crystallinite and 'vitrinite' reflectance. *J. geol. Soc. Lond.* **137**, 271–288.

Klemme, H. D. 1971: What giants and their basins have in common. *Oil Gas J.* **69**(9), 85–90.

Koch, C. J. W. 1987: Preparation and characterization by X-ray diffraction of kerogen from Cambrian and Silurian sedimentary rocks from North Greenland. Unpubl. intern. GGU rep., 13 pp.

Koch, L. 1925: The geology of North Greenland. *Am. J. Sci.* **9**, 271–285.

Koch, L. 1929: Stratigraphy of Greenland. *Meddr Grønland* **73**(2), 205–320.

Kontorovich, A. E. 1984: Geochemical methods for the quantitative evaluation of the petroleum potential of sedimentary basins. *In* Demaison, G. & Murris, R. J. (edit.) Petroleum geochemistry and basin evaluation. *Mem. Am. Ass. Petrol. Geol.* **35**, 79–109.

Krebs, W. & Macqueen, R. W. 1984: Sequence of diagenetic and mineralization events, Pine-Point lead-zinc property, Northwest Territories, Canada. *Bull. Can. Petrol. Geol.* **32**, 434–464.

Larsen, N. H. 1985: Cambrian endolithic alga from North Greenland. Sec. Int. Phycol. Congr., Book of abstracts, 88. Copenhagen.

Larsen, N. H. 1989: Fossil algae from North Greenland. *Open File Ser. Grønlands geol. Unders.* **89/3**, 32 pp. + 42 figs.

Larsen, O. 1982: The age of the Kap Washington Group volcanics, North Greenland. *Bull. geol. Soc. Denmark* **31**, 49–55.

Larsen, O., Dawes, P. R. & Soper, N. J. 1978: Rb/Sr age of the Kap Washington Group, Peary Land, North Greenland, and its geotectonic implications. *Rapp. Grønlands geol. Unders.* **90**, 115–119.

Larsen, P.-H. & Escher, J. C. 1985: The Silurian turbidite sequence of the Peary Land Group between Newman Bugt and Victoria Fjord, western North Greenland. *Rapp. Grønlands geol. Unders.* **126**, 47–67.

Larsen, P.-H. & Escher, J. C. 1987: Additions to the lithostratigraphy of the Peary Land Group (Silurian) in western and central North Greenland. *Rapp. Grønlands geol. Unders.* **133**, 65–80.

Larsen, P.-H., Edwards, D. & Escher, J. C. 1987: Late Silurian plant megafossils from the Peary Land Group, North Greenland. *Rapp. Grønlands geol. Unders.* **133**, 107–112.

Legall, F. D., Barnes, C. R. & Macqueen, R. W. 1981: Thermal maturation, burial history and hotspot development, Paleozoic strata of southern Ontario–Québec, from conodont and acritarch colour alteration studies. *Bull. Can. Petrol. Geol.* **29**, 492–539.

Leggett, J. K., McKerrow, W. S., Cocks, L. R. M. & Richards, R. B. 1981: Perodicity in the early Palaeozoic marine realm. *J. geol. Soc. Lond.* **138**, 167–176.

Lewan, M. D. 1983: Effects of thermal maturation on stable organic carbon isotopes as determined by hydrous pyrolysis of Woodford Shale. *Geochim. cosmochim. Acta* **47**, 1471–1479.

Lewan, M. D. 1986: Stable carbon isotopes of amorphous kerogens from Phanerozoic rocks. *Geochim. cosmochim. Acta* **50**, 1583–1591.

Leythaeuser, D. 1973: Effects of weathering on organic matter in shales. *Geochim. cosmochim. Acta* **37**, 113–120.

Link, W. K. 1952: Significance of oil and gas seeps in World oil exploration. *Bull. Am. Ass. Petrol. Geol.* **36**, 1505–1540.

Macauley, G., Snowdon, L. R. & Ball, F. D. 1985: Geochemistry and geological factors governing exploitation of selected Canadian oil shale deposits. *Pap. geol. Surv. Can.* **85–13**, 65 pp.

Mackenzie, A. G. 1984: Applications of biological markers in petroleum geochemistry. *In* Brooks, J. & Welte, D. H. (edit.) *Advances in petroleum geochemistry* **1**, 115–214. London: Academic Press.

Macqueen, R. W. & Powell, T. G. 1983: Organic geochemistry of the Pine Point lead-zinc ore field and region, Northwest Territories, Canada. *Econ. Geol.* **78**, 1–15.

Marcussen, C., Christiansen, F. G., Larsen, P.-H., Olsen, H., Piasecki, S., Stemmerik, L., Bojesen-Koefoed, J., Jepsen, H. F. & Nøhr-Hansen, H. 1987: Studies of the onshore hydrocarbon potential in East Greenland 1986–87: field work from 72° to 74°N. *Rapp. Grønlands geol. Unders.* **135**, 72–81.

McKerrow, W. S. 1979: Ordovician and Silurian changes in sea level. *J. geol. Soc. Lond.* **136**, 137–145.

McKirdy, D. M., Aldridge, A. K. & Ypma, P. J. M. 1983: A geochemical comparison of some crude oils from Pre-Ordovician carbonate rocks. *In* Bjoroy, M. *et al.* (edit.) *Advances in organic geochemistry 1981*, 99–107. London: Wiley & Sons Ltd.

McKirdy, D. M., Kantsler, A. J., Emmett, J. K. & Aldridge, A. K. 1984: Hydrocarbon genesis and organic facies in Cambrian carbonates of the eastern Officer basin, South Australia. *In* Palacas, J. G. (edit.) Petroleum geochemistry and source rock potential of carbonate rocks. *Am. Ass. Petrol. Geol. Stud. Geol.* **18**, 13–31.

Miller, B. M. 1986: Resource appraisal methods, choice and outcome. *In* Rice, D. D. (edit.) Oil and gas assessment. *Am. Ass. Petrol. Geol. Stud. Geol.* **21**, 1–23.

Moldowan, J. M. Seifert, W. K. & Gallegos, E. J. 1985: Relationship between petroleum composition and depositional environment of petroleum source rocks. *Bull. Am. Ass. Petrol. Geol.* **69**, 1255–1268.

Moore, L. V. 1984: Significance, classification of asphaltic material in petroleum exploration. *Oil Gas J.* **82**(41), 109–112.

Nassichuk, W. W. 1983: Petroleum potential in Arctic North

America and Greenland. *Cold Regions Science and Technology* **7**, 51–88.

Nielsen, E. 1941: Remarks on the map and the geology of Kronprins Christians Land. *Meddr Grønland* **126**(2), 34 pp.

Norford, B. S. 1972: Silurian stratigraphic sections at Kap Tyson, Offley Ø and Kap Schuchert, northwestern Greenland. *Meddr Grønland* **195**(2), 40 pp.

Nøhr-Hansen, H. & Koppelhus, E. B. 1988: Ordovician spores with trilete rays from Washington Land, North Greenland. *Rev. Palaeobot. Palynol.* **56**, 305–311.

O'Connor, B. 1979: The Portfjeld Formation (?early Cambrian) of eastern North Greenland. *Rapp. Grønlands geol. Unders.* **88**, 23–28.

Ogunyami, O., Hesse, R. & Héroux, Y. 1980: Pre-orogenic and synorogenic diagenesis and anchimetamorphism in Lower Paleozoic continental margin sequences of the northern Appalachians in and around Quebec City, Canada. *Bull. Can. Petrol. Geol.* **28**, 559–577.

Ourisson, G., Albrecht, P. & Rohmer, M. 1979: Paleochemistry and biochemistry of a group of natural products: the hopanoids. *Pure Appl. Chem.* **51**, 709–729.

Østfeldt, P. 1987a: Oil-source rock correlation in the Danish North Sea. *In* Brooks, J. & Glennie, K. (edit.): *Petroleum geology of North West Europe,* 419–429. London: Graham & Trotman.

Østfeldt, P. 1987b: Organic geochemistry of North Greenland samples. Unpubl. intern. GGU rep., 43 pp.

Parrish, J. T. 1982: Upwelling and petroleum source beds, with reference to Paleozoic. *Bull. Am. Ass. Petrol. Geol.* **66**, 750–774.

Parrish, J. T. 1987: Palaeo-upwelling and the distribution of organic-rich rocks. *In* Brooks, J. & Fleet, A. J. (edit.) Marine petroleum source rocks. *Spec. Publ. geol. Soc. Lond.* **26**, 199–205.

Peel, J. S. 1979: Cambrian – Middle Ordovician stratigraphy of the Adams Gletscher region, south-west Peary Land, North Greenland. *Rapp. Grønlands geol. Unders.* **88**, 29–39.

Peel, J. S. 1980: Cambrian and Ordovician geology of Warming Land and southern Wulff Land, central North Greenland. *Rapp. Grønlands geol. Unders.* **101**, 55–60.

Peel, J. S. 1982: The Lower Paleozoic of Greenland. *In* Embry, A. F. & Balkwill, H. R. (edit.) Arctic geology and geophysics. *Mem. Can. Soc. Petrol. Geol.* **8**, 309–330.

Peel, J. S. 1985: Cambrian – Silurian platform stratigraphy of eastern North Greenland. *In* Gee, D. G. & Sturt, B. A. (edit.) *The Caledonide Orogen – Scandinavia and related areas,* 1077–1094. London: John Wiley & Sons Ltd.

Peel, J. S. & Christie, R. L. 1982: Cambrian–Ordovician stratigraphy, correlations around Kane basin. *In* Dawes, P. R. & Kerr, J. W. (edit.) Nares Strait and the drift of Greenland: a conflict in plate tectonics. *Meddr Grønland Geosci.* **8**, 117–135.

Peel, J. S. & Hurst, J. M. 1980: Late Ordovician and early Silurian stratigraphy of Washington Land, western North Greenland. *Rapp. Grønlands geol. Unders.* **100**, 18–24.

Peel, J. S. & Wright, S. C. 1985: Cambrian platform stratigraphy in the Warming Land – Freuchen Land region, North Greenland. *Rapp. Grønlands geol. Unders.* **126**, 17–24.

Peel, J. S., Dawes, P. R., Collinson, J. D. & Christie, R.L. 1982: Proterozoic – basal Cambrian stratigraphy across Nares Strait: correlation between Inglefield Land and Bache Peninsula. *In* Dawes, P. R. & Kerr, J. W. (edit.) Nares Strait and the drift of Greenland: a conflict in plate tectonics. *Meddr Grønland Geosci.* **8**, 105–115.

Perregaard, J. 1979: Organic geochemistry of sedimentary organic matter from Greenland: a petroleum source rock evaluation. Unpubl. intern. GGU rep., 81 pp. + appendix.

Philp, R. P. & Lewis, C. A. 1987: Organic geochemistry of biomarkers. *Ann. Rev. Earth Planet. Sci.* **15**, 363–395.

Poty, B., Leroy, J. & Jachimowicz, 1976: A new device for measuring temperatures under microscope: the Chaixmeca microthermometry apparatus. *In* Roedder, E. & Kozlowski, A. (edit) *Fluid inclusion research* **9**, 173–178.

Powell, T. G. 1978: An assessment of the hydrocarbon source potential of the Canadian Arctic Island. *Pap. geol. Surv. Can.* **78–12**, 82 pp.

Powell, T. G., Macqueen, R. W., Barker, J. F. & Bree, D. G. 1984: Geochemical character and origin of Ontario oils. *Bull. Can. Petrol. Geol.* **32**, 289–312.

Procter, R. M., Tayor, G. C. & Wade, J. A. 1984: Oil and gas resources of Canada. *Pap. geol. Surv. Can.* **83–31**, 59 pp.

Radke, B. M. & Mathis, R. L. 1980: On the formation and occurrence of saddle dolomite. *J. sed. Petrol.* **50**, 1149–1168.

Rayer, F. G. 1981: Exploration prospects and future petroleum potential of the Canadian Arctic Islands. *J. petrol. Geol.* **3**, 367–412.

Reed, J. D., Illich, H. A. & Horsfield, B. 1986: Biochemical evolutionary significance of Ordovician oils and their sources. *In* Leythaeuser, D. & Rullkötter, J. (edit.) Advances in organic geochemistry 1985. *Org. Geochem.* **10**, 347–358.

Rice, D. D. (edit.) 1986: Oil and gas assessment. *Am. Ass. Petrol. Geol. Stud. Geol.* **21**, 267 pp.

Robert, P. 1974: Analyse microscopique des charbons et des bitumen dispersés dans roches et mesure de leur pouvoir réflecteur. Application à l'étude de la paléogéothermie des bassins sédimentaires et de la genèse des hydrocarbures. *In* Tissot, B. & Bienner, F. (edit.) *Advanced organic geochemistry,* 549–569. Rueil-Malmaison.

Rogers, M. A., McAlary, J. D. & Baily, N. J. L. 1974: Significance of reservoir bitumens to thermal-maturation studies, Western Canada basin. *Bull. Am. Ass. Petrol. Geol.* **58**, 1806–1824.

Rolle, F. 1981: Hydrocarbon source rock sampling in Peary Land 1980. *Rapp. Grønlands geol. Unders.* **106**, 99–103.

Rolle, F. & Wrang, P. 1981: En foreløbig oliegeologisk vurdering af Peary Land området i Nordgrønland. Unpubl. intern. GGU rep., 21 pp.

Rullkötter, J., Meyers, P. A., Schaefer, R. G. & Dunham, K. W. 1986: Oil generation in the Michigan Basin: a biological marker and carbon isotope approach. *In* Leythaeuser, D. & Rullkötter, J. (edit.) Advances in organic geochemistry 1985. *Org. Geochem.* **10**, 359–375.

St. John, B., Bally, A. W. & Klemme, H. D. 1984: Sedimentary provinces of the world – hydrocarbon productive and nonproductive. *Am. Assoc. Petrol. Geol. Map Library,* 36 pp. + maps.

Schoell, M. 1984: Wasserstoff- und Kohlenstoffisotope in organischen Substanzen, Erdölen und Erdgassen. *Geol Jahrb. Reihe D.* **67**, 167 pp.

Schopf, T. J. M. 1983: Paleozoic black shales in relation to continental margin upwelling. *In* Thiede, J. & Suess, E. (edit.) *Coastal upwelling, its sediment record, part B: Sedimentary records of ancient coastal upwelling,* 570–596. New York: Plenum Press.

Scotese, C. R., Bambach, R. K., Barton, C., Van der Voo, R. & Ziegler, A. M. 1979: Palaeozoic base maps. *J. Geol.* **87**, 217–278.

Sikander, A. H. & Pittion, J. L. 1978: Reflectance studies on organic matter in Lower Paleozoic sediments of Quebec. *Bull. Can. Petrol. Geol.* **26**, 132–151.

Sluijk, D. & Nederlof, M. H. 1984: Worldwide geological experience as a systematic basis for prospect appraisal. *In* Demaison, G. & Murris, R. J. (edit.) Petroleum geochemistry and basin evaluation. *Mem. Am. Ass. Petrol. Geol.* **35,** 15–26.

Smith, M. P., Sønderholm, M. & Tull, S. J. 1989: The Morris Bugt Group (Middle Ordovician – Early Silurian) of North Greenland and its correlatives. *Rapp. Grønlands geol. Unders.* **143**.

Sønderholm, M. & Due, P. H. 1985: Lower and Middle Ordovician platform carbonate lithostratigraphy of Warming Land, Wulff Land and Nares Land, North Greenland. *Rapp. Grønlands geol. Unders.* **126**, 31–46.

Sønderholm, M. & Harland, T. L. 1989a: Franklinian reef belt, Silurian, North Greenland. *In* Geldsetzer, H. J. J., James, N. P. & Tebbutt, G. E. (edit.) Reefs, Canada and adjacent area. *Mem. Can. Soc. Petrol. Geol.* **13,** 356-366.

Sønderholm, M. & Harland, T. L. 1989b: Latest Ordovician – earliest Silurian reef mounds in western North Greenland. *In* Geldsetzer, H. J. J., James, N. P. & Tebbutt, G. E. (edit.) Reefs, Canada and adjacent area. *Mem. Can. Soc. Petrol. Geol.* **13,** 241-243.

Sønderholm, M., Harland, T. L., Due, P. H., Jørgensen, L. N. & Peel, J. S. 1987: Lithostratigraphy and depositional history of Upper Ordovician – Silurian shelf carbonates in central and western North Greenland. *Rapp. Grønlands geol. Unders.* **133**, 27–40.

Soper, N. J. & Higgins, A. K. 1987: A shallow detachment beneath the North Greenland fold belt: implications for sedimentation and tectonics. *Geol. Mag.* **124**, 441–450.

Soper, N. J., Dawes, P. R. & Higgins, A. K. 1982: Cretaceous–Tertiary magmatic and tectonic events in North Greenland and the history of adjacent ocean basins. *In* Dawes, P. R. & Kerr, J. W. (edit.) Nares Strait and the drift of Greenland: a conflict in plate tectonics. *Meddr Grønland Geosci.* **8**, 205–220.

Springer, N. 1981: Preliminary Rb-Sr age determinations from the North Greenland fold belt, Johannes V. Jensen Land, with comments on the metamorphic grade. *Rapp. Grønlands geol. Unders.* **106**, 77–84.

Springer, N. (compiler) 1987: Conventional core analysis for GGU. Cambrian sandstones from North Greenland (Nordolie). Unpubl. intern. GGU rep., 17 pp.

Sproule, J. C. 1966: Oil and gas prospects of the Canadian Arctic Islands. *Proc. 8th Commonwealth Mining and Metallurgical Congress, Australia and New Zealand 1965,* Vol. **5** (Petroleum), 57–64.

Staplin, F. L. 1969: Sedimentary organic matter, organic metamorphism, and oil and gas occurrence. *Bull. Can. Soc. Petrol. Geol.* **17**, 47–66.

Stemmerik, L. & Håkansson, E. 1989: Stratigraphy and depositional history of the Upper Palaeozoic and Triassic sediments in the Wandel Sea Basin, eastern North Greenland. *Rapp. Grønlands geol. Unders.* **143**.

Stoneley, R. 1981: Petroleum: the sedimentary basin. *In* Tarling, D. H. (edit.) *Economic geology and geotectonics,* 51–71. London: John Wiley & Sons Ltd.

Stouge, S., Thomsen, E. & Guvad, C. 1988: Reflected light microscopy of graptolite periderm material of Ordovician/Silurian strata in North Greenland. Unpubl. intern. GGU rep., 58 pp.

Strother, P. K. & Traverse, A. 1979: Plant microfossils from Llandoverian and Wenlockian rocks of Pennsylvania. *Palynology* **3**, 1–21.

Stuart-Smith, J. H. 1970: Hydrocarbon potential of northern Greenland. *Bull. Am. Ass. Petrol. Geol.* **54**, 2507 only.

Stuart-Smith, J. H. & Wennekers, J. H. N. 1977: Geology and hydrocarbon discoveries of Canadian Arctic Islands. *Bull. Am. Ass. Petrol. Geol.* **61**, 1–27.

Surlyk, F. 1982: Nares Strait and the down-current termination of the Silurian turbidite basin of North Greenland. *In* Dawes, P. R. & Kerr, J. W. (edit.) Nares Strait and the drift of Greenland: a conflict in plate tectonics. *Meddr Grønland Geosci.* **8**, 147–150.

Surlyk, F. 1983: Source rock sampling, stratigraphical and sedimentological studies in the Upper Palaeozoic of the Jameson Land basin, East Greenland. *Rapp. Grønlands geol. Unders.* **115**, 88–93.

Surlyk, F. & Hurst, J. M. 1983: Evolution of the early Paleozoic deep-water basin of North Greenland – aulacogen or narrow ocean? *Geology* **11**, 77–81.

Surlyk, F. & Hurst, J. M. 1984: The evolution of the early Paleozoic deep-water basin of North Greenland. *Bull. geol. Soc. Am.* **95**, 131–154.

Surlyk, F., Hurst, J. M., Marcussen, C., Piasecki, S., Rolle, F., Scholle, P. A., Stemmerik, L. & Thomsen, E. 1984: Oil geological studies in the Jameson Land basin, East Greenland. *Rapp. Grønlands geol. Unders.* **120**, 85–90.

Surlyk, F. & Ineson, J. R. 1987a: Aspects of Franklinian shelf, slope and trough evolution and stratigraphy of North Greenland. *Rapp. Grønlands geol. Unders.* **133**, 41–58.

Surlyk, F. & Ineson, J. R. 1987b: The Navarana Fjord Member (new) – an Upper Llandovery platform derived carbonate conglomerate. *Rapp. Grønlands geol. Unders.* **133**, 59–63.

Thickpenny, A. & Leggett, J. K. 1987: Stratigraphic distribution and palaeo-oceanographic significance of European early Palaeozoic organic-rich sediments. *In* Brooks, J. &

Fleet, A. J. (edit.) Marine petroleum source rocks. *Spec. Publ. geol. Soc. Lond.* **26**, 231–247.

Thomsen, E. & Guvad, C. 1987: Organic petrology and thermal maturity of Lower Palaeozoic deposits from western and central North Greenland. Unpubl. intern. GGU rep., part 1 (text) 40 pp. and part 2 (figures) 49 pp.

Tissot, B. P. & Welte D. H. 1984: *Petroleum formation and occurrence,* 699 pp. Berlin, Heidelberg, New York, Tokyo: Springer Verlag.

Trettin, H. P. 1987: Pearya: a composite terrane with Caledonian affinities in northern Ellesmere Island. *Can. J. Earth Sci.* **24**, 224–245.

Trettin, H. P. & Balkwill, H. R. 1979: Contributions to the tectonic history of the Innuitian Province, Arctic Canada. *Can. J. Earth Sci.* **16**, 748–769.

Trettin, H. P., Frisch, T. O., Sobczak, L. W., Weber, J. R., Law, L. R., Delaurier, I., Niblett, E. R. & Whitnam, K. 1972: The Innuitian Province. *In* Price, R. A. & Douglas, R. J. W. (edit.) Variation in tectonic styles in Canada. *Spec. Pap. geol. Ass. Can.* **11**, 83–179.

Troelsen, J. C. 1949: Contributions to the geology of the area round Jørgen Brønlunds Fjord, Peary Land, North Greenland. *Meddr Grønland* **149**(2), 29 pp.

Troelsen, J. C. 1950: Contributions to the geology of Northwest Greenland, Ellesmere Island and Axel Heiberg Island. *Meddr Grønland* **149**(7), 85 pp.

Tyson, R. V. 1987: The genesis and palynofacies characteristics of marine petroleum source rocks. *In* Brooks, J. & Fleet, A. J. (edit.) Marine petroleum source rocks. *Spec. Publ. geol. Soc. Lond.* **26**, 47–67.

Ungerer, P., Bessis, F., Chenet, P. Y., Durand, B., Nogaret, A., Chiarelli, A., Oudin, J. L. & Perrin, J. F. 1984: Geological and geochemical models in oil exploration; principles and practical examples. *In* Demaison, G. & Murris, R. J. (edit.) Petroleum geochemistry and basin evaluation. *Mem. Am. Ass. Petrol. Geol.* **35,** 53–77.

Vavrdová, N. 1984: Some plant microfossils of possible terrestrial origin from the Ordovician of Central Bohemia. *Věstnik Ústředniho ústavu geologického* **59**, 165–170.

Venkatachala, B. S. 1981: Differentiation of amorphous organic matter types in sediments. *In* Brooks, J. (edit.) *Organic maturation studies and fossil fuel exploration,* 177–200. London: Academic Press.

Waples, D. W. 1985: *Geochemistry in petroleum exploration,* 232 pp. Dordrecht: Reidel Publ. Com.

Wedeking, K. W. & Hayes, J. M. 1983: Carbonization of Precambrian kerogens. *In* Bjorøy *et al.* (edit.) *Advances in organic geochemistry 1981,* 546–553. London: Wiley & Sons Ltd.

Welte, D. H., Kalkreuth, W. & Hoefs, J. 1975: Age-trend in carbon isotopic composition in Palaeozoic sediments. *Naturwissenschaften* **62**, 482–483.

Welte, D. H. & Yukler, M. A. 1981: Petroleum origin and accumulation in basin evolution – a quantitative model. *Bull. Am. Ass. Petrol. Geol.* **65**, 1387–1396.

Yarbrough, S. C. 1986: Oil and gas developments in Europe 1985. *Bull. Am. Ass. Petrol. Geol.* **70**, 1578–1610.

Plate 1. Kerogen

A. Sample with a relatively low (0.21% TOC) kerogen content and a dominance of finely disseminated amorphous kerogen in a silica gel, Lafayette Bugt Formation, Nyeboe Land, GGU 316490–1, unsieved organic material.

B. As A., Lafayette Bugt Formation, Nyeboe Land, GGU 316490–2, sieved organic material (on 10 μm nylon mesh).

C. Sample with a relatively moderate (1.15% TOC) kerogen content and small to moderate amounts of large amorphous kerogen particles, Thors Fjord Member, Nares Land, GGU 318007–18–1 unsieved organic material.

D. As C., Thors Fjord Member, Nares Land, GGU 318007–18–2, sieved organic material (on 10 μm nylon mesh).

E. Sample with a relatively large (5.09% TOC) kerogen content and a dominance of large amorphous kerogen particles, Thors Fjord Member, Nares Land, GGU 318007–32–1, unsieved organic material.

F. As E., Thors Fjord Member, Nares Land, GGU 318007–32–2, sieved organic material (on 10 μm nylon mesh).

Scale bar: 20 μm.

Plate 2. Cambrian palynomorphs

A. Acritarch-like folded alga. Middle Cambrian Sydpasset Formation, Freuchen Land, MGUH 19334 from GGU 315873–2; 139.5–13.9.

B. Acritarch-like folded alga. Middle Cambrian Sydpasset Formation, Freuchen Land, MGUH 19335 from GGU 315873–2; 150.6–7.0.

C. Two acritarch-like folded algae. Middle Cambrian Sydpasset Formation, Freuchen Land, MGUH 19336 (large light body), MGUH 19337 (dark small body), both from GGU 315873–2; 122.0–15.3.

D. Acritarch-like folded alga. Middle Cambrian, Ekspedition Bræ Formation, Freuchen Land, MGUH 19338 from GGU 324217–2; 139.2–14.9.

E. Acritarch-like folded alga. Middle Cambrian, Ekspedition Bræ Formation, Freuchen Land, MGUH 19339 from GGU 324300–2; 131.2–13.4.

F. Acritarch-like folded alga. Middle Cambrian, Ekspedition Bræ Formation, Freuchen Land, MGUH 19340 from GGU 324217–2; 141.9–11.4.

G. Lump of algal or spore-like elements. Middle Cambrian, Ekspedition Bræ Formation, Freuchen Land, MGUH 19341 from GGU 324300–2; 127.8–14.4.

H. Diad-like lump of algal or spore-like elements. Middle Cambrian, Ekspedition Bræ Formation, Freuchen Land, MGUH 19342 from GGU 314300–2; 138.5–17.8.

I. Lump of alga or spore-like elements. Middle Cambrian, Ekspedition Bræ Formation, Freuchen Land, MGUH 19343 from GGU 324300–2; 157.7–14.7.

Scale bar: 20 μm.

Plate 3. Ordovician palynomorphs

A. Acritarch. Upper Ordovician Troedsson Cliff Member, Washington Land, MGUH 19344 from GGU 316968–2; 145.3–17.8.

B. Acritarch. Upper Ordovician – Lower Silurian Aleqatsiaq Fjord Formation, Washington Land, MGUH 19345 from GGU 316085–4; 124.1–21.3.

C. Graptolite fragment, Upper Ordovician Troedsson Cliff Member, Washington Land, MGUH 19346 from GGU 316968–2; 128.1–2.9.

D. Scolecodont, Upper Ordovician, Troedsson Cliff Member, Washington Land, MGUH 19347 from GGU 316968–2; 148.8–15.1.

E. Alga. Upper Ordovician – Lower Silurian Aleqatsiaq Formation, Nyeboe Land, MGUH 19348 from GGU 316103–2; 135.0–15.0.

F. Filamentous alga. Upper Ordovician – Lower Silurian Aleqatsiaq Formation, Washington Land, MGUH 19349 from GGU 316058–2; 135.1–4.2.

G.-L. Spores with trilete rays. Upper Ordovician, Troedsson Cliff Member, Washington Land (Nøhr-Hansen & Koppelhus, 1988).

G.-I. *Besselia nunaatica*, MGUH 17539 from GGU 316968–2; 125.5–8.3.

G. Distal view illustrating the minute ornamentation.

H. Equatorial view.

I. Internal proximal view.

J. *Besselia nunaatica*, two connected spores, internal proximal view, MGUH 17541 from GGU 316968–2; 155.1–11.9.

K.-L. *Besselia nunaatica*. MGUH 17542 from GGU 316968–2; 123.8–15.9.

K. Distal view illustrating the ornamentation.

L. Internal proximal view.

Scale bar: 20 μm.

Plate 4. Silurian palynomorphs

A. Chitinozoan, *Angochitina* cf. *A. elongata*. Upper Silurian Wulff Land Formation, Wulff Land, MGUH 19350 from GGU 315950–3; 136.9–17.2.

B. Chitinozoans, *Linochitina erratica*. Upper Silurian Wulff Land Formation, Wulff Land, MGUH 19351 from GGU 315950–2; 154.3–9.6.

C. *Retiolites*, graptolite fragment. Upper Silurian, Wulff Land Formation, Wulff Land, MGUH 19352 from GGU 315950–3; 155.1–11.1.

D. Graptolite fragment, Upper Silurian, Wulff Land Formation, Wulff Land, MGUH 19353 from GGU 315950–2; 127.3–5.7.

E.-H. Trilete spore-like bodies, figs E and F with a degraded bitumen-like appearance.

E. Lower Silurian Lafayette Bugt Formation, Washington Land, MGUH 19354 from GGU 211760–2; 143.3–17.2.

F. Upper Silurian Wulff Land Formation, Wulff Land, MGUH 19355 from GGU 315950–3; 15950–3; 155.5–8.2.

G. Upper Silurian Nyeboe Land Formation, Nyeboe Land, MGUH 19356 from GGU 319234–2; 119.3–11.0.

H. Upper Silurian Nyeboe Land Formation, Wulff Land, MGUH 19357 from GGU 319210–3; 130.6–21.4.

I. Spherical folded algae, acritarchs? Lower Silurian Lafayette Bugt Formation, Hall Land, MGUH 19358 from GGU 324157–2; 144.2–8.5.

J. Tubular structure. Upper Silurian Nyeboe Land Formation, Wulff Land, MGUH 19359 from GGU 319210–3; 146.6–16.5.

K. Tubular structure. Upper Silurian Nyeboe Land Formation, Nyeboe Land, MGUH 19360 from GGU 319234–2; 138.8–8.0.

L. Rounded drop-shaped palynomorphs. Lower Silurian Lafayette Bugt Formation, Washington Land, MGUH 19361 from GGU 316061–2; 137.1–14.8.

Scale bar: 20 μm.

Plate 1. Kerogen

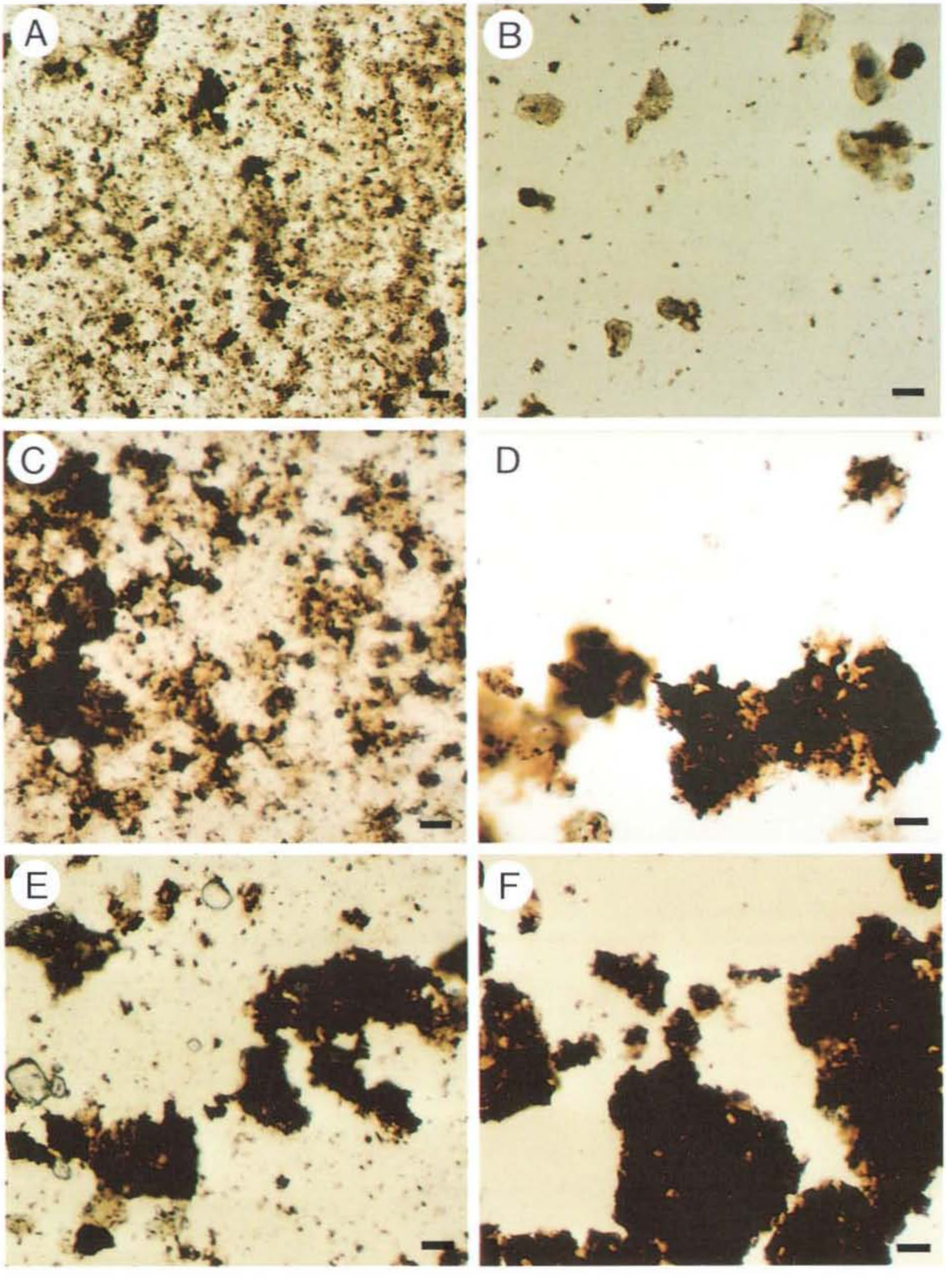

Plate 2. Cambrian palynomorphs

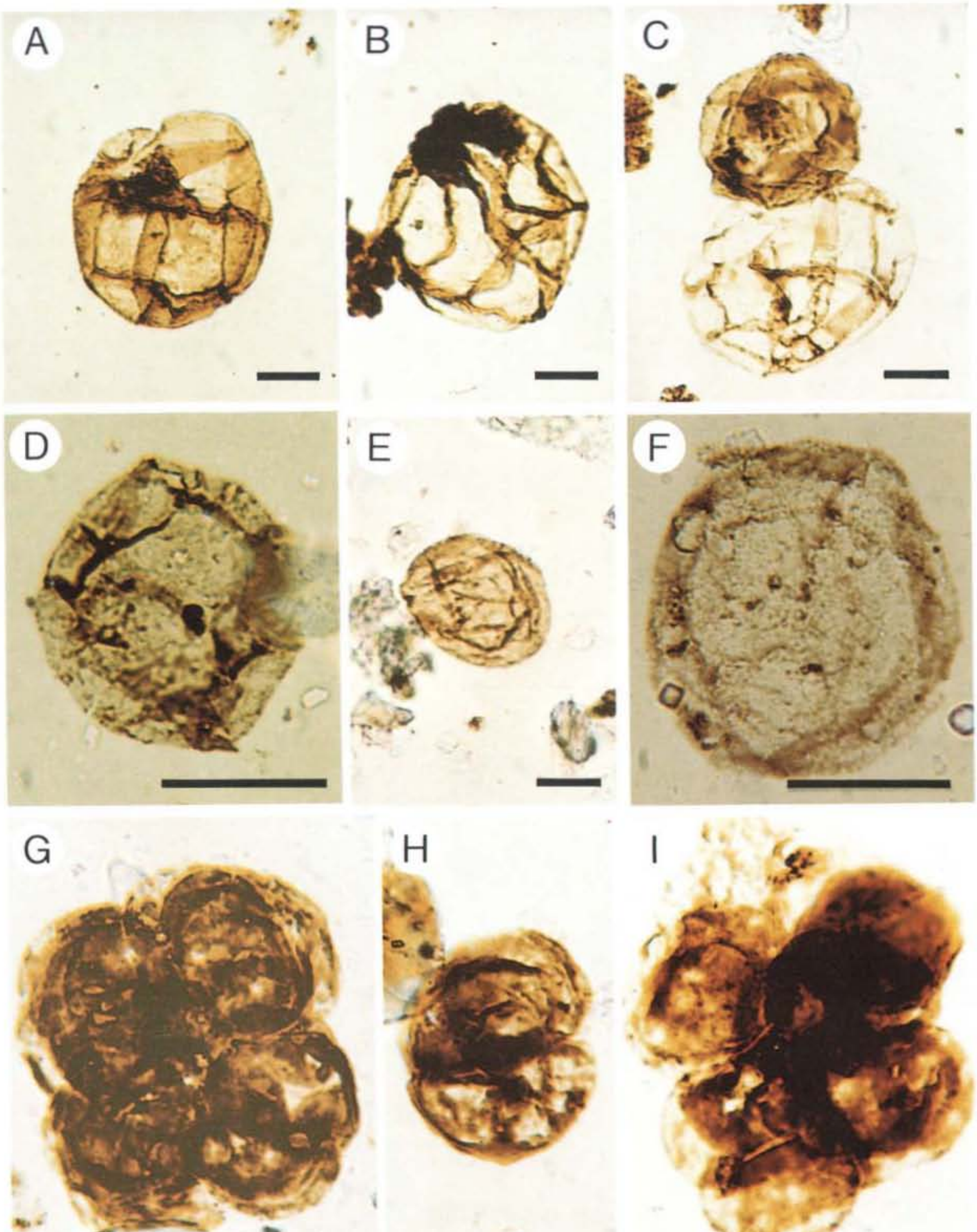

Plate 3. Ordovician palynomorphs

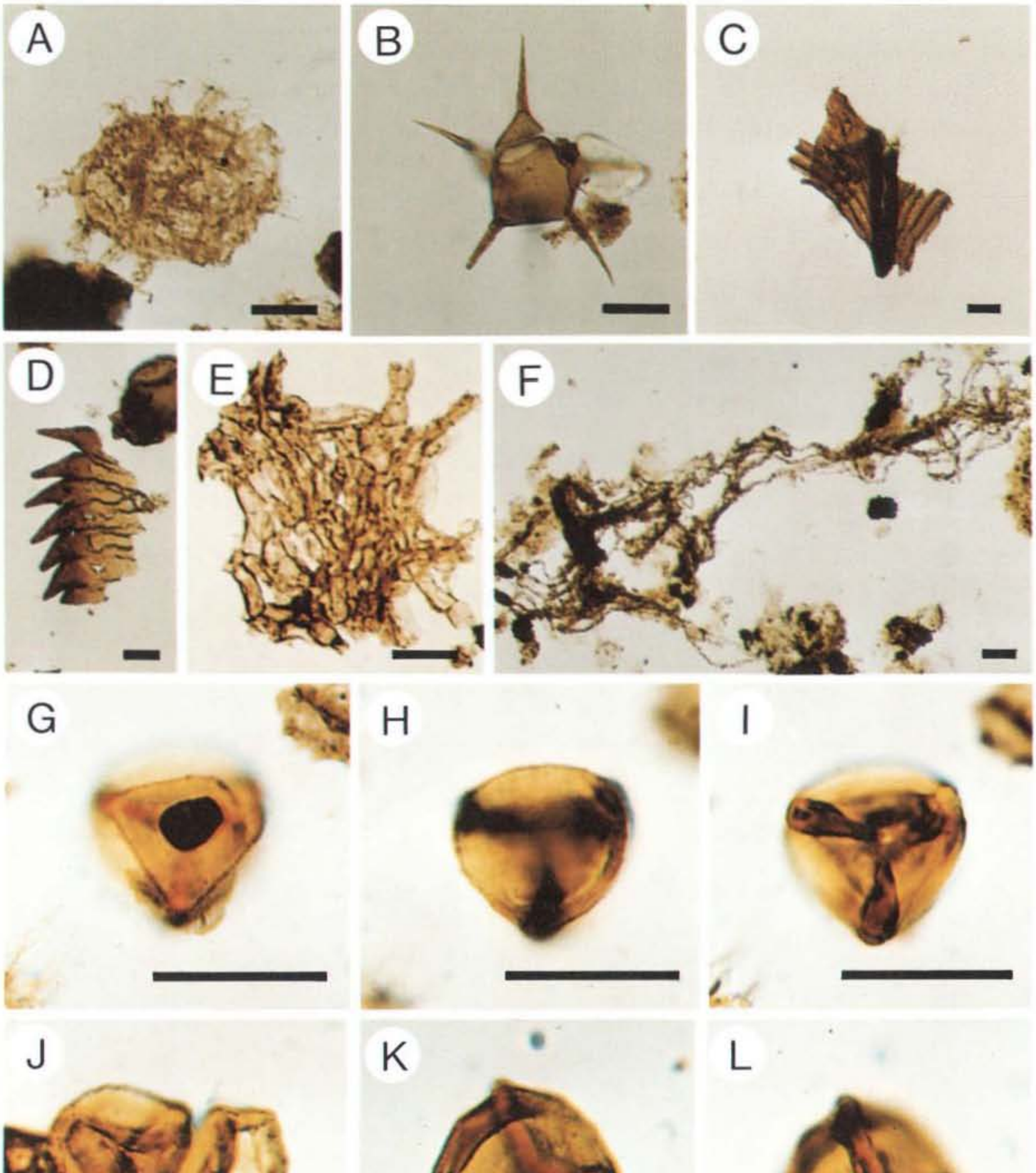

Plate 4. Silurian palynomorphs

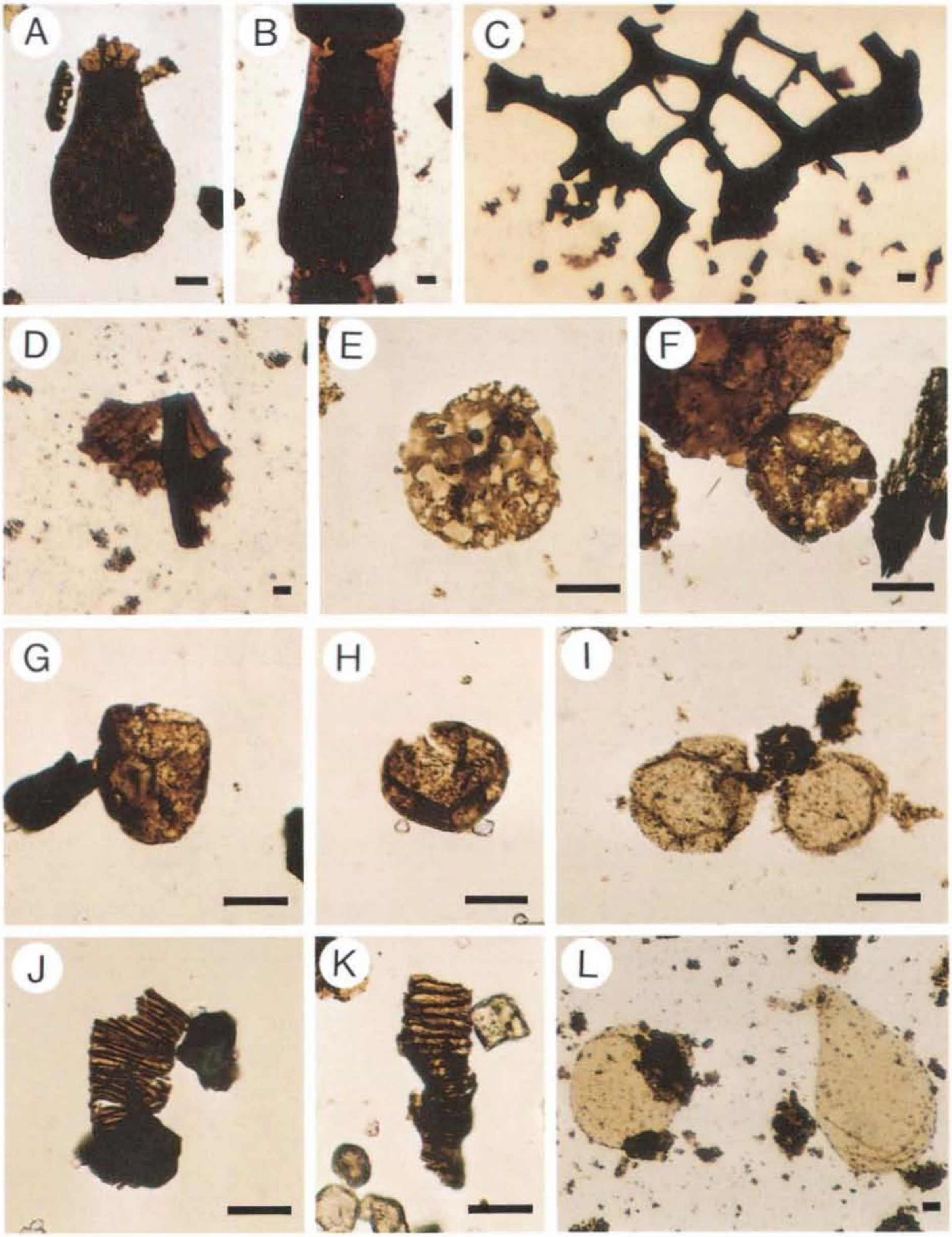

Plate 5. Progressive coloration of amorphous kerogen with increasing thermal alteration

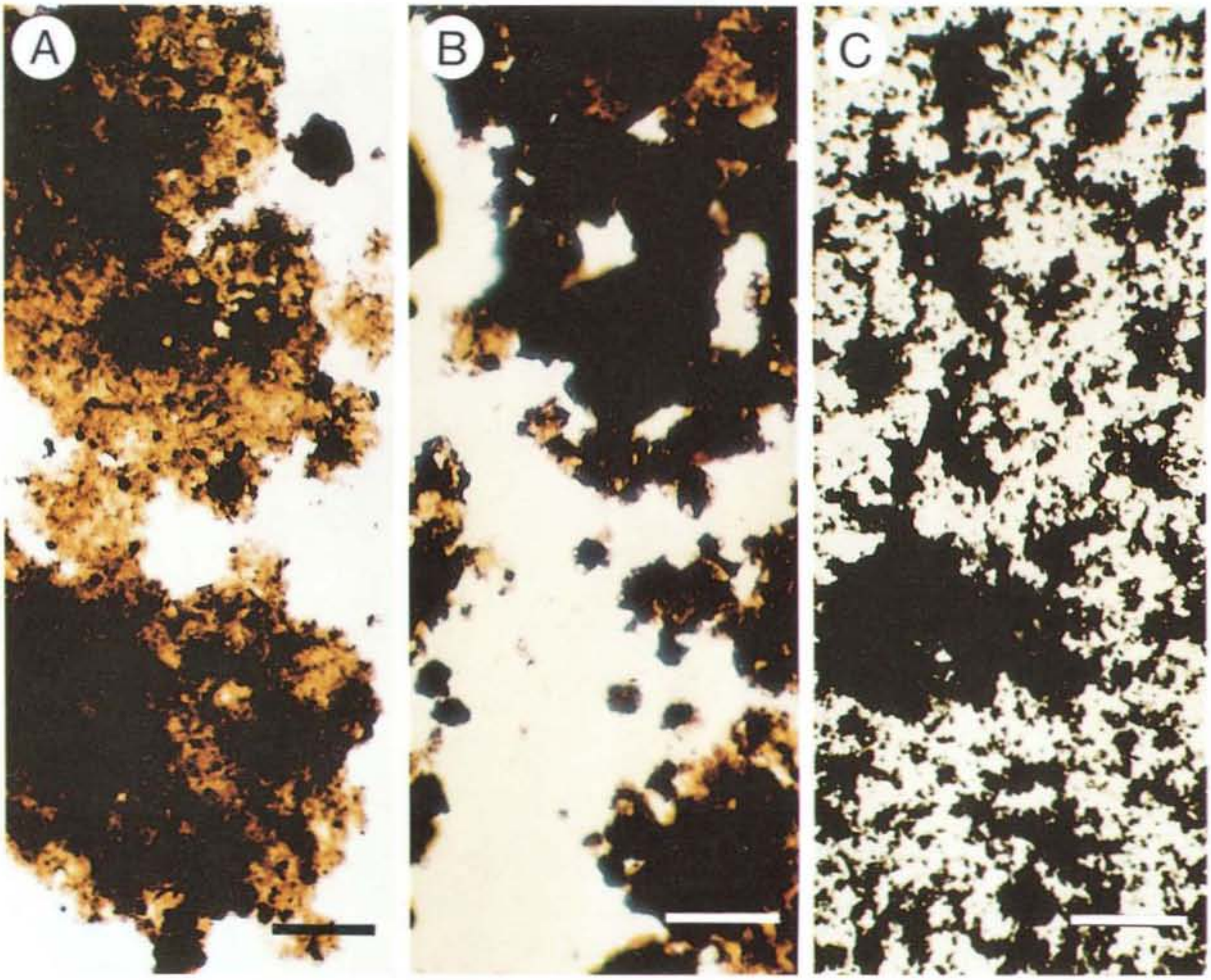

Plate 5. Progressive coloration of amorphous kerogen with increasing thermal alteration

Scale bar: 50 μm

A. TAI: (2)–2^+, GGU 211759–2.   B. TAI: 2^+–(3^-), GGU 324405–2.   C. TAI: 4^+, GGU 316475–1.

Plate 6. Change in structure of amorphous kerogen with increasing thermal alteration as observed in the scanning electron microscope

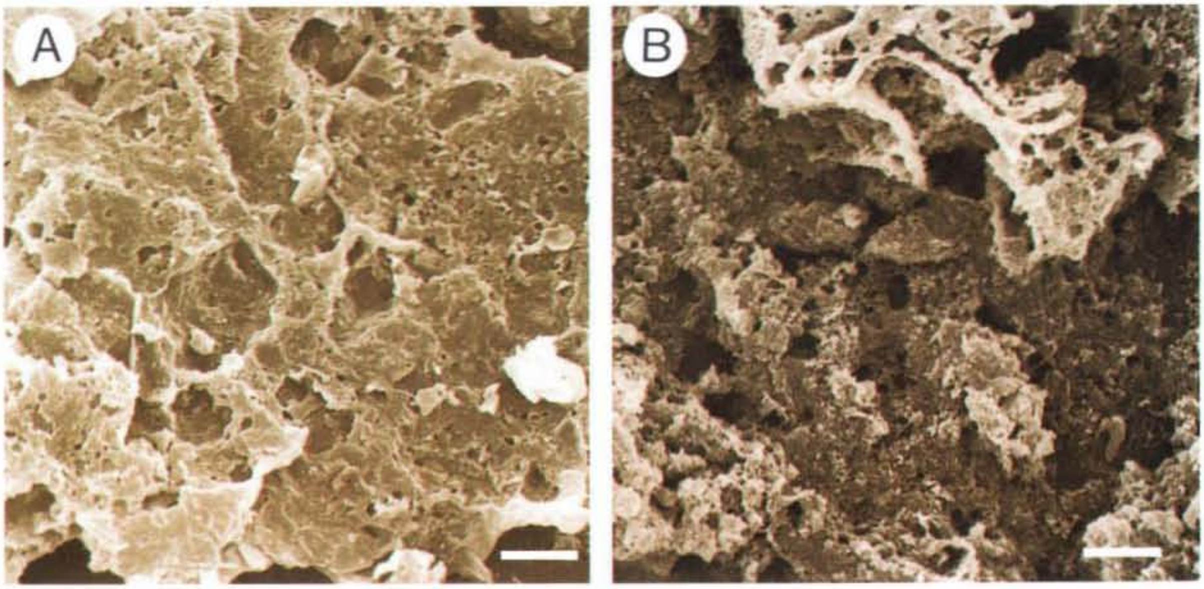

Plate 6. Change in structure of amorphous kerogen with increasing thermal alteration as observed in the scanning electron microscope

A. TAI: 2⁺–(3⁻), T_{max}: 446, GGU 324405–2, scale bar: 10 μm.

B. TAI: 4⁺, T_{max}: n.d., GGU 316475–2, scale bar: 10 μm.

Plate 7. Field appearance of bitumen

A. Seeping asphalt from southern Wulff Land (equivalent to GGU 324200).

B. Hard solid bitumen in dolomite vug in the Sydpasset Formation (equivalent to GGU 324287–324299, core GGU 318003).

Plate 8. Macroscopic bitumen in slabs

A. Asphalt from seep in dolomite breccia. GGU 324200A.

B. Like A. Stained. D0, D1, D2, C1, C2 correspond to generations of dolomite and calcite.

C. Asphalt from seep in dolomite breccia. Stained. Same generations of carbonates as A and B. GGU 324200E.

D. Hard solid bitumen in vugs and veins in dolomite grainstone. DO: dolomite grainstone, D1: saddle dolomite. Core GGU 318003.

Plate 9. Bitumen in thin section

A. Bitumen in coral. GGU 324130B, Lafayette Bugt Formation, Nyeboe Land. Plane light, stained, C: calcite, Fe-C: Fe-rich calcite, B: bitumen, scale bar: 1 mm.

B. Bitumen in coral. GGU 316067, Lafayette Bugt Formation, Washington Land. Crossed nicols + gypsum plate. Q: quartz, C: calcite, B: bitumen, scale bar: 1 mm.

C. Bitumen-filled fracture in calcarenite. GGU 318013–09, Lafayette Bugt Formation, Nyeboe Land. Plane light, scale bar: 2 mm.

D. Two-phased bitumen (black and yellow) (B1, B2) in saddle dolomite veins (D1) cross-cutting dolomite grainstone (D0). See close-up (arrow) in Plate 11. GGU 318003–53, Henson Gletscher Formation, Freuchen Land. Plane light, scale bar: 2 mm.

E.-F. Saddle dolomite vein (D1) in dolomite grainstone (D0). Bitumen occurs as impregnation in DO (B1), as residual matter in the contact between D0 and D1 (B2, R_o: 0.92%) and in the centre of the vein (B3, R_o: 1.21%). GGU 318003–21, Sydpasset Formation, Freuchen Land. Plane light, scale bars: 1 mm.

Plate 10. Bitumen in palynologically prepared samples observed in microscope or in SEM

A. Bitumen with flaky appearance (note crystal impressions). GGU 315172–1. Ryder Gletscher Group Fm 6, Wulff Land. Scale bar: 25 μm.

B. Globular bitumen. GGU 315865–2, Aftenstjernesø Formation, Nares Land, scale bar: 50 μm.

C. Globular bitumen which has been extruded during and after sample preparation by the xylene-containing mounting medium. GGU 315199, Ryder Gletscher Group Fm 6, Warming Land. Scale bar: 12.5 μm.

D. Bitumen with flaky appearance (note crystal impressions). GGU 315172–1, Ryder Gletscher Group Fm 6, Wulff Land. Scale bar: 10 μm.

E. Bitumen mirroring imprints of crystals from coral space. GGU 316067–2, Lafayette Bugt Formation, Washington Land. Scale bar: 10 μm.

F. Thread-like bitumen. GGU 324453, Buen Formation, Wulff Land. Scale bar: 25 μm.

Plate 7. Field appearance of bitumen

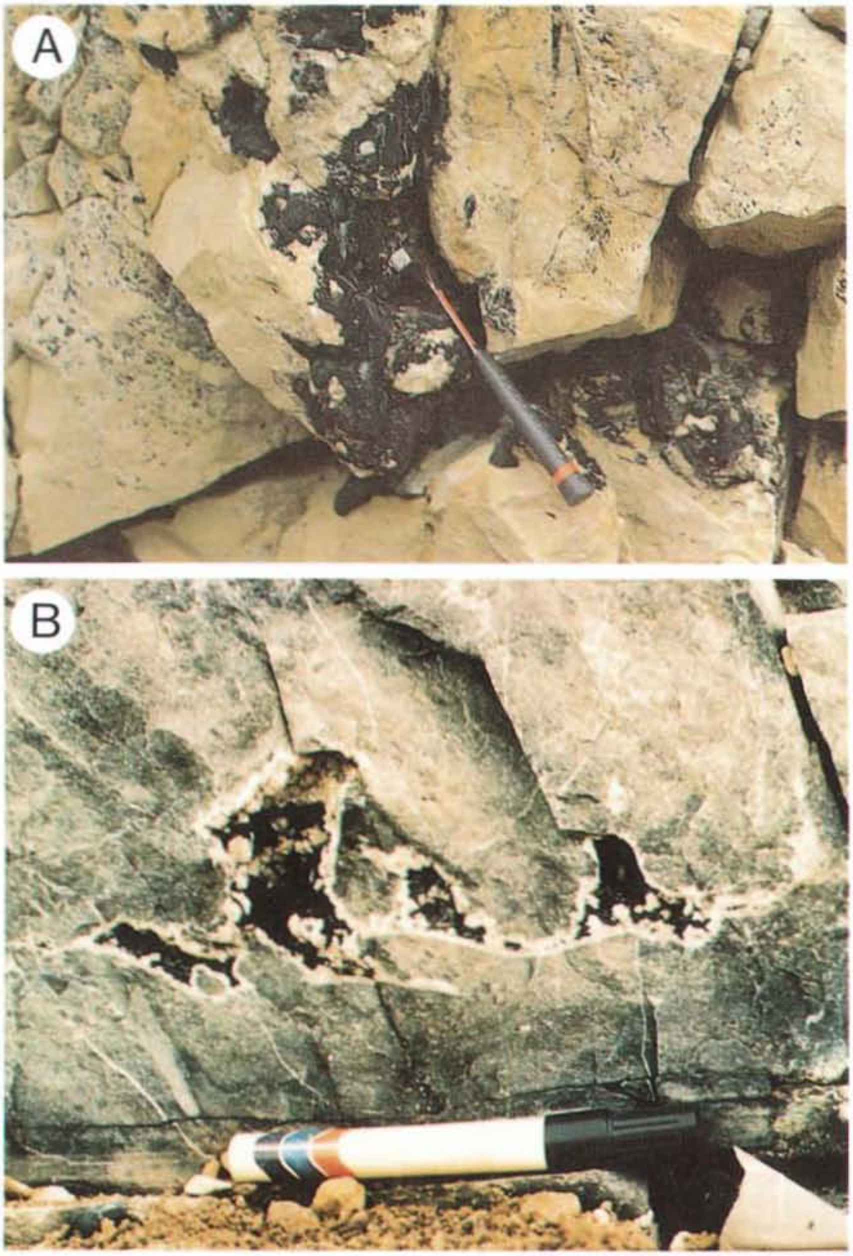

Plate 8. Macroscopic bitumen in slabs

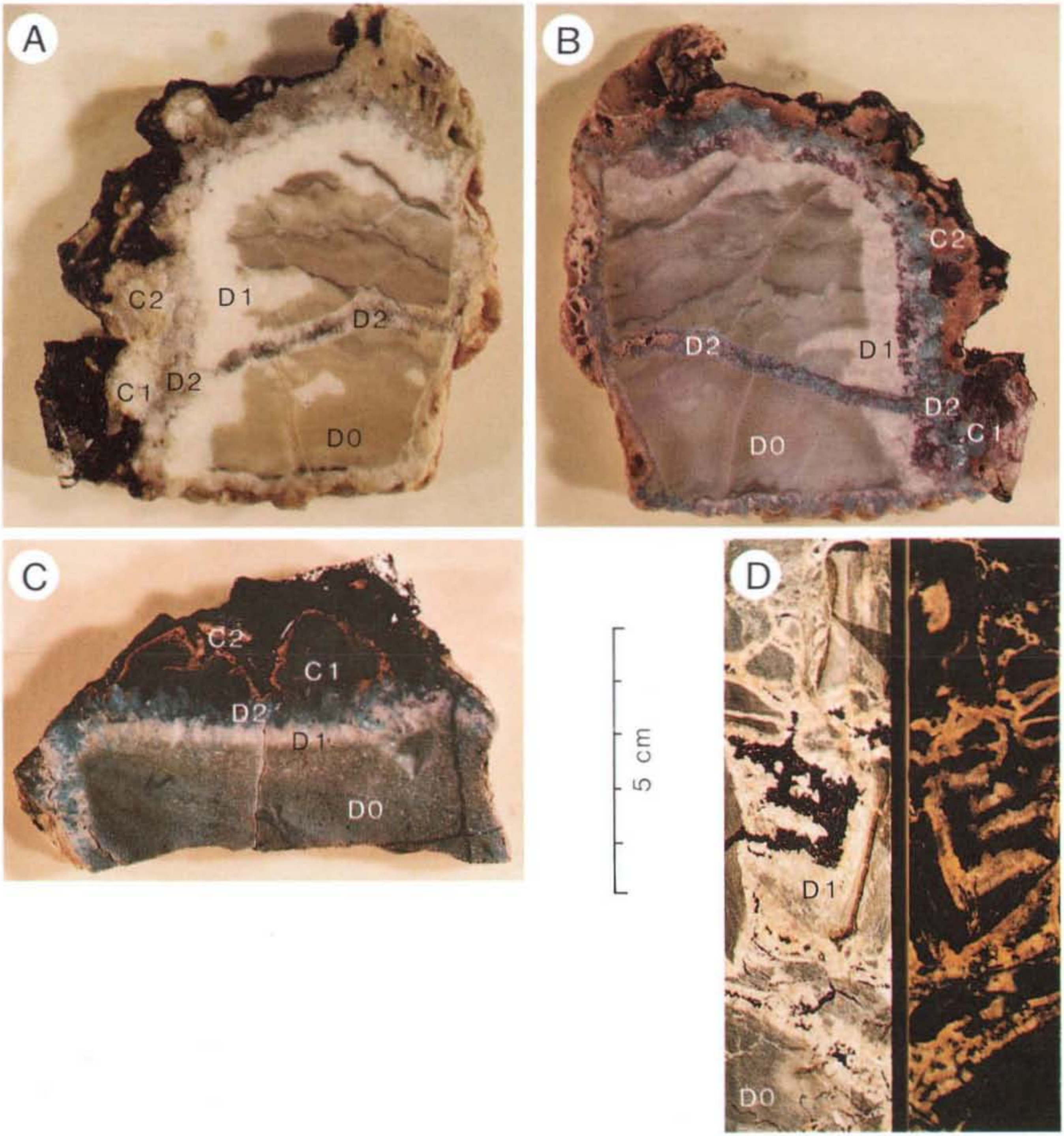

Plate 9. Bitumen in thin section

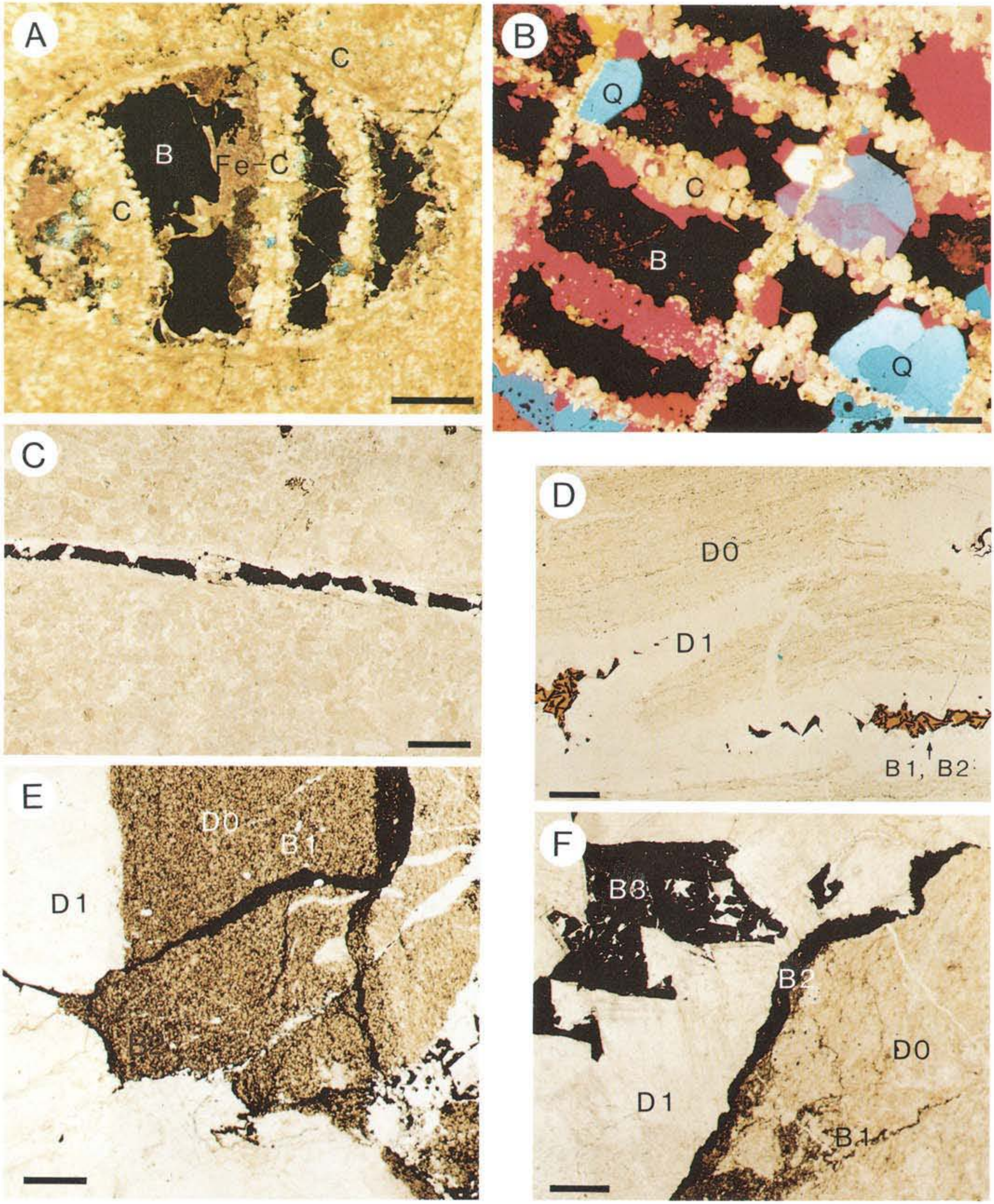

Plate 10. Bitumen in palynologically prepared samples observed in microscope or in SEM

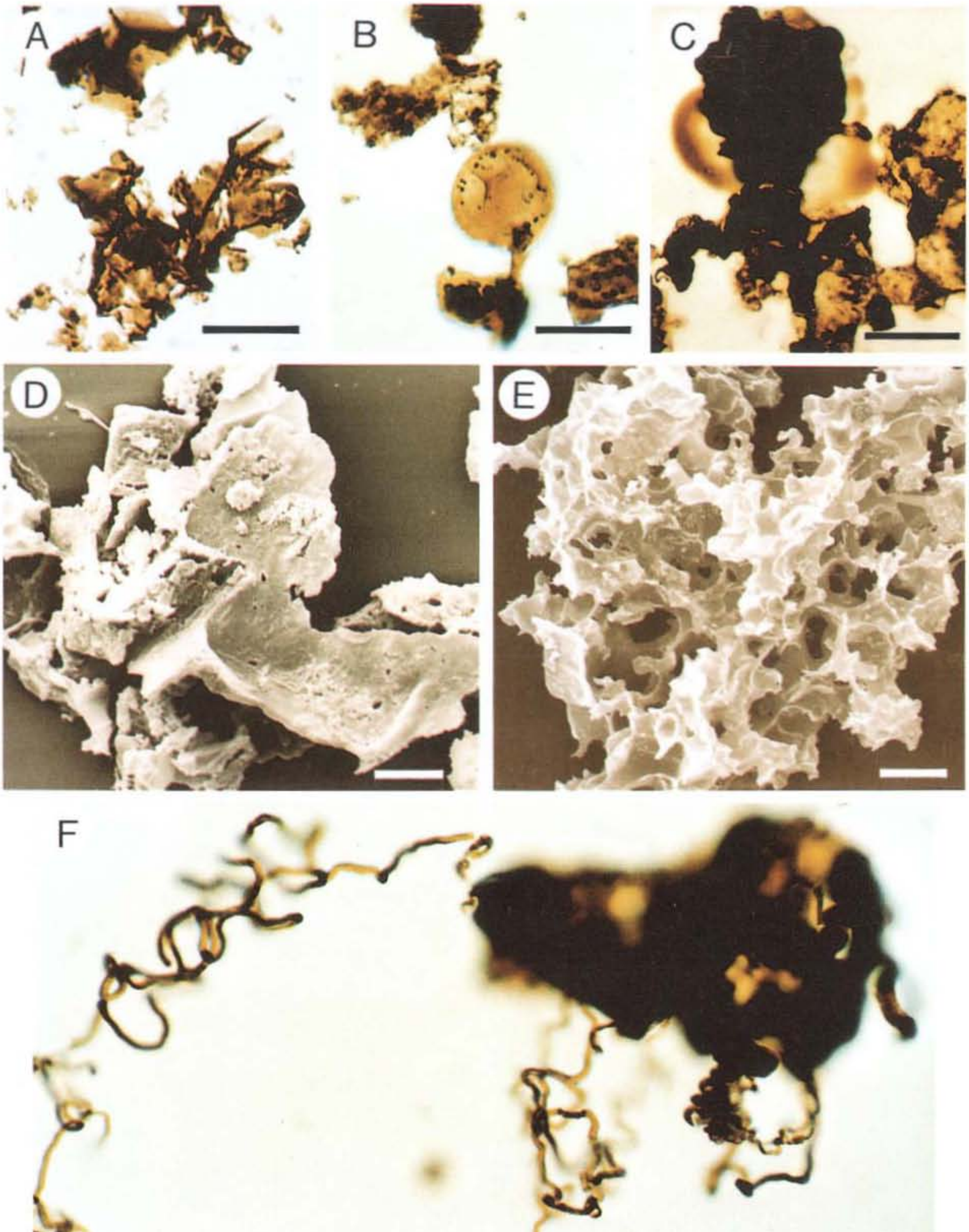

Plate 11. Bitumen in polished section

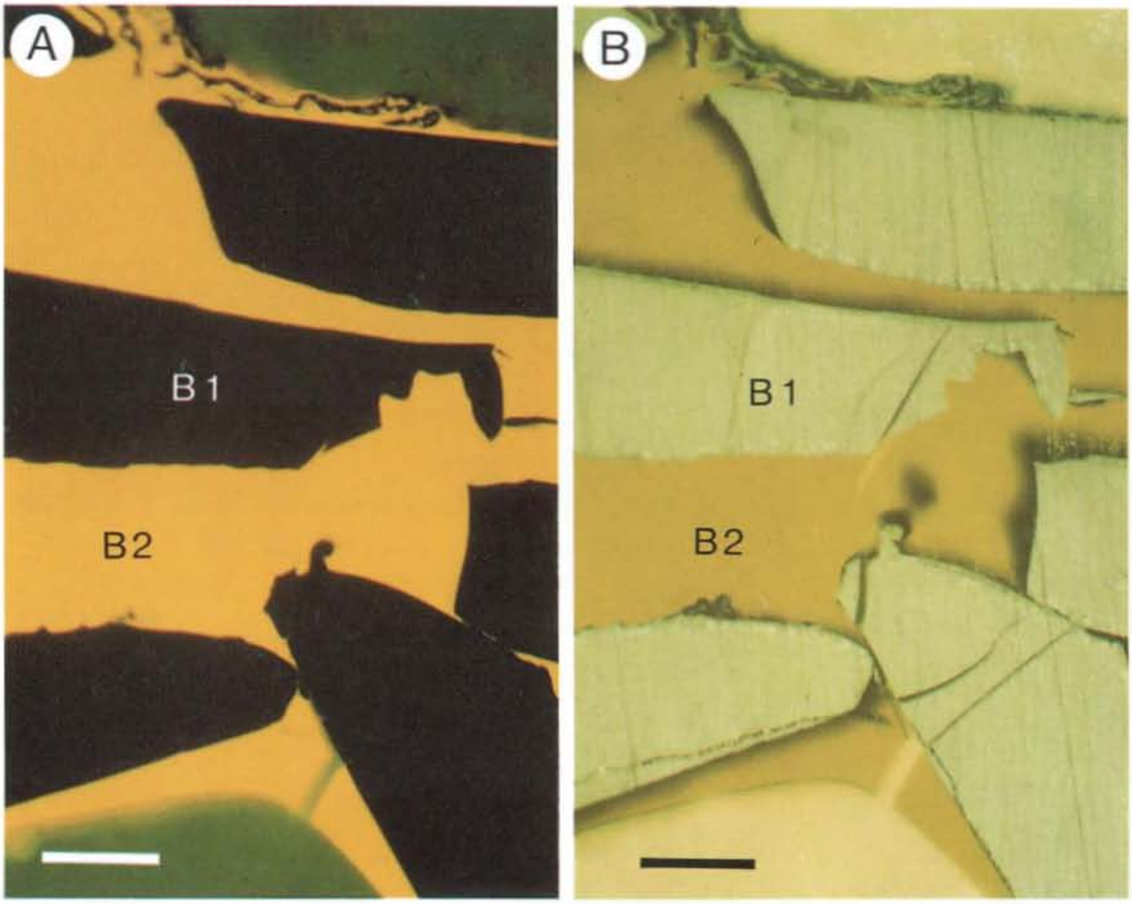

Plate 11. Bitumen in polished section

GGU 318003–53, Henson Gletscher Formation, Freuchen Land.
Scale bar: 50 μm

A. Fluorescent light photograph of two-phase bitumen.

B. Normal reflected light photograph of same field. The yellow-fluorescent low-reflecting bitumen (B2) has a R_o of 0.08% and the dark non-fluorescent high-reflecting bitumen (B1) a R_o of 1.17%.

Cover picture

Cambrian and Ordovician strata at Blue Cliffs, Wulff Land, North Greenland. Photo: J. Lautrup, GGU.